External Transmittal
Authorized

CF 57-8-15
Copy 67

OAK RIDGE SCHOOL OF REACTOR TECHNOLOGY

Reactor Design and Feasibility Study

200 MW NUCLEAR POWER STATION USING A NATURAL URANIUM, ORGANIC COOLED, HEAVY WATER MODERATED, HETEROGENEOUS POWER REACTOR

Prepared by:

A. F. Veras, Group Leader
F. S. Beal
G. L. Hartfield
H. D. Irwin
E. A. Licitra
H. I. Lill, Jr.
H. McNeill
C. B. Magee
W. J. Roesener
K. A. Wheeler

August 1957

DISCLAIMER

Distribution:

1. A. M. Weinberg
2. J. A. Swartout
3. R. A. Charpie
4. W. H. Jordan
5. Lewis Nelson
6. D. C. Hamilton
7. C. O. Smith
8. J. H. Marable
9. P. G. Lafyatis
10. Herbert Pomerance
11. W. A. Lloyd
12. W. Zobel
13. E. D. Arnold
14. J. W. Ullmann
15. A. T. Gresky
16. C. S. Walker
17. E. P. Blizard
18. L. B. Holland
19. W. R. Gall
20. A. P. Fraas
21. J. A. Lane
22. P. R. Kasten
23. A. F. Rupp
24. E. S. Bettis
25. C. E. Winters
26. R. B. Briggs
27. A. L. Boch
28. W. T. Furgerson
29. R. V. Meghreblian
30. L. Dresner
31. S. Jaye
32. C. A. Trilling, Atomics International, North American Aviation
33. Malcolm McEwen, Monsanto Chemical Company
34-35. Martin Skinner
36-37. REED Library
38-39. Central Research Library
40-50. Laboratory Records
51-56. ORSORT Files
57-71. TISE
72. A. F. Veras
73. F. S. Beal
74. G. L. Hartfield
75. H. D. Irwin
76. E. A. Licitra
77. H. I. Lill, Jr.
78. H. McNeill
79. C. B. Magee
80. W. J. Roesener
81. K. A. Wheeler
82. Document Reference Section

PREFACE

In September, 1955, a group of men experienced in various scientific and engineering fields embarked on the twelve months of study which culminated in this report. For nine of those months, formal classroom and student laboratory work occupied their time. At the end of that period, these seven students were presented with a problem in reactor design. They studied it for ten weeks, the final period of the school term.

This is a summary report of their effort. It must be realized that, in so short a time, a study of this scope can not be guaranteed complete or free of error. This "thesis" is not offered as a polished engineering report, but rather as a record of the work done by the group under the leadership of the group leader. It is issued for use by those persons competent to assess the uncertainties inherent in the results obtained in terms of the preciseness of the technical data and analytical methods employed in the study. In the opinion of the students and faculty of ORSORT, the problem has served the pedagogical purpose for which it was intended.

The faculty joins the authors in an expression of appreciation for the generous assistance which various members of the Oak Ridge National Laboratory gave. In particular, the guidance of the group consultants, James A. Lane and Paul R. Kasten, are gratefully acknowledged.

Lewis Nelson
for
The Faculty of ORSORT

ACKNOWLEDGEMENT

The members of this group wish to express their sincere gratitude to their advisors, Mr. J. A. Lane and Mr. P. R. Kasten, without whose patient help and wise counsel this report could not have been written.

Our thanks go also to Mr. E. C. Miller and Mr. J. E. Cunningham for their assitance in materials selection, to Mr. S. Jaye and Mrs. M. P. Lietzke for reactor analysis and computer assistance, to Mr. M. McEwen of the Monsanto Chemical Company and Mr. C. A. Trilling of Atomics International for their technical aid on organic coolants, to Mrs. Marjory Watts for her invaluable assistance with reference materials, and to Miss Sue Wassom and Mrs. Francis Boyd whose skillful art work on graphs and illustrations have added much to the professional appearance of this report.

Finally, we thank the ORSORT faculty and staff for their able assistance in producing this report.

ABSTRACT

A preliminary design and feasibility study has been completed for an organic cooled, heavy water moderated, natural uranium fuel, heterogeneous reactor for a central station power plant with an electrical capability of 200 MW. This study indicates that such a plant is capable of producing electrical energy in the range of 6 to 7 mills/KWH with burnups of the order of 3000 MWD/ton.

The use of organic coolants permits high temperature operation at low pressure and thereby eliminates the necessity for thick-walled, expensive reactor components. Compatability of the organic coolant with uranium dioxide and aluminum together with the low pressure features of the system allows the use of inexpensive fuel elements.

TABLE OF CONTENTS

LIST OF FIGURES

LIST OF TABLES

UNCLASSIFIED
ORNL-LR-DWG. 23257

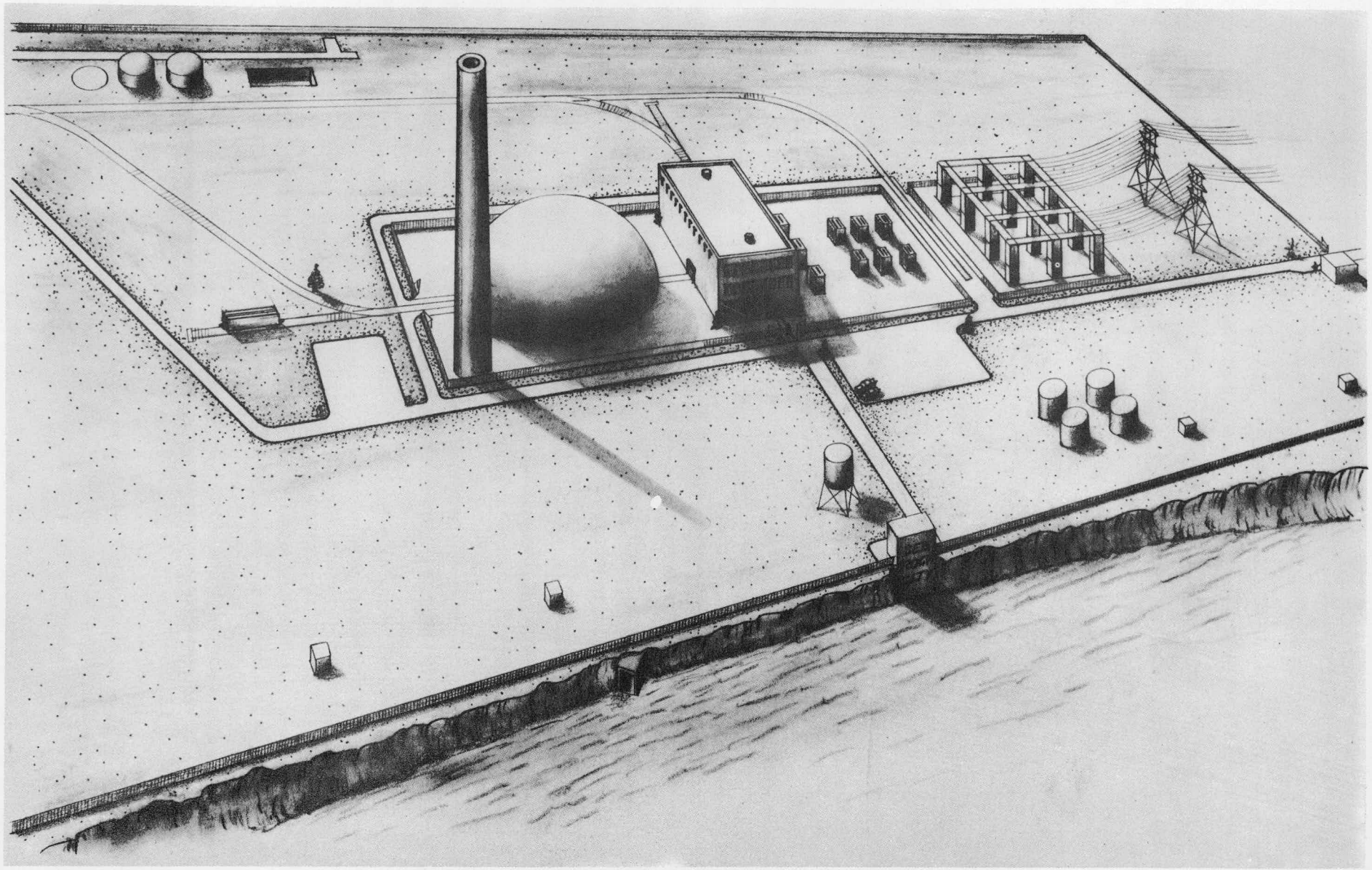

FOREWORD

In the early days of the nuclear reactor program, the challenge was demonstrable power from nuclear fuel, with little regard for cost. During this early period, the basic objectives were that the reactor be critical and controllable, and that energy be removed continuously and used for power generation. With the maturing of nuclear technology, it is no longer significant, from a commercial power viewpoint, to demonstrate merely that reactor power systems will work. The present challenge is nuclear power at reasonable cost.

In commercial power reactor design, there has been, in the past, a tendency to design for an absolute minimum predicted power cost. We feel that the most important requirement is not this minimum possible predicted power cost but rather moderate power costs which can be accurately predicted. A utility company might be more interested in a large scale power experiment which could be relied upon to operate at a small loss than in a minimum cost system based on high risk technological extrapolations. Likewise, the foreign market is best served not by high risk minimum predicted cost systems but rather by reliably predicted moderate cost systems.

One of the major impacts of the principles outlined above is in choosing the balance of capital and fuel costs. Probably the highest risk technological extrapolation in current use in power reactor design is the high fuel burn-up requirement. The desire for minimum fuel costs is the prime motivation for basing designs on high burn-ups. These high burnups have not been achieved to date and if they are not obtained, power costs can go up dramatically for many power reactors being built today. There is another difficulty in basing nuclear power designs on high fuel burn-ups. Often, an attempt is made to construct complex fuel elements from exotic alloys in order to make the large burn-up required appear reasonable. Since the fuel elements are exceedingly difficult to fabricate, they may ultimately cost so much that even if theoretical burn-up is achieved the reactor is uneconomic. The net result of basing a nuclear power design on high fuel burn-up may well be a predicted power cost of 6 mills per KWH and an actual cost of over 10.

We feel that a better measure of the worth of a reactor design is the overall cost per megawatt hour of heat delivered to the prime movers. It seems reasonable to believe that the design required for best overall heat cost is

not likely to be the one that minimizes fuel costs. We have attempted to strike a balance between reactor capital costs and fuel costs to achieve minimum heat costs consistent with a high degree of confidence in the cost estimates.

It is apparent that emphasis on a high degree of confidence in the predicted economics of the reactor requires the most conservative technological approach possible. As an example suppose one pick a reactor operating at a moderate pressure and is thus able to use conventional design and fabrication practices for the vessel; or suppose one picks a reactor operating at a high pressure and obtains the required safety factors by using a high strength, difficult to fabricate alloy of a thickness and diameter beyond conventional practice. All other things being equal, we would regard the moderate pressure approach as "conservative", and the high pressure approach as unconservative.

Recently, there has been a resurgence of interest in this country in natural uranium, high neutron economy systems for commercial power generation. England, Canada, and Norway have, of course, been interested in these systems in a growing realization that economic commercial power from such reactors is possible. Further, such systems do not perhaps involve quite so many engineering unknowns as do the highly enriched, high thermal performance, low neutron economy reactors. Many high neutron economy systems have been and are being investigated. Examples are the Calder Hall, gas cooled, graphite moderated reactors; the Savannah River heavy water moderated, heavy water cooled reactors; the Chalk River heavy water moderated light water cooled reactors; and the Atomics International graphite moderated, sodium cooled reactors. One type which has not received much attention to date is the heavy water moderated, organic cooled reactor. This study is concerned with a large power generating station of 200 megawatts electrical output using a heavy water moderated, organic cooled reactor, fueled with natural uranium. We feel that our investigation is a timely one because of the renewed interest in high neutron economy systems and because of the change in economic conditions brought about by the recently published increase in the AEC guaranteed fair price for plutonium and the low cost of heavy water.

SUMMARY

Economic Summary

Commercial power reactor design requires full recognition of the economic import of the special features of the system under consideration. The successful design must obviously make full use of the desirable qualities of the design elements while minimizing the deleterious effects of any inherent difficulties. It is of course much easier to recognize these requirements than to do anything about them. The difficulty arises in attempting to juggle simultaneously ten or fifteen engineering parameters pertinent to the economics of the system. We do not feel, however, that the difficulty of the task excuses us from attempting it.

First, to identify the gross economic effects of our choice of design elements, let us see in what way this reactor is likely to be different from other more or less similar reactors. Probably the most outstanding feature is that our "fuel costs" can never be much less than a mill/kwh regardless of irradiation time. This situation is brought about by our choice of moderator and coolant both of which occasion moderately high costs, independent of irradiation.

Generally speaking, for best economics one would desire to use natural uranium as the fuel in a high neutron economy system. However, since our primary coolant is a moderately bad nuclear poison, we might expect that our permissible fuel irradiation with natural uranium would be low. Short irradiation times can be tolerated only if low fuel element fabrication and processing costs can be realized. Fortunately, the newly published fair price for reactor grade plutonium of $30/gram might be expected to help keep fuel costs in line at the short irradiation times, since plutonium production per unit exposure is greatest for short fuel cycles.

From the above discussion it would appear that this reactor is likely to have moderately high fuel costs in spite of anything we do. This distinguishes it from many reactors which have essentially zero fuel costs at irradiations in excess of 10 to 15,000 mwd/ton. This being the case, to synthesize an economic reactor we must hold capital costs down. Happily, proper use of the special characteristics of our design elements will permit us to accomplish this objective.

Our primary coolant is an organic which has a low vapor pressure at

moderately high operating temperatures, and is essentially non-corrosive to ordinary engineering materials at these temperatures. Choice of process tubes surrounded by cool moderator maintains pressure and corrosion rate in the reactor vessel at a low value. These features permit low reactor plant investment and low fuel element fabrication and processing costs. Further, our operating temperature yields a fairly good steam cycle efficiency and hence, low investment in the electrical portion of the plant.

We have by no means given an exhaustive discussion of the economic factors involved in this study. Enough has been said to indicate that we had some reason to believe that we might achieve our best economics by trying to strike a balance between operating and capital costs. The economic arguments for the various design choices are given in considerable more detail in the Economics section of this report.

Our capital cost was estimated to be $195/installed kw. Table 1A gives our overall energy cost in mills/kwh at fuel irradiations of 3,000 and 6,000 mwd/ton. Energy costs are 6.73 mills/kwh at our proposed operating point (3,000 mwd/ton) of which 4.45 mills/kwh is the carrying cost, and 2.26 mills/kwh is the net operating cost. Total operating cost was estimated to be 5.82 mills/kwh with a fissionable material credit of 3.56 mills/kwh. The graph, Fig. 1, shows overall energy costs in mills/kwh as a function of fuel irradiation in mwd/ton. The predicted lifetime is of the order of 3,000 mwd/ton and lifetimes approximately double that might be achieved by arranging fuel elements periodically. The detailed breakdown on costs is given in the Economics Section of this report.

Technical Summary

In the design of the reactor, the objective, as noted above, was to take best advantage of those properties of organic coolants which allow substantial engineering gains, namely; low organic vapor pressure, which permits reduction of pressure vessel design and fabrication problems; and secondly, low corrosion rates of organics with ordinary engineering materials. Reductions in volumes of structural materials, made possible by low pressure and low corrosion designs, were translated into substantial gains in neutron economy. Mechanical gains were further enhanced by restricting fluid flow to "pressure tubes" (relatively low pressure) joining upper and lower coolant plenum chambers. The pressure tube concept allowed optimum strength characteristics and in

addition simple and convenient fuel channels and good coolant flow properties. "Bulk" moderator cooling was employed. The 10% of total power generated in the moderator is removed by pumping heavy water through heat exchangers and then back to the moderator tank surrounding the core pressure tubes. Baffling in this tank serves both to promote uniform moderator temperature in the core and to provide rigidity to the fuel element channels. Subsequent sections of the report substantiate the simplicity of structure of this reactor.

As with general reactor features, fuel element design developed around inherent properties of the organic coolant. The basic objective was to obtain highest possible thermal cycle efficiency consistant with the use of a low cost fuel element. It was also desirable to minimize the holdup of organic coolant in the reactor core, in order to increase reactivity and reduce organic make-up requirements. Since the overall limiting factor in this design was the maximum allowable wall temperature of the fuel element cladding, as determined by material considerations, the relatively poor heat transfer properties of the cooling medium dictated large flow channels and good flow-mixing characteristics. On the other hand, the compatibility of the organics with the uranium-oxide fuel materially reduced the importance of maintaining integrity of fuel cladding. For this reason, exotic cladding material could be avoided in favor of inexpensive and easily fabricated aluminum. It is fully expected that should cladding failures occur, continued reactor operation will occasion only minor fission product contamination of the coolant. The fuel element consists of nine 24" long 19-rod clusters of 0.3"O.D. aluminum tubing, wire spaced to provide flow channels, and fitted into 3.5"diameter 18 foot long fuel element tubes. Each end of the element tube is open to coolant flow. The upper end is fitted with an adjustable orificing device and a simple twist-lock device to hold the fuel element against the upward thrust of coolant flow. This design produces an element which is inexpensive to manufacture and easy to handle in and out of the reactor core.

The steam-electric plant is similar to that found in standard central power stations. Steam supplied by the generators is at 430 psia and 560^{o}F. The steam generating plant together with all storage, purification and reactor service equipment is located within the 200 foot diameter containment vessel. Maximum use is made of natural shielding afforded by locations below grade. Arrangement is such that concrete foundations provide shielding as well as support and compartmentation.

TABLE 1A

TOTAL INVESTMENT AND ANNUAL OPERATING COSTS FOR THE ODPR

Electric Capacity	Gross	222,000 KW
	Net	200,000 KW

Cost of Plant

Land	500,000
Reactor and Associated Equipment	24,038,000
Turbogenerator Plant	14,360,000
Total	38,898,000
Working Capital(1)	5,390,000

Carrying Costs

Land 11%	55,000
Reactor and Associated Equipment at 15.25%(2)	3,670,000
Turbogenerator plant at 14%	2,010,000
Working Capital at 9%	485,000
Total	6,220,000

Total Annual Costs

Net Annual Output (millions of KWH)(3)			1,400	
Irradiation (MWD/Ton)	3,000		6,000	
	Annual Cost,	Mills/KWH	Annual Cost,	Mills/KWH
Annual Carrying Charges	6,220,000	4.45	6,220,000	4.45
Annual Operating Costs				
Labor and Maintenance	1,300,000		1,300,000	
Fuel Element Fabricat.	1,400,000		710,000	
Fissionable Material Rental	308,000		308,000	
Cost of Fissionable Material Consumed	2,840,000		1,420,000	
Shipping and Processing	1,420,000		710,000	
Water and Misc. Supplies	80,000		80,000	
D_2O Rental (120 tons)	269,000		269,000	
D_2O Depletion Allowance	269,000		269,000	
Organic Makeup	280,000		280,000	
Total Operating Cost	8,186,000		5,346,000	
Credit Fissionable Material Produced	4,995,000		2,940,000	
Total Net Operating Cost	3,191,000	2.28	2,406,000	1.70
Total Energy Cost		6.73		6.15

(1) Includes the cost of fabricating two cores
(2) Includes Interim Replacement at 1.25%
(3) Assumes .8 Plant Factor

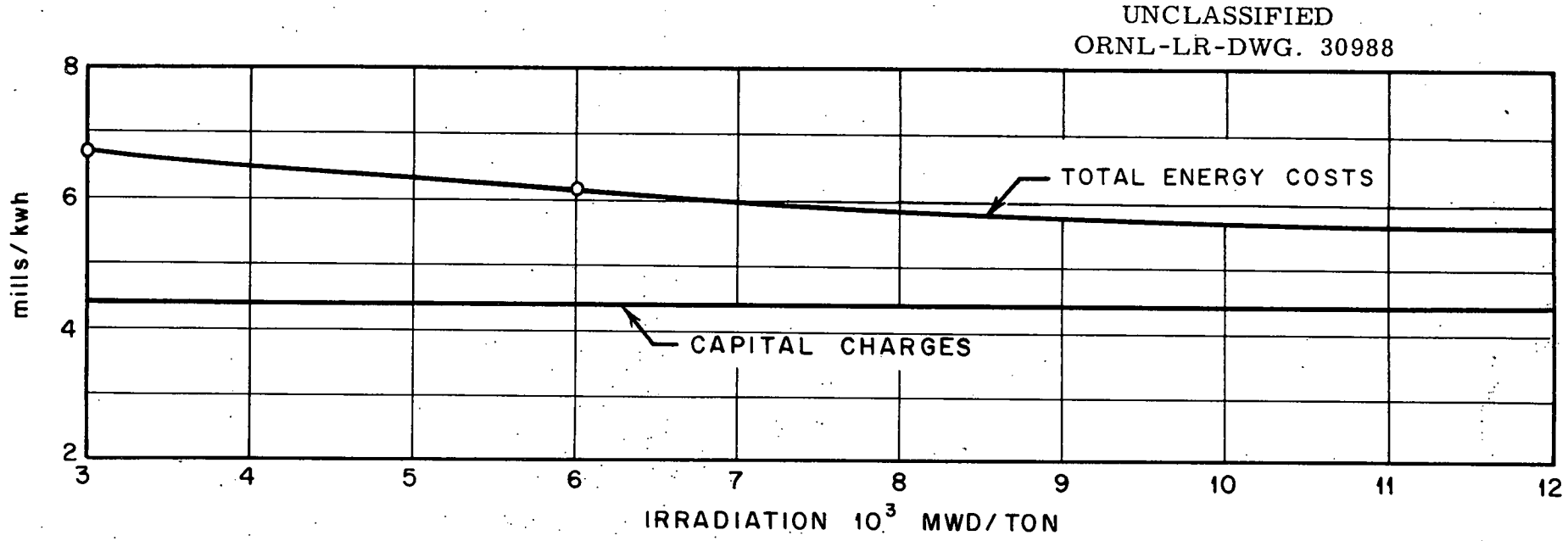

Fig. 1. Total Energy Costs

TABLE 1B

SUMMARY OF TECHNICAL DATA

General Plant

Net Electrical Output at 1.5-in Hg abs, kw	203,260
Reactor Thermal Power Level, mw	800,000
Plant Net Heat Rate, Btu/kwh	13,433
Plant Net Thermal Efficiency, %	25.4
Reactor Type	Heterogeneous
Neutron Energy	Thermal
Fuel (UO_2)	Natural Uranium
Coolant	"Santowax-R" *
Moderator	Heavy Water

Reactor

General

Core Size	
Diameter, ft - in	16 - 11
Length, ft - in	16 - 0
Number of Fuel Tubes	745
Number of Fuel Rods per Tube	19
Fuel Tube Lattice Spacing, in	7
Number of Control Rods	130
Reflector Material	Heavy Water
Reflector Thickness, in	6
Biological Shield Material	Barytes Concrete
Biological Shield Thickness, ft	8

Power

Heat Released in Reactor, mw	800
Heat Flux	
Maximum, Btu/hr sq ft	242,000
Average, Btu/hr sq ft	81,300
Reactor Heat Transfer Area, sq ft	35,300
Specific Power, mw/t uranium	8
Power Density,	
kw/liter	65
mw/t D_2O moderator	0.7 **
mw/t organic	101

* Commercial mixture of terphenyls available through Monsanto Chemical Co.
**Based on 10% of total heat being generated in moderator

Reactor (con't)

Fuel	
Enrichment	Natural
Composition	UO_2
Form	Pellet
Cladding Material	Aluminum
Size of fuel container	
Outside diameter, in	0.60
Length, in	24
Thickness, mils	25
Number of fuel containers per element	152
Uranium in Reactor, tons	106
Aluminum in Cladding, tons	6.5
Fuel Tubes and Coolant Channels	
Number	745
Shape	Circular
Dimensions	
Outside diameter, in	3.5
Length, ft	18
Tube Material	
Inner	Aluminum
Outer	Aluminum
Tube Thickness	
Inner, in	0.125
Outer, in	0.125
Channel Thickness	
Gas space, in	0.125
Aluminum, tons	21
Physics	
Estimated Burnup, MWD/Ton	3050
Initial Conversion Ratio	0.686
k_∞ (hot,clean)	1.12
k_{eff} (hot, clean)	1.089
Thermal Neutron Flux, neutrons/sq cm sec	2.55×10^{13}
Temperature Coefficient of Reactivity, Moderator per ^oC	-1.5×10^{-5}

Reactor (con't)

Physics (con't)

Temperature coefficient of Reactivity, Coolant per °C	-1.6×10^{-5}
Organic/Uranium ratio	0.57
Heavy Water/Uranium ratio	7.8

Reactor Systems

Organic Velocities	
Entrance, ft/sec	7.4
Exit, ft/sec	7.4
In Channels, Average, ft/sec	15
In Channels, Maximum, ft/sec	30
Organic Pressures	
Entrance, psig	250
Exit, psig	60
Organic Temperatures	
Entrance, °F	518
Exit, °F	625
Total Organic Flow Rate, lb/hr	41,000,000
Heavy Water Velocities	
Entrance, ft/sec	34
Exit, ft/sec	34
In reactor, ft/sec	0.2
Heavy Water Pressures	
Entrance, psig	110
Exit, psig	100
Heavy Water Temperatures	
Entrance, °F	140
Exit, °F	190
Heavy Water Flow Rate, lb/hr	5,460,000
Number of Organic Recirculating Feed Pumps	8
Capacity of Organic Recirculating Feed Pumps, (ea), gpm	10,500
Total Organic Pumping Power, kw	12,600
Number of Heavy Water Recirculating Pumps	4
Capacity of Heavy Water Recirculating Feed Pumps, (ea)gpm	3500
Number of Heavy Water Exchangers	2
Surface of Heavy Water Heat Exchangers (ea),sq ft	6280
Heavy Water Velocity in Heat Exchangers,ft/sec	15
Circulating Cooling Water Flow, gpm	4200

Steam Generating System

Number of Reboiler-Superheater Units	4
Surface Area	
Reboiler, (ea) sq ft	22,100
Superheater, (ea) sq ft	5200
Organic Velocities	
Entrance Superheater, ft/sec	7.4
In Superheater, ft/sec	9.8
Entrance Reboiler, ft/sec	7.4
In Reboiler, ft/sec	10
Exit Reboiler, ft/sec	9.5
Water Entrance Reboiler Velocity, ft/sec	18.7
Steam Velocities	
Entrance Superheater, ft/sec	105
In Superheater, ft/sec	75
Exit Superheater, ft/sec	100
Organic Pressures	
Entrance Superheater, psig	60
Exit Reboiler, psig	20
Organic Temperatures	
Entrance Superheater, ^{o}F	625
Entrance Reboiler, ^{o}F	617
Exit Reboiler, ^{o}F	518
Total Organic Flow Rate, lb/hr	41,000,000
Water Entrance Reboiler Pressure, psia	450
Steam Exit Superheater Pressure, psia	430
Water Entrance Reboiler Temperature, ^{o}F	354
Steam Entrance Superheater Temperature, ^{o}F	456
Steam Exit Superheater Temperature, ^{o}F	560
Total Water Entrance Flow Rate, lb/hr	2,590,000
Total Steam Exit Flow Rate, lb/hr	2,566,000
Total Blowdown Flow Rate, lb/hr	24,000
Number of Feedwater Pumps	5
Capacity of Feedwater Pumps, (ea)gpm	1300
Number of Hotwell (Condensate) Pumps	3
Capacity of Hotwell Pumps, (ea) gpm	1900
Number of Feedwater Heaters	4

Turbine - Generator

Turbine Type	Compound, Double Flow
Turbine Speed, rpm	1800
Throttle Steam Pressure, psia	400
Throttle Steam Temperature, ^{o}F	550
Turbine Throttle Steam Flow at 1.5 in Hg abs, lb/hr	2,563,000
Capability of Turbine at 1.5 in Hg abs, kw	225,000
Capability of Generator, 30 psig Hydrogen, 0.85 P.F., 0.64 S.C.R., kva	260,000

Condenser

Condenser Type	Two Pass, Divided Water Box
Condenser Surface, sq ft	202,000
Condenser Circulating Water Flow, gpm	256,400
Circulating Water Pumps	
Number (including heavy water cooling)	8
Capacity, (ea)gpm	50,000

Station Performance

Total Steam Flow at 1.5 in Hg Abs, lb/hr	222,200
Total Turbine-Generator Output at 1.5 in Hg abs, kw	222,200
Auxiliary Power, kw	18,940
Auxiliary Power, %	8.5
Net Electrical Output at 1.5 in Hg abs, kw	203,260
Net Station Heat Rate at 1.5 in Hg abs, B/kwh	13,433

Materials of Construction

Fuel	UO_2
Fuel Cladding	Aluminum Alloy X-2219
Fuel Assembly Tube	Aluminum Alloy X-2219
Process Tube	Aluminum Alloy 61S-T6
Tube Sheets	Alfin Clad Carbon Steel SA-212B
Pressure Vessel	Carbon Steel SA-212B
Moderator and Reflector	Heavy Water
Coolant	"Santo-wax R"
Piping	
Main Power Loop	Seamless Carbon Steel, SA-106 Gr. A, Sch.80

Moderator Loop	Stainless Steel, 304, 316, or 347
Steam and Water	Carbon Steel SA-106, Gr.A, Sch. 80
Container Shell	SA 212 or 312 Aluminum killed

ENGINEERING

Description of Power Plant

General - This study is concerned with a nominal 200 megawatt electric power generating plant using an 800 megawatt heat output, organic cooled, heavy water moderated nuclear reactor. This section of the report deals with an engineering description of this power plant.

Plant Site - The property for this plant is a typical river site approximately one mile in length and three-quarters of a mile in depth back from the river, encompassing about 480 acres. The reactor building is located near the center of the property, with the turbine-generator building, including administrative offices, being situated next to it; Fig. 2 and Frontispiece. Just beyond the turbine-generator building are the electrical transformers, the switchyard, and the transmission facilities. The screen house is located on the river bank about 2000 feet from the turbine-generator building. Waste disposal facilities are at the back corner of the property about 2500 feet from the reactor building and 3500 feet from the river. A 300-foot stack is adjacent to the reactor building for venting mildly radioactive decomposition gases. Railroad facilities enter the plant site next to the waste disposal area and provide service into the reactor building, into the turbine-generator building, and to the electrical transformer and switch-yard area. Deepwells on the property provide the water for the steam cycle, shield cooling, and miscellaneous bearing and oil cooling, as well as for the fire protection system and the drinking water and sanitary system.

Reactor Building - This building is in the form of a 200-foot diameter steel hemisphere above grade, with a 200-foot diameter steel cylindrical section extending 50 feet below grade and being closed on the bottom by a spherical segment with a 215-foot radius of curvature, thus giving an additional 25 foot below grade at the center of the building. Below grade this safety shell is surrounded on the outside by four feet of concrete plus a considerably thicker section of concrete below the center portion of the bottom. A large pressure seal door is on one side of the building to allow railroad entry into the building. A small pressure seal door is provided opposite the railroad entrance to allow personnel passage to and from the turbine-generator building.

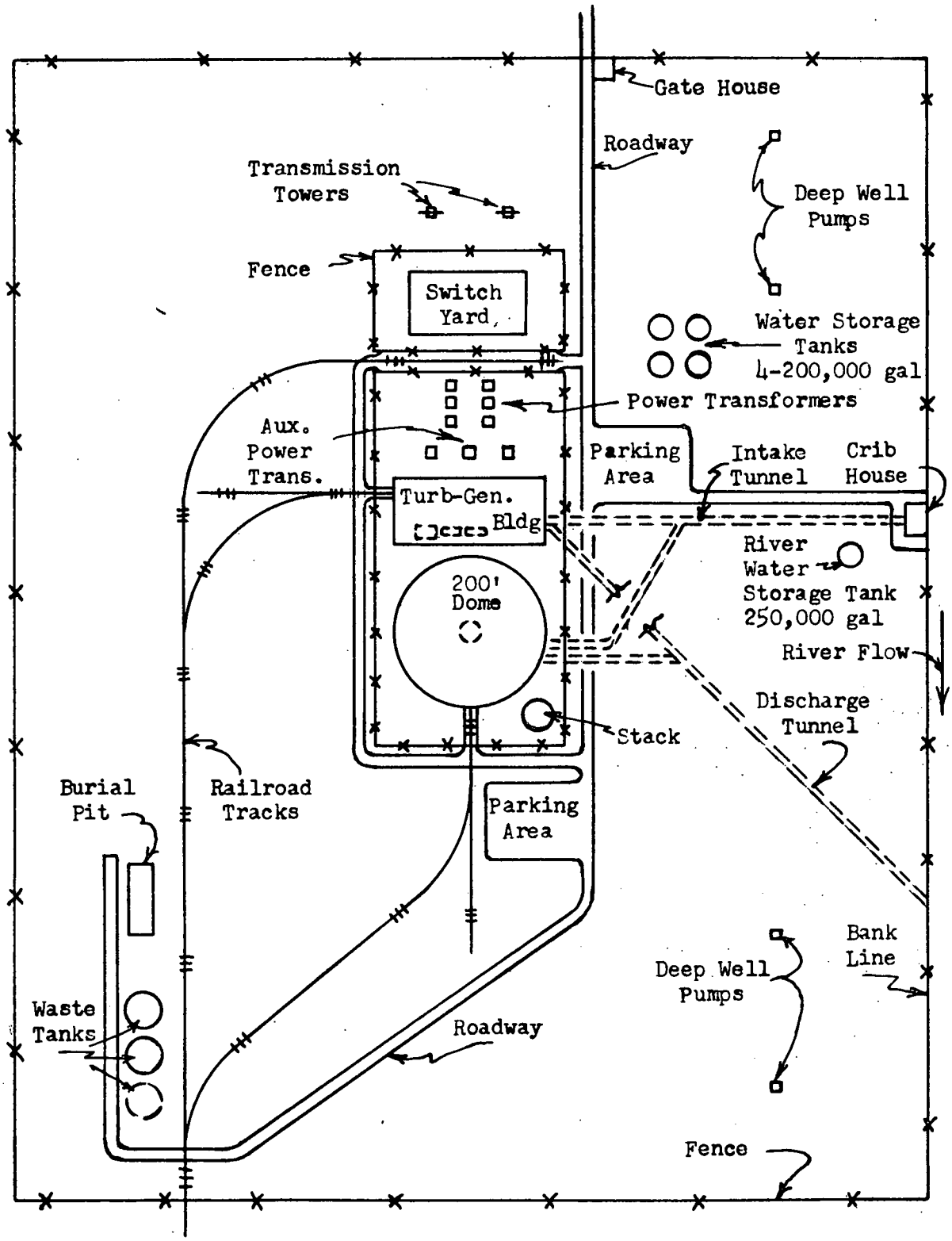

PROPERTY PLAT
Figure No. 2

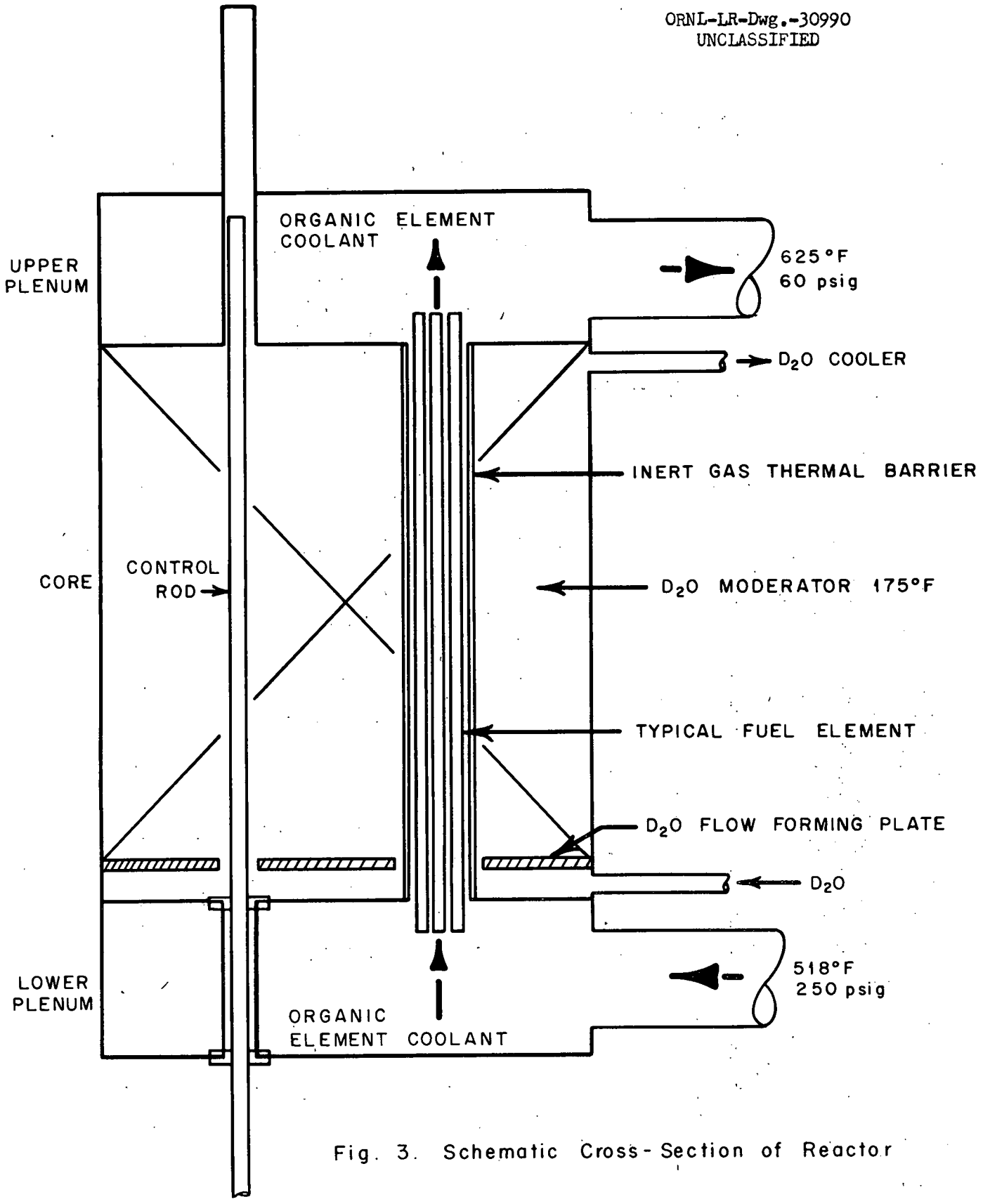

Fig. 3. Schematic Cross-Section of Reactor

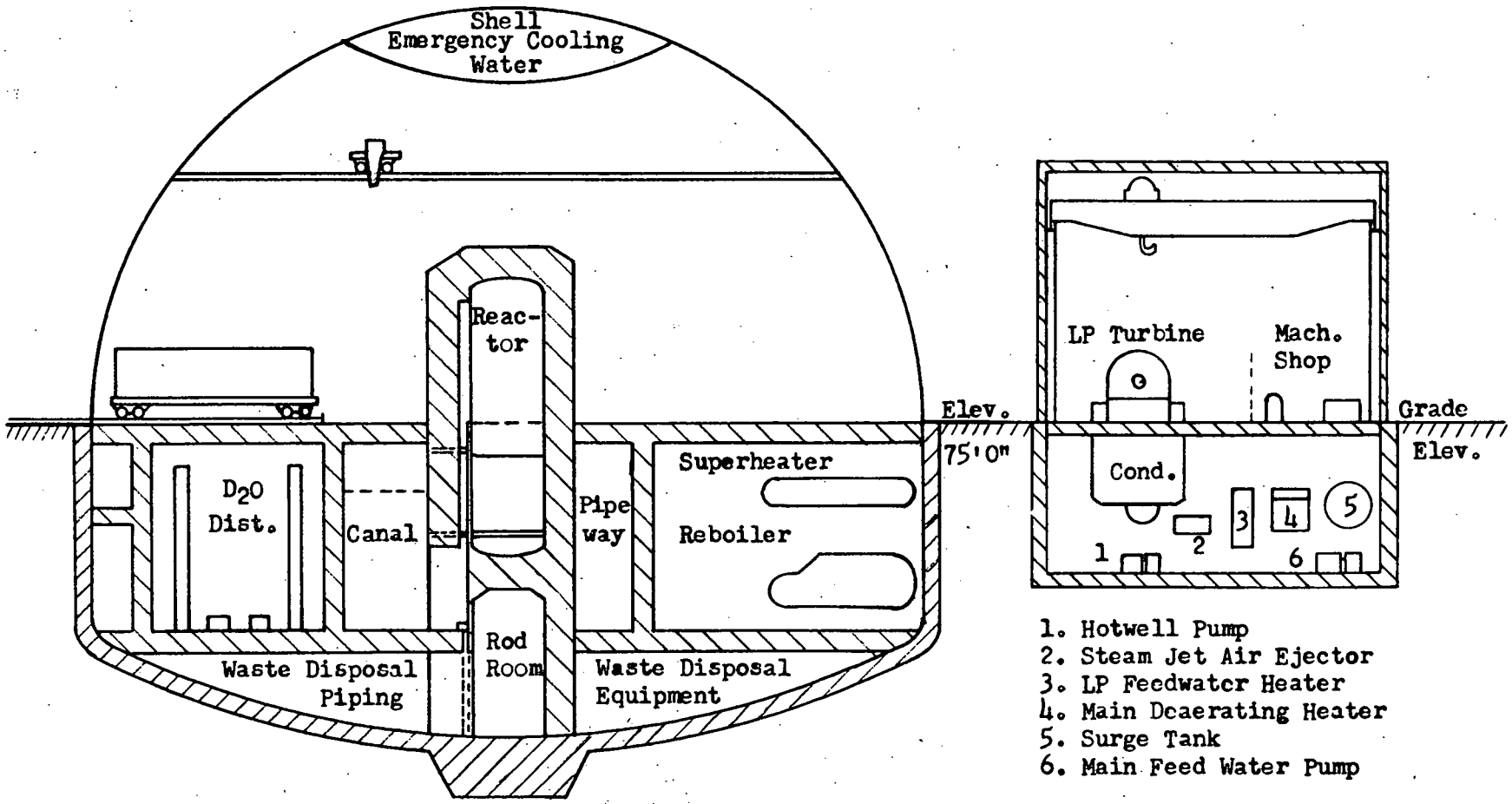

Section A-A

Elevation Cross Section Through Reactor and Turbine-Generator Buildings

Figure No. 4

ORNL-LR-Dwg.-30991
UNCLASSIFIED

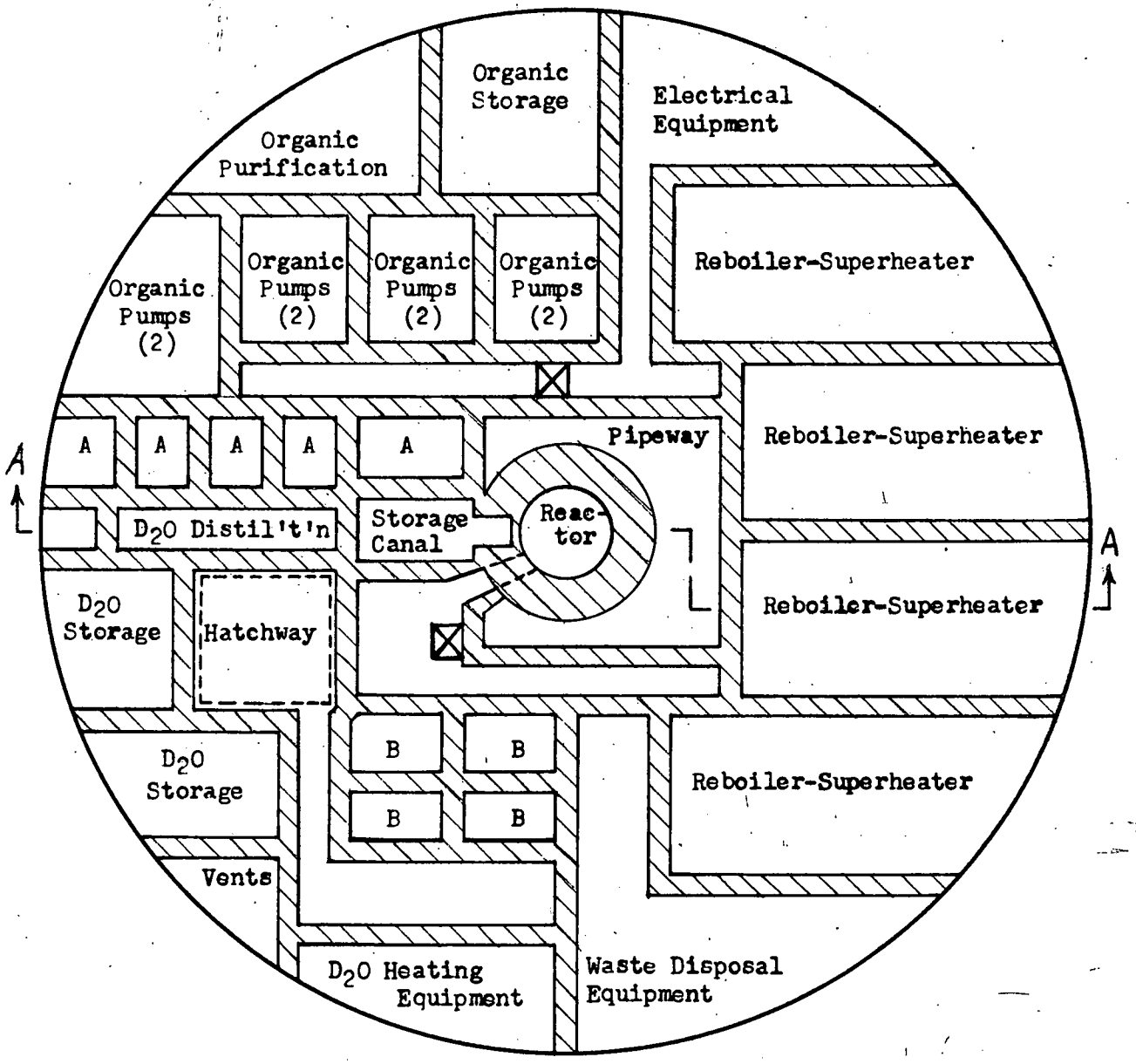

A - D_2O Purification Cell
B - D_2O Pump
⊠ - Elevator

PLANT LAYOUT
Elevation 25'-0"
Plan View
Figure No. 5

ORNL-LR-Dwg 23227
UNCLASSIFIED

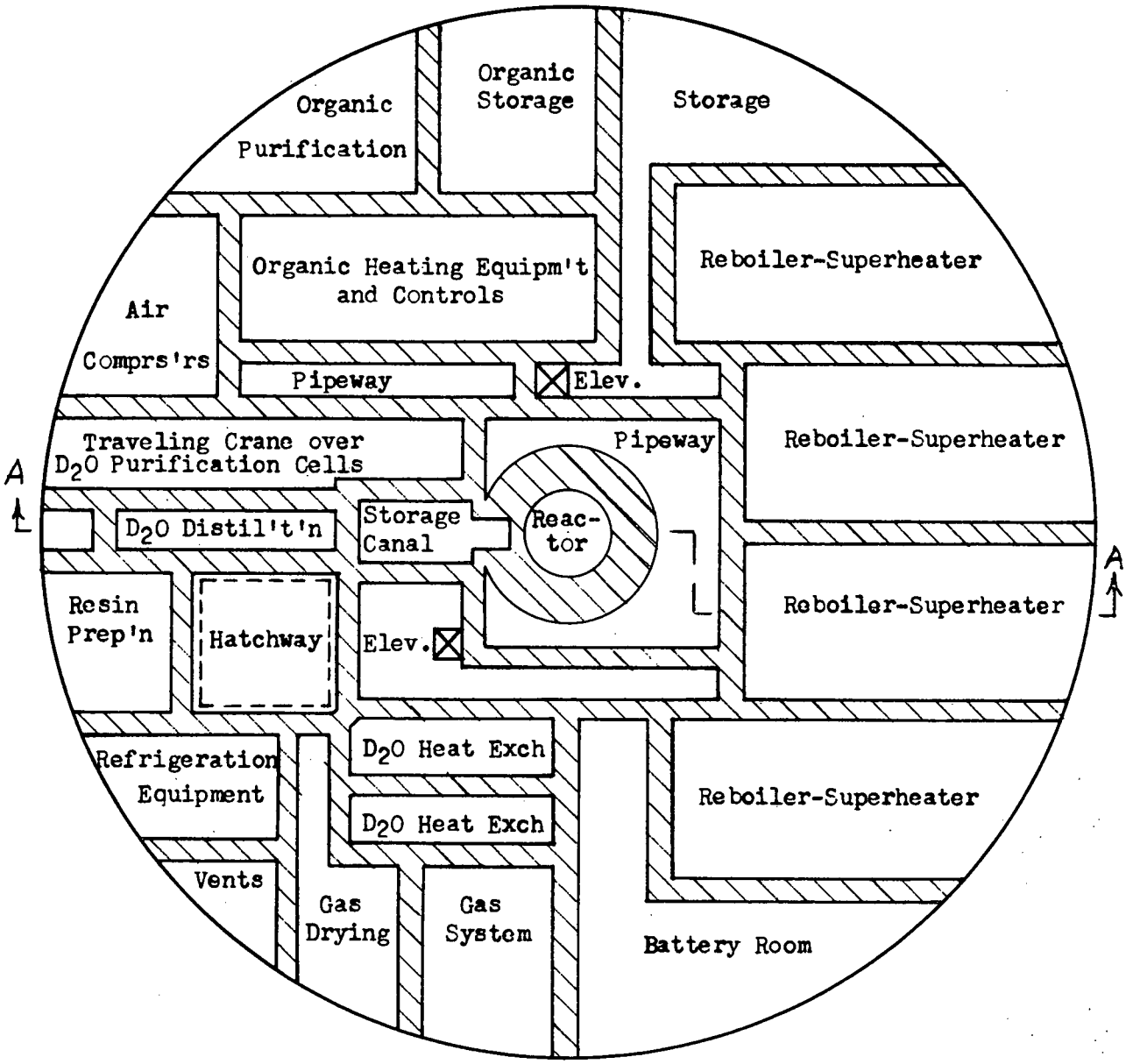

PLANT LAYOUT

Elevation 55'-0"
Plan View
Figure No. 6

UNCLASSIFIED
ORNL-LR-DWG. 30993

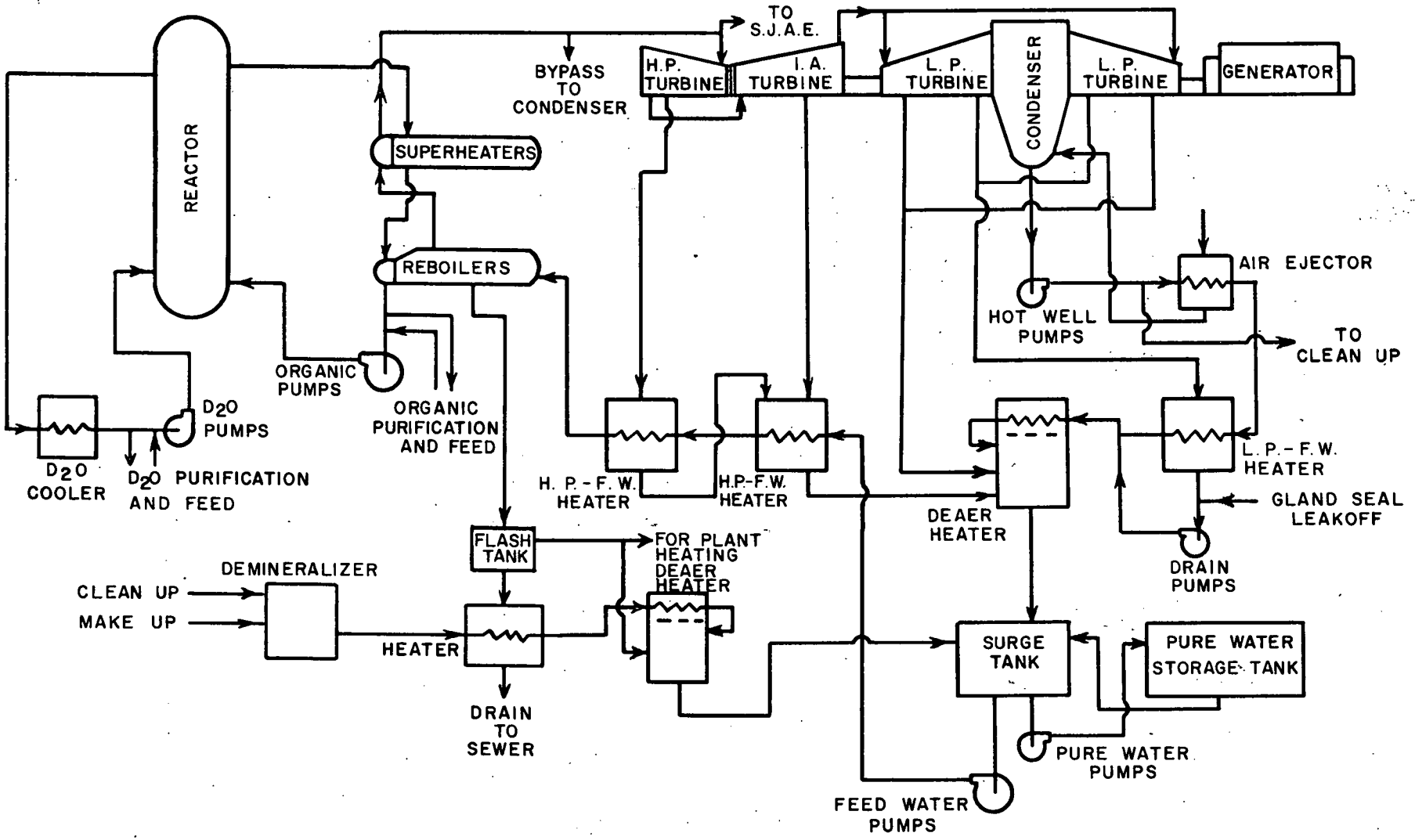

The reactor itself is in the middle of the building extending some 34 feet above and below grade elevation. Also located in this building are the reboiler-superheater units, the organic and heavy water systems and their separate purification equipment, the gas system, and the waste disposal equipment. The reactor and its various components are assembled in an arrangement designed to provide adequate protective shielding and maximum accessibility of equipment, Figs. 4, 5, and 6. The reactor is surrounded by 8 feet of Barytes concrete while the associated equipment cells are constructed of walls 2 to 4 feet thick. The simplified flow diagram of the O.D.P.R. system is shown in Fig. 7.

Turbine-Generator Building - This building houses the turbine-generator and its associated steam cycle and electrical equipment, along with the main control room, administrative offices, emergency diesel generators, and personnel decontamination locker facilities, Fig. 4. The building is 200 feet in length, 80 feet in width, and extends 60 feet above grade and 35 feet below grade. Railroad facilities extend into the building for easy access by the 100 ton overhead crane.

Screen House - This building contains the traveling screens, trash racks, screen wash pumps and circulating water pumps. It is connected to the reactor building and to the turbine generator building by circulating water intake tunnels. An elevated circulating water storage tank with a 250,000 gallon capacity is about 75 feet from the screen house toward the reactor building.

Deep Wells - Four deep wells are located on the property, each being about 200 feet back from the river bank and being well set apart from each other. The deep well pumps supply the water for plant services as well as to the four 200,000 gallon storage tanks located near the main parking area across from the turbine generator building.

Reactor

The Fuel Element

a. Mechanical Description - The fuel element consists of an aluminum tube 3.5" in diameter and 18 ft long in which are held eight two foot long bundles of UO_2 fuel rods. Each bundle contains 19 symetrically spaced fuel rods 0.60 " in diameter made of pressed cylindrical UO_2 pellets of 92%

theoretical density, and sealed in 0.025" wall thickness aluminum tubes. Each pellet contains a 1/8" diameter gas expansion void space. The inner circle of rods is spaced from the center rod and from the outer rod by 0.065" diameter aluminum wire wrapping. Rods in the outer circle are spaced from each other and from the inner rods by welded space sleeves made of 2" long tubing sections spaced six inches longitudinally along the rod bundle. The entire bundle is aluminum wire wrapped to space the rod bundle from the element tube. Each bundle assembly is made by a furnace welding procedure such as used in manufacture of MTR elements.

The upper and lower ends of the element tube are ported to allow flow of the organic heat transfer fluid through the element tube and through the rod bundles. The upper end is provided with an orificing arrangement for adjustment of individual element heat removal, and with a "twist-lock" devise for securing the element assembly in the reactor core. A conceptual design for the element is shown in Fig. 9.

The element tube fits within the reactor process tube and is spaced 1/16" from the process tube by process tube ribbing. An "O-ring" seal at the upper junction of the element and the process tube together with a labyrinth seal at the lower junction, form a nitrogen gas insulating barrier space to prevent loss of heat from the hot fuel tube to the relatively cool heavy water moderator. Nitrogen is distributed to this space by 3/16" tubing arranged in the upper organic plenum. The gas pressure is sufficient to overcome the pressure in the lower organic plenum. This pressure differential allows slight gas leakage and prevents organic from entering the nitrogen space.

b. Selection - As noted previously, an organic cooled reactor requires a large degree of subdivision of the fuel in order to provide the required heat transfer area. Also, the choice of UO_2 as the fuel for this study limited the choice of elements to simple shapes that could be easily fabricated. The combination of these two requirements led to the use of small diameter cylindrical rods. In order to obtain the lattice spacing required by physics it was necessary to group several of these rods into a cluster. Preliminary calculations indicated that single and seven rod clusters did not provide sufficient heat transfer surface. The final design of nineteen rods in a cluster provided adequate surface area without increasing the amount of cladding unduly.

The possibility of using extended surfaces to obtain the required heat

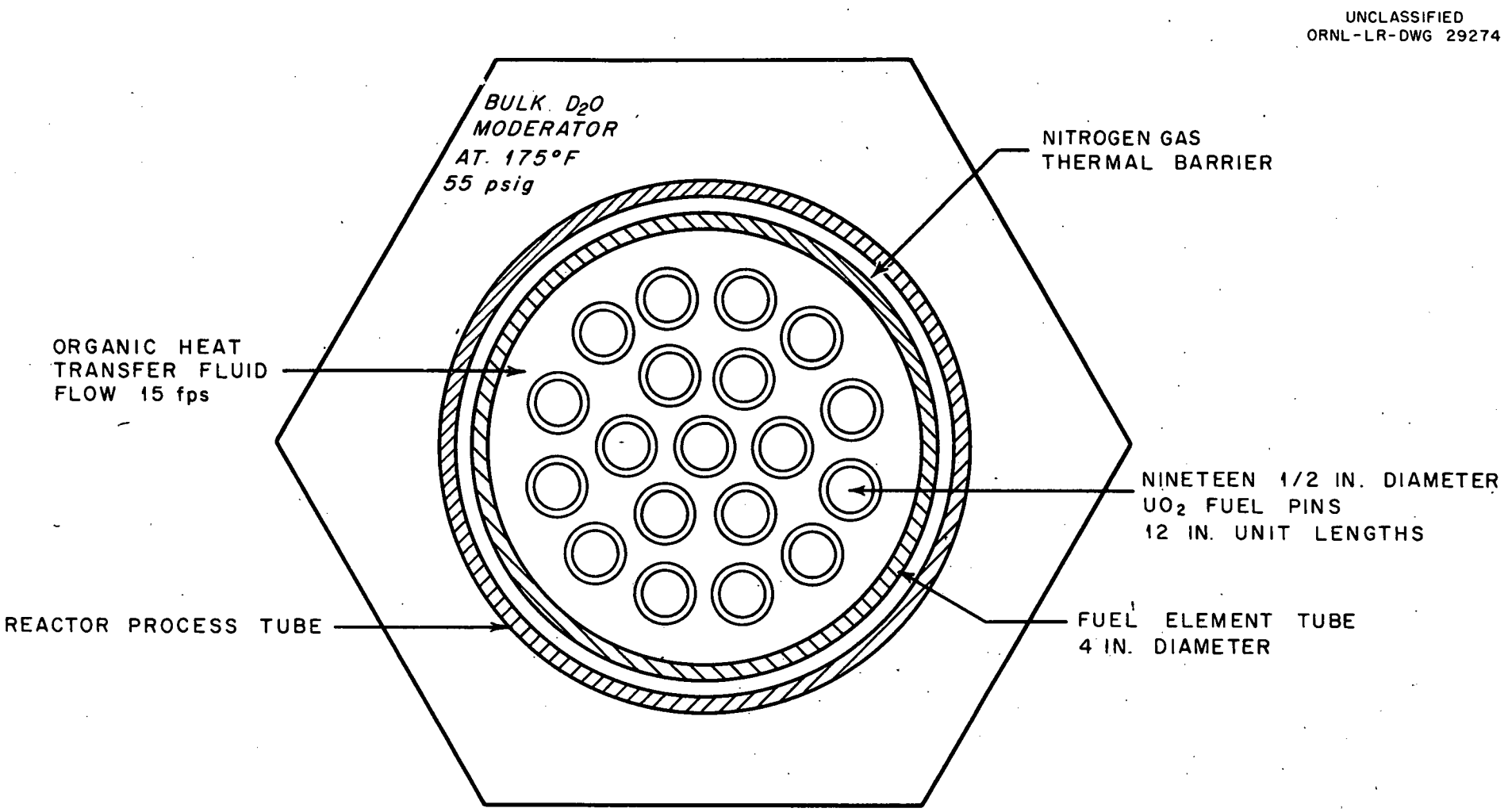

Fig. 8. Fuel Tube Flow Channel and Unit Cell Schematic

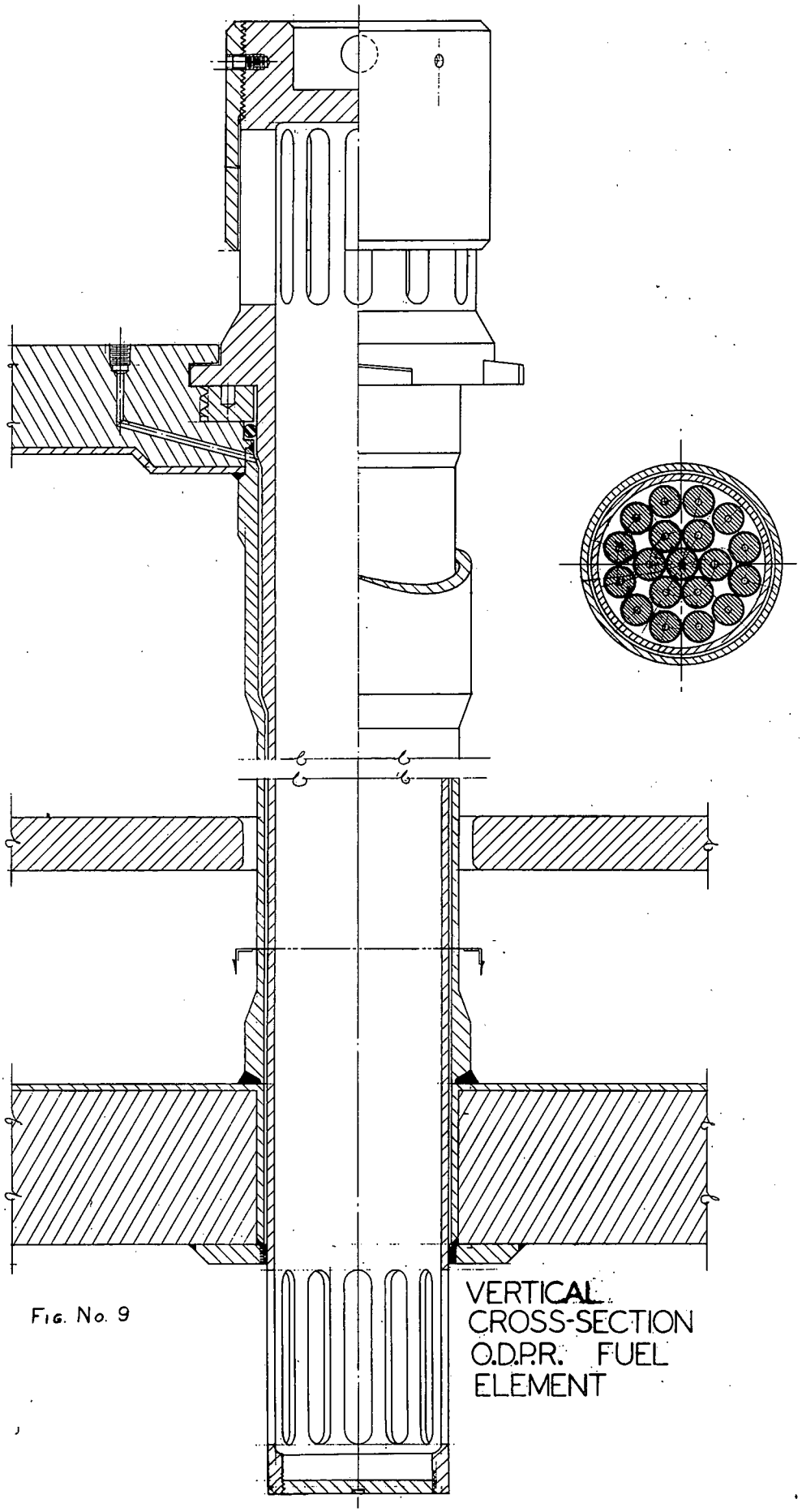

FIG. No. 9

VERTICAL CROSS-SECTION O.D.P.R. FUEL ELEMENT

transfer area was considered briefly. A careful examination of finned rods would certainly be justified in a more detailed study.

c. Characteristics - Fuel elements similar to the one selected for this study have been proposed for several reactors 1-2, 1-3, and work has been done on the determination of their hydraulic and heat transfer characteristics. One problem of interest is that of mixing of the coolant flowing in the various channels within the element. Since the neutron flux is depressed in the inner rods the heat generation rate here is less than in the outer ring of rods. However, the fluid in the inner channels is totally in contact with the fuel rods while the fluid in the outer channels is partially in contact with the fuel element tube. As a consequence the coolant in the inner channels tends to become hotter than the outer channel fluid as it passes through the reactor, unless mixing between the various channels occurs.

Experimental work on a seven rod cluster 1-3, 1-4 has shown that very high degrees of mixing may be obtained by wrapping some of the rods with spiral spacer wires. Therefore, it was assumed that there was no radial variation in coolant temperature within the rod cluster. Similiarly, no account was taken of the radial variations in the heat generation rate within the cluster, since physics calculations indicated that these variations were not large. The errors incurred by neglecting these two factors tend to cancel each other, since the heat generation rate is highest at the outer ring where the fluid would tend to be coolest, due to less than perfect mixing.

The use of spacer wires causes a large increase in the pressure drop through the element. Measurements made on a seven rod cluster 1-5 indicate that a friction factor approximately $2\frac{1}{2}$ times that of the Moody friction factor should be used in computing the pressure loss. The pressure drop of a fluid flowing axially along the outside of a closely packed array of small tubes, but without spacer wires, has also been determined 1-6 and found to agree closely with the pressure drop computed using the conventional Moody friction factor. Therefore, it appears that the increase in pressure drop is due entirely to the presence of the spacer wires. Since the 19 rod cluster has proportionally fewer spacers than the seven rod cluster, the friction factor used in this study was taken as twice the Moody friction factor at the Reynolds number of interest. Reference 1-6 indicates that measurements made on a 19 rod cluster do indicate a smaller friction factor than that for the seven rod cluster.

The large value of the friction factor found in this type of element should be reflected in an increase in the film coefficient for heat transfer, h. The Reynolds analogy between the transfer of heat and momentum states that, for a given system, the friction factor is directly proportional to the film coefficient. Experimental data on a similar system is available, and a correlation of this data was made to determine the magnitude of the increase in film coefficient. The film coefficient computed by the Sieder-Tate equation was then corrected by this factor.

d. Stress Analysis - The fuel elements in this reactor will be subject to a number of stresses. These stresses will be caused by the flow of the coolant, the difference in pressure between the lower and upper coolant plenums, thermal expansion, and the difference in pressure between the coolant on the outside and the gases on the inside of the cladding material. The last mentioned cause of stress is considered the most serious as far as limiting the usable lifetime of the fuel elements is concerned because of the build up of fission product gases with the burn up of the fuel. In order to analyze this problem a number of assumptions had to be made. These assumptions were:

(1) That the total porosity in the UO_2 disks (8% of the volume) is available as free volume to contain the liberated gases.

(2) That all of the free volume within the element (including the hole in the center of the disks, the porosity in the UO_2, and the gap between the cladding and the fuel) is interconnected so that isolated pockets of gas cannot form.

(3) That all of the stable gases produced by fission are not released from UO_2, but only a fraction of the total is free to cause pressure. For the purpose of this analysis, gas releases of 20%, 10% , and 1% were considered.

On the basis of these assumptions the hoop stress acting on the interior surface of the fuel element cladding of the hottest fuel element was calculated as a function of the time of reactor operation at full power, (See Appendix C) The results of this calculation are plotted in Fig. 10. It will be noted that for the first few thousand hours of reactor operation (for 20 & 10% gas release) the stress is negative. This is because the external hoop stress caused by the coolant pressure exceeds the internal stress due to gases. There are no stresses attributable to differential expansion of the aluminum cladding and

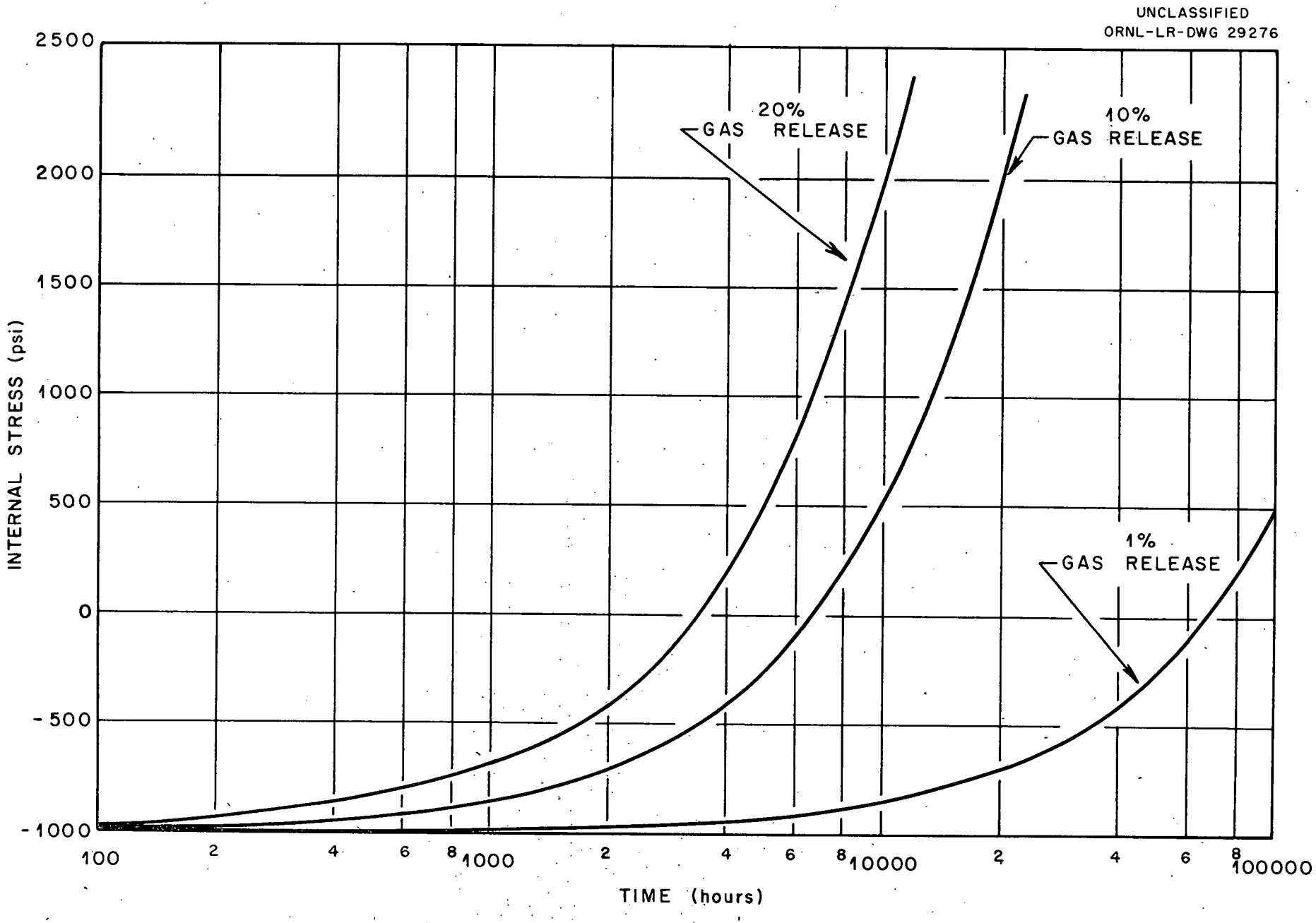

Fig. 10. Internal Stress Build Up From Stable Fission Product Gases as a Function of Time.

UO_2 fuel because there is a gap between the two at all times of reactor operation. As the operating time increases the internal stress due to gas build up increases. It becomes equal to the external stress and then continues to increase linearly with time.

The data contained in Fig. 10 are independent of the type of cladding used. In order to determine how this stress effects the aluminum alloy (X-2219) used for the cladding, it is necessary to relate the creep, time, and stress for this alloy. In the Materials Selection section, See Fig. 36 the log of creep rate is plotted against the log of stress at 600°F for this material. Also two extrapolations of the 600°F data to 750°F are shown. In Appendix F the functional relationships obtained from these straight line plots are given. These relationships are in the form:

$$\epsilon = k_1 t \left(\frac{\sigma}{k_2}\right)^n$$

where ϵ is strain in % elongation, t is time in 1000 hours, σ is stress in psi, and k_1, k_2, and n are constants. From the calculation of stress due to fission product gases as a function of time the following linear relationship was found (See Appendix C):

$$\sigma = k_3 t - k_4$$

where σ is stress in psi, t is time in 1000 hours and k_3 & k_4 are constants. Substituting this relationship into the one above gives:

$$\epsilon = k_1 t \left(\frac{k_3 t - k_4}{k_2}\right)^n$$

which is a functional relationship between the strain in the cladding and the time of reactor operation. This relationship is plotted in Fig. 11 (starting from the point where $\epsilon = 0$, i.e., where internal stress equals external stress) for the three different fractions of fission product gas release, and under the following temperature conditions:

(1) 600°F
(2) 750°F ("½" extrapolation)*
(3) 750°F ("¼" extrapolation)*

*For an explanation of these extrapolations see the Section on Material Selection, Fuel and Fuel Element Cladding.

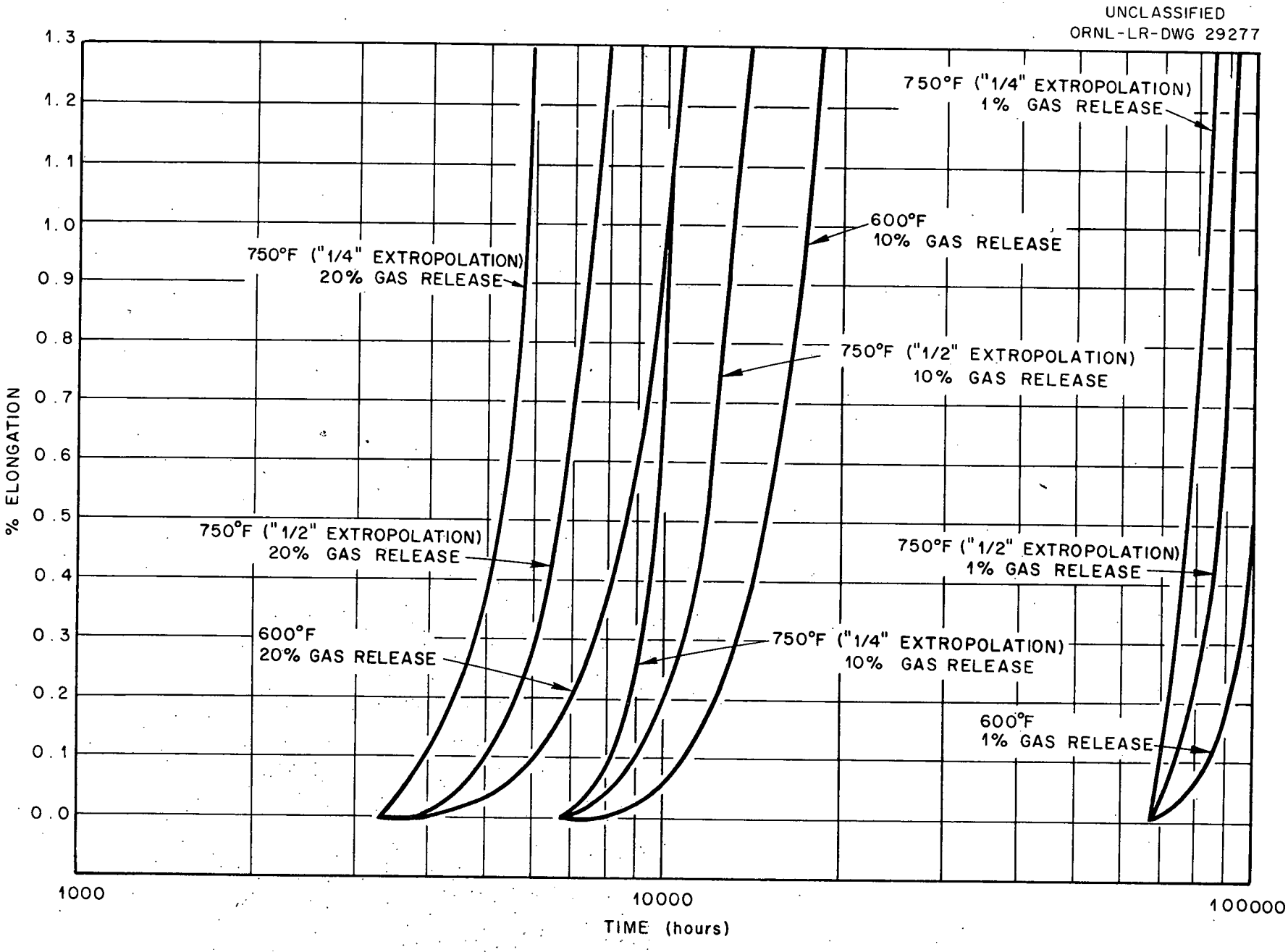

Fig. 11. Strain Build Up from Stable Fission Product Gases for Aluminum Alloy X-2219 as a Function of Time

If an allowable strain is selected, Fig. 11 gives the time that the reactor can operate before this strain is imposed upon the cladding. Since for aluminum alloy X-2219 the stress required to produce rupture in any given time is not too much larger than that required to produce 1% elongation, this latter figure will be used as the allowable strain. With this criterion the allowable fuel element life times for the various conditions of temperature and fission gas release were determined from Fig. 11. This information is summarized in Table 2.

TABLE 2

TIME AND BURN UP TO PRODUCE 1% ELONGATION
IN ALUMINUM ALLOY X-2219

Temp.(^{o}F)	% Fission Gas Release	Time (hours)	MWD/T
600	20	10200	3240
600	10	17300	5500
600	1	>100000	>30000
750 ("$\frac{1}{2}$" Extrapolation)	20	7500	2380
750 ("$\frac{1}{2}$" Extrapolation)	10	13200	4200
750 ("$\frac{1}{2}$" Extrapolation)	1	910000	29000
750 ("$\frac{1}{4}$" Extrapolation)	20	5750	1830
750 ("$\frac{1}{4}$" Extrapolation)	10	10200	3240
750 ("$\frac{1}{4}$" Extrapolation)	1	820000	26000

For the reactor under consideration 3000 megawatt days per ton of uranium is an acceptable fuel burn up. Table 2 shows that if the fuel cladding does not exceed 600^{o}F, fission gas release of 20% would not cause sufficient strain to limit the useful life of the fuel elements to below an acceptable figure. For a fuel element cladding temperature of 750^{o}F, (the design temperature for the reactor) and using the "$\frac{1}{2}$" extrapolation of creep data, a 20% gas release would limit the lifetime to an unacceptably low value. A 10% gas release under these conditions however, permits an acceptably long life. If the "$\frac{1}{4}$" extrapolation is used a 10% gas release is just about the maximum that can be tolerated and still allow the reactor to operate for the desired length of time.

Two questions now might be legitimately asked: (1) How good are the assumptions that were used in making this analysis? and (2) What is known about the actual fraction of fission gas release from UO_2? In answer to the

second question it must be admitted that not enough is known at this time to say definitely what the exact fraction of fission gas escape is. The problem is being studied extensively in connection with the Pressurized Water Reactor blanket fuel elements. Reports of many "in pile" experiments involving use of UO_2 disks in Zircaloy cladding are found in the recent progress reports on this project.[1-7] The percentages of fission gas release reported from these experiments range from 36% down to .05%. In almost every case, however, where the percentage of gas release exceeded a few percent, the temperature at the center of the element was high enough to melt the UO_2. For example, the UO_2 in the center of a sample element similar to the one giving the low value of .05% gas release was allowed to melt and the value obtained was 23%. Atomic Energy of Canada has been performing experiments with similar elements at Chalk River[1-8], and they report a 20% gas release for elements with molten centers. Since the elements proposed for this reactor are designed to prevent melting of the UO_2 fuel, it is not unreasonable to expect that the gas release would be less than 10%.

What then of the assumption made in this analysis? With regard to the open porosity of UO_2, the question of how it is effected by the density is presently under study by Lustman and others at the Bettis Plant of Westinghouse Electric Corporation.[1-9] There is some descrepancy in the experimental results, but it is generally found that not all of the porosity is open. Thus, the assumption that the total porosity (8%) in the UO_2 proposed for this fuel element (92% of theoretical density) is open, probably overestimates the free volume available for fission gas occupancy. However, since the mechanism of gas release from UO_2 is believed to be one of diffusion[1-9], and the amount of diffusion is dependent on the amount of free surface area, it seems likely that a decrease in open porosity would bring about a corresponding decrease in gas release. Thus the overestimation of free volume should be compensated by a decrease in gas atoms reaching this volume.

The assumption concerning the interconnection between all free volume pockets seems quite justified if only the open porosity in the UO_2 is considered. The assumption concerning the amount of fission product gas released has already been discussed. The assumed decrease in creep strength from 600°F to 750°F is discussed under the section on Material Selection. Suffice it to say here that the "$\frac{1}{4}$" extrapolation seems conservative.

In conclusion it can be said that this analysis has shown that the fuel element designed for this reactor could give satisfactory service. Whereas many assumed quantities have been used in this analysis, most of the areas of doubt are being investigated today and a much better analysis should be possible in the near future. In the last analysis, however, any fuel element must be accepted or rejected in actual experimental tests. It is felt that on the basis of the evidence available and presented here this element deserves such tests.

The Core

Introduction - The reactor core is similar in design to that of various other heavy water moderated reactors such as the Canadian Chalk River units, the chief variation being in the use of an organic as the primary coolant. Since reactors of this type have been built and operated successfully for a number of years there is little reason to doubt the feasibility of the basic design proposed in this study.

General Arrangement - The reactor core consists of a right circular cylinder, 16' - 11" in diameter and 16' - 0" long, as shown in Figs. 13 and 14. The core is surrounded both axially and radially by a 6" D_2O reflector. The 745 process tubes containing the fuel elements are arranged within the D_2O moderator on a 7" hexagonal pitch, as determined by Reactor analysis calculations. The 130 control rods are spaced approximately 15" apart within the process tube lattice. Details of the control system are given elsewhere in the report.

Primary Coolant - The organic coolant enters the reactor core by means of a bottom plenum chamber, formed by the pressure vessel and the lower tube sheet, flows upward through the fuel elements and then into the upper plenum chamber. At full load the coolant will enter the core at 517°F and leave at 625°F removing 720 MW of heat. The pressure drop of the coolant across the core is 190 psi, with an inlet pressure of 250 psig. Each fuel element is orificed so that the temperature rise and overall pressure drop through each element is the same.

Moderator and Reflector - The temperature of the heavy water moderator will be maintained below 200 F in order to reduce the pressure in the core and to increase reactivity. The D_2O will be circulated upward through the core at a very low velocity in order to remove the 80 MW of heat generated within it by fast neutrons and gamma rays. Because of the large gas space separating the D_2O from the fuel element the heat given up to the moderator by conduction is negligible.

The D_2O enters the core through a bottom plenum chamber formed by the lower tube sheet and an orifice plate, and is removed by a collector ring assembly located below the upper primary coolant plenum. The D_2O is also used to cool the reactor vessel by means of baffles which direct the fluid along the inner face of the vessel. In addition, heat generated in the control rods will be removed by the moderator.

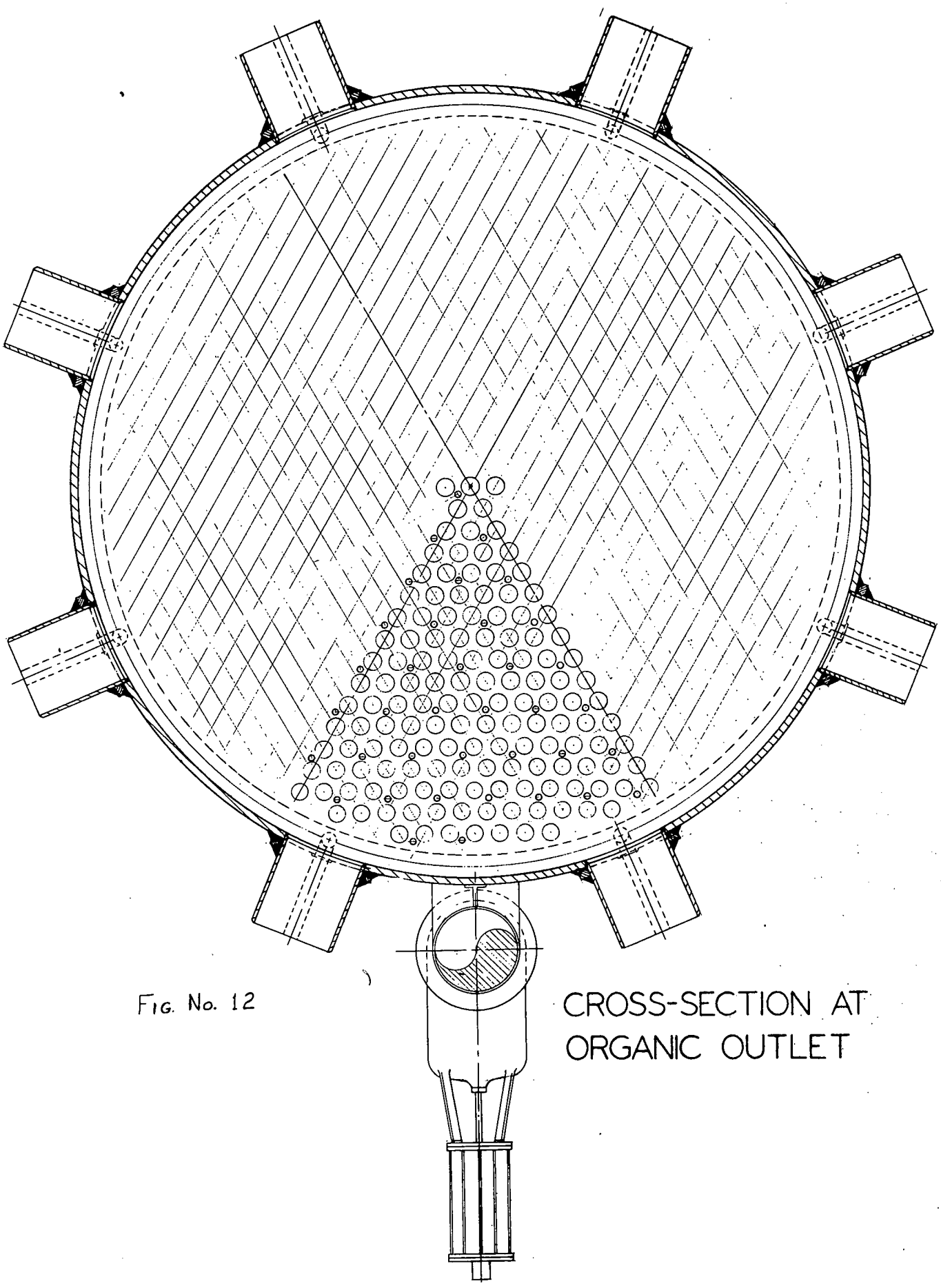

FIG. No. 12

CROSS-SECTION AT ORGANIC OUTLET

UNCLASSIFIED
ORNL-LR-DWG. 23380

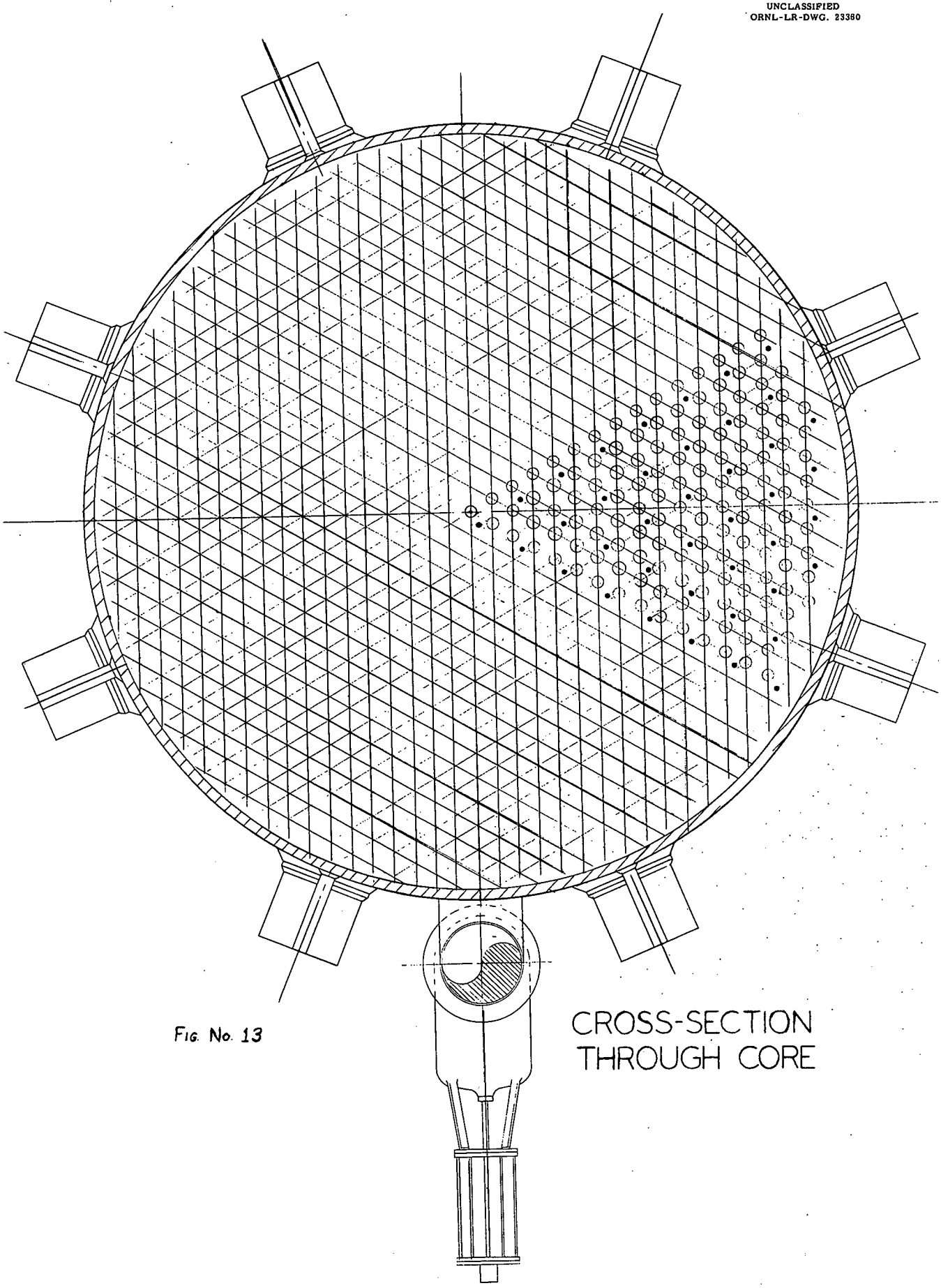

FIG. No. 13

CROSS-SECTION
THROUGH CORE

UNCLASSIFIED
ORNL-LR-DWG. 23259

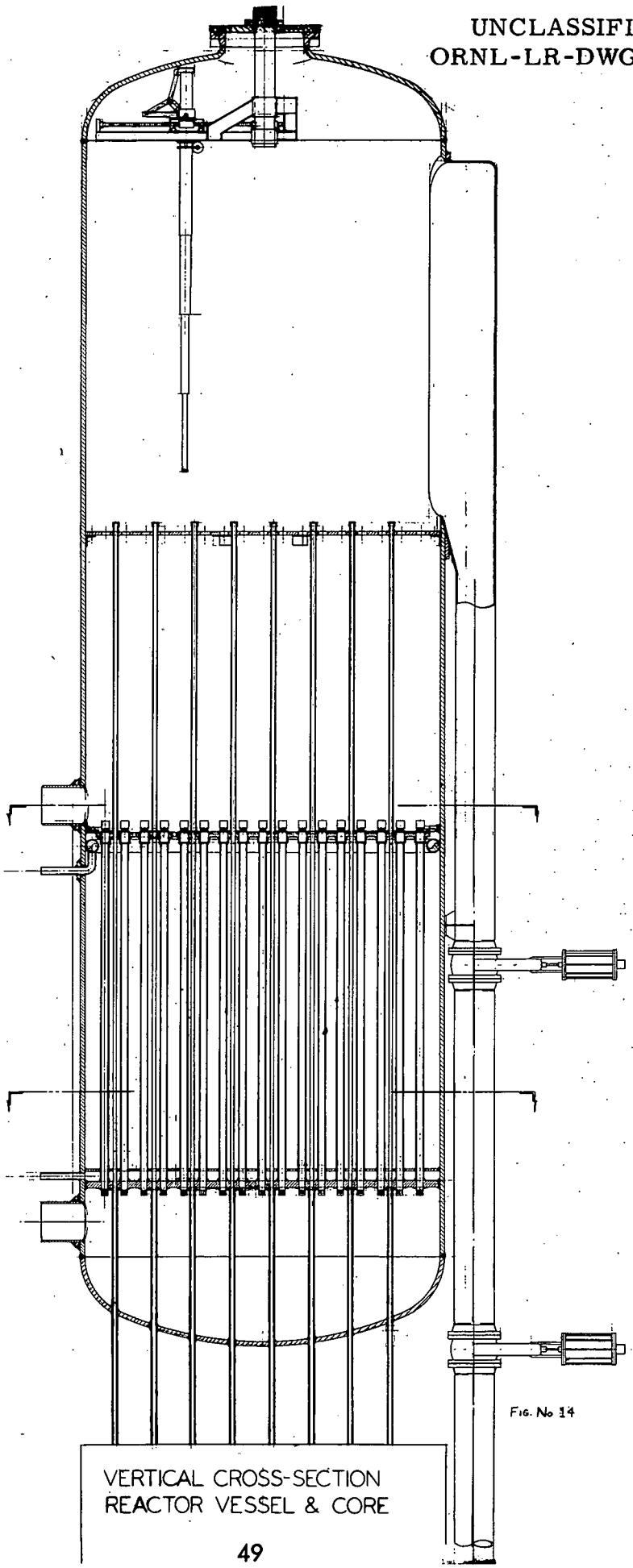

Fig. No 14

VERTICAL CROSS-SECTION
REACTOR VESSEL & CORE

Gas System - During operation the large void space above the upper plenum will be filled with Nitrogen gas. Although the saturation pressure of the organic in the upper plenum is only 9 psig, a 60 psig over pressure is necessary in order to maintain a pressure above atmospheric at all points in the system. The D_2O moderator will be pressurized to 100 psig as a precaution against possible boiling due to local variations in heat generation and removal.

Nitrogen gas will also be introduced into the 1/8" gap between the process tube and the fuel element. The pressure in this space will be balanced against the pressure of the organic in the bottom plenum, eliminating the need for a positive seal between the fuel element and lower tube sheet.

Mechanical and Structural Arrangement of Core - The loads on the core originate from three sources:

1. Hydraulic drag forces on fuel elements
2. Hydraulic pressures on tubes, plenums and tube sheets
3. Thermal stresses from temperature gradients.

Figures 12, 13, and 14 indicate the mechanical configuration of the core. The lower tube sheet is welded to the reactor vessel. The process tube which is the primary strength member for equilibrating drag forces and hydraulic pressure is welded to the top and bottom tube sheets with a strength weld. The maximum stress in this tube is 2600 psi and since the estimated allowable stress at 200°F is 10,000 for 61S aluminum alloy there is ample margin of safety. Since the tubes are approximately 16' long and 3.5" in diameter, instability was considered. Operating loads, however, stress this tube in tension and only the loss of D_2O pressure would result in compressive forces. Midway in the core is a lattice arrangement which affords pin-ended support to column mid-length to reduce the $(\frac{\ell}{\rho})$ ratio. The tube may then be considered fixed-pinned for instability purposes and the critical stress is increased greatly. To prevent thermal stress resulting from differential thermal expansion of the core and pressure vessel, the top tube sheet is not welded to the vessel wall but is arranged to float vertically with lateral constraint. The leakage of D_2O to organic is prevented by a membrane type seal.

Pressure Vessel

The pressure vessel was designed using the criteria established by the ASME Boiler Code using an allowable stress of 17,000 psi for SA-212B. This

criteria is based on membrane stress and is conservative enough to allow an additional increment of stress for thermal effects. This extension of the code is allowable because of the similarity of thermal stress with bending stress, thus allowing an additional 1.5 on the allowable membrane stress.

Calculations were completed for internal heat generation in the vessel wall. The vessel wall is only 1-1/2" thick therefore, although the specific energy deposition is high, the heat flux to be removed on the inner surface is relatively low and the temperature gradient not severe. The pressure vessel thus acts as an effective thermal shield for the concrete biological shielding.

Calculations were not done for thermal stress in the concrete shielding. Gradients could be reduced by cooling the shield with circulating water which would also act as an effective fast neutron barrier.

Biological Shielding

The National Committee For Radiation Protection has established limits for maximum permissible exposure to radiation which are published in the National Bureau of Standards Handbook [1-1].

These limits are based on a conservatively established radiation dose rate that is known to produce no measurable physical effect on humans when received continuously over a lifetime of exposure. This established or standard dose rate if 0.3 rem/wh.

For shield optimization it is necessary to consider the following operational and maintenance characteristics of the reactor plant:

(1) Some regions will not require continuous access.

(2) The average power level of the reactor over a time interval may be lower than the rated power.

Careful consideration of these two factors and possibly averaging dose rate over a quarterly operating period will result in shield optimization.

Since this report is essentially a feasibility study, these important aspects of shielding design were not fully considered and the dose rate of 0.3 rem/wk or 7.5 mr/hr was established for maximum permissible exposure at rated power.

The value of 0.3 rem/wk is the cumulative dose of both neutrons and gammas. Since the RBE for neutrons is 10 compared to 1 for gammas the greater attenuation of neutrons by the biological shield will result in a more effective reduction of dose than a similar attenuation of gammas.

The maximum permissible radiation fluxes were established as follows:

$$MPE = \frac{4000}{E} \quad \frac{\text{photons}}{\text{cm}^2 - \text{sec}}$$

$$MPE = \frac{3.6 \times 10^{-22}}{\sigma E} \quad \frac{\text{fast neutrons}}{\text{cm}^2 - \text{sec}}$$

The maximum neutron flux can be conservatively estimated at 30 $\frac{\text{neutrons}}{\text{cm}^2\text{-sec}}$ for fast neutrons, and arbitrarily assuming 10 $\frac{\text{neutrons}}{\text{cm}^2\text{-sec}}$ as the allowable flux, the preliminary design tolerance levels were established as follows:

Radiation	Flux	Dose
Neutrons	10 $\frac{\text{neutrons}}{\text{cm}^2\text{-sec}}$	2.5 mr/hr
Gammas	$\frac{3340}{2}$	5.0 mr/hr

The calculations in appendix show that a more effective shielding arrangement is possible by using a barytes concrete 8 ft thick which is more effective in attenuating gammas and allowing the fast neutron dose rate to go up to 3.2 mr/hr. No calculations have been done for thermal neutrons since the MPE for slow neutrons is much greater than for fast neutrons, also, the only source of thermal neutrons in the concrete biological shield is that associated with the slowing down of fast neutrons.

The calculations indicate that Barytes concrete is so effective in attenuating gammas that fast neutrons are the most important dose source. If a hydrogeneous material was placed at or near the exterior of the reactor vessel, a more effective and less bulky shield would be possible.

The following tabulation indicates the dose rate expected from the non-negligible sources.

TABLE 3

Type Radiation	Dose Rate MR/HR
Fast neutrons from core	3.200
Capture γ's from fast neutrons slowed down in concrete	.410
Capture γ's from thermal neutron capture in reactor vessel	.008
	$\Sigma =$ 3.618

Control and Instrumentation

Reactor Protection System - The protection of this reactor following plant incidents which are normally termed accidents does not appear to present any problems not normally encountered with power reactors. The accidents that must be protected against include:

(a) Startup accident-short periods due to excess reactivity insertions when reactor is below power range.

(b) Loss of coolant flow - decreased coolant flow due to loss of one or more coolant pumps.

(c) Excessive nuclear level - reactor power beyond safe level.

(d) Excessive reactor temperatures - temperatures that endanger the integrity of the core.

(e) Cold coolant or cold moderator accident - reactor transients following sudden injection of cold coolant or cold moderator.

The power level that the reactor reaches during a start-up accident is an inverse function of the magnitude of the temperature coefficient if no protective or control action such as control rod insertion is initiated. Since the temperature coefficient of this reactor is small and perhaps positive, extra precautionary measures must be included to compensate for this weakness. These measures should include: (1) Limiting rod-withdrawal rates such that many seconds will be required to add .1 % reactivity, (2) a period cutback protection system that automatically increases the reactor period by inserting control rods when the period becomes shorter than some arbitrary limit, probably about 30 seconds, and (3) a period scram that will shut down the reactor when the period is shorter than some safe value, probably about 20 seconds.

Loss of coolant flow and excessive nuclear level accidents could be protected against simultaneously since they are related. The protection system could include a power-flow comparator which operates a non-lock-in cutback at one power-flow ratio and a scram at another ratio. The cutback and scram levels would be some values above the design level, which would require an analytical study to determine. The nuclear level would be determined by the ionization chambers which measure reactor power, while loss of flow could probably be determined quickest by monitoring the power to the coolant pumps.

Excessive reactor temperatures could be prevented in the same manner as the other accidents, by first a cutback and then a scram if the cutback does

alleviate the condition. The protective action should be initiated by either the reactor coolant outlet temperature as measured in the loops or by the coolant temperatures as measured by the thermocouples in the core.

Cold coolant or cold moderator accidents are a function of the magnitude of the negative temperature coefficient of the fluid that suddenly changes temperature. The magnitude of the coolant temperature coefficient is such that any transient due to the startup of a colder loop could probably be limited by a power-flow scram if a temperature interlock is included to prevent the starting of a pump unless the temperature of that loop is near the reactor temperature.

The moderator temperature coefficient is such that the reactivity insertion due to a sudden temperature change is about the same as that produced by the same change in coolant temperature. Since there are four moderator loops, temperature interlocking would have to be used to prevent adding a cold moderator loop to hot loops already operating. Loss of all moderator flow should initiate a scram. It is not expected that loss of moderator pressure should cause reactor shut down unless the flow is low.

In addition to the automatic protection system, the usual features of manual or operator-initiated scram and an alarm system would be included.

Reactor Control System Under Normal Operation - An automatic control system is desirable for a nuclear power plant of this size. In general, central station power plants employ automatic systems to regulate steam pressure by controlling the rate of fuel input. To comply with this practice, an automatic system for controlling reactor power and temperature is proposed.

A reactor with negative temperature coefficient is capable of self-adjusting its power generation to meet the steam plant demands in a closed loop system such as this. However, with a temperature coefficient as small as $-1.6 \times 10^{-5}/^{\circ}C$, the transient response of the plant would be poor, i.e., the reactor would be sluggish in responding to load fluctuations. Wide reactor temperature variations may also occur following load changes, which might result in damage to the reactor.

Automatic control of a reactor is also desirable because of the reactivity transients due to xenon buildup and decay that follow load changes. If the control rods were not moved to compensate for the poison variations, the temperature of the reactor would change.

Thus, it seems justifiable for both the reactor power and the coolant temperatures to be controlled automatically by moving the control rods.

In general, a control system that generates a control signal of the following form should be adequate:

$$\varepsilon = \frac{n - n_o}{n_o} + T_c - T_{ref.}$$

where:

ε = error or reactivity demand signal

n = reactor power level as measured by ion chambers

n_o = power demand signal determined from steam flow or generator output

T_c = reactor inlet temperature as measured by resistance thermometer

T_{ref} = reference point for controlling reactor inlet temperature.

The $n - n_o$ signal is divided by n_o since the gain of a control loop of which the reactor is a part is proportional to the power level of the reactor[1-10] Dividing by n_o gives this control loop constant gain. It was decided to control cold leg temperature instead of average temperature or steam pressure because: (1) if the average temperature were controlled at 600°F, the steam pressure would vary from 400 psi at full load to approximately 1550 psi at no load, and (2) if the steam pressure were controlled at 400 psi, the average temperature of the coolant would vary from 600°F at full load to approximately 440°F at no load. The variation of steam pressure in the first case seems unreasonable since the steam plant would then be designed for 1550 psi and operate at 400 psi. The variation in coolant temperature in the second case may result in a large expansion of the coolant requiring a large expansion tank. However, the expansion may be tolerable and the steam pressure could be substituted in the error signal equation for cold leg temperature.

The error signal generated would be used to actuate rods-in or rods-out relays, which would then move a group of rods until the error is corrected. This control system would operate in conjunction with the rod programmer as discussed later in this section.

Time did not permit a detailed stability study of the plant and proposed control system. Such a study would reveal what design features were required to insure stable operation and control.

Reactor Instrumentation - Reactor instrumentation is required to provide an adequate amount of information to the control system, to the protection system, and to the operator. This information is presented in the main control room. A main control console and a main instrument panel are provided along with auxiliary control panels.

Instruments required include those which measure the reactor power from complete shutdown to the maximum level that causes shutdown. At least two types of neutron detectors will be provided to cover this range which usually extends some ten to twelve decades in power reactors. The detectors will probably be compensated ionization chambers and BF^3 counters. At least two and probably three of each are necessary to supply accurate and reliable information. These detectors provide signals for period meters, log-level meters below the power range, and linear-level meters in the power range. Period and level signals are sent to the protection system while level signals are sent to the reactor control system.

A number of thermocouples are provided to measure the outlet coolant temperature of a number of fuel cells. The thermocouples will be located to give a radial temperature distribution that might be used in flattening the radial neutron flux. A vertical row of thermocouples is also provided to determine a vertical temperature variation.

A system is also provided to locate any ruptured or failed fuel element. The system proposed entails continuous sampling of the bulk coolant to determine when a failure occurs somewhere in the core. The next step is to take a sample from each coolant channel, using the fuel changing indexing equipment. The defective element is then removed.

The position of each of the control rods will also be determined and indicated. The method of detection of rod position could involve either hydraulic or electrical position measuring equipment.

In addition to the direct reactor instrumentation, a basic list of variables which should be monitored is as follows:

(1) Bulk coolant temperature at outlet of reactor for each loop
(2) Bulk coolant temperature at inlet of reactor for each loop
(3) Coolant flow each loop
(4) Coolant pump head
(5) Reactor pressure drop
(6) Heat exchanger pressure drop

(7) Moderator outlet temperature for each loop
(8) Moderator inlet temperature for each loop
(9) Moderator pressure
(10) Moderator flow for each loop
(11) Moderator plenum liquid level
(12) Organic plenum liquid level
(13) Steam pressure for each loop
(14) Steam flow for each loop
(15) Feedwater flow for each loop
(16) Evaporator liquid level
(17) Total Steam flow
(18) Condenser pressure
(19) Feed-pump head
(20) Hotwell temperature

Numerous other instruments and monitors are necessary for plant operation which are not listed. These would include such measurements as pump bearing temperatures, cooling water temperatures, various radiation levels, electrical quantities such as voltages and currents, and the various measurements associated with the sampling and auxiliary systems.

An annunciator system in line with conventional power plant practice is provided to warn operators of abnormal situations.

Temperature Coefficients of Reactivity - It is usually advantageous for the temperature coefficient of reactivity of a reactor to be negative. A coefficient of this type is very helpful in regulating the reactor and may be regarded as an inherent control system. The requirements of a reactor control system are thereby reduced and the safety of the reactor is enhanced.

This reactor may be considered to have three separate temperature coefficients: (1) a metal coefficient, (2) a moderator coefficient, and (3) a coolant coefficient. Since the coolant and metal are normally at or near the same temperature, their coefficients may be lumped. It is therefore desirable to know the magnitude and sign of two temperature coefficients of reactivity.

The coolant and moderator are insulated from each other, and it is necessary that each exhibit a negative reactivity effect with increasing temperature. The reactor could be inherently unstable if either coefficient were positive.

(a) Coolant Temperature Coefficient - The temperature coefficient of the coolant was calculated and found to be negative but small in magnitude. The equations and calculations are contained in Appendix D.

The net coolant coefficient is determined by the summation of five components:

(1) $\frac{1}{\epsilon} \frac{\partial \epsilon}{\partial T_c}$	0
(2) $\frac{1}{\eta} \frac{\partial \eta}{\partial T_c}$	$.1 \times 10^{-5/^0C}$
(3) $\frac{1}{p} \frac{\partial p}{\partial T_c}$	$-3.65 \times 10^{-5/^0C}$
(4) $\frac{1}{f} \frac{\partial f}{\partial T_c}$	$3.6 \times 10^{-5/^0C}$
(5) $-B_g^2 \frac{\partial M^2}{\partial T_c}$	$-1.65 \times 10^{-5/^0C}$
Net coefficient	$-1.65 \times 10^{-5/^0C}$

The magnitude of the net coefficient is not as large as may be desired. It can be seen that the two large components approximately cancel each other. The large positive term $\frac{1}{f} \frac{\partial f}{\partial T_c}$ could be reduced by decreasing the amount of coolant per channel since the coolant is a poison. A decrease in lattice spacing would increase the magnitudes of the $\frac{1}{\eta} \frac{\partial \eta}{\partial T_c}$ and $B_g^2 \frac{\partial M^2}{\partial T_c}$ terms because of an increase in neutron temperature. A decrease in lattice spacing would also increase the magnitude of the $\frac{1}{p} \frac{\partial p}{\partial T_c}$ term. The net effect of a decreased lattice spacing would probably be an increase in the magnitude since the negative terms affected are larger. Thus there are two design variations which would probably lead to an increased negative coolant temperature coefficient:

(1) decreased coolant/ fuel cell

(2) decreased lattice spacing

The coolant temperature coefficient calculation was for a clean reactor at operating temperature with natural uranium as fuel. As U^{235} burns out and Pu^{239} builds up the magnitude of the coefficient may become smaller. This is a result of the increased resonance integral for Pu^{239} over U^{235} which leads to a decreased resonance absorption integral for U^{238}, since U^{238}, Pu^{239},

and U^{235} are all competing for the resonance energy neutrons. The net effect of the Pu^{239} increase is then a decrease in the magnitude of $\frac{1}{p}\frac{\partial p}{\partial T_c}$ and a decrease in the temperature coefficient such that it may even become positive.

(2) Moderator Temperature Coefficient - The calculation of the moderator temperature coefficient was made using the same equations as those for the coolant temperature coefficient (Appendix D)

The components of the coefficient were found to be:

(1) $\frac{1}{n}\frac{\partial n}{\partial T_m}$	$.3 \times 10^{-5/^oC}$
(2) $\frac{1}{\epsilon}\frac{\partial \epsilon}{T_m}$	0
(3) $\frac{1}{f}\frac{\partial f}{\partial T_n}$	$.45 \times 10^{-5/^oC}$
(4) $\frac{1}{p}\frac{\partial p}{\partial T_m}$	0
(5) $-B_g^2\frac{\partial M^2}{\partial T_m}$	$-2.35 \times 10^{-5/^oC}$
Net coefficient	$-1.6 \times 10^{-5/^oC}$

The magnitude of the net coefficient is approximately the same as that of the coolant. However, there is no reason for having a large negative moderator coefficient since it is not used to transport heat to the steam plant.

The calculation was again based on a hot, clean condition. The effect of the reflector was not included and would probably be small.

A decreased lattice spacing together with decreased overall dimensions would increase the net coefficient by increasing the leakage term $-B_g^2\frac{\partial M^2}{\partial T_m}$.

Control Rods - Excess reactivity is controlled by neutron absorbing rods inserted into the reactor from the bottom. The rods are housed in perforated aluminum tubes as described on page 46 and located in the moderator region.

The rods are spaced symmetrically in triangular array with a 15 inch pitch as shown in Fig. 13. It is assumed that all rods are similar and black. They will probably be constructed of steel containing about 2% boron.

The rods must be capable of maintaining the reactor subcritical when the reactor is clean and at its lowest temperature. The excess reactivity of the

reactor at operating temperature is approximately 9%. The gain in reactivity due to lowering the coolant temperature from 600°F to 0°F and the moderator temperature from 200°F to 0°F would not exceed 1%. It thus appears that at least 10% of controllable reactivity must be supplied by the control rods.

(1) Rod Effectiveness - The calculations of the effectivness of the rods are contained in the Appendix. The following is a list of the results of these calculations.

Group	δ k/local	δ k/rod	No. rods	δ k Group
I	.196	.004	1	.004
II	.196	.00378	6	.0227
III	.196	.00304	12	.0365
IV	.196	.00222	18	.0400
V	.196	.00118	24	.0283
VI	.196	.00046	30	.0138
VII	.196	.000085	40	.0034
			Total k	.1487

The total δ k of the rods is seen to be 14.8% by this calculation. However, this must be considered as an approximation since it is subject to limitations. It was assumed that the flux varied radially according to the Bessel function J_o, which applies to unreflected cores only. The radial flux variation is flatter for a reflected system which increases the worth of the outer rods and decreases the worth of the inner rods. The above list indicates that the outer group of rods is negligible in worth. However, the worth of this group would be increased in a reflected system.

It was decided to determine the total worth of the rods if the radial flux were flat instead of varying according to J_o. In this case the position factor is 1, and each rod is worth approximately .0011. The worth of 130 rods in this case would be 14.3%.

The effect of shadowing was not considered. However, it is felt that this effect will be small and that there is sufficient margin to insure complete reactor shutdown.

(2) Rod Programming - None of the rods has been designated as a shim or a safety rod. Since all rods would probably be positioned to flatten the

radial flux, it seems that no restriction should be applied.

A logical way of programming the rods is to move them in groups, i.e., each concentric ring of rods could be positioned in unison. A programming mechanism is then required to determine the sequence for moving the various groups. This programmer would be required to keep the groups in the same relative positions as they are moved through the core.

The drive mechanisms for the rods are located beneath the reactor vessel and push the rods out the top of the core. Either hydraulic or electrical drives could be used. All rod guides in the moderator and rod extensions are perforated aluminum tubes to minimize poison and permit moderator to fill as much of the rod guide as possible when the rods are out of the core.

The maximum reactivity of a group of rods is seen to be approximately 0.04. Since the core is sixteen feet high, the average worth of this group per foot is 0.0025. If a maximum to average worth of 2 is assumed, the maximum δ k/foot is 0.005. If the rods are then moved at a constant speed of 2 ft/minute, the maximum rate of reactivity insertion is approximately .0100/minute. This rate would prevent an operator from obtaining a prompt critical start-up condition for at least forty seconds after passing criticality in which time safety circuits could easily operate to protect the reactor.

It is also required that the rods speeds permit the operator or an automatic control system to follow xenon transients following reactor load changes. It is estimated that the xenon transients that could be encountered with this reactor plant should not exceed 10^{-5} δ k/sec or 60×10^{-5} δ k/min and do not introduce any control problem with the rod rates chosen.

The time required to pull all rods from the bottom of the core to the top of the core, or the maximum time to achieve criticality would be of the order of 55 minutes.

It is therefore concluded that a choice of 2 ft/min is adequate for all operating conditions.

Fuel Handling - This system consists of a storage canal, discharge tube, fuel racks, hydraulic lift, and a remote operated special indexing fuel handling crane within the reactor head, Fig. 4 and 14.

The principal requirements of the fuel handling system include:

a. The provision for removal and replacement of all of the components of the reactor core.

b. Provision for storage of fresh fuel elements and cooling space for used fuel elements.

c. Provision for transferral of fuel elements to and from railroad shipping cars

d. Provision for refueling during a weekend shutdown.

A general description of the system and facilities may best be accomplished by describing the replacement of fuel elements.

The reactor is shut down and the coolant is kept circulating at a reduced rate to remove the decay heat. In the storage canal six fresh fuel elements are loaded into one of the fuel racks, which have provisions for holding seven elements, and the fuel rack is moved onto the platform of the hydraulic lift at the end of the canal next to the reactor and immediately below the discharge tube. The lower gate valve of the discharge tube is opened and the water level in the canal and discharge tube is raised from the normal level, which is approximately twenty feet above the fuel elements in storage, up to the upper gate valve in the discharge tube. The hydraulic lift, including the fuel rack and elements, is raised until the lift platform seats against the bottom of the discharge tube. The upper gate valve is then opened.

In the reactor, the special crane is indexed to the proper element and the first lifting device is attached to the fuel elements extension which protudes above the spacing tube sheet near the top of the control rod "cans". Visual observation is accomplished by a television camera lowered through an access opening in the top of the reactor. The element is given a fraction of a turn to unlock it from the tube sheet and is lifted by this first lifting device until the top end of the fuel element itself, including the discharge ports, is above the top of the control rod cans. Another lifting device, provided with a gas blast tube, is attached to the element at its top head and gas is forced through the element for cooling. The extension is then detached and moved away by the first lift system for future installation on the new element.

The old fuel element is lifted until the bottom is clear of the control rod cans and is then transferred to the blank space in the fuel rack. The new element is then lifted from the rack and installation procedure is the reverse of the removal.

After the sixth fresh element has been removed from the rack the hydraulic lift is lowered and the fuel rack is removed into the storage canal and another rack is set on the lift platform in order to continue the replacement procedure if so desired.

When all replacements desired have been made, and the hydraulic lift is in the lowered position, the upper gate valve is closed and the water level in the storage canal and discharge tube is lowered to the normal level. The lower gate valve is then closed.

For shipment of spent fuel elements for reprocessing, the elements are loaded into a special shipping cask under water in the storage canal. The cask is closed and sealed and is transferred onto the shipping car by the crane. The cask is lifted up through an opening in the four foot concrete floor above the storage canal provided by removable sections of this concrete.

Primary System

The flow of the organic in this system is from the pumps to the bottom of the reactor, from the top of the reactor to the superheater, to the reboiler, and thence back to the pumps, see Fig. 16. A side stream of organic is taken off downstream from the reboiler to pass through the purification system and be returned along with the organic feed to the suction of the pumps.

The four cellular enclosures for the eight 11,600 gpm organic recirculating-feed pumps are arranged along the side of a pipeway which connects to the piping cell which surrounds the reactor. Each of the four reboiler-superheater units are separately shielded in compartments along the side of the reactor building next to the turbine-generator building so as to reduce the steam cycle piping in the reactor building to a minimum and prevent radioactive contamination of the secondary system. Organic purification and storage equipment are in cells in a quadrant of the reactor building adjacent to the railroad facility and close to the organic recirculating-feed pumps. The organic storage tank is heated by electrical coils placed inside the tank in several horizontal banks one above the other in order to maintain the organic as a liquid regardless of the depth of organic in the tank. Heating control equipment is located in a room adjacent to the storage tank. This tank also acts as an expansion reservoir for the primary system along with the space at the top of the reactor.

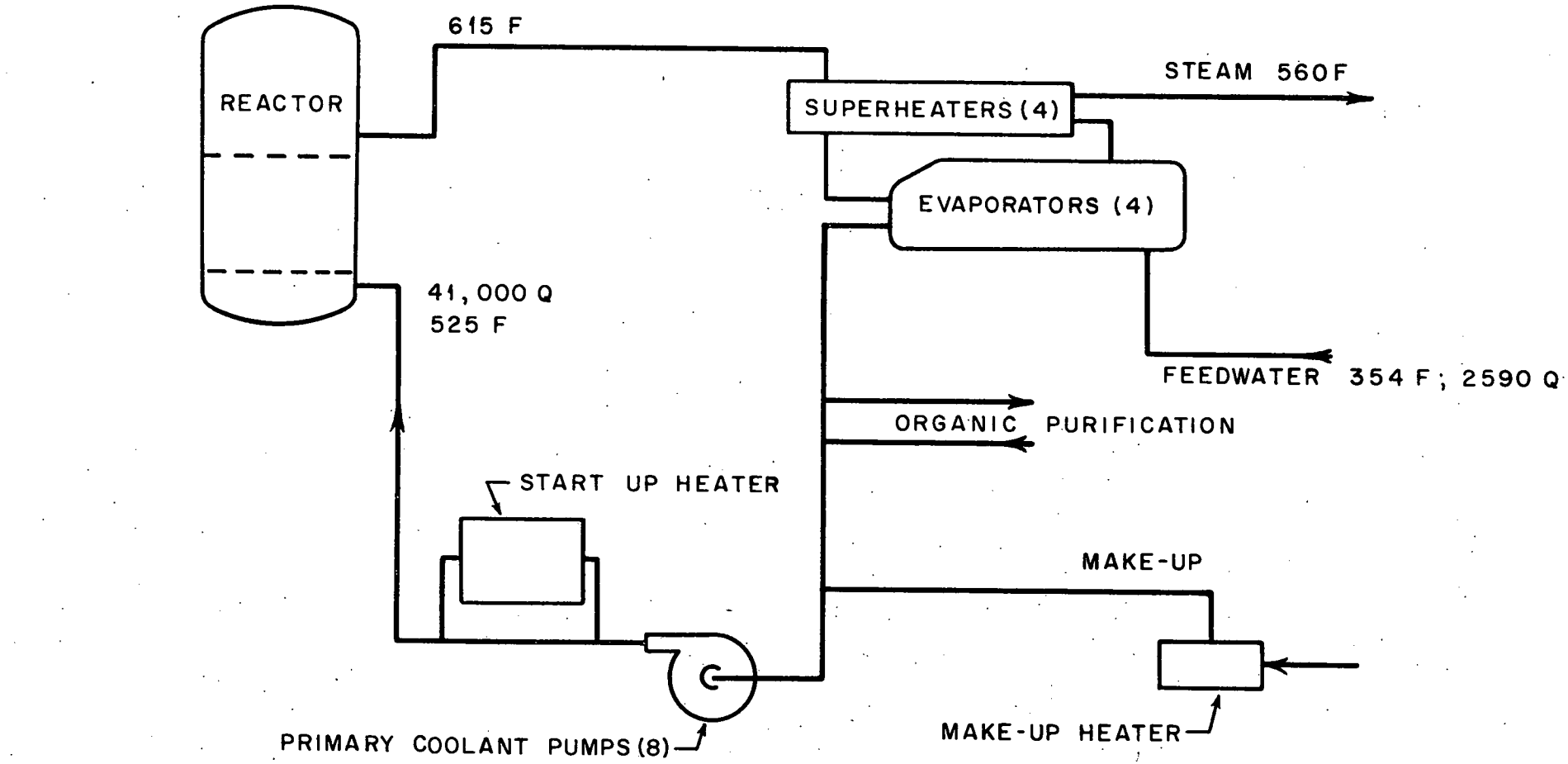

Q = FLOW, 1000's #/HOUR
F = TEMPERATURE, °F

Fig. 16. Primary Coolant Flow Diagram

The organic enters the reactor through eight 24-inch lines which feed into the lower chamber of the reactor vessel. The organic flows upward through the core section around the fuel slugs inside the aluminum fuel tube. The annular gas space around the outside of the fuel tube is open to the organic at the bottom tube sheet with leakage of gas into the organic being minimized by a labyrinth seal and balanced gas pressure. The organic flows out of the core region into the upper chamber of the reactor, with the level of the organic in this chamber being maintained at approximately seven feet above the top tube sheet. The organic leaves the reactor through eight 24-inch lines to go to the superheater.

The organic passes through the shell side of the four superheaters and exits through eight 24-inch lines which combine into four 30-inch lines for entrance to the four reboilers, Fig. 17. It passes through the tubes of the reboilers and leaves in four 30-inch lines which connect to the organic recirculating-feed pumps and to the organic storage-expansion tank.

The shell of the reboiler and superheater are made of boiler grade carbon-silicon steel to A.S.M.E. specification SA-212, grade A. The tubes of the reboiler and superheater are seamless carbon steel tubes, A.S.M.E. specification SA-83; 1/2-inch OD by .065 wall in the reboiler and 5/8-inch OD by .065 wall in the superheater. All organic piping is seamless carbon steel pipe, A.S.M.E. specification SA-106, grade A, Sch.80, and is induction heated by electrical coils wrapped around the pipe under the insulation.

The reboilers have an 8-foot internal diameter at the head end, a 13-foot 3-inch internal diameter at the opposite end, and are 19 feet long. The superheaters have a 3-foot 9-inch internal diameter and are 12 feet in length.

Secondary System

This system includes the turbine-generator and all of its associated equipment and piping. The make-up feed water for this system is supplied by the deep well pumps, which pump directly into the water treating equipment as well as into the four storage tanks near the main parking lot and into the emergency water storage tank in the upper region of the turbine-generator building. The water purification system handles a side stream of water from the main loop of the secondary system as well as the make up water. The

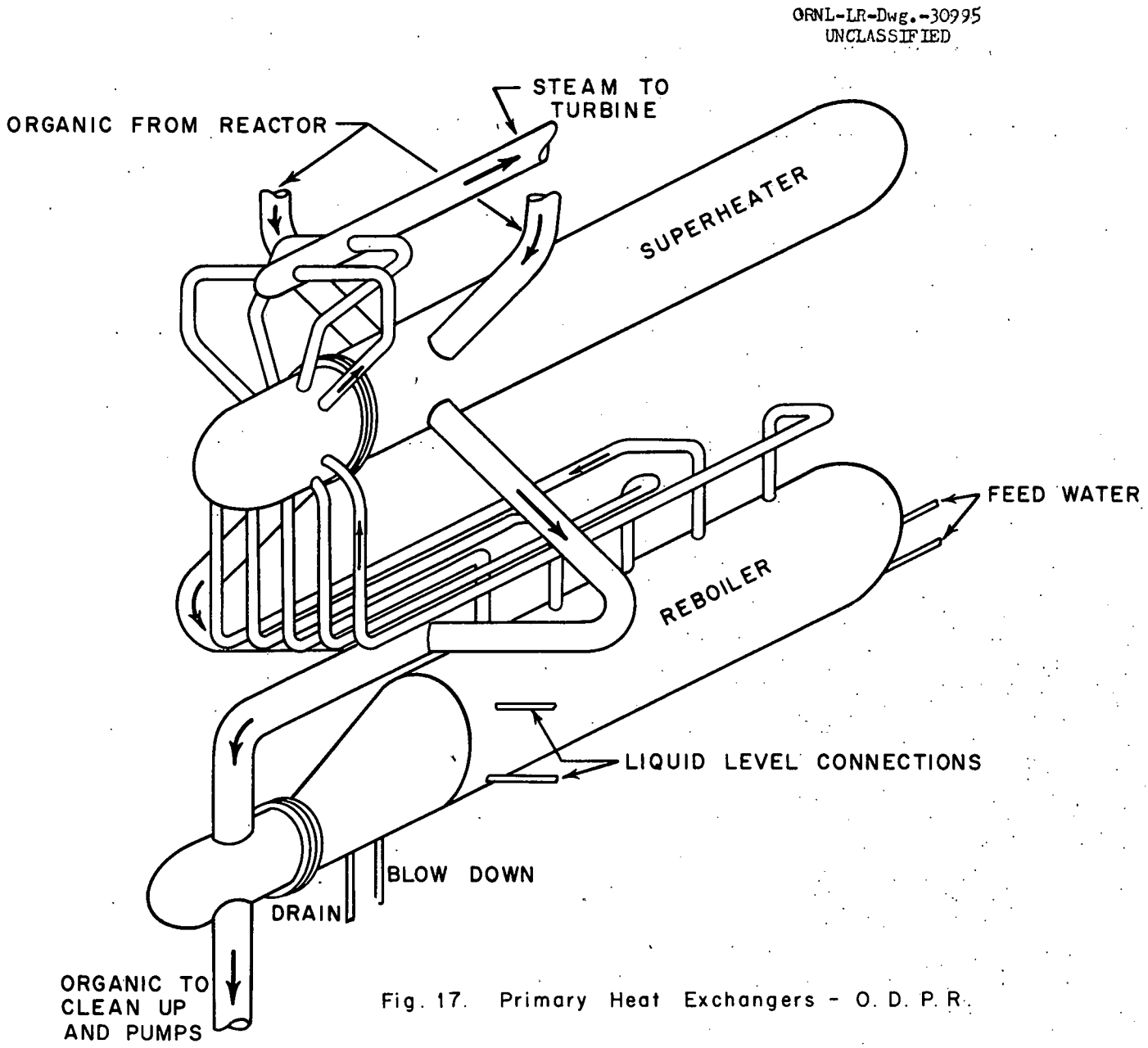

Fig. 17. Primary Heat Exchangers - O. D. P. R.

water from the treating plant is passed into the surge tank of the main feedwater system. From the surge tank it is pumped by the main feedwater pumps through two high pressure extraction heaters and into the reboiler-superheater units located in the reactor building. The steam from the superheater comes back into the turbine-generator building to supply the throttle steam for the turbine as well as the jet steam for the steam jet air ejector. Exhaust steam from the turbine is condensed and pumped by the hotwell pumps through the steam jet air ejector, the low pressure feedwater heater, the main deaerating heater, and into the surge tank. The side stream for clean up of any contamination in the main loop is taken off the discharge of the hotwell pumps.

Reboiler and Superheater - Steam generation and superheating is accomplished as shown in Fig. 17. Each reboiler is equipped with a horizontal, perforated baffle plate located about six inches above the tube bundle and with screen type steam driers as shown in Fig. 18. Water enters the reboiler through two 4-inch pipes which extend along the lower side of the tube bundle for about 90% of its length; the water flowing out of these pipes through slots along the top of the pipes. The steam, after passing through the driers, is taken from the reboiler to the superheater by five 8-inch pipes.

Steam passes through the tubes of the superheater and exits through four 10-inch pipes which then combine into one 20-inch pipe to flow to the turbine. All piping in the secondary system is A.S.M.E. specification SA-106, Grade A, seamless carbon steel pipe, Sch. 80.

Heat is supplied to each of these units by hot organic flowing directly from the reactor through two 24-inch pipes into the shell of the superheater, then through two 24-inch pipes joining the one 30-inch pipe into the reboiler, through the tubes of the reboiler and out through one 30-inch pipe to the organic recirculating pumps.

Turbine-Generator - The turbine-generator unit is a compound, double flow, 1800 rpm, 225,000 kw turbine consisting of a single flow high pressure unit, a single flow intermediate pressure unit and a double flow low pressure unit coupled directly to a 260,000 kva hydrogen cooled generator.

Steam is extracted from the turbine at five points to heat the feedwater and to supply deaeration of the feedwater. One extraction point on the high pressure turbine and one extraction point on the intermediate pressure turbine

supply the steam for the two high pressure feedwater heaters. Extraction from two different stages in the early portion of the low pressure turbine supply the proper temperature and pressure steam for the deaerating heater. Extraction from a later stage in the low pressure turbine supplies the low pressure feedwater heater. Several rows of moisture removal blading are used in the low pressure turbine to assist in the moisture removal. By employing special turbine blading of this kind the moisture content in the last stage can be maintained below 15%, without the aid of an external moisture removal system.

At full load operation steam at 400 psia pressure and 550°F is supplied to the turbine throttle at the first stage of the high pressure turbine section. Full load operation calls for a steam flow of 2.563 million pounds per hour at the turbine throttle. Exhaust pressure conditions will vary between 1.5 and 3.0 inches of Hg abs.

There are two steam seals on the high pressure turbine, two on the intermediate pressure turbine and four on the low pressure turbine. Labyrinth seals that operate in a conventional manner are used. The shaft seals are connected in a system that disposes of the steam that leaked past the labyrinth rings and also supplies sealing steam to prevent leakage of air into the turbine. During start up or at light loads, when a vacuum exists in the turbine shell, a regulator admits steam at 2 psig to seal the labyrinth. During full load, leak-off steam from the high pressure labyrinth rings is used to seal the lower pressure ends and any excess is dumped to the gland seal leak-off system. The outer chamber of each ring assembly is connected to a steam-seal gland exhausting system which prevents steam from escaping past the outermost rings into the plant. A slight vacuum (10-in of water) is maintained in the outer chamber. Steam and air leakage from each labyrinth section is discharged to the gland seal leak-off system and later returned to the main loop.

Steam to the turbine passes through two emergency stop valves in parallel and then through two sets of control valves which feed separate halves of the turbine shell.

The main generator is a 14,400 volt, three phase, 60 cycle, 225,000 kw hydrogen cooled machine. The name plate rating at 30 psig hydrogen pressure and a power factor of 0.85 is 260,000 kva. The generator is of the double winding type with a short circuit ratio of 0.64 and a current rating of 5230 amp per winding.

UNCLASSIFIED
ORNL-LR-DWG. 23361

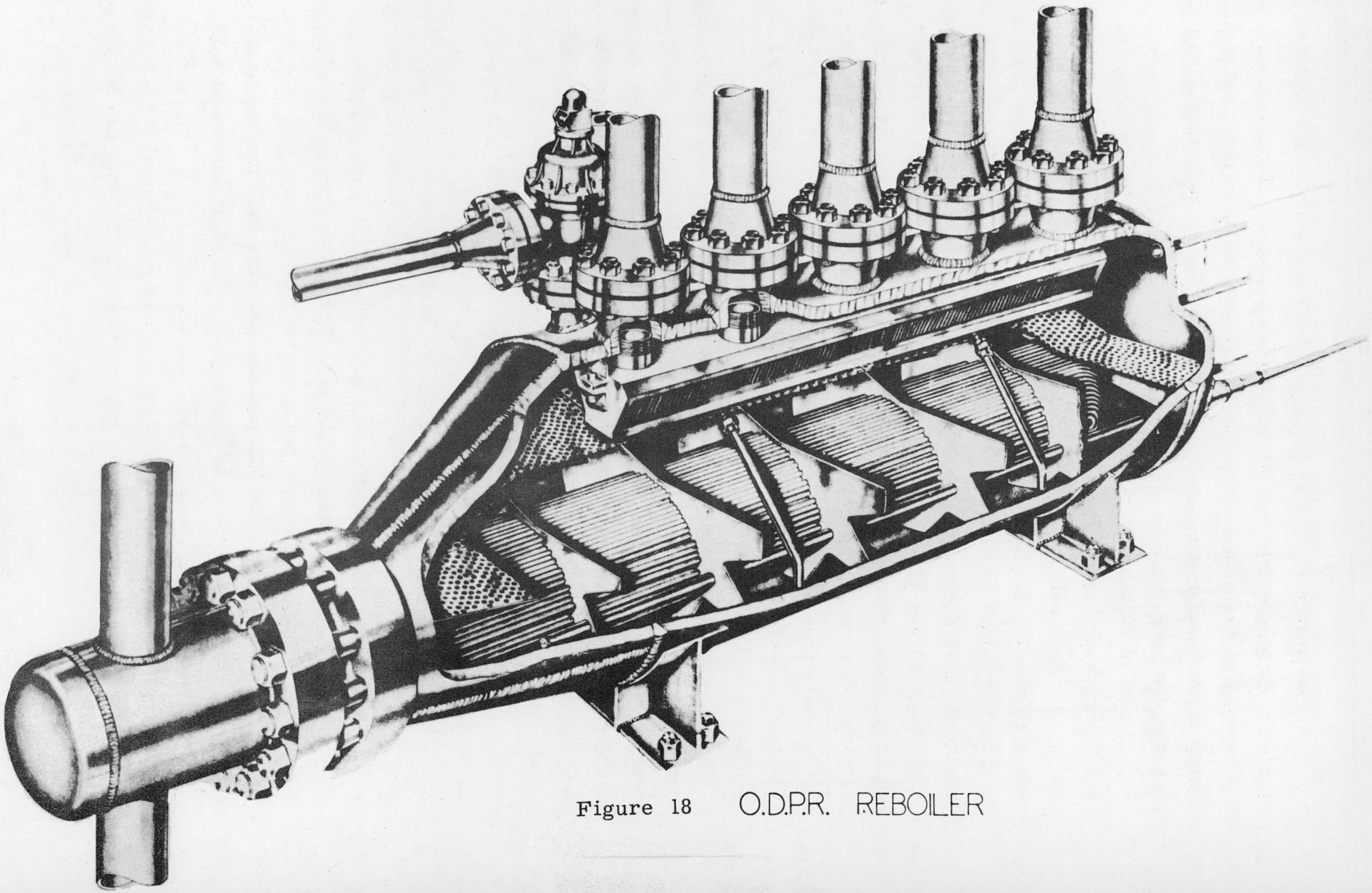

Figure 18 O.D.P.R. REBOILER

The generator is cooled by circulating gas within the sealed generator casing. Rotor mounted fans circulate the hydrogen. Heat absorbed by the gas is removed in six coolers mounted at the generator casing. Station cooling water flows through the cooler at a rate regulated to maintain 90 to 95°F gas temperatures.

Field excitation for the generator is provided by two high response, wide range stabilized, motor driven exciters. Each exciter is rated 500 kw at 375 v. Each exciter set consists of an induction motor, a dc generator, and a flywheel. The flywheel is designed to provide the specific inertia constant required to maintain operation equivalent to that of a shaft driven exciter. This feature is essential during periods of transient disturbances and faults in the power system. Both exciters are operated remotely from the control room. Normally, only one is operating. The second exciter is a reserve machine. Each set is provided with a unit excitation cubicle. This installation consists of three compartments housing the field circuit breakers, discharge resistor, motor operated field rheostat, and the amplidyne voltage regulator.

The generator casing is sealed against hydrogen loss at the shaft by oil seals. Seal oil is pumped from the vacuum tank, through a cooler, and then to the seal housings. At the seal housing, the oil flows in two direction along the shaft. The seal oil that flows toward the bearing mixes with the bearing oil and is drained to an air detrainor. Oil from the generator side of the shaft seals drains into a hydrogen detrainor. From the two detraining tanks, oil is returned to the vacuum tank. A 2 hp vacuum pump is required to maintain a vacuum of about 29.6 in of hg abs.

The lubricating oil system provides high pressure oil to the hydraulic governor mechanism and low pressure oil to the bearings. The system includes a 5400 gal storage tank equipped with a motor driven vapor extractor, a main centrifugal oil pump driven by the main turbine shaft, an auxiliary motor driven oil pump, an emergency motor driven bearing oil pump, and a motor driven turning gear oil pump. Two oil coolers are provided, one being sufficient for normal operation. Flow of cooling water through the coolers is adjusted to maintain 110 to 120 °F oil outlet temperature.

The supervisory instrumentation and control devices for the turbine-generator includes not only the conventional instruments, but also some

special and duplicate instrumentation and control. Numerous devices are provided to protect the turbine-generator from various types of failures. Many of these protective devices will automatically initiate a complete shut down of the unit by tripping closed the stop valves, tripping open the two generator circuit breakers and the tripping open of the two auxiliary power transformer breakers.

Condenser - The main turbine condenser is a two pass divided water box type, equipped with external valving for backwashing each section. Condensed steam is collected in a storage type hotwell from which it is pumped by the hotwell pumps through the various heaters to the surge tank. There are three 1900 gpm hotwell pumps, two being sufficient for normal operation. Approximately 202,000 sq ft of effective condensing surface is provided. At full load, the circulating water flow to the condenser is 256,400 gpm and the steam flow is 1,920,000 lb/hr.

Steam-Condensate-Feedwater - Most of the secondary cycle is of conventional design, general data of which may be found in Table 4. An emergency water storage tank is provided in the upper region of the turbine-generator building. Some special instrumentation is provided beyond the normal scope of the conventional system.

Circulating Water System - The circulating water system consists essentially of an intake structure, pump house, chlorinating apparatus, a supply tunnel and a discharge tunnel. Circulating water is provided mainly for condenser cooling and heavy water cooling, but is used for numerous other small coolers within the plant. There are eight 50,000 gpm circulating water pumps. To provide for river elevation fluctuations up to fifty feet, the total height of the pump house atructure is 60 feet.

Heat Cycle - Much of the full load heat cycle data has been tabulated in Table 13 . At full load, operating with a condenser pressure of 1.5 in Hg abs a gross electrical output of 222,200 kw is obtained. The gross thermal efficiency is 31.1% , which corresponds to a gross heat rate of 10,982 Btu/kwh (See Heat Balance, Fig. 19) An approximately 75% full load heat balance, corresponding to one reboiler-superheater unit being out of service, gives a gross electrical output of 163,800 kw. The gross thermal efficiency is 30.4% and the gross heat rate is 11,229 Btu/kwh. (See Heat Balance, Fig. 20.)

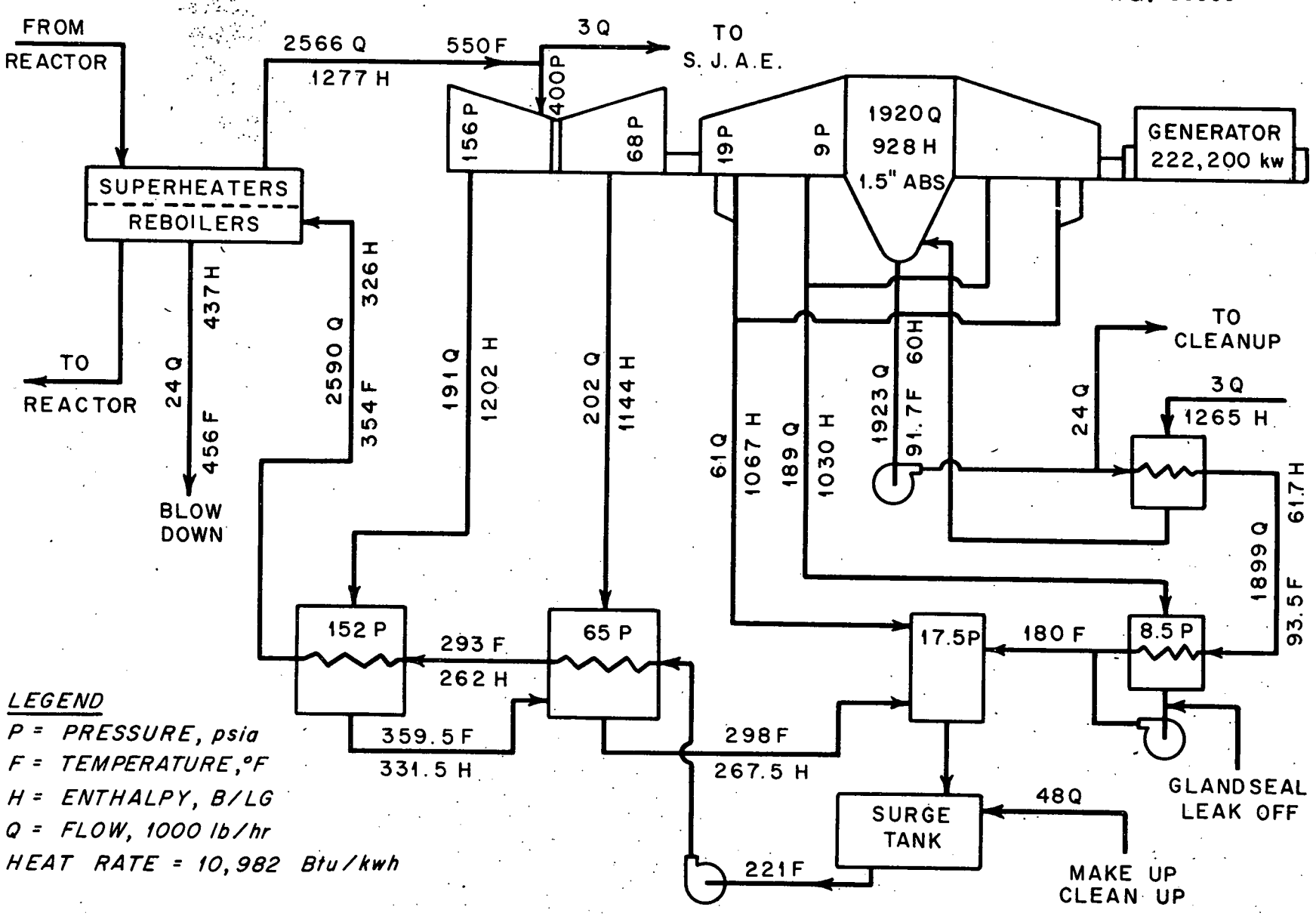

Fig. 19. O.D.P.R. Heat Balance - 222,200 kw - Full Load

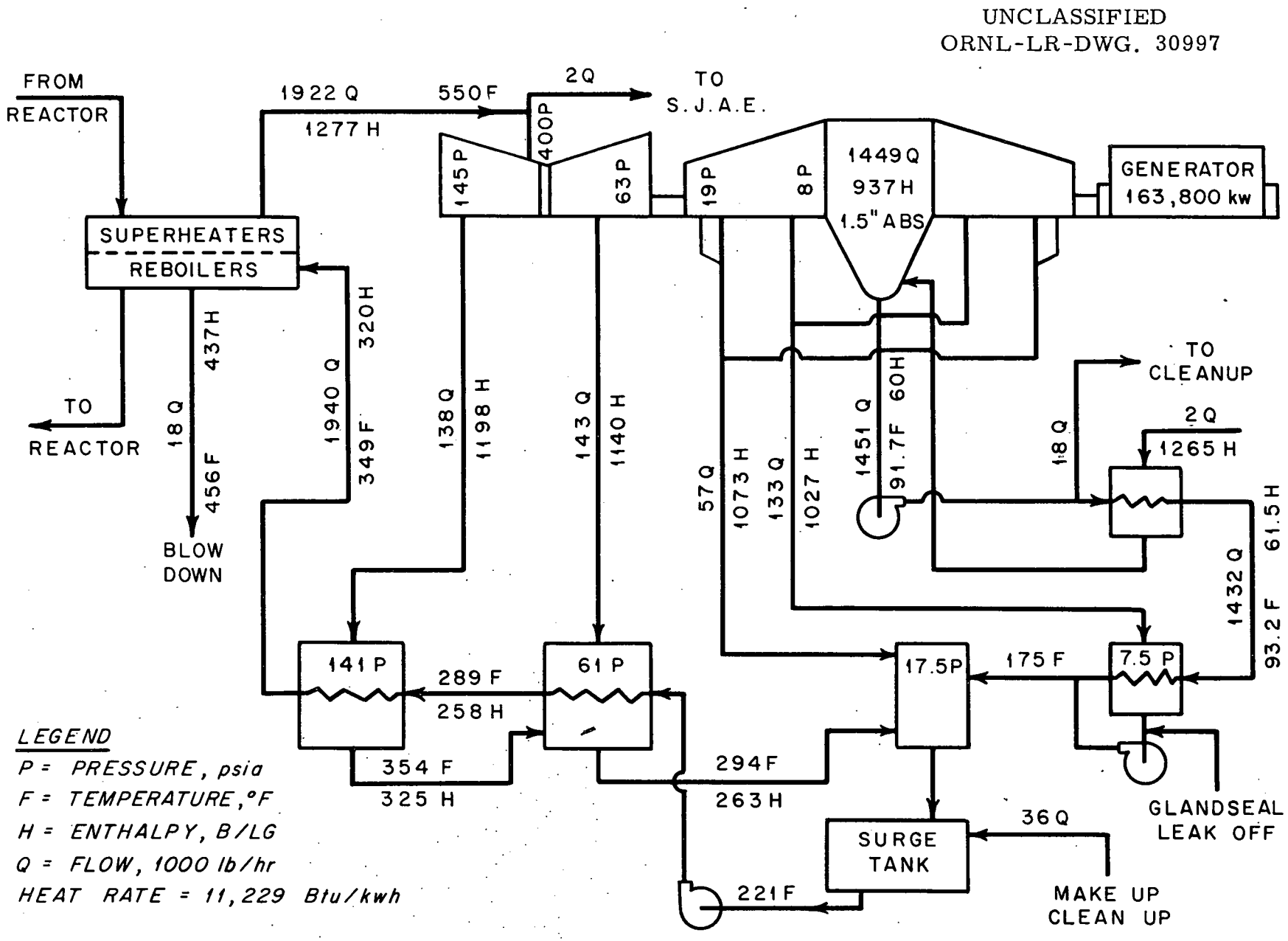

Fig. 20. O.D.P.R. Heat Balance - 163,800 kw - 3/4 Load

Electrical System

The electrical system required for the generation and transmission of electrical energy is shown by the One-line Electrical Diagrams, Figs. 21 and 22. It consists of a single circuit generator feeding the high voltage network through the main power transformer and a high voltage bus in the switch-yard on which four lines of the high voltage network are terminated.

The auxiliary power system shown in these diagrams consists of three transformers and three high voltage auxiliary power buses from which the various motor control centers and lighting buses are served. One of the auxiliary power buses is connected to the generator, another to the high voltage network bus, and the third to the sub-transmission system.

The net electrical output of the plant will be 203,260 kw. This energy will be generated at 14.4 kv and stepped up by means of a single three-phase main power transformer to the transmission voltage of 138 kv.

Generator - The 1800 rpm conventional hydrogen cooled generator is rated 260,000 Kva at 0.85 power factor, 30 psig hydrogen pressure and 14.4 kv. Its short circuit ratio is 0.64. This double winding machine is connected to the 10,000 ampere self-cooled isolated phase buses which feeds the low voltage terminals of the main power transformer. The generator neutral is grounded through a resistor loaded distribution transformer. Two sets of potential transformers supply metering, relaying, and control potentials. Lightening arresters and surge protection capacitors have also been included within the generator housing.

Excitation System - Two motor-driven exciters (one to serve as standby) are provided for excitation. Each is rated 500 kw at 375 volts and is driven by a 4160-volt induction motor, and is provided with the necessary equipment to connect to the generator's main field breakers. The motor-driven amplidyne-voltage regulator is capable of being switched to either exciter. All associated auxiliary equipment is contained in conventional metal clad cubicals.

Main Power Transformer - The two-winding, forced-oil, air-cooled, three-phase main power transformer is rated at 245,000 Kva with a full load voltage rating of 14.4 to 138 kv. The high voltage winding is wye connected and the low delta connected. It is provided with two 2.5% taps above and below the rated voltage. The high voltage winding's neutral is solidly grounded.

TABLE 4

TURBINE CYCLE HEAT EXCHANGER DATA

		Steam Jet Air Ejector	No. 1 Feed Water Heater-LP	No. 2 Feed Water Heater Deaerating		No. 3 Feed Water Heater High Pres.		No. 4 Feed Water Heater-HP	Condenser	Flash Tank	Demineralizer		Recovery Heat Exchanger	Make Up and Clean Up Deaerating Heater
Hot side				Extract'n	Cascade	Extract'n	Cascade				Make Up	Clean Up		
Flow	10^3 #/hr	3	189	61	393	202	191	191	1920	24	19	24	18	5
Inlet Pressure	psia	390	9	19	65	68	152	156	1.5"Hg abs	450	35	35	20	20
Inlet Temperature	°F	530	185.6	222	298	298	359.5	373	91.7	456	60	91.7	228	228
Inlet Enthalpy	Btu/#	1265	1030	1067	267.5	1144	331.5	1202	928	437	28	60	196	1156
Outlet Pressure	psia	17.5	8 5	17.5	17.5	65	65	152	1.5"Hg abs		30	30	15	17.5
Outlet Temperature	°F	221	185.6	221	221	298	298	359.5	91.7		77.9	77.9	154	221
Outlet Enthalpy	Btu/#	189	154	189	189	267.5	267.5	331.5	60		45.9	45.9	122	189
Enthalpy Loss	Btu/#	1076	876	878	78.5	876.5	64	870.5	868		17.9	14.1	74	967
Heat Released	10^6Btu/hr	3.2	165.8	53.5	30.9	177.0	12.2	166.0	1,666.6		(340)	(340)	1.3	4.8
				84.4		189.2					(10^3)			
Cold Side														
Flow	10^3 #/hr	1899	1899	1899	189	2590	2590	128,200	6	18	43		43	43
Inlet Pressure	psia	35	30	25	25	550	530	25' H_2O	450	450			30	25
Inlet Temperature	°F	91.7	93.5	180	185.6	221	293	70	456	456			77.9	109
Inlet Enthalpy	Btu/#	60	61.7	148	154	189	262	38	437	437			45.9	76.6
Outlet Pressure	psia	30	25	17.5	17.5	530	510	20' H_2O	20	20	30		25	17.5
Outlet Temperature	°F	93.5	180	221	221	293	354	83	228	228	77.9		109	221
Outlet Enthalpy	Btu/#	61.7	148	189	189	262	326	48	1156	196	45.9		76.6	189
Enthalpy Gain	Btu/#	1.7	86.3	41	35	73	64	13	719	241			30.7	112.4
Heat Absorbed	10^6Btu/hr	3.2	165.8	77.8	6.6	189.2	166.0	1,666.6	4.3	4.3			1.3	4.8
				84.4										
Surface Area	10^3 sq ft	0.62	13.4	(12) equiv.		18	17	202					0.10	(2) equiv.

High Voltage Switchyard - High voltage switchyard consists of a main and transfer bus, four transmission line terminals, two sectionalized buses, one sectionalizing breaker, two transformer connections, and a bus paralleling breaker.

a. Circuit Breakers and Disconnect Switches - All 138 kv oil circuit breakers have a continuous rating of 1200 amperes, a momentary rating of 36,000 amperes, and an interupting capability of 5,000,000 Kva. All associated disconnect switches are rated at 1200 amperes except the one in the tap to the 138 kv auxiliary power transformer which is 600 amperes.

b. Potential Devices - Potential transformers are located on bus section 1 for metering and relaying whereas coupling capacitors and bushing potential devices are located on bus section 2 for the same purpose.

Auxiliary Power System

Four sources of auxiliary power are available as indicated below:

1. Main generator
2. 138 kv transmission system
3. 34.5 kv sub-transmission system
4. Diesel generators

The last two are provided as backup for the 138 kv transmission system during shutdown conditions. The three 4160-volt buses are each connected to independent power sources: Bus 1 to the 138 kv transmission system via auxiliary power transformer No. 1; bus No. 2 to the generator via auxiliary power transformer No. 2; and bus No. 3 to the sub-transmission system via standby transformer No. 3. All 4160-volt bus sections and load centers are completely separated from one another and their sources to reduce the probability of a single incident rendering the auxiliary power system inoperable.

a. Normal Power - Auxiliary power is normally supplied from the two main auxiliary power transformers via the 4160-volt bus sections No. 1 and 2 with either bus tie 1-3 or 3-2 open. Each source is capable of supplying the total auxiliary power load. The three 4160-volt buses supply the loads indicated:

	Bus 1	Bus 3	Bus 2
Primary feed pump motors	3	2	3
Secondary feed pump motors			
Condensate (hotwell)	1	1	1
Main feed water	2	1	2
Circulating water pump motors	3	2	3
Exciters	1		1
Load center transformers	1	2	1

b. Shutdown or Emergency Power - Power is required for shutdown or emergency conditions to allow station auxiliaries vital to the protection of the equipment, plant, and personnel to operate. This power is supplied from either the 138-kv system via the 138-kv auxiliary power transformer, the 34.5 kv sub-transmission system via the unit substation, or the diesel driven generators.

Station Auxiliary Power Equipment

a. 14.4 kv Auxiliary Power Transformers - The auxiliary power transformer fed from the main generator is a three-phase, three-winding, oil-immersed, air-cooled transformer. This wye-delta-wye connected transformer delivers power to the plant auxiliary system at 4160 volts, with a duel feed arrangement to supply buses 1 and 2. It is rated 15,000 KVA self cooled and 20,000 KVA forced-air cooled.

b. 138 kv Auxiliary Power Transformers - The auxiliary power transformer connected to the 138-kv transmission system is a conventional oil-air cooled, three-phase unit with a self cooling rating of 15,000 KVA and a forced air cooled rating of 20,000 KVA. This delta-wye connected transformer delivers power to the plant auxiliary system through a duel feed arrangement to supply buses 1 and 2 at 4160 volts.

c. 34.5 kv Unit Sub-station - The 34.5 kv unit sub-station consists of an oil-air self cooled 2,500 KVA three-phase transformer packaged with a 1200-ampere 250,000 KVA 4160-volt metal-clad switch gear compartment. This unit is connected to bus No. 3 of the 4160-volt auxiliary power system.

d. Diesel Generators - The diesel generators consist of a diesel engine, a 60-cycle AC generator, a shalf-driven exciter, and the necessary field control and regulating equipment.

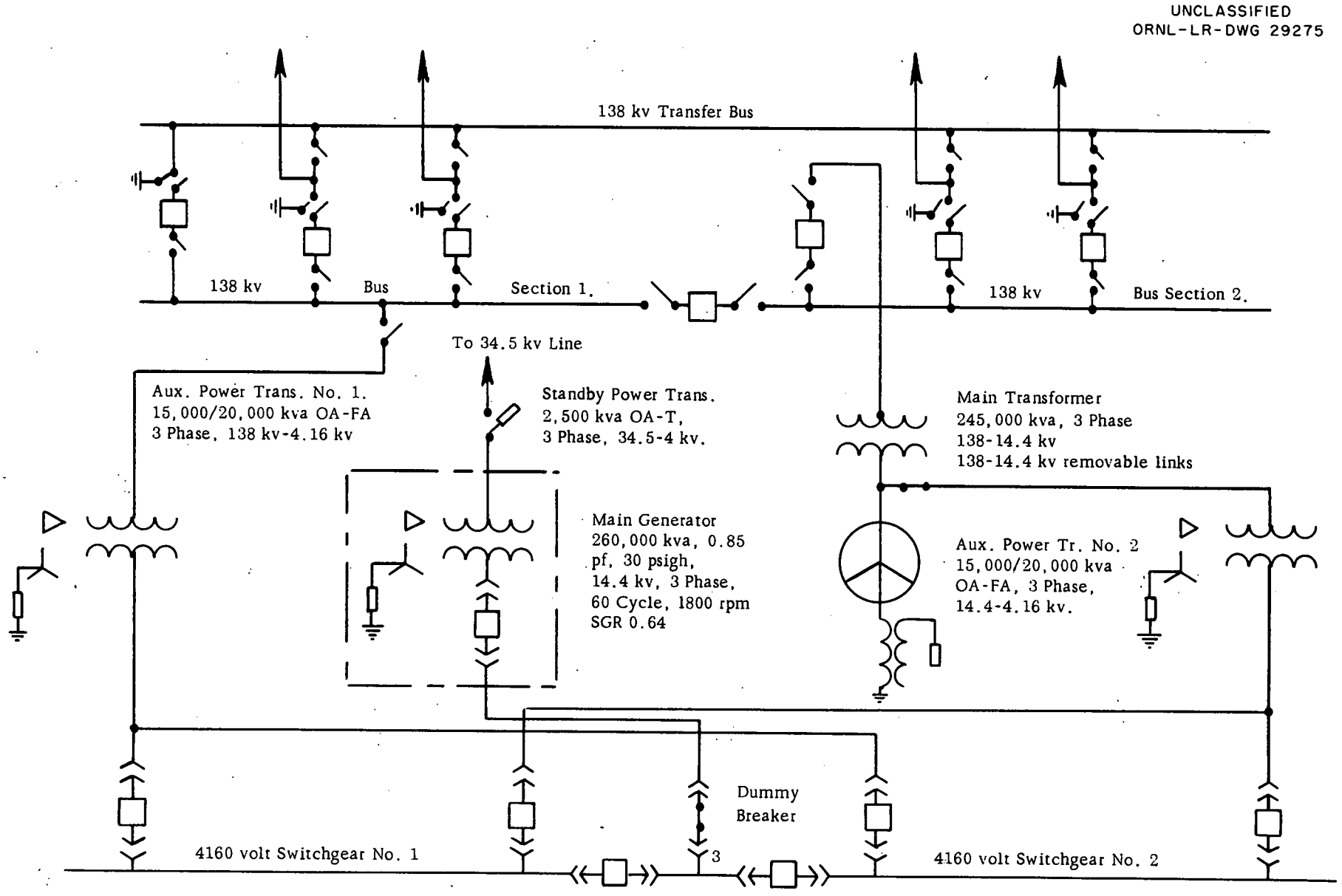

FIG. 21. ELECTRICAL SINGLE LINE DIAGRAM - HIGH VOLTAGE SYSTEM.

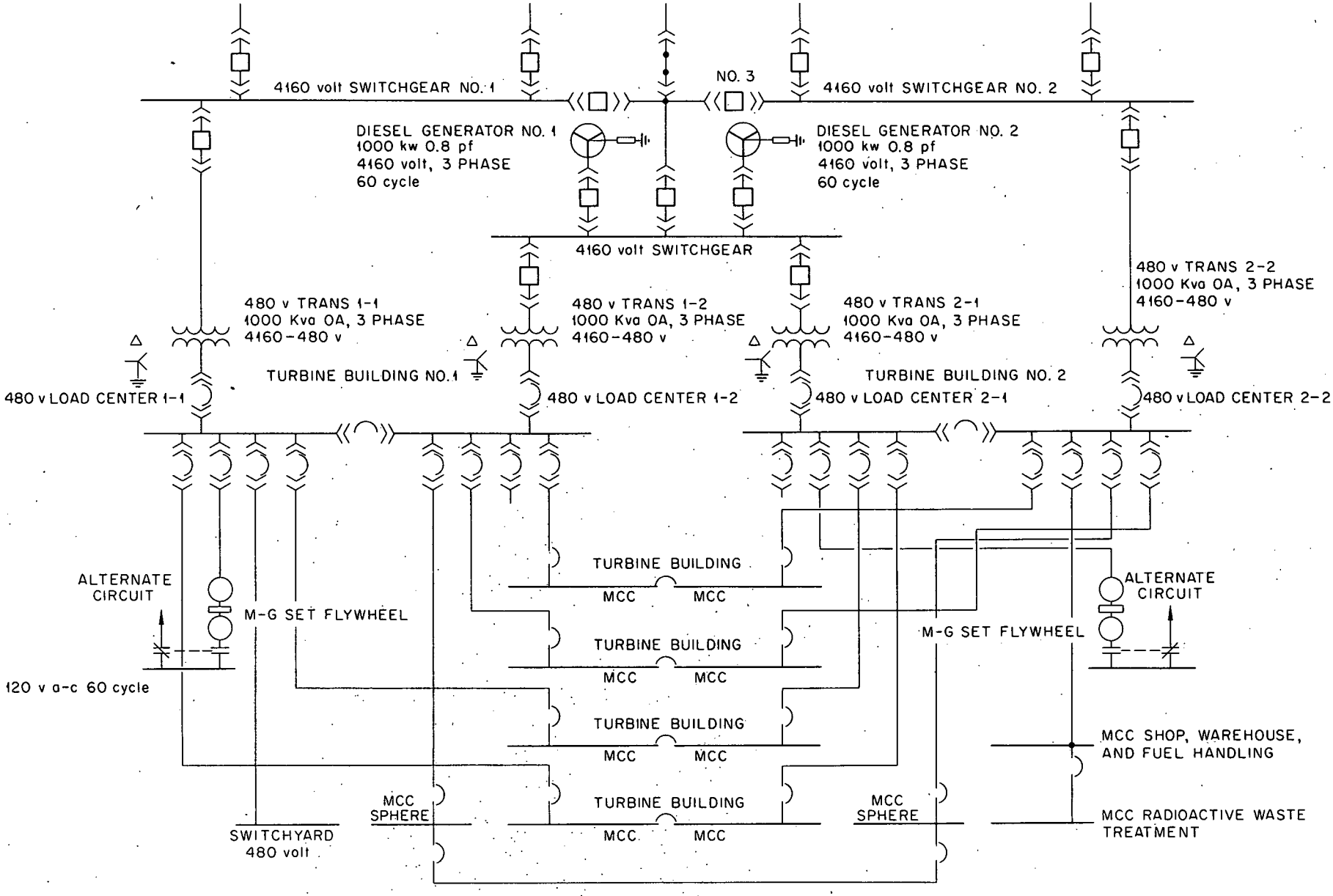

Fig. 22. Electrical Single Line Diagram–Auxillary Power System.

e. 4160-volt Switchgear - Auxiliary power is distributed by means of three metal-clad switchgear units making up the three 4160-volt buses. Buses 1 and 2 are connected to their respective main auxiliary power transformers by bus duct. All incoming and feeder circuit breakers are rated at 1200 amperes and 250,000 KVA. Each bus contains appropriate metering, relaying instrument transformers and control devices.

f. 480-volt Load Centers - Two indoor double-ended 480-volt load centers supply 480-volt auxiliary power requirements. Each load center transformer is pyranol filled with a self-cooled rating of 1000 KVA. Each switchgear section is completely metal enclosed and contains a low voltage draw-out breaker and an instrument compartment. The circuit breakers are co-ordinated for selective tripping.

g. 480-volt Motor Control Centers - The 480-volt motor control centers feed all motors up to and including 100 hp., lighting and miscellaneous plant services. They consist of grouped or packaged metal enclosed control and switching equipment.

Protective Relaying - Differential protection is provided for all buses rated 4 kv and higher, major transformers, and the main generator. Overlapping protection zones exist throughout with back-up relaying and ground protection throughout. Carrier-current directional comparison transmission line relaying with single-shot reclosing is provided for all 138 kv transmission lines.

The generator is protected by loss of field relaying, negative sequence relaying and overcurrent with voltage restraint. The generator neutral is grounded through a resistance loaded distribution transformer which limits its fault current and provides for ground relaying.

All incoming lines and feeders connected to the 4160-volt auxiliary power system have phase and ground overcurrent relays. The transformer neutrals are resistance grounded to limit damage due to ground fault currents and to provide fast effective ground relaying.

The 480-volt switchgear is designed for selective tripping. Solid grounding of the load center transformers provides for fast breaker tripping. Circuit breaker controlled loads and contractor controlled loads utilize circuit breaker overcurrant devices and contractor overload heaters, respectively, for circuit protection rather than separate protective relays as used in the higher voltage systems.

Special Electrical Services - The special electrical services are those systems which provide for the control, instrumentation, and special emergency power. These systems are grouped into an isolated AC system and the station battery DC system.

a. A-C Reactor Safety and Instrumentation System - All safety circuits and equipment are provided in duplicate, fail safe and are supplied from separate isolated 120-volt, 60-cycle AC power sources. The sources are AC motor generator sets equipped with fly wheels to override momentary interruptions of power. Emergency operation is achieved by switching to the 120-volt station power system in event of an outage of either of these sources.

b. Station Battery DC System - Two separate and independent station batteries and DC buses provide 125- and 250-volt DC control, instrumentation, and special emergency power. Certain essential loads are connected to both batteries through silicon rectifiers. Duel feed and source isolation is thus maintained.

Motors - All motors larger than 250 h.p. are connected to 4160-volt, 3-phase, 60-cycle AC buses. Most motors larger than 3/4 h.p. up to and including 250 h.p. are connected to 440-volt, 3-phase, 60-cycle, AC motor control buses. All motors are either drip proof or splash proof and may either be totally enclosed and/or weather protected, depending upon their location.

Auxiliary Power Requirements - The total auxiliary power requirements is broken down and the major auxiliary power uses exhibited in the following tabulation:

AUXILIARY POWER REQUIREMENTS

	Total Connected Load, kw	Normal Load, kw
Organic Recirculating-feed Pumps	12,600	12,600
Circulating Water Pumps	2,840	2,130
Main Feed Water Pumps	1,910	1,520
Condensate (hotwell) Pumps	225	150
Heavy Water Circulating-feed Pumps	585	440
Screen Wash Pumps	150	75
Exciters	710	355
Miscellaneous Motors and Equipment	1,200	1,150
Lighting Circuits	520	520
Total	20,740	18,940

This auxiliary power represents 8.5% of gross electrical output and 2.37% of total heat input at reactor.

Heavy Water System - The essential entities of the moderator system are four D_2O recirculating-feed pumps, two D_2O coolers, two D_2O storage tanks, a purification system and a start-up heating system, see Fig. 23.

The D_2O flows from three of the pumps (one being held as spare) into the lower D_2O plenum of the reactor, entering the reactor vessel through eight 4-inch pipes. This lower plenum provides proper distribution of D_2O around the outside of the process tubes of the core, and to the tubes extending below the reactor vessel for control rod cooling. The D_2O flows bulkwise upward through the core region serving as both a moderator and a reflector. It flows into a ring header at the top of the core region, and from this out of the reactor through eight 4-inch pipes. It also flows on upward out of the core region through the tubes surrounding the upper portion of the control rods to provide cooling for these rods. From the tops of these tubes (cans) the D_2O and decomposition gases are sent to the purification system along with the side stream from the main loop taken off from the downstream side of the D_2O coolers.

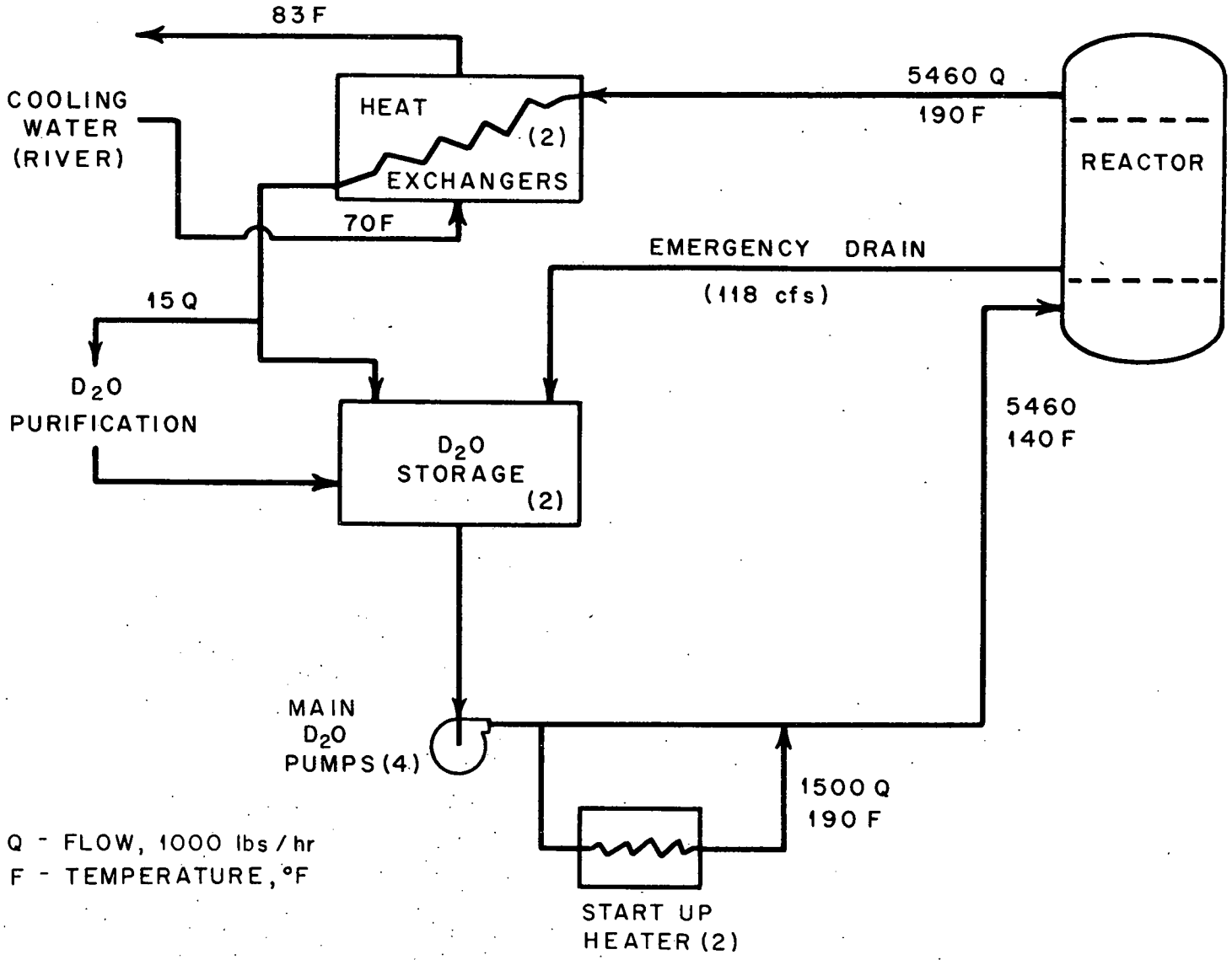

Fig. 23. O.D.P.R. Simplified D_2O Flow Diagram

ORNL-LR-Dwg.-30998
UNCLASSIFIED

From the reactor the main stream of the D_2O flows to one of the coolers (the second one serving as spare in case of leakage in the first,) through the tubes of the cooler, and then to the storage tanks. The D_2O is cooled by river water from the regular circulating water system. The D_2O coolers are 4-foot inside diameter by 19-feet long cylindrical heat exchangers with stainless steel single wall tubes and a carbon steel shell. The storage tanks are cylindrical; 14-foot inside diameter by 20-feet long, and are stainless steel. The storage tanks supply the suction for the D_2O pumps.

Make up for the D_2O system is fed, along with the purified side stream, into the storage tanks. In case of a reactor scram the D_2O in the reactor is drained to the storage tanks through a 30-inch pipe.

All piping in the D_2O system is stainless steel.

Heavy Water Purification Cycle

a. Purpose - To maintain the necessary high purity of the heavy water in the moderator system, means are provided to remove such undesirables as light water, ionic impurities and suspended materials. This action is necessary to:

(1) Minimize parasitic capture of neutrons by foreign materials
(2) Reduce corrosion effects to a minimum
(3) Remove and recombine moderator radiolytic decomposition products

b. Purification Equipment - The system to be used for purification of the heavy water consists of the following (See Figure 24):

(1) A degasifier or cyclone separator (to seperate entrained gases from the liquid)
(2) A recombiner (to recombine decomposed D_2O in the gas exit of the degasifier)
(3) A prefilter (to remove suspended material)
(4) An ion exchange column (to remove dissolved impurities)
(5) An afterfilter (to prevent any of the resin bed from depositing small particles in the D_2O)
(6) A distillation column (to separate light water from the moderator)
(7) A gas dryer and cooler (to keep heavy water losses to a minimum)

c. Description of Cycle - The purification cycle described herein is similar to that of Savannah River and is of the type recommended by NPG[1-2].

For moderator cooling purposes, heavy water is pumped at the rate of 10,900 gpm through heat exchange equipment. From this main stream, a side flow of about 30 gpm is removed and circulated through the purification cycle. Side stream flow is such that there is complete clean-up of the D_2O system in 12 hours following any major contamination. A small amount of make-up is required to account for losses in the system.

d. Gas Separation and Removal - Gas separation and removal are accomplished by means of a degasifier and a recombiner. The 30 gpm side stream of moderator is let down to atmospheric pressure and passed through the degasifier. The degasifier consists of a cyclone-type separator connected to a condenser on the vapor discharge and to the purification feed surge tank on the liquid discharge. Gas leaving the condenser is passed through the recombiner in order to avoid any loss of dissociated D_2O. Gases from the recombiner are sent through heat exchangers to condense the heavy water, which is returned to storage, the gas being exhausted to the atmosphere through refrigerated vents where all but a trace of D_2O is removed.

Before entering the next step of the purification cycle, the D_2O in the purification feed surge tank passes through a cooler where the temperature is lowered below $100^{\circ}F$. This is necessary, as the anion resin bed becomes highly ineffective above $100^{\circ}F$.

e. Ionic and Suspended Material Impurity Removal - The system for ionic and suspended material impurity removal consists of three units: each having a prefilter, a deionizer (ion exchange column) and an afterfilter. One unit is used during normal operation but all are available for emergency purification.

Cooled water from the purification feed surge tank enters the prefilter which provides a filtering surface of about 15 ft^2. capable of removing particles above 10 microns, thus preventing them from entering the deionizer which follows. The passage of the D_2O through the ion exchange column (about 27 ft^3 of mixture) removes most of the dissolved impurities. On leaving the deionizer, heavy water passes through an afterfilter used primarily to prevent suspended matter, expelled from the resin bed, from entering D_2O storage.

"Spent" beds will be detected by conductivity measurements on the exit stream, and when replacement becomes necessary, as much D_2O as is practical is removed from the equipment by helium drying. Gas is sent to the gas drying

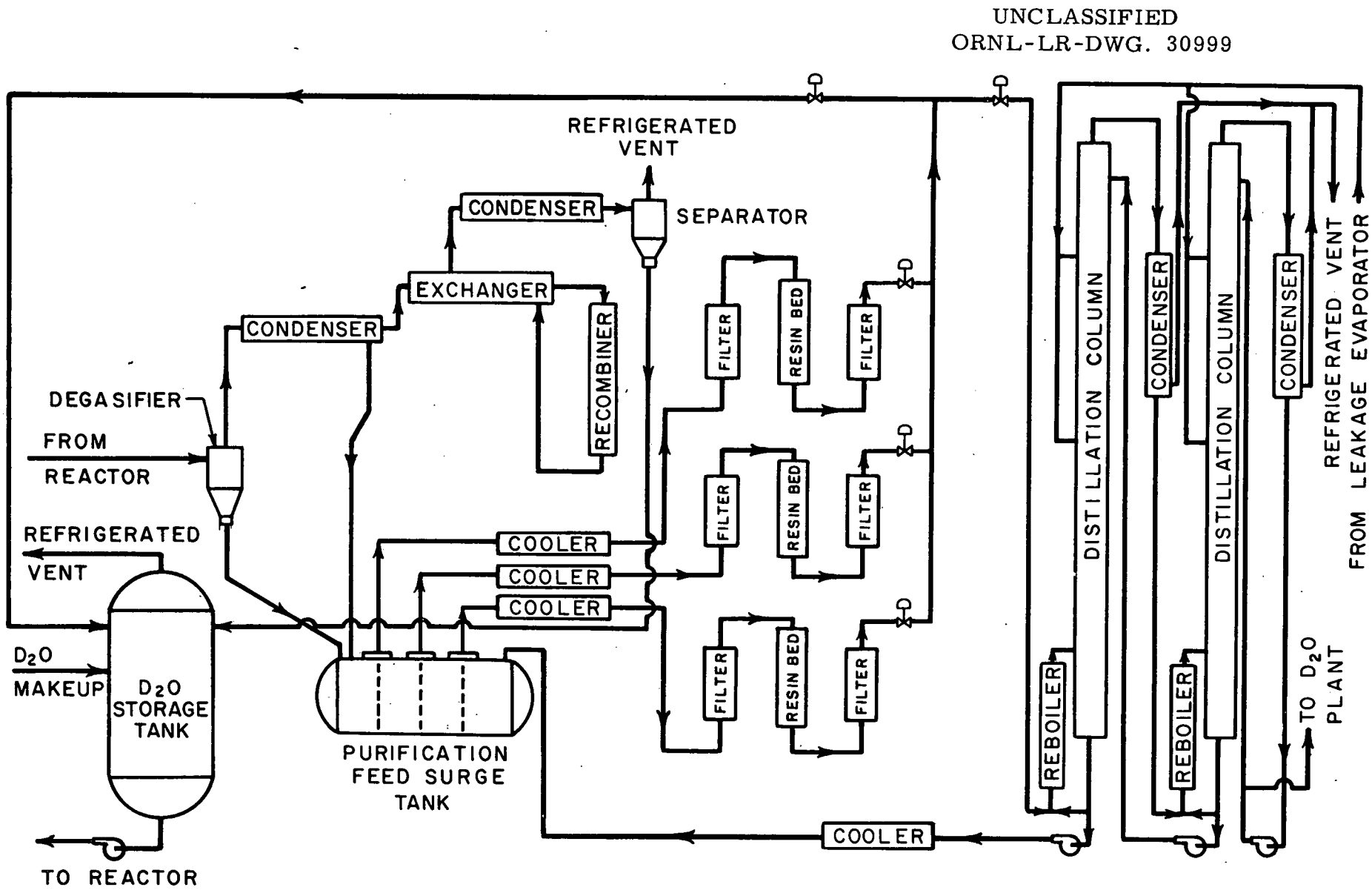

Fig. 24. D_2O Degasifier and Purification System

system for D_2O recovery, while replacement of the bed is performed by remote operation because of radioactivity of the "spent" resin. The fresh column, containing a mixture of anion and cation exchange resins, must be deuterized prior to use.

f. Light Water Removal - After the moderator has passed through the afterfilter, a stream of about 5 gpm is put through an isotopic distillation system while the remainder is sent to D_2O storage. The distillation equipment consists of two 90 plate columns operated in series, at reduced pressure, so as to remove light water from the system as 20 mol percent H_2O.

Light water can be picked up by the moderator in the following manner:

(1) Absorption from the atmosphere upon initial loading in the reactor.

(2) Contamination of heavy water used in preparing the resin beds

(3) Any possible H_2O leaks in the D_2O system.

Although H_2O is produced in the moderator due to a γ, n reaction, the amount thus formed is negligible.

The flow of D_2O is sent to the reboiler of the first column. The condensate from the first column is sent to the reboiler of the second column, while the bottoms are returned to the D_2O purification feed surge tank as product. The condensate from the second column is returned to a heavy water production plant after removal of a side stream as second column reflux, while the bottoms are returned to the first column as reflux.

The condensers are vented through vacuum pumps to refrigerated condensers where all but a trace of D_2O is removed and returned to process.

Distillation also serves as a means of processing leakage that collects at various points in the plant. The leakage D_2O is evaporated to remove suspended matter and the vapor is sent to an appropriate elevation on the distillation column depending upon its concentration; if the concentration is less than 80 mol percent heavy water, the material is collected and returned to the D_2O production plant.

The distillation column is in an unshielded area so care is taken to avoid the introduction of radioactive D_2O. This is accomplished by means of a monitor located on the feed stream originating at the afterfilter discharge which closes the control valve feeding the distillation system and at the same time sounds an alarm.

g. Gas Drying and Cooling - The purpose of the gas drying and cooling system is to provide a means of drying and cooling helium that is used in the following way:

(1) Drying filters

(2) Drying ion exchange beds

The equipment includes a water cooled condenser, refrigerated chiller, refrigerated freezer, gas heaters, blower and storage for 5000 standard cubic feet. During operation, wet or hot gas flowing at 200 to 300 cfm is routed through the water cooled condenser to storage, where it is ready for reuse. D_2O collected is tested for purity and returned to the appropriate point in the system.

If the helium has become contaminated and must be exhausted to the stack, it is sent through the chiller and freezer, after going through the condenser. The freezer removes all but a trace of D_2O before the helium is exhausted.

Water Feed System - Water for the main steam cycle is supplied from the deepwell pumps and water storage tanks on the property site via the miscellaneous bearing cooling and oil cooling units in the turbine-generator building. The pumps flow the water through the turbine-generator building cooling service system, the demineralizer, the recovery heat exchanger, the make-up deaerating heater and into the surge tank. The clean-up stream from the main steam cycle is mixed with the make-up feed in the demineralizer. Water may be pumped directly into the make-up system demineralizer by the deepwell pumps when more water is required for make-up than is supplied from the cooling service water system. An emergency cooling water storage tank in the upper region of the turbine-generator building is kept full of treated water, with no normal flow either to or from this tank. This tank supplies emergency cooling for the reboiler-superheater circuit only, with back-up cooling for bearings, etc. being supplied by a deepwell pump operating from the emergency bus.

Water Service - Water service including fire protection, shield cooling, miscellaneous bearing and oil cooling, drinking and sanitary systems, is provided by deepwell water. Water is supplied to these systems by the deepwell pumps directly or by the water storage tanks. This water service may be divided into several systems. First is the drinking water and sanitary system; second

is the fire protection system; third is the shield cooling and reactor building bearing and oil cooling system; and last is the miscellaneous bearing and oil cooling system in the turbine-generator building.

In the reactor building the water service flows through the piping embedded in the first few inches of the concrete biological shield next to the reactor, and through the various bearing coolers and oil coolers associated with the coolant and moderator systems. This water then flows through a mixed bed ion exchanger and to a hold up system before being discharged from the plant site. The emergency water tank for shell cooling is kept full of deepwell water, with no normal flow either to or from this tank.

In the turbine-generator building the water service flows through the various bearing coolers and oil coolers and then into the make-up demineralizer. If there is more water flow from the turbine-generator building cooling service system than is required for make-up, the surplus is dumped to the river via the discharge tunnel piping.

Organic Purification Cycle

a. Purpose - In the decomposition of the organic coolant during irradiation, both tars (higher polymers) and gases are formed. Means must be provided to remove the higher polymers from the system so as to:

(1) Minimize the buildup of fouling on heat transfer surfaces and thereby
    a) reduce resistance to heat transfer
    b) prevent a decrease in coolant flow area
(2) Maintain good heat transport characteristics in the coolant.
(3) Prevent an increase in the organic viscosity so as to minimize
    a) pressure drop and
    b) pumping requirements

b. Equipment - The purification of the organic coolant is accomplished by continuous removal of tars by means of a distillation column. For this purpose, a packed column is used, operating under reduced pressure to maintain the column below 700°F and thus keep further pyrolytic decomposition down to a negligible amount. In addition, a make-up tank and a storage tank are used, both of which are equipped with heaters so as to prevent solidification of the organic.

c. Make Up Requirements (See Appendix) - Organic purchased for the reactor is a byproduct of bi-phenyl manufacture and contains 20% higher boilers. The decomposition rate of coolant in the reactor core is 175 lbs/hr of which 8 lbs/hr are gases. At 20% tar content, the make up requirements of Santowax-R are 219 lbs/hr (175 lbs/hr of lower boilers), making the total amount of tar removed by distillation 211 lbs/hr.

d. Description of Cycle (See Figure 25) - Coolant is circulated through the core at the rate of 41×10^6 lbs/hr. After passing through heat exchangers, part of the flow (10^6 lbs/hr) is directed through the 10,000 gal organic storage tank before entering the reactor. The storage tank is used to provide feed for the distillation column, and at the same time picks up the product from the still plus fresh Santowax-R from the 2000 gal make up tank. In this way the three streams are blended.

The flow rate to the still is 703 lbs/hr at 30% tar concentration. Operating at 5 psig pressure, the 2 ft diameter, 12 ft high column removes 211 lbs/hr from the bottom and returns approximately 492 lbs of terphenyl/hr to the storage tank.

The purification system contains 2 packed columns so that a change over can be made in case of any operational difficulties encountered with the still in use. To start up a fresh column, melted Santowax-R from the make up tank is sent to the appropriate level of the new column. When the proper equilibrium conditions have been reached, the feed is switched to the fresh still. The old column continues to operate so as to recover as much terphenyl as is practical. After shutdown, the remaining organic is removed as waste, and maintenance can be accomplished.

e. Waste Disposal - All irradiated organic waste will be disposed of by burial. The waste produced by the system is 211 lbs/hr or twelve 55 gal drums/day. Therefore, one acre of land will provide sufficient ground area to bury 10 years of waste in drums piled 4 high.

If at any time a use can be found for this organic waste, it can be easily recovered from burial and conveniently shipped. Care must be taken, however, to move them only after the residual readioactivity has reached a safe level.

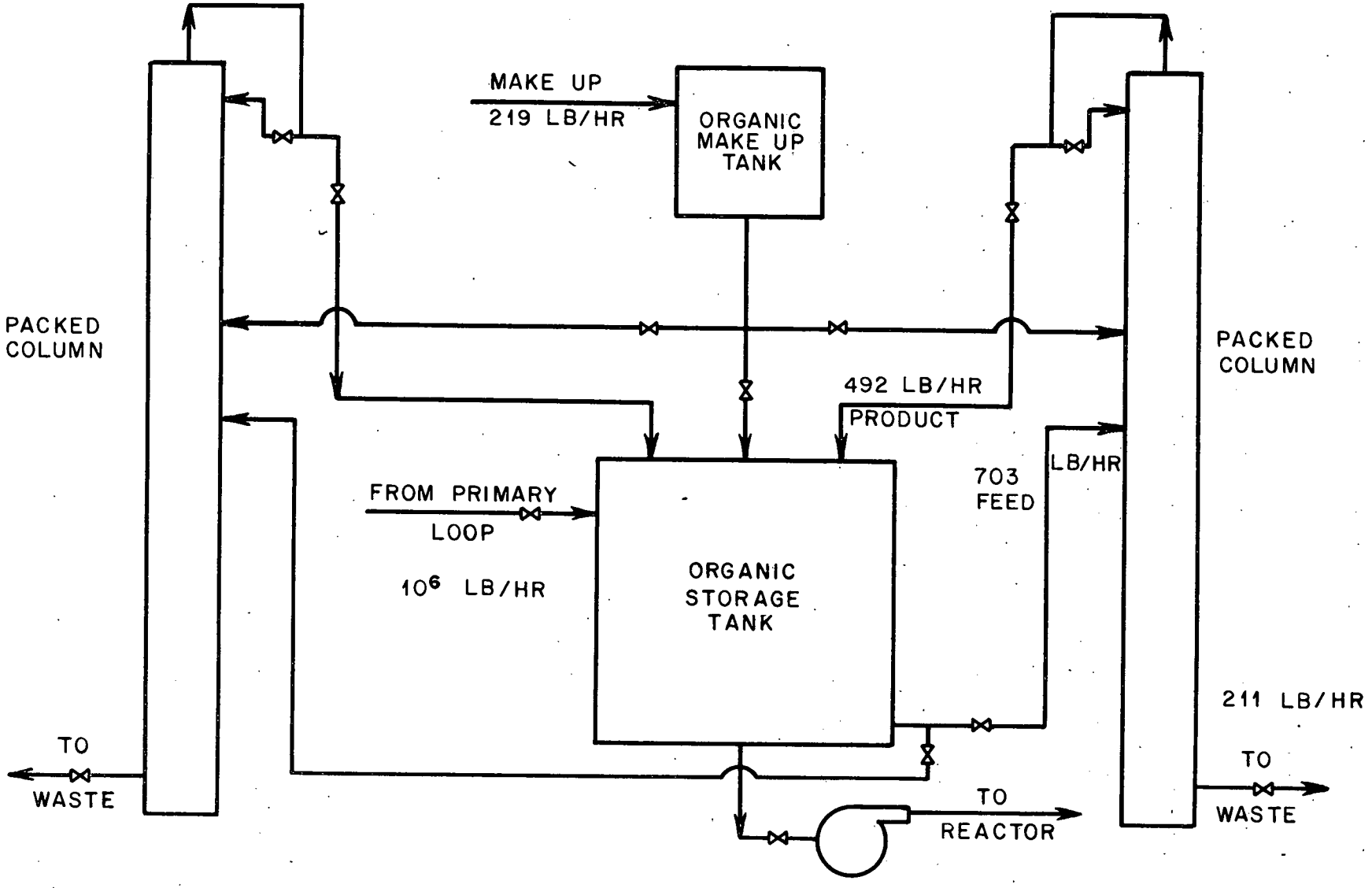

Fig. 25. Organic Makeup and Purification System

Gas, Purge and Gas Disposal System

a. Purpose - During reactor operation, some of the products formed due to the decomposition of the organic coolant, are combustible gases. Also, due to possible leakage of fission gases through ruptured fuel elements, the gases above the organic can be radioactive. Hence a gas purge and disposal system is necessary to provide:

(1) a gas blanket to supplement the vapor pressure of the organic
(2) an inert atmosphere to insure against any possible fires or explosions.
(3) a means of continually removing decomposition gases
(4) a means of safely disposing of any radioactive gases

b. Equipment - The equipment to be used for the gas purge and disposal system consists of the following:

(1) High pressure nitrogen supply and low pressure storage tank (to supply the organic with an inert nitrogen blanket)
(2) Charcoal beds (to absorb any radioactive fission gases that may escape through a fuel element)
(3) Shielded pressurized storage tanks (to store any gases which are too radioactive to exhaust to atmosphere)

c. Description of Cycle(See Figure 26) - The gas formation rate, due to the decomposition of the organic, is 8 lbs/hr. To provide an inert atmosphere and to supplement the vapor pressure of the organic in the reactor, N_2 is added to the gases from a high pressure supply tank through a low pressure storage tank. These gases are continually removed from the system and, after dilution with air, are exhausted through the stack.

d. Charcoal Beds - Before being expelled, the gases are monitored for radioactivity. If the activity is found to be above the allowable limit, the gases must be "stripped" through a charcoal bed before being vented. Gases to be stripped first pass through a cooler so as to increase the absorbing efficiency of the beds.

The radioactivity stripping section contains three charcoal beds in series one of which is used during operation. When a bed becomes spent, gas flow is transferred over to a fresh bed. The spent bed can either be replaced from the line with a fresh one, or if time permits, be slowly stripped with steam and the gases discharged to the atmosphere after air dilution. The latter

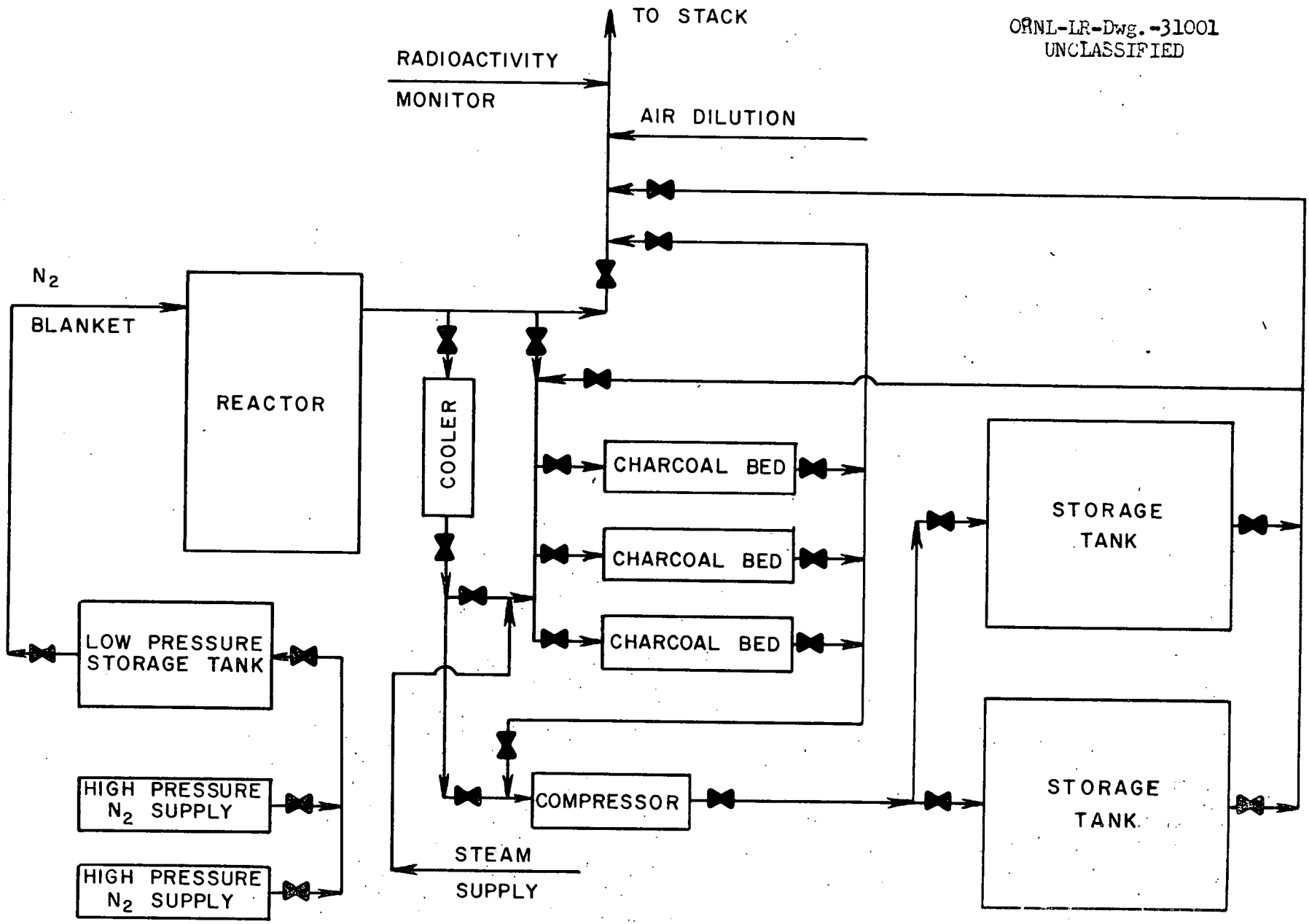

Fig. 26. Gas Purge And Disposal System

alternative can only be accomplished when the reactor exit gas stream does not contain any "hot" constituents.

e. Storage Tanks - If, after stripping, the gases cannot be sent to the stack due to excessive radioactivity, they are sent to a storage tank via the compressor. Under these conditions the reactor must be shut down, and the source of radioactivity is determined and eliminated. In all probability this represents several ruptured fuel elements.

The storage section contains 2 large shielded, pressurized storage tanks. The gases to be stored can either be sent directly to a tank after the cooler, or if more convenient, go through a charcoal bed first. Disposal of the gases in storage is accomplished by slowly releasing them to the atmosphere after air dilution. If necessary, the gases can be kept in the tank awhile before venting.

Reactor Emergency Cooling System - The emergency cooling system includes emergency driven organic pumps, emergency driven feedwater and condensate pumps, emergency driven circulating water pumps, and elevated cooling water and river water storage tanks, Fig. 27.

In an emergency shut down, for example, in the case of total power failure, all pumps will stop and the reactor will scram. Immediately upon any such power failure two 2000 horsepower diesel engines, clutched to the shaft of two organic pumps, will automatically start up in order to supply organic coolant flow through the reactor to remove decay heat. At the same time two 2000 horsepower diesel generators will automatically start up to supply power to the emergency electrical bus. This emergency bus supplies power for two organic pumps (other than the diesel driven ones), a feedwater pump, a condensate pump, two circulating water pumps and an auxiliary transformer for lower voltage emergency demand. The feedwater pump, condensate pump and one circulating water pump start immediately, whereas the two organic pumps start only if the two diesel driven pumps fail to function, and the second circulating water pump starts only if the first one fails to operate or if the return circulating water temperature rises too high. The cooling water in the secondary system bypasses the turbine unit through the bypass valve, which opens in the case of power failure, and goes directly to the condenser.

The valve admitting pure water to the system from the 250,000 gallon emergency cooling water tank will open if the feedwater and condensate pumps

fail; and at the same time the cooling water emergency drain valve on the condenser will open to release this water from the system to the floor drains. If all of the water from this emergency cooling water tank should be used, a deep well pump will start and supply raw water for the cooling. There is enough water in this emergency cooling water tank to remove the decay reactor heat from the organic for approximately 24 hours.

The valve on the 250,000 gallon river water storage tank will open to furnish water to that system if both circulating water pumps fail to operate or provide sufficient cooling water.

REACTOR ANALYSIS

Reactor analysis was done on the Oak Ridge automatic computer (ORACLE) using a code for large heterogeneous reactors. The code[2-1] is based on a one-group Fermi age model, which is considered adequate for large, heavy water moderated thermal reactors. A complete description of the mathematical basis of the code, the calculations required to obtain code inputs and the valves of the inputs for this reactor are given in Appendix A.

Core and Nuclear Design Data

The reactor core is a right circular cylinder, 16 feet high and 16.92 feet in diameter, surrounded by a six inch thick heavy water reflector. Table 5 gives the basic design data for the core. Basic design data for the fuel element are given in Section I.

TABLE 5

REACTOR CORE DESIGN DATA

Diameter (unreflected), ft	16.92
Diameter (reflected), ft	17.92
Height (unreflected), ft	16.00
Height (reflected), ft	17.00
Reflector	D_2O
Number of elements	745
Fuel Inventory (UO_2), tons	119
Cell spacing (hexagonal), inches	7.0

TABLE 6

NUCLEAR DESIGN DATA - HOT, CLEAN REACTOR

k_{eff} (hot, clean)	1.089
k_∞ (hot, clean)	1.120
η	1.33
f	0.946
p*	0.865

*Resonance escape probability and age from fission to resonance for each uranium and plutonium isotope are given in Appendix A.

TABLE 6 (Con't)

ϵ	1.036
Non-fast leakage probability	0.977
Non-thermal leakage probability	0.990
L^2, cm^2	67.2
$\tau_{thermal}, cm^2$	203
B^2(reflected), cm^{-2}	1.139×10^{-4}
Reactivity lifetime, MWD/ton	3050
Reactivity lifetime, days (full power)	495
Initial Conversion Ratio	0.686
Power, heat megawatts	800
Power density, watts/cm^3(unreflected core)	7.80
Thermal flux, neutrons/cm^2-sec	2.55×10^{13}
Moderator temperature, ^oF	200
Neutron temperature, ^oF	260
Δ k, equilibrium Xe^{135} and Sm^{149}, %	-3.4

Nuclear design data for the hot, clean reactor are given in Table 6. Data for room temperature are not given because the reactor must be kept at a minimum temperature of 300°F during shutdown to insure that the terphenyl coolant does not freeze. Sufficient control with rods alone exists to keep the reactor sub-critical to moderator temperature of 0°C should external heating fail during shutdown (See Section I). Should danger of lower temperature exist, all or part of the moderator may be drained from the core.

Lattice Spacing

The size of the core and the design of the fuel element were determined primarily by heat removal considerations. The number of elements and their spacing were determined by heat removal, reactor analysis and economic considerations.

The primary objective of reactor analysis was to determine the lattice spacing that would give maximum fuel lifetime. The optimum figure given by analysis was first reconciled with heat removal requirements and finally with the overall design objective of minimum power cost. Fig. 28 shows

results of the initial parameter study made to establish lattice spacing. In this study the following parameters are fixed throughout:

(1) Core size - the smallest size consistent with heat removal and D_2O inventory requirements,

(2) Fuel element composition and configuration.

These parameters vary:

(1) Lattice spacing

(2) Fuel loading (fixed for given spacing)

Fuel loading, initial conversion ratio and fuel lifetime for hexagonal lattice spacings are:

Lattice spacing (inches)	Fuel Loading (tons)	Lifetime (MWD/ton)	Initial Conversion (ratio)
6	168	2030	0.77
7	119	3050	0.68
8	96	3140	0.64
9	78	3110	0.62
10	71	3100	0.61

The eight inch lattice gave maximum fuel lifetime, but lifetime was found to be relatively independent of spacing for spacing greater than 6.75 inches. Initial conversion ratio decreased rapidly with increased spacing. While the eight inch lattice gave maximum lifetime, seven inches was selected for further study because it gave:

(1) nearly maximum lifetime

(2) high conversion ratio, and

(3) a fuel loading that

  (a) met all heat transfer requirements

  (b) gave low neutron flux and high initial excess reactivity.

The low flux decreases reactivity loss due to equilibrium xenon and samarium and, combined with high initial reactivity, minimizes xenon override problem in case of shutdown.

A second parameter study was made to confirm and expand the results of the first. In this study the following parameters were fixed throughout:

(1) Fuel loading (119 tons, from first study)

(2) Fuel element number, composition and configuration

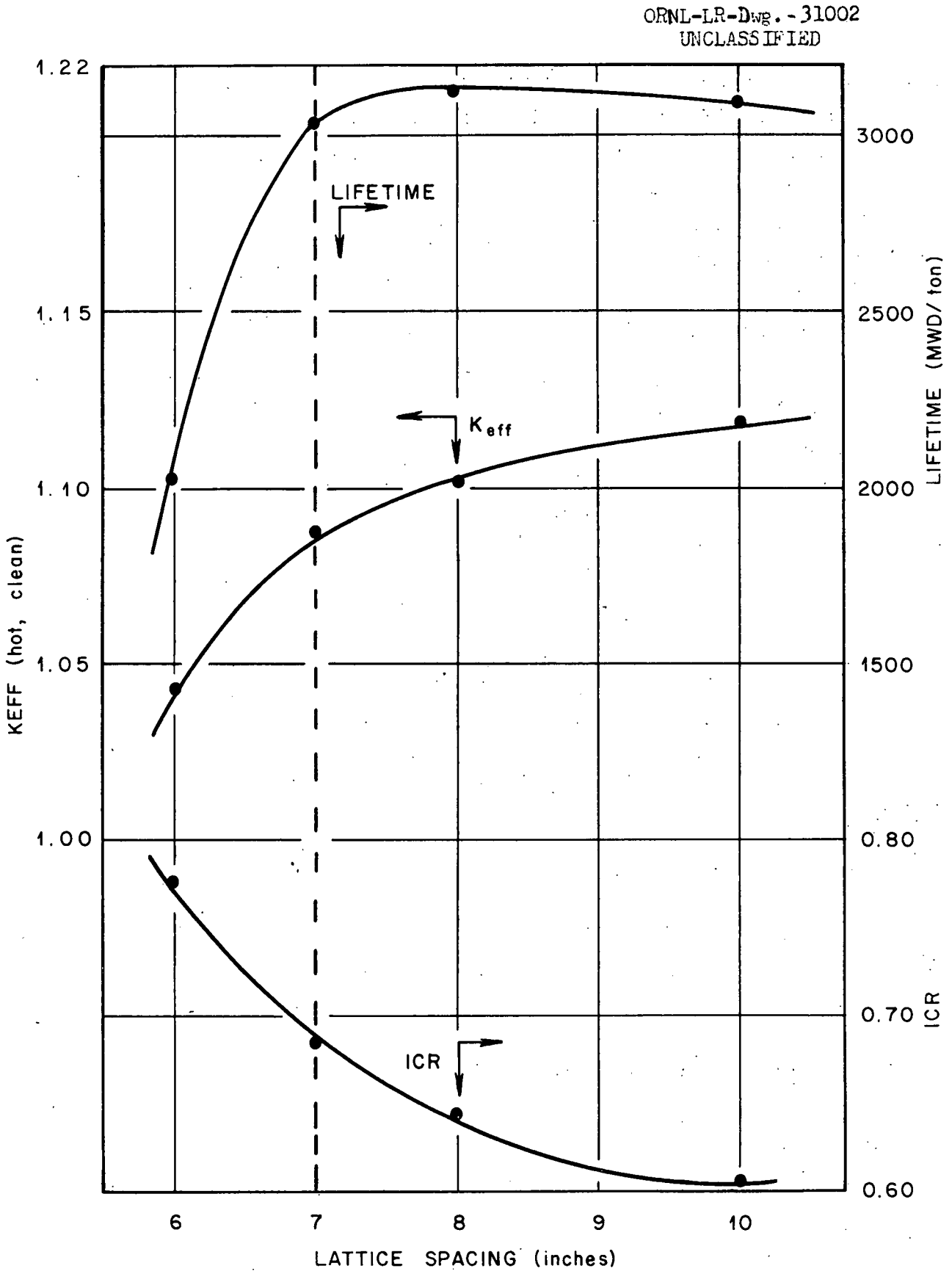

Fig. 28. Initial Reactivity, Initial Conversion Ratio and Lifetime vs. Lattice Spacing

(3) Core length (16 feet

These parameters varied:

(1) Lattice spacing

(2) Reactor diameter

Results are shown in Fig. 29. Core diameter, fuel lifetime and initial conversion ratio for lattice spacings are:

Lattice Spacing (inches)	K_{eff} Initial	Core Diameter Unreflected (feet)	Lifetime (MWD/ton)	Initial Converstion Ratio
6	1.058	13.6	1475	0.77
7	1.088	16.9	3050	0.68
8	1.110	18.6	3350	0.64
9	1.125	20.4	3500	0.62
10	1.133	22.6	3475	0.61

Maximum lifetime occurred with nine inch spacing, but once again lifetime was relatively independent of spacing for spacing greater than 6.75 inches. Initial conversion ratio fell off sharply with increased spacing and D_2O inventory requirements rose rapidly with increased diameter.

A very rapid fall-off in lifetime and k_{eff} occurred for spacing less than seven inches. At six inches k_{eff} was so low that after reactivity loss due to xenon and samarium (3.4%) was subtracted the remaining reactivity is only 0.006. The accuracy of the code is not believed such that design could be based on such a narrow margin even if the economics (through higher conversion ratio) showed such a spacing desirable.

Figure 30 shows Pu^{239} concentration versus lifetime for several lattice spacings. For example, at 3000 MWD/ton and end of life, Pu^{239} concentrations are:

Lattice spacing (inches)	Pu^{239} Concentration, 3000 MWD/ton (grams/ton U)	Pu Concentration end of lifetime (grams/ton U)
6	---	2680
7	2060	2080
8	1600	1650
10	940	980

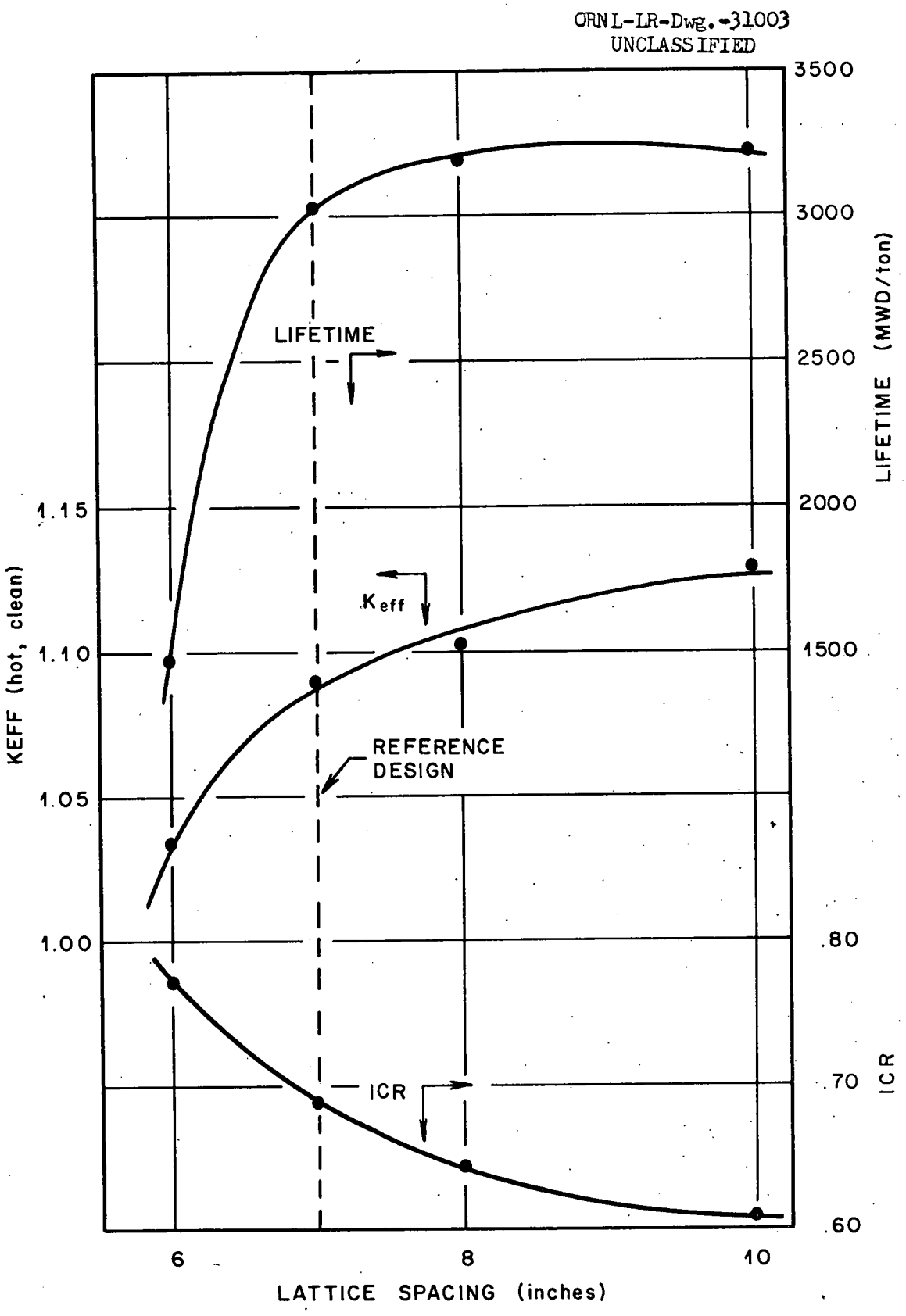

Fig. 29. Initial Reactivity, Initial Conversion Ratio and Lifetime vs. Lattice Spacing Fuel Loading = 119 Tons UO_2.

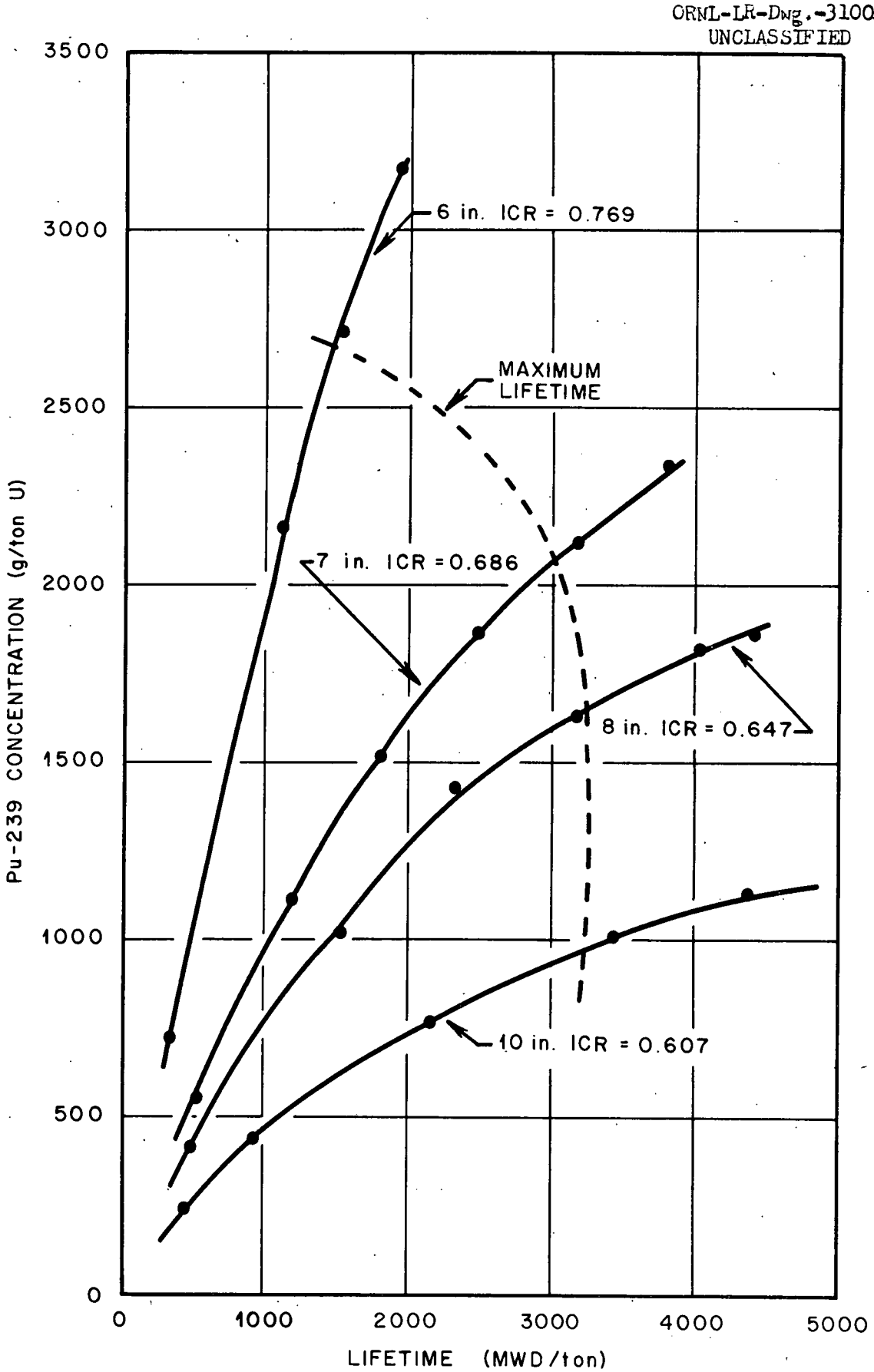

Fig. 30. Pu^{239} Concentration for Various Lattice Spacings

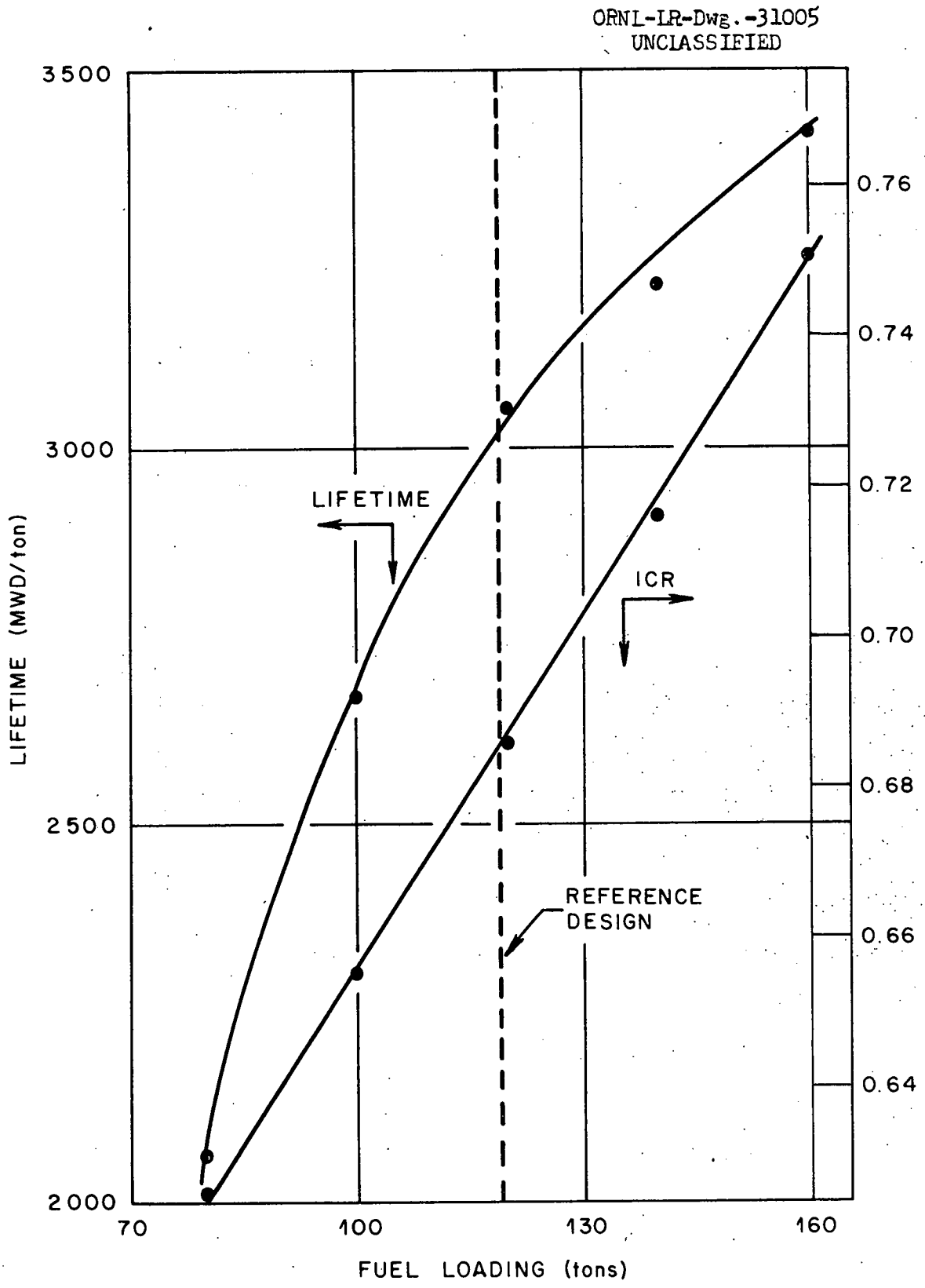

Fig. 31. Lifetime and Conversion Ratio vs. Fuel Loading.

The figures show the price paid in loss of plutonium to get slightly longer lifetime by wider lattice spacing. The economics of the reactor are largely governed by plutonium credit (see Section VI), so every effort is made to maximize plutonium credit.

On the basis of these two parameters studies a hexagonal seven inch lattice spacing was selected. This spacing gives:

(1) nearly maximum fuel lifetime

(2) High initial conversion ratio and net plutonium production, without undue sacrifice of reactivity and lifetime

(3) high enough initial reactivity to overcome xenon override through out most of lifetime (See H below) and

(4) a reactor of reasonable size.

Tables 5 and 6 give the important data on the reference design core.

Fuel Loading Optimization

Figure 31 shows the results of a study of the effect of fuel loading on fuel lifetime and initial conversion ratio. In this study the following parameters were constant:

(1) core size (h = 16', d = 16.9')

(2) lattice spacing (7 inches)

(3) number of fuel elements (745)

The fuel loading was varied by varying the diameter of the fuel rods.

Important results from this study are:

Fuel loading (tons)	Pu^{239} Concentration 3000 MWD/ton (gms/ton U)	Pu^{239} Production 3000 MWD/ton (Kg/year)
80	--	--
100	--	--
120	2020	158
140	2200	171
160	2320	181

The effect of the increased plutonium production on net fuel cost was studied. The lower cost due to the plutonium is partially offset by greater

fuel inventory and fabrication costs, but a net decrease of about 0.2 mil per KWH could be realized by using 160 tons of UO_2 rather than 120 tons. The decision of fuel loading had to be made before this study was completed, so the design fuel loading is not optimum.

Fuel Enrichment

Figure 32 shows the dependence of lifetime, initial reactivity and initial conversion ratio of fuel enrichment. Reference design core and fuel element were used. The results of the study are summarized below:

Enrichment (% U^{235})	Lifetime (MWD/ton)	Pu Concentration 3000 MWD/ton (gm/ton U)	Pu Concentration 3000 MWD/ton (Kg/year)
0.713	3050	2050	158
0.90	5400	1960	153
1.20	8750	1750	137

The effect of enrichment on net power cost is analyzed in Section VI. Natural uranium gives the lowest cost.

Fuel Density

UO_2 density of 10.0 grams/cm^3 was assumed in all previous studies and in the reference design. Since UO_2 density can vary greatly with fabrication method[2-2], a study was made of the effect of density on lifetime. Reference design was used except for fuel density (and consequently fuel loading). Figure 33a shows the results of this study, which are summarized below:

UO_2 Density (gm/cm^3)	Fuel Loading (tons)	Lifetime (MWD/ton)
9.5	113	2810
10.0	119	3050
10.5	125	3460

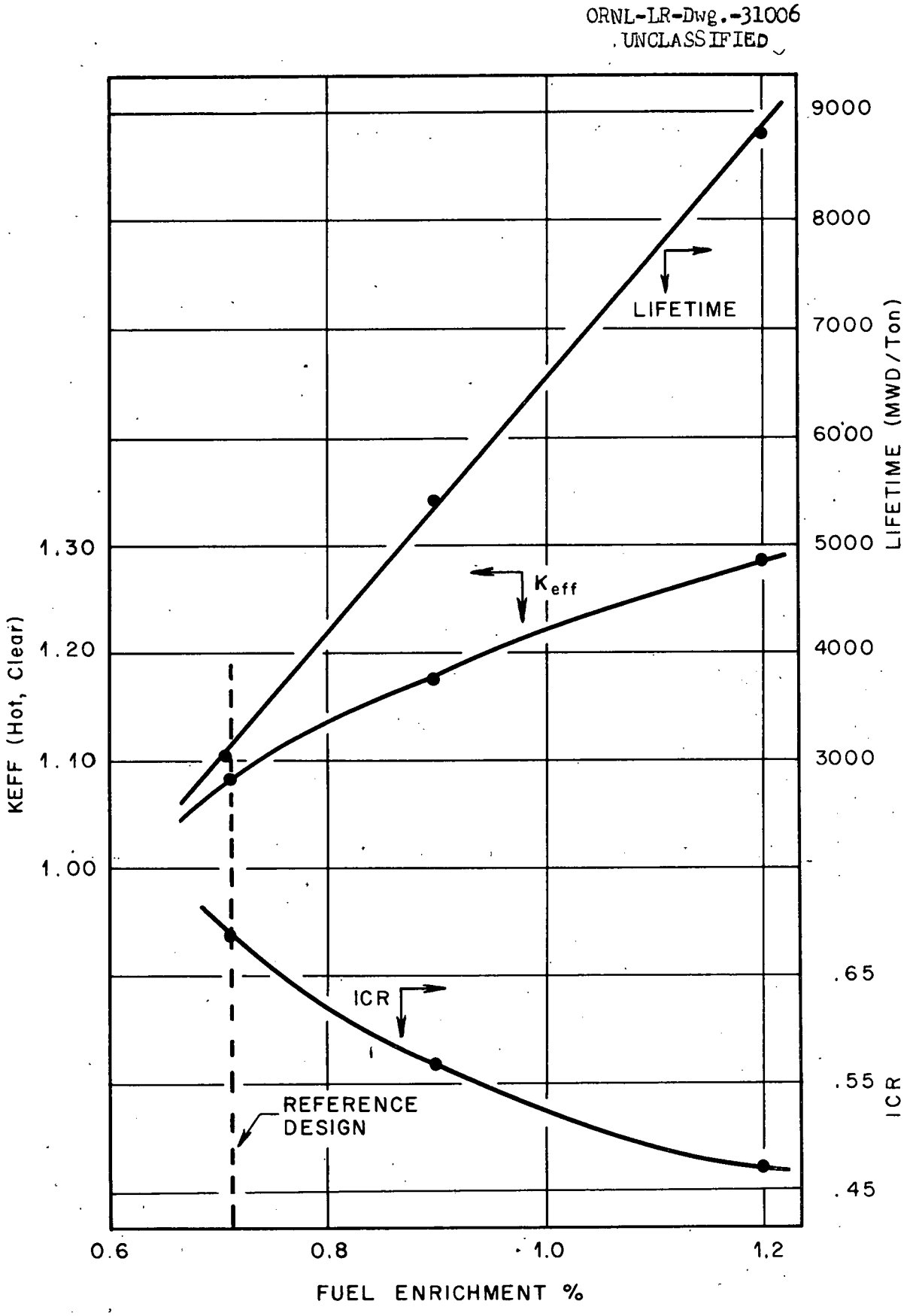

Fig. 32. Initial Reactivity, Initial Conversion Ratio and Lifetime vs. Fuel Enrichment

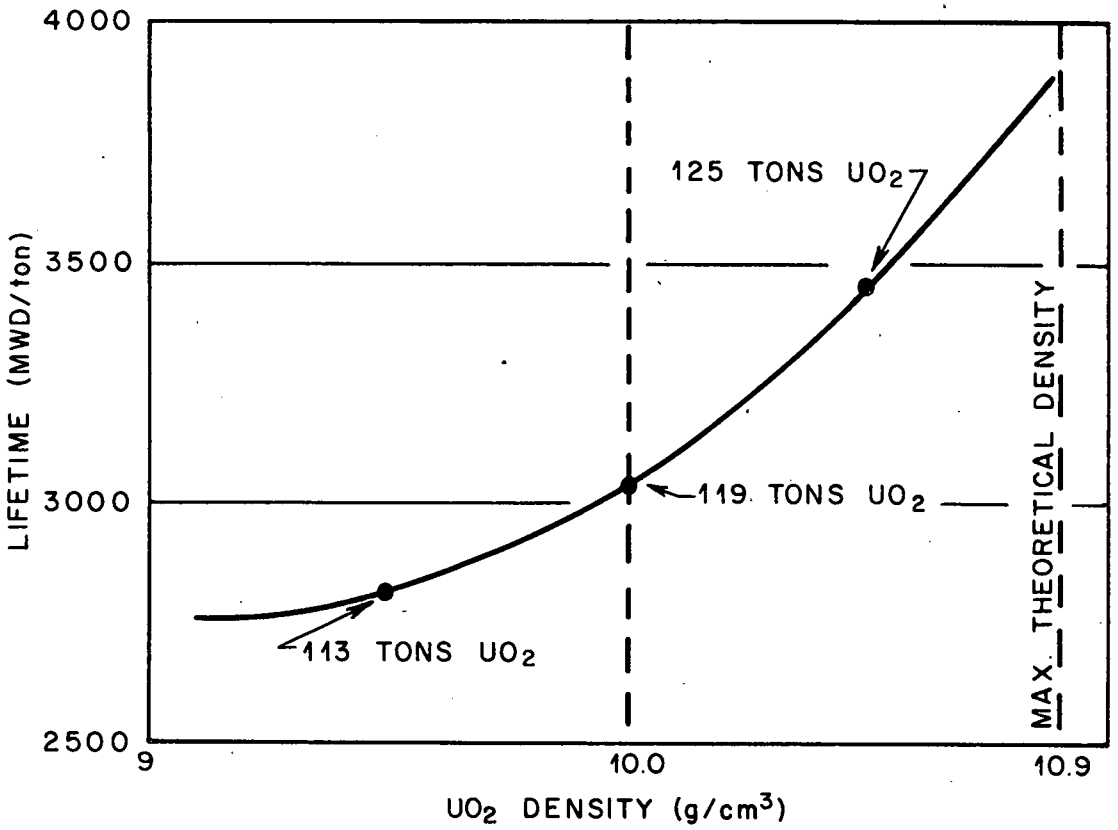

Fig. 33A. Lifetime vs. UO_2 Density

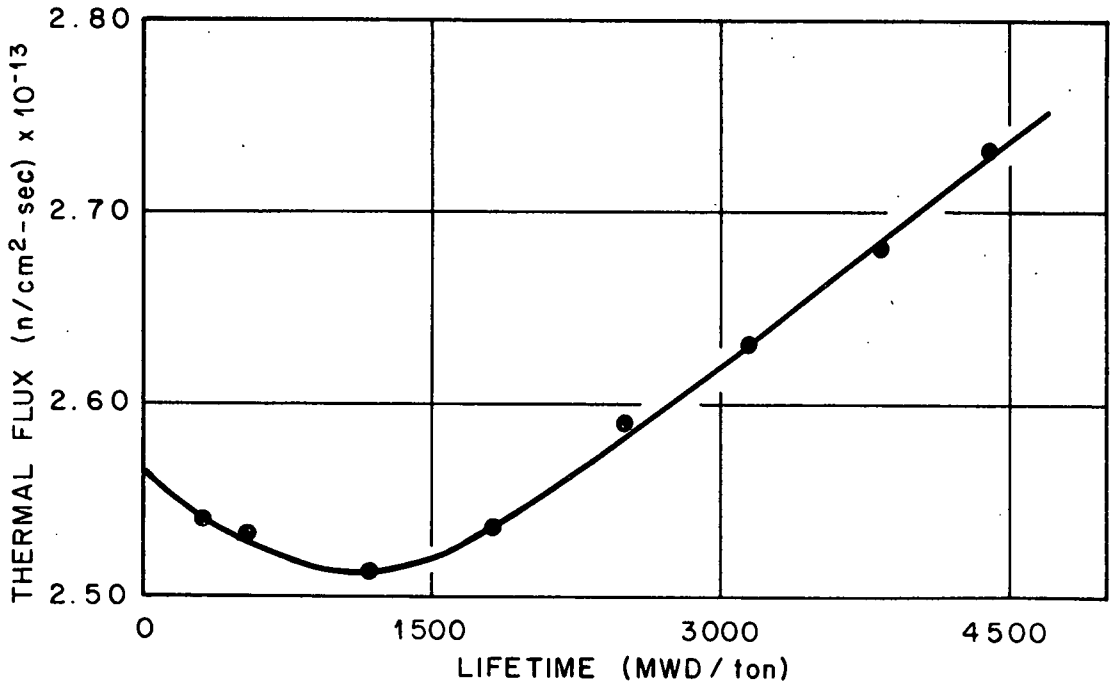

Fig. 33B. Thermal Flux vs. Lifetime

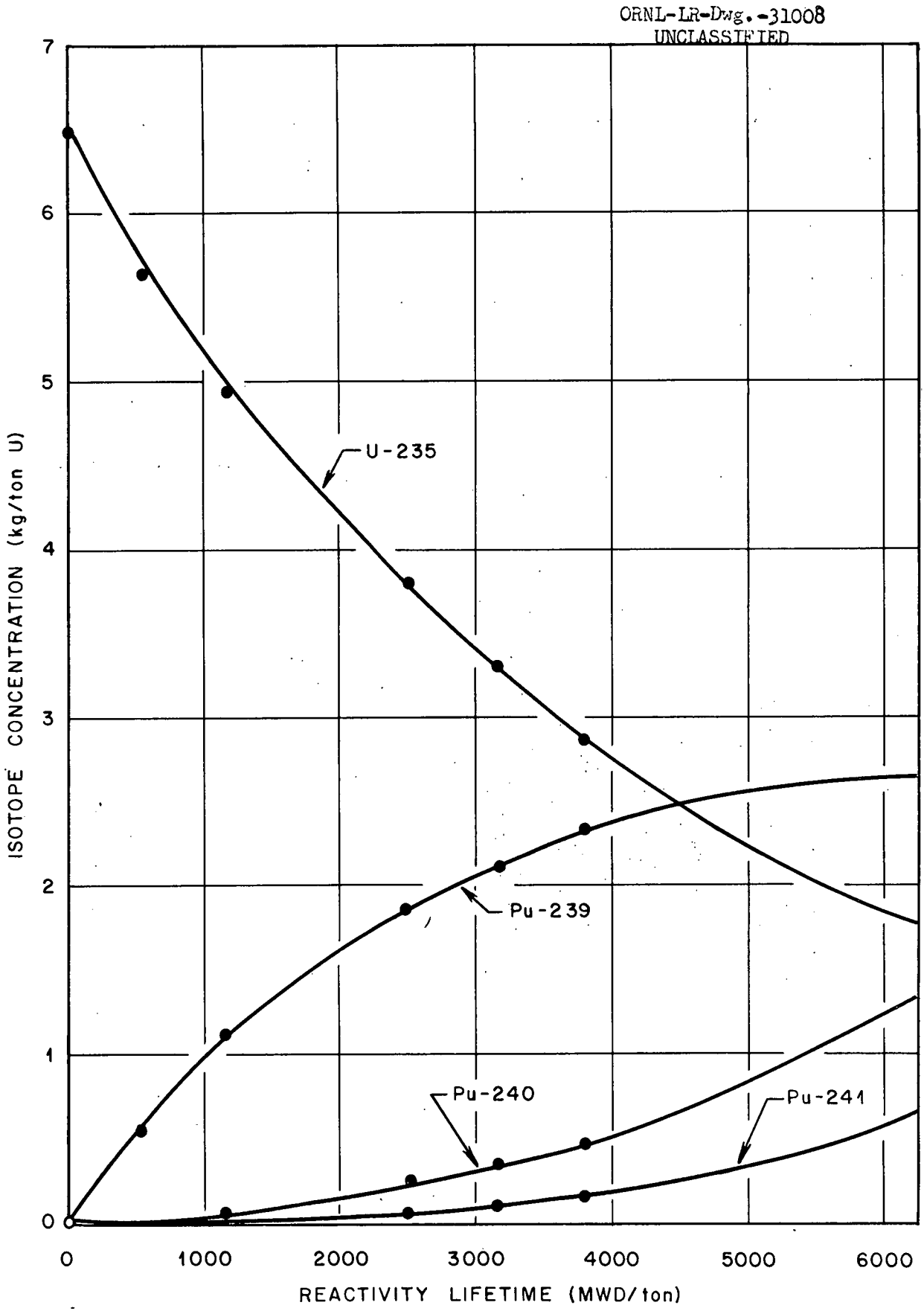

Fig. 34. Isotope Concentration Vs. Reactivity Lifetime

UNCLASSIFIED
ORNL-LR-DWG. 31009

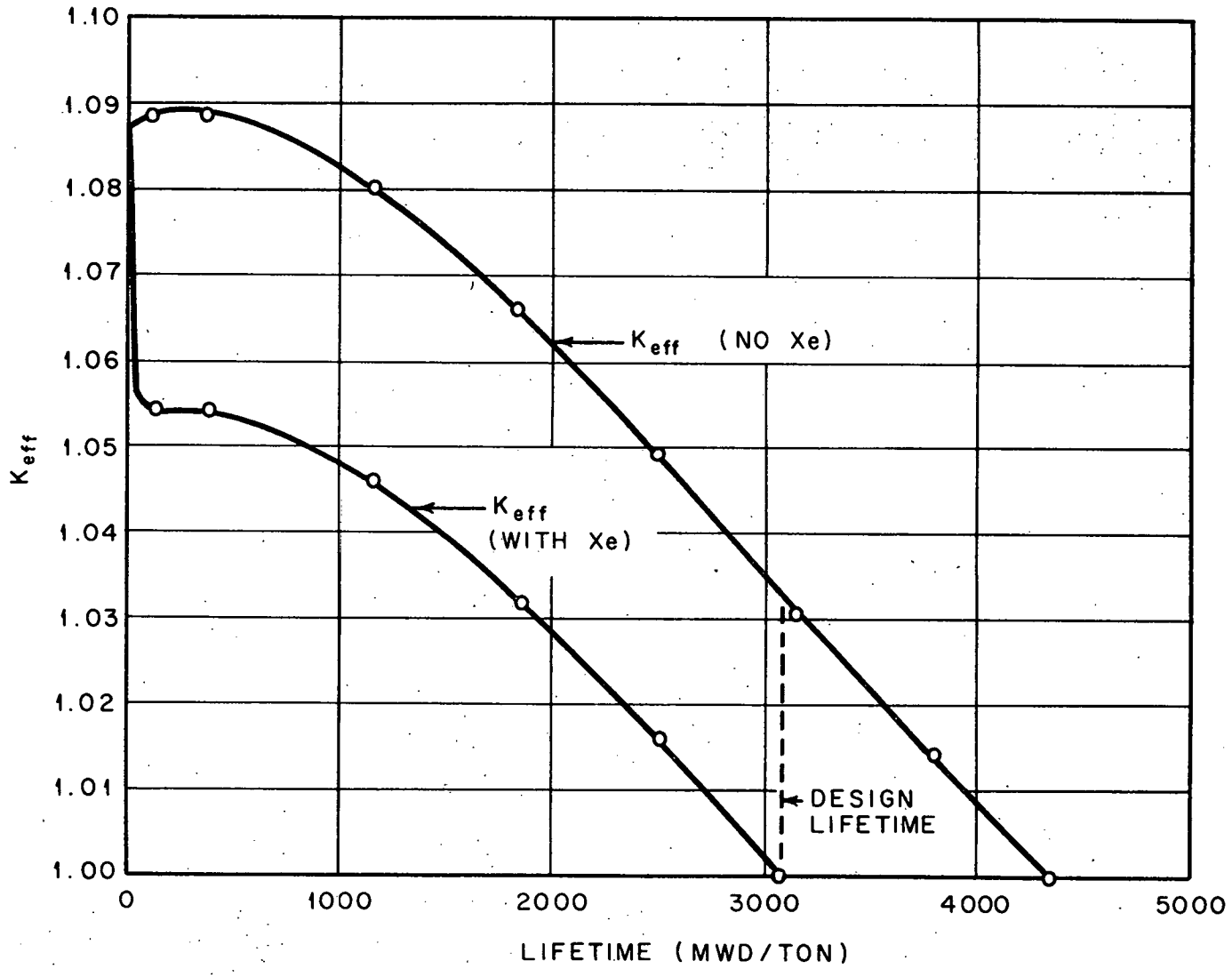

Fig. 35. K_{eff} vs. Fuel Lifetime

Isotope Concentrations

Figure 34 shows the concentration of U^{235} and the three principal plutonium isotopes as a function of fuel lifetime. The concentrations at end of life are:

Isotope	Concentration 3050 MWD/ton (g/tonU)
U^{235}	3320
Pu^{239}	2100
Pu^{240}	375
Pu^{241}	100

Thermal Neutron Flux

Reactor analysis calculations were based on constant power density. Since fuel concentrations vary with time, the thermal flux must also vary to keep power density constant. Figure 33b shows the variation of thermal flux (mean flux for the core) with lifetime.

The initial drop in flux shows the increase in macroscopic fission cross-section caused by rapid Pu^{239} buildup (see Figure 34). The later rise in flux shows the decrease in macroscopic fission cross section which occurs when increase in Pu^{239} and Pu^{241} macroscopic fission cross-section no longer is equal to or greater than loss of U^{235} macroscopic fission cross-section. This is the result of low conversion ratio and the parasitic absorption of neutrons by Pu^{239} to form non-fissionable Pu^{240}.

Xenon and Samarium Buildup and Override

Figure 35 shows the variation of k_{eff} with fuel lifetime. The upper curve is k_{eff} without Xe and Sm, the lower curve is k_{eff} with Xe^{135} and Sm^{149} reactivity loss included.

The loss due to xenon is given by the formula (modified from 2.3) for natural uranium reactors:

$$\Delta k \cong \frac{y \, \Sigma_{f_U} / \Sigma_{fuel}}{1 + \lambda / \sigma_{a\,T} \phi_T} \cong \frac{.0312}{1 + \frac{6.0 \times 10^{12}}{\phi_T}} \quad \text{(for natural uranium)}$$

where y = yield fraction of Xe^{135}

λ = radioactive decay constant of Xe^{135}

ϕ_T = thermal neutron flux in neutrons/cm^2 - sec.

For a mean flux during lifetime of 2.55×10^{13} neutrons/cm^2 - sec (see Fig. 33b) and $\Delta k \cong -2.5\%$. The fuel element contains a hole in the center where xenon will accumulate. Since thermal flux is least at the center of the rod, xenon effect will actually be somewhat less than these figures indicate. A Δk of -2.2% was therefore used for xenon equilibrium.

Reactivity loss due to Sm^{149} is independent of thermal flux and is about 1.2 % at equilibrium [2-4]. Total reactivity loss due to equilibrium xenon and samarium poisoning is 3.4%.

After instantaneous shutdown the concentrations of xenon and samarium increase with time. Changes in reactivity due to increased samarium concentration is slight, about -0.3%, for a flux of 2.55×10^{13} neuts/cm^2-sec [2-4]. Xenon concentration increases significantly with time after shutdown, reaches a maximum in about twelve hours and then decreases slowly. At time of maximum xenon concentration, an excess reactivity of about 9% would be necessary to overcome the xenon and samarium poisoning and permit startup.

The control system must therefore be designed to minimize unnecessary shutdown, and required shutdowns should be for short periods (or very long periods) only. Table 7 shows [1] the maximum allow shutdown time to permit immediate start up and [2] the waiting time to startup should the maximum allowable shutdown be exceeded [2-3].

TABLE 7

MAXIMUM ALLOWABLE SHUTDOWN

Fuel lifetime (MWD Hour)	Maximum allowable shutdown time (hours)	Waiting time if maximum exceeded (hours after shutdown)
500	9	10
1000	8	13
1500	6	18
2000	3	25
2500	1	30
3000	0.1	40

Effect of Reflector

The effect of reflector thickness on initial reactivity and lifetime are summarized below:

Reflector Thickness (inches)	Initial Reactivity	Lifetime (MWD/ton)
0	1.085	2950
6	1.089	3050
10 (effectively ∞)	1.091	3140

It can be seen that reflector thickness has little effect on fuel lifetime. To minimize D_2O inventory and pressure vessel size, less than effectively infinite reflector was used.

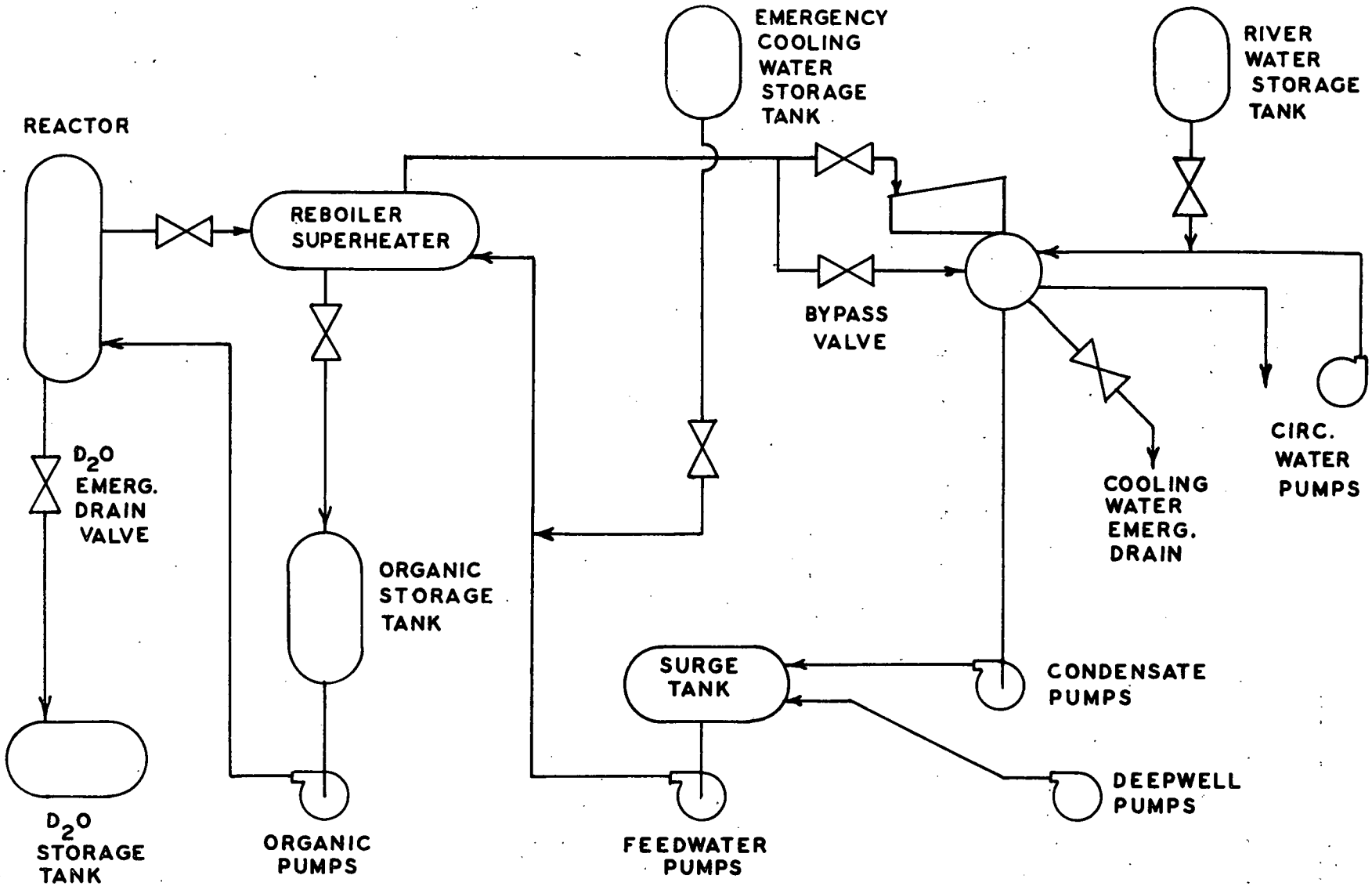

REACTOR EMERGENCY COOLING SYSTEM

Figure No. 27

MATERIALS

Introduction

The criteria for the selection of the materials for this reactor were to a great extent established by the nature of the study itself; that is, the feasibility of an organic cooled, D_2O moderated, natural uranium fueled, power reactor. Thus the moderator was fixed, the general type of coolant was fixed, and the area of selection of the actual type of fuel was severely limited. Furthermore, the use of natural uranium imposed the necessity of great neutron frugality, and the aim for a power reactor (as competitive with present power stations as possible) imposed restrictions on the cost of materials and of the cost of material fabrication.

The approach to the problem taken by this group established a further criterion: it was determined that wherever possible known technology would be used in the design. This has not been possible in every area, i.e., the fuel rod cladding, but it is felt that the material selected would require the least amount of development to provide satisfactory service. Other criteria were, of course, compatability of materials and, particularly with regard to the organic selection, to make the best use of the inherent advantages of the system under study.

On the basis of these criteria the following reactor material selection was made:

Fuel - UO_2
Fuel cladding - Al alloy, X-2219
Fuel assembly tube - Al alloy, X-2219
Process tube - Al Alloy, 61S-T6
Tube sheets - Alfin Clad carbon steel, SA-212B
Pressure vessel - Carbon Steel, SA-212B
Moderator and Reflector - D_2O
Coolant - "Santowax-R"*

Some of these materials will be discussed in detail below.

* A commercially available mixture of polyphenyl compounds consisting mainly of the isomeric terphenyls.

Fuel and Fuel Cladding

The individual fuel rods, the fuel element bundles, and the fuel element assembly, as well as the heat transfer characteristics of the elements are described under the section on Engineering. To some extent the individual fuel rods are patterned after the blanket elements proposed for the Pressurized Water Reactor[3-1]. That is, natural uranium in the form of sintered UO_2 disks is contained in a closed cylindrical can. The choice of UO_2 disks rather than metallic uranium slugs was dictated by the fear of severe dimensional changes in uranium slugs effected by relatively short "in pile" operation. This problem, which has been studied at Hanford and elsewhere for some years, does not appear to be near enough solution to warrant the use of metallic uranium in a reactor of this design and for this purpose. Table 8 compares some of the pertinent properties of uranium metal and UO_2.

TABLE 8

COMPARISON OF SOME PROPERTIES OF UO_2 AND URANIUM METAL

	Density	Fission Product Gas Release	Dimensional Stability
Uranium Metal	18.7 gm/cc	No problem	Poor
UO_2	10.9 gm/cc (theoretical)	Can be a serious Problem	No problem

On the basis of the properties listed in Table 8 it is apparent that selecting UO_2 over uranium metal, while obviating the problem of dimensional in stability, introduces two other problems: a substantial reduction in density from that of uranium metal and a possible internal pressure build-up caused by fission product gases. The lower density of UO_2 is compensated by increasing the size of the reactor. This increase in size is not of a magnitude to greatly effect the reactor design. The problem of pressure buildup from fission product gases is not as easily disposed of; this problem is discussed in the section of Fuel Element Stress Analysis. The technology of the production and fabrication of UO_2 specimens has progressed very rapidly in the last few years[3-1,3-2].

It is now possible to prepare sintered disks of a specified fraction of the theoretical density by control of the particle size and the conditions of pressing and sintering. Further, it is possible to make these disks within quite restrictive dimensional tolerances so that little machining of the finished product is necessary. Thus the fabrication of the fuel sections for this reactor does not appear to present any serious problems. Some of the important physical and thermodynamic properties of UO_2 are listed in Table 9.

TABLE 9

PROPERTIES OF URANIUM DIOXIDE[3-2]

Property	Temperature (°C)	Value
Melting Point	2405	
Thermal Conductivity (cal/sec/°C/cm) Extrapolated from 73% to 100% of theoretical density	200	0.0190
	400	0.0138
	600	0.01055
	800	0.00885
	1000	0.00815
Heat Capacity (cal/gm/°C)	100	0.063
	200	0.067
	500	0.074
	1000	0.078
	1500	0.082
Heat of Formation (cal/mole)	25-1200	-259,500 $\pm$ 2,000
Free energy of Formation (Cal/mole	25	-246,600
	1227	-197,700
Heat of Fusion (cal/mole)	2405	16,000
Heat of Vaporization (cal/mole)		137,000
Entropy (cal/mole/°C)	25	18.6
Vapor pressure (mm of Hg)	1326	1.65×10^{-8}
Coefficient of Linear Expansion (cm/cm/°C)	27-400	9.1×10^{6}
	400-800	10.8×10^{6}
	800-1260	13.0×10^{6}

Theoretical Density (gm/cm^3)	26	10.968
Young's modulus of elasticity (psi)	20	25×10^6
Modulus of rupture (psi)	25	10,000 - 12,000

The cladding material proposed for the PWR blanket fuel elements is Zircaloy[3-1]. Other possibilities include stainless steel, aluminum and magnesium. Table 10 compares, qualitatively, some important properties of these cladding materials with reference to this reactor.

TABLE 10

QUALITATIVE COMPARISON OF SOME PROPERTIES OF POSSIBLE CLADDING MATERIALS

	Thermal Neutron Absorption Cross-section	Compatibility with Organic	Strength at Relatively High Temperature	Cost
Zircaloy	Excellent	Poor	Good	High
Stainless Steel	Poor	Good	Excellent	Medium
Aluminum	Good	Good	Poor	Low
Magnesium	Excellent	Fair	Poor	Low

Stainless steel will be used as the cladding material in the Organic Moderated Reactor Experiment[3-3]. The resistance to corrosion of stainless steel in a high temperature (600-800°F) organic medium has been demonstrated[3-4,3-5]. Stainless steel possesses excellent mechanical properties at the temperature being considered. Despite these qualities the use of natural uranium in this reactor precludes the use of stainless steel because of its high neutron absorption.

Zircaloy rates high on two points; its low neutron absorption cross-section and its good strength at 700-800°F. However, Zircaloy is subject to excessive embrittlement in organic media at these temperatures[3-4,3-5]. This

embrittlement is the result of hydride formation, the source of hydrogen being the radiolytic decomposition of the organic. Thus, unless Zircaloy could be protected by an impervious cladding, its service life in this reactor would be severely limited. Application of such a cladding on Zircaloy may be possible, but it is far from being standard practice. Furthermore, the high cost of zirconium and the high cost of its fabrication argue against its use in a reactor that purports to provide relatively low cost power.

Magnesium and aluminum fall into the same general category; they are both low cost metals, their compatibility with organics is acceptable, They have low neutron absorption cross sections, and the metals and their alloys have low strength at 700-800°F. Since the major problem with these metals is strength, and since magnesium alloys generally are not as strong as aluminum alloys, magnesium was given no further consideration.

Thus, having somewhat arbitrarily disposed of stainless steel, zirconium, and magnesium, it remains to choose an aluminum alloy that will withstand the expected loads on the fuel element cladding at temperatures up to 750°F. This task is made very difficult because of the lack of experimental data on the mechanical properties of aluminum alloys at this temperature. Some data are available on the tensile and yield strengths of the more common aluminum alloys as a function of temperature up to 700°F. These data are included in the tables of properties (Table 11 and 12) of the alloys 61S and 75S.

TABLE 11

MECHANICAL PROPERTIES OF ALUMINUM ALLOY : 61 S-T6

Property	Temperature	Value
Density (gm/cc)	70°F	2.70
Liquid	1205°F	
Specific Heat (cal/gm)	212°F	.23
Thermal Expansion (per °F)	68°F to 212°F	.000013
Thermal Conductivity (cal/sq cm/cm/°C/sec)	77°F	.37
Recrystallization Temperature (75% Reduction)	650°F	
Modulus of Elasticity (psi)		10×10^6
Poisson's Ratio		.33

Composition: Al-1.0 Mg - .6 Si - .25 Cu - .25 Cr

Property	Temperature(°F)					
	75	300	400	500	600	700
Tensile Strength(psi)	45000	31000	19000	7500	3500	3000
Yield Strength (psi	40000	29000	15000	5000	2500	2000
% Elongation	15	23	29	55	90	105

TABLE 12

MECHANICAL PROPERTIES OF ALUMINUM ALLOY: 75S -T6

Property	Temperature	Value
Density gm/cc	68°F	2.80
Liquid	1180°F	
Thermal Expansion (per °F)	68°F to 572°F	.0000145
Specific Heat (cal/gm)	212°F	.23
Thermal Conductivity (cal/cm^2/cm/°C/sec)	77°F	.29
Recrystallization Temperature (50% reduction)	775°F	
Modulus of Elasticity (psi)		10.4 x 10^6
Poisson's Ratio		.33

Composition : Al - 5.5 Zr - 2.5 Mg - 1.5 Cu - .3 Cr - .2 Mn

Property	Temperature (°F)					
	75	300	400	500	600	700
Tensile Strength (psi)	88000	25000	15000	12000	8500	6500
Yield Strength (psi)	80000	22000	12000	8000	6000	5000
% elongation	10	32	55	60	68	75

Of more significance than the short time tensile and yield strengths of the alloys are creep and rupture strengths. Mr. J. E. Cunningham of the Metallurgy Division of ORNL has provided some data on the creep strengths of some high strength aluminum alloys.* This data is reproduced in Table 13.

* Mr. Cunningham obtained this information from E. T. Wanderer of the Alcoa Research Laboratory in New Kensington, Pennsylvania.

TABLE 13

CREEP STRENGTH DATA ON SELECTED HIGH STRENGTH ALUMINUM ALLOYS

Creep Level	Time Hr.	Temp. °F	Creep Strength in psi of Indicated Alloy: 7075 75S	M-257 Al_2O_3 Pulver	X-2219 Experimental
Rupture	1	600	7000	14000	15000
Rupture	10	600	5500	13000	12000
Rupture	100	600	4500	11500	9000
Rupture	1000	600	3500	10000	6500
1% Deformation	1	600	6000	14000	13000
"	10	600	4500	12500	10000
"	100	600	3500	11000	7500
"	1000	600	3000	10000	6000
.5% deformation	1	600	5500	14000	12000
"	10	600	4000	12000	9000
"	100	600	3000	10500	7000
"	1000	600	2500	-	5000
.1% deformation	1	600	3500	9500	7500
"	10	600	2500	--	5000
"	100	600	2000	--	3500
"	1000	600	1500	--	2000

It will be noted that all the data in Table 13 were obtained at 600°F. Unfortunately, data at higher temperature were not available and in order to predict the behavior of these materials at 750°F an extrapolation must be made. Some limited data are available on the creep strength of M-257 versus temperature[3-6]. These data indicate a decrease in creep strength to cause 0.5% extension in 100 hours from 15,000 psi to about 10,000 psi when the temperature is raised 200°F (400°F to 600°F). If this behavior is assumed to be a linear function of the temperature, an increase in temperature from 600°F to 750°F would reduce the creep strength by roughly one third. For most metals and alloys this is not a linear relationship, in fact at higher temperatures the slope changes in such a way that the decrease in strength

per increase in temperature becomes less.[3-7] None the less it will be assumed here that the slope changes in the opposite way, i.e., that the rate of decrease in strength with increasing temperature increases. Two extrapolations will be used: one assuming that the strength decreases by a factor of two for an increase in temperature from 600°F to 750°F, the other will assume a decrease factor of four. The former extrapolation will be referred to as the "$\frac{1}{2}$" extrapolation and the latter as the "$\frac{1}{4}$" extrapolation. The data from Table 13 as well as the two extrapolations mentioned above are plotted for the 75S and the X-2219 alloy in Fig. 36. The "log-log" method (log creep rate vs. log stress) was used in interpreting these data. This is one of the recommended methods of relating strain, stress and time.[3-8] The functional relationship between these variables obtained from the straight lines for X-2219 in Fig. 36 are given in the Appendix. These relationships are used in the analysis of the stresses in the fuel element (see section on Fuel Element Stress Analysis)

It will be noted from Table 13 that the Pulver Alloy M-257 is the strongest, with regard to creep, of the alloys compared. The experimental alloy X-2219 (Al - 6.0 Cu - .3 Ma - .1 V- .15 Zr) is the next strongest. All three are much stronger in this regard than the commercially available, weldable alloys such as 52S. Unfortunately none of the three strongest alloys are recommended at the present time for welded construction. However, X-2219 has been welded in special cases and probably the least amount of development would be necessary to fabricate satisfactorily the fuel rod cladding for this reactor from X-2219. This fact combined with the results obtained from the stress analysis of the fuel element, indicate that the choice of X-2219 for the fuel rod cladding is the best one under the conditions of this reactor.

Fuel Element Assembly Tube

The fuel element assembly tube is described in the section on Engineering. This tube requires no welding in its construction. The operating temperature is 600°F. The greatest stress on this tube is the hoop stress caused by the difference in pressure at the top between the gas on the outside and the organic on the inside. This stress is about 2500 psi. Since this is a constant stress under operating conditions, it could lead to creep. Hence, a high creep strength aluminum alloy is required. The alloy 75S-T6 was considered for use

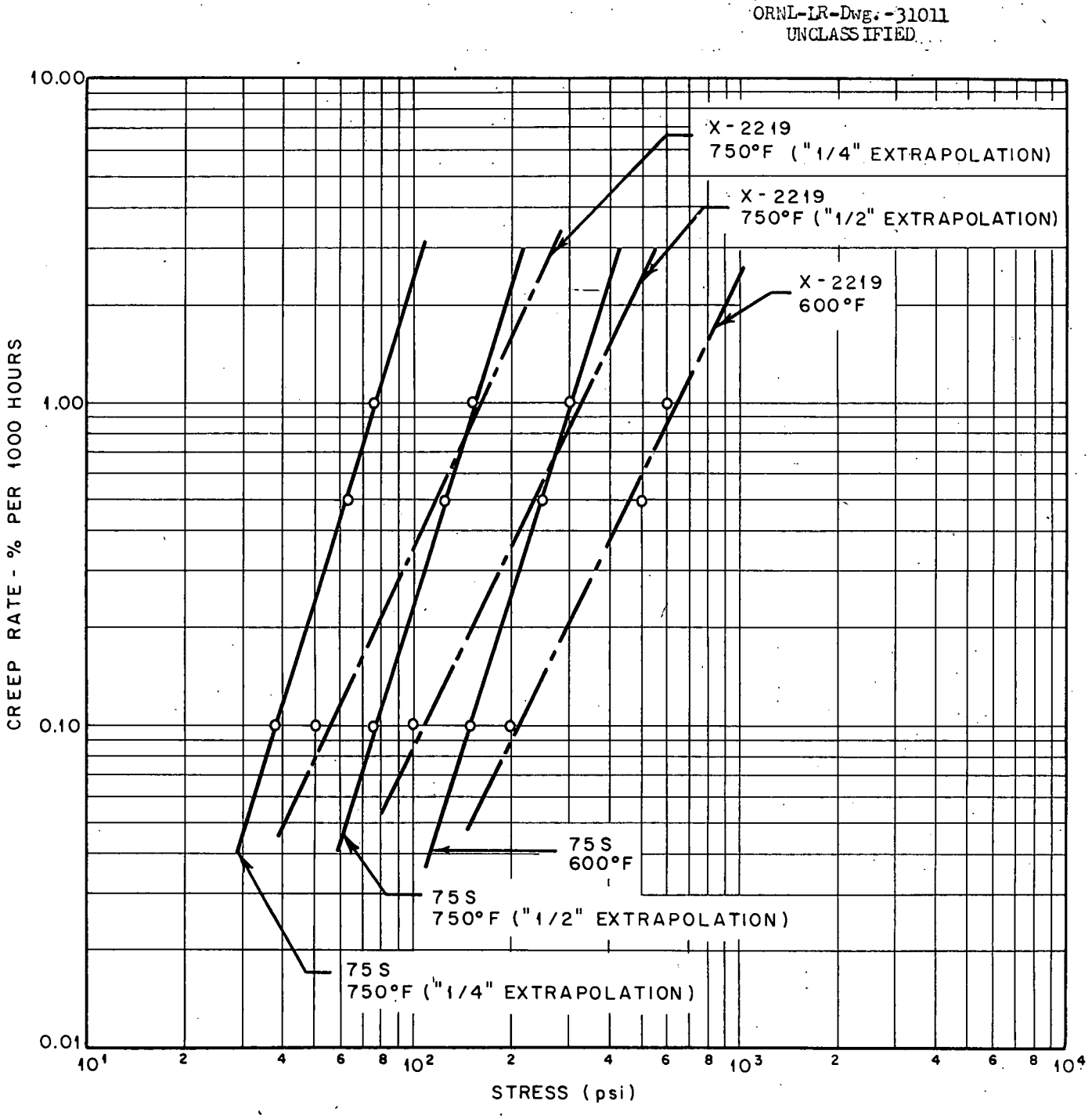

Fig. 36. Creep Rate vs. Stress for Aluminum Alloys: 75S and X-2219 at 600°F and 750°F.

in making this tube because of its high strength and availability. However, since alloy X-2219 has considerably greater creep strength (See Table 13) at 600°F than 75S, it seemed advisable to use this alloy for the assemble tube as well as the fuel rod cladding.

The Process Tube

For a description of this tube and the loads it must carry see the section on Engineering. Since the operating temperature for this tube is low (200°F), there is little difficulty in selecting an alloy that is acceptable. The Boiler Code recommends the alloy 61S-T6 for applications such as this. For the properties of this alloy see Table 11. The boiler Code Specifies the allowable stress for this alloy at 200°F as 10,000 psi. Since the actual stress on this tube is much below 10,000 psi, the use of 61S-T6 aluminum alloy for this application should be completely satisfactory.

Organic Coolant

There are a number of properties of organic liquids that make them desirable for use as coolants in nuclear reactors. These properties are:

1. Low vapor pressure. This property, of course, varies with the organic, but all organics considered for high temperature use have significantly lower vapor pressure than water. This property is graphically displayed in Fig. 39.
2. Negligible corrosion of most low cost construction materials. Such materials include low carbon steel and aluminum.
3. Low activation. This property allows a lessening (from that of a water system, for example) of the shielding around the coolant piping.
4. No hazardous chemical reactions between fuel or water and the coolant. This property is of particular significance if metallic uranium is used as the fuel.

There are, however, certain technical difficulties that are encountered with the use of organics in a reactor. These are:

1. Pyrolytic and radiolytic decomposition. This results in the formation of gases and higher polymers. Since these higher polymers (usually called "tars") tend to increase the viscosity of the fluid and may

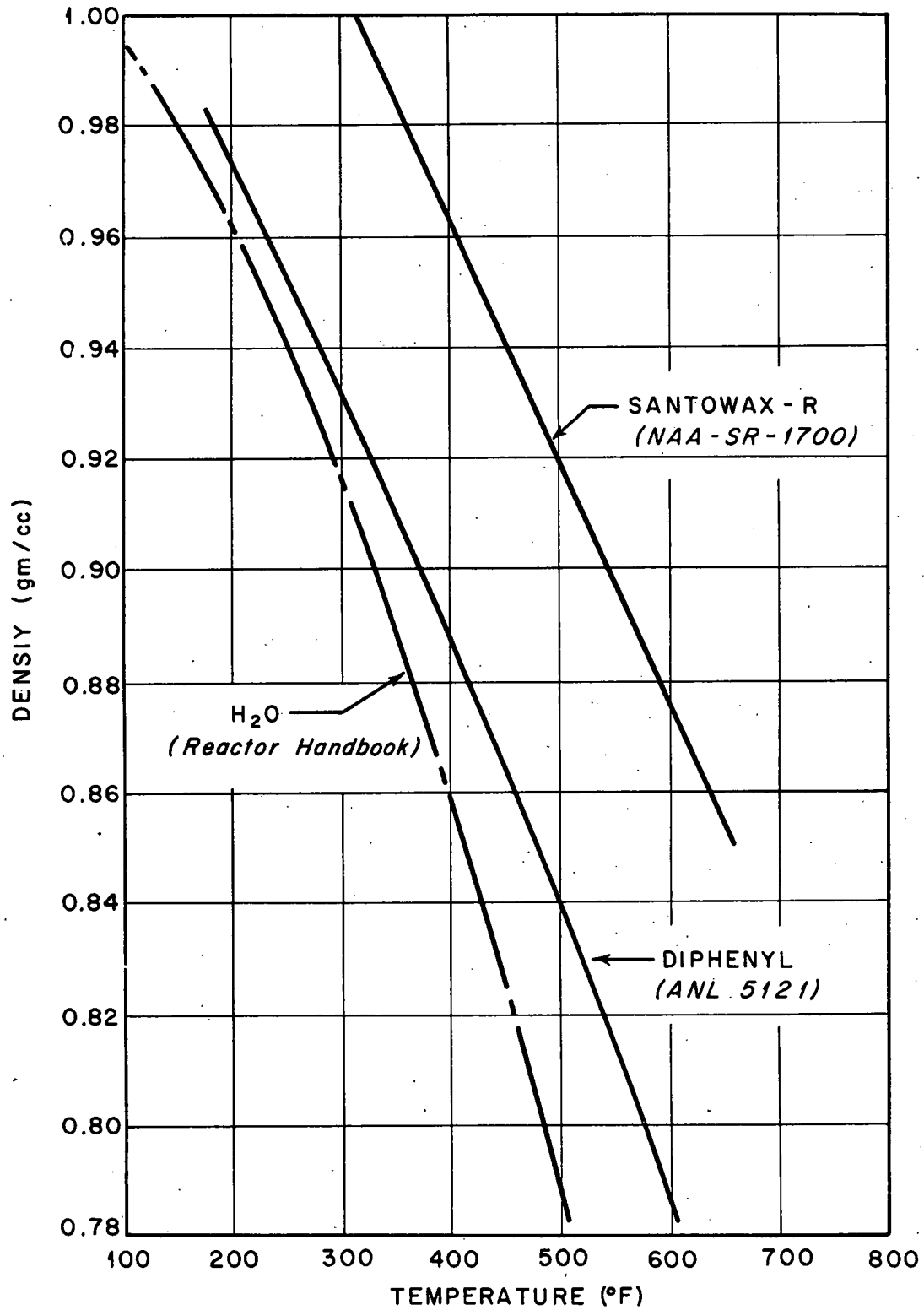

Fig. 37. Density of Selected Reactor Coolants

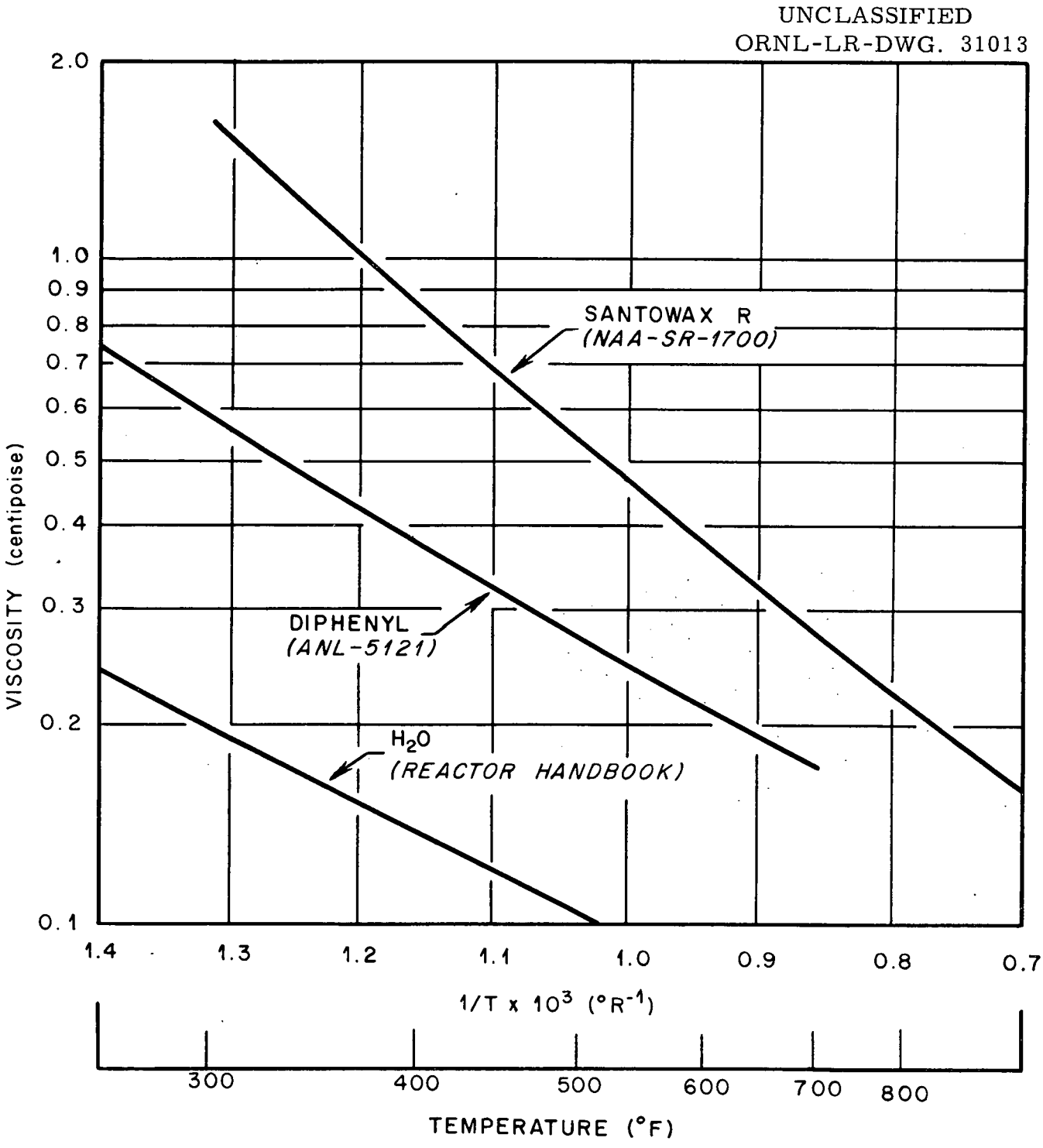

Fig. 38 Viscosity of Selected Reactor Coolants

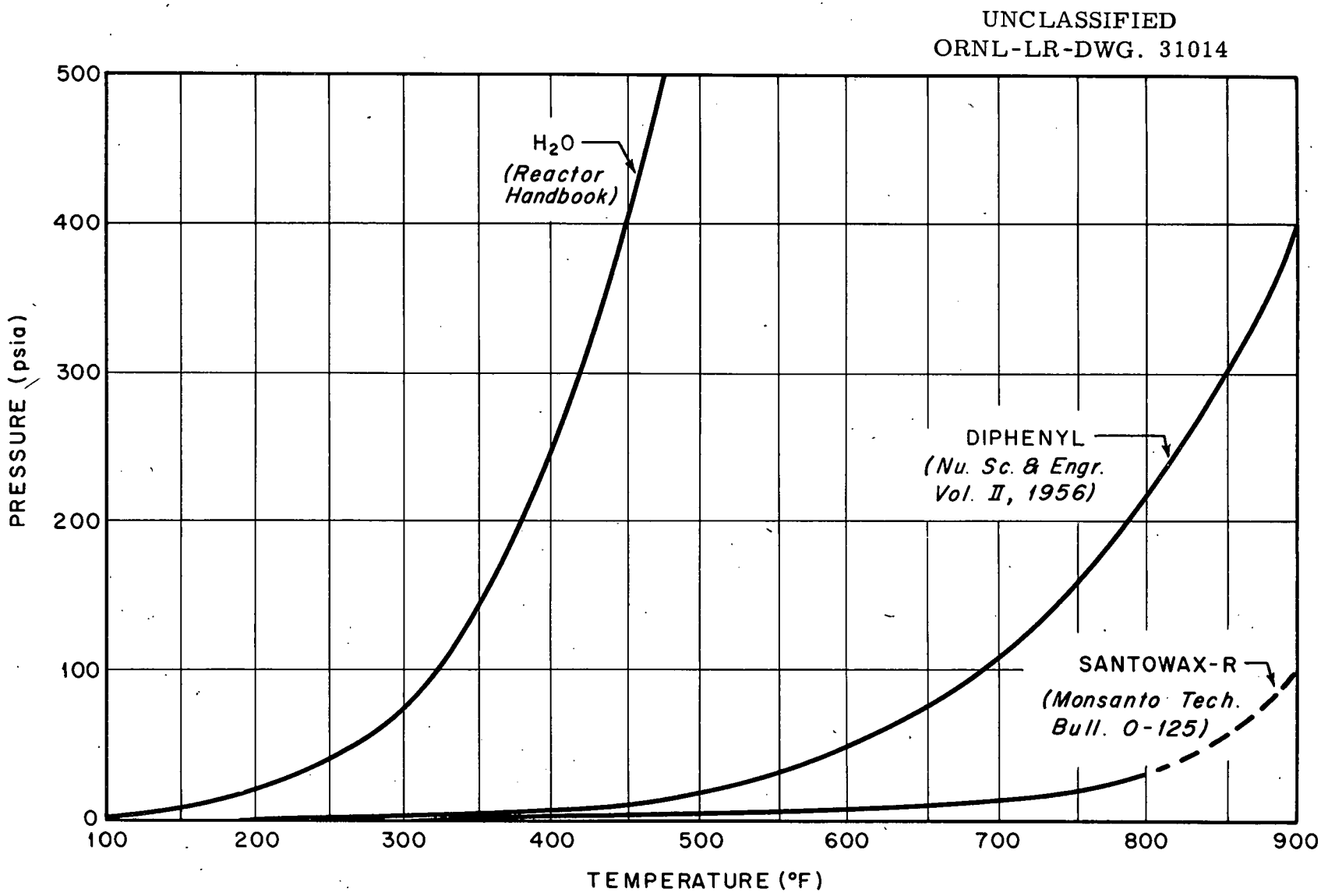

Fig. 39. Vapor Pressures of Selected Coolants

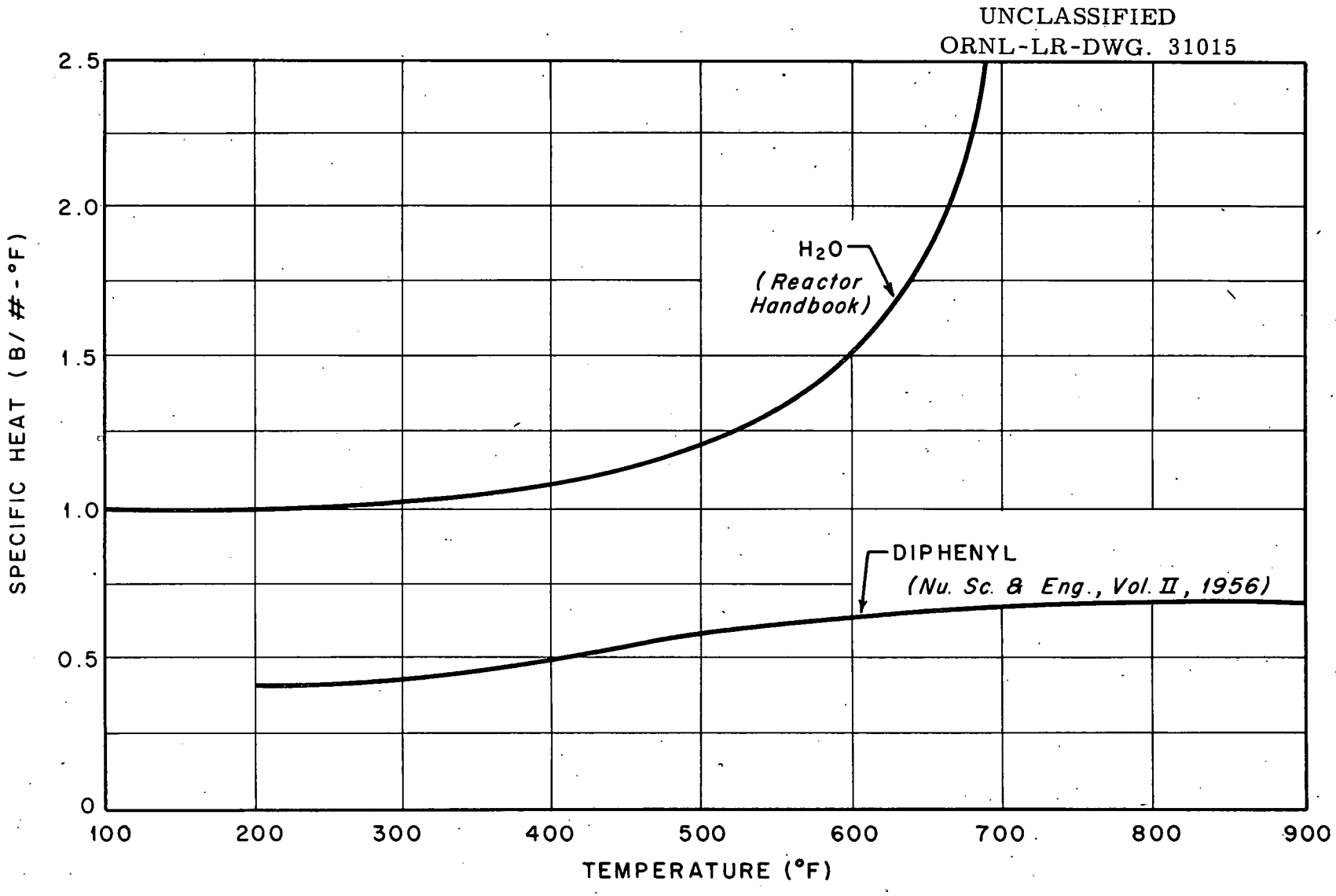

Fig. 40. Specific Heat of Selected Coolants

in certain cases foul the heat transfer surfaces in the reactor, they must be continuously or periodically removed.

2. Many organics considered for high temperature use are solids at room temperature. Thus a heating system is required to prevent solidification when the reactor is not operating.
3. Flammability. This is important in organic systems since the coolant is above the fire point (temperature at which ignition in air is possible) under reactor operating conditions. Because of the possibility of fire from any leakage, precautions must be taken in the reactor design to eliminate ignition sources.

Furthermore, in comparison to water, organics suffer the disadvantages of having inferior heat transfer characteristics. That is, they have higher viscosities and lower specific heats and thermal conductivities than water. (See Fig. 38 and 40). However, this disadvantage is compensated by the possible use of organics at higher temperatures than can be used with water and with a much lower vapor pressure than water exhibits at even much lower temperatures.

Over the past several years much work has been done in screening and testing organics for possible reactor applications[3-3,3-9,3-10,3-11,3-13]. In general this work has determined the following:

1. Alyphatic Hydrocarbons generally show much higher radiolytic damage than do the aromatics.
2. Because of the possible introduction of corrosion problems due to liberation of oxygen during irradiation, organic compounds containing oxygen are not recommended for reactor application.
3. Among the aromatics, the condensed ring class (e.g., napthalene) show a high degree of radiation resistance, but have the disadvantage of forming insoluble cokes during decomposition.
4. Most organic materials exhibit a temperature threshold for pyrolytic damage. That is, below a certain temperature the damage caused by irradiation is independent of the temperature.

Most of the organic compounds that have an acceptable combination of properties (e.g., viscosity, boiling point, melting point, and over-all radiation stability) to be considered for reactor coolant use are benzene derivatives such as diphenyl, the terphenyls, alkyl benzenes, and alkyl diphenyls. The alkylated derivatives, particularly alkyl diphenyls, have some attractive

properties, namely, they are liquid at room temperature and (with respect to their use as a moderator as well as coolant) they have a higher hydrogen density than the polyphenyls. However, they are somewhat less stable to irradiation than the polyphenyls and their cost is slightly higher. Also in D_2O moderated reactors, such as the one being considered here, hydrogen acts more like a poison than a moderator, and an increase in hydrogen density is not an advantage.

At the present time Atomics International, Division of North American Aviation, Inc. is conducting the Organic Moderated Reactor Experiment (OMRE) Those materials given the most consideration for the moderator- coolants of the OMRE are diphenyl and the terphenyls. In the opinion of those responsible for the OMRE these materials are the most stable commercially available hydrocarbons[3-13]. Because these compounds are being considered for use in the OMRE, and because more pertinent information was available concerning these compounds* than for any others, it was determined to limit the choice for the coolant for this reactor to either diphenyl or a mixture of the terphenyls.

Diphenyl - Because of its low cost (15¢ per pound) and availability, diphenyl (also called byphenyl) has undergone more tests as a heat transfer fluid than perhaps any other hydrocarbon. It has the best heat transfer characteristics of the polyphenyl compounds. Some of the important properties of diphenyl, compared to those of "Santowax-R" (see below) and water are shown in Figures 37, 38, 39, 40. It will be noted from these figures that, compared to water, diphenyl has a higher density and a higher viscosity but a lower specific heat and a lower vapor pressure. Its lower specific heat and higher viscosity account for the fact that it has poorer heat transfer characteristics than water. These same properties as well as others are compared for the same three coolants in Table 14.

Terphenyls - There are three isometric terphenyls, ortho, meta, and para terphenyl. All of the isomers have higher densities; higher viscosities, and low vapor pressures than has diphenyl. The radiation stability of o-terphenyl is about the same as that of diphenyl, whereas m-terphenyl is slightly more stable and p-terphenyl considerably more stable than diphenyl[3-14]. Unfortunately the cost of any single isomer is quite high, running from $0.90 per pound to $1.40 per pound[3-14]. Mixtures of the terphenyls are commercially available

* Much of this information was supplied by C.A. Trilling, Project Engineer, and others concerned with the OMRE.

at much lower cost. One such mixture available from the Monsanto Chemical Co. is called "Santo-wax-R". The composition of this mixture is reported to be[3-15]:

Diphenyl	1%
Ortho-phenyl	10%
meta-terphenyl	45%
para-terphenyl	20%
Triphenylene	4%
para-quaterphenyl	2%
Higher boiling Compounds	18%

The vapor pressure and radiation stability of this mixture are about the same as those of m-terphenyl. Reference is again made to Figures 37, 38, 39, 40 and Table 14 wherein the properties of "Santowax-R" are compared to those of diphenyl and water. It will be noted that the viscosity is higher and the specific heat lower than for diphenyl, and thus, the heat transfer characteristics are not quite as good. The melting point is higher but neither are liquid at room temperature. The cost of the two materials is about the same. Of great significance for this reactor is the low vapor pressure of "Santowax-R" compared to that of diphenyl. For a large reactor it is advantageous from the standpoint of both cost and safety to keep the pressure in the core to as low a value as possible. To make the best use of the organic coolant with regard to the reactor under study it seemed advisable to take advantage of the low vapor pressure of "Santowax-R".

Another promising mixture of the terphenyls which is available from the Monsanto Chemical Company is called "Santowax-OM". This mixture consists mainly of ortho and meta-terphenyl with a trace of para-terphenyl. This material is very similar to "Santowax-R" in its physical properties and radiation stability. Its vapor pressure is slightly higher than that of "Santowax-R"[3-14], but its metling point is lower.[3-13] Because of this lower melting point, "Santowax-OM" is the material being first used in the OMRE[3-13]. The present cost of "Santowax-OM" is $0.75 per pound, however, if large scale production is demanded the cost would drop to about $0.25 per pound[3-15].

"Santowax-R" was chosen for use as the coolant in this reactor for the following reasons:

1. Low vapor pressure
2. Low cost
3. Availability
4. High radiation stability

It should be pointed out that because of the relatively high melting point of this coolant means must be provided to melt the material before its introduction into the reactor. Means must be provided also to prevent freezing of the coolant in the reactor and piping during prolonged shutdown of the reactor.

"Santowax-R" may not be the best organic reactor coolant. The best coolant can be determined only after the most promising organics have been tested under actual reactor conditions. The OMRE is set up to perform just such tests. With the completion of this experiment much more information will be available regarding the pertinent properties of the various hydrocarbons and their behavior as reactor coolants.

Thermal Stability of The Terphenyls - Experimental evidence[3-21] has shown that the thermal decomposition is small and practically constant with time for all the terphenyls at 750°F. This temperature is below the threshold value (See above) for these compounds. Since the hottest surface temperature of the fuel elements is 750°F and the bulk temperature of the coolant is about 600°F, there is no danger of excessive pyrolytic damage to the organic coolant in this reactor under normal operation. When hydrocarbons of this kind are heated to temperatures around 900°F coking takes place. This could be a serious problem as far as fouling the heat transfer surfaces is concerned. Thus, it is important to prevent hot spots in the coolant channels. A rupture of the fuel element cladding, while not disastrous from the point of view of a chemical reaction, might cause such hot spots. If it were found that such hot spots did not form, the problem of the fuel element cladding would not be nearly so great.

Effects of Irradiation on the Terphenyls - In reactor applications most damage to organics is caused by gamma photons and fast neutrons. The interactions of these particles with organics leads to the formation of gases and higher polymers. Fortunately in the case of the terphenyls the gas formation is not excessive and the higher polymers are soluble in the terphenyls. Also, the higher polymers are more radiation stable than the original terphenyls (See Fig. 62 in Appendix H). Thus the rate of decomposition decreases as the concentration of higher polymers increases. It is not possible to allow the higher polymer concentration to increase without limit, however, because the

addition of these materials change the properties of the fluid. The most significant change is an increase in viscosity. It has been estimated[3-13] that a concentration of 30% higher polymers in "Santowax-R" increases the viscosity by 50%. This has been selected as the limiting concentration for steady state operation.

The effects of higher polymer concentration on the properties of Santowax-R are shown in Figures 41 and 42 and in Table 15. It will be noted that there is a decrease in final melting point with increasing higher polymer concentration. Unfortunately this decrease is not great enough to cause the mixture to be liquid at room temperature. The increase in density shown in Figure 42 brings about an increase in hydrogen density. This can be important from the point of view of reactor physics.

The properties compared in Table 15 are the most significant for heat transfer considerations. The values given for 30% higher polymer concentration have been estimated from the effects of higher polymers on the properties of similar organic materials[3-12].

In order to calculate the rate of decomposition of organics in radiation fields it is necessary to assume that the decomposition rate is a function only of the amount of energy absorbed. There are exceptions to this rule. For example, fission fragments cause more damage for equal energy deposition than do gamma photons or fast neutrons. For this reason it is important to protect organic coolants from the surface of the fuel in reactors. None the less, the rule is generally accepted to hold when comparing , for example, damage caused by electrons from Van de Graff generators with that caused by gammas and neutrons. Some data are available relating the decomposition of the terphenyls with the energy absorbed from Van de Graff electrons[3-21]. Since the main constituent of Santowax-R is m-terphenyl, the data for the latter was used in calculating the decomposition rate for santowax-R in this reactor. The results of this calculation are given in Appendix H.

Activation of Organic Coolants - It has been stated that one of the advantages of organics over water in reactor application is the low activity found in organic systems. The activity that is found is due mainly to impurities in the organic. An estimate of the activity expected for common impurities in organics and under the radiation conditions of the OMRE has been made[3-22] Table 16. The activity as well as the radiation expected at

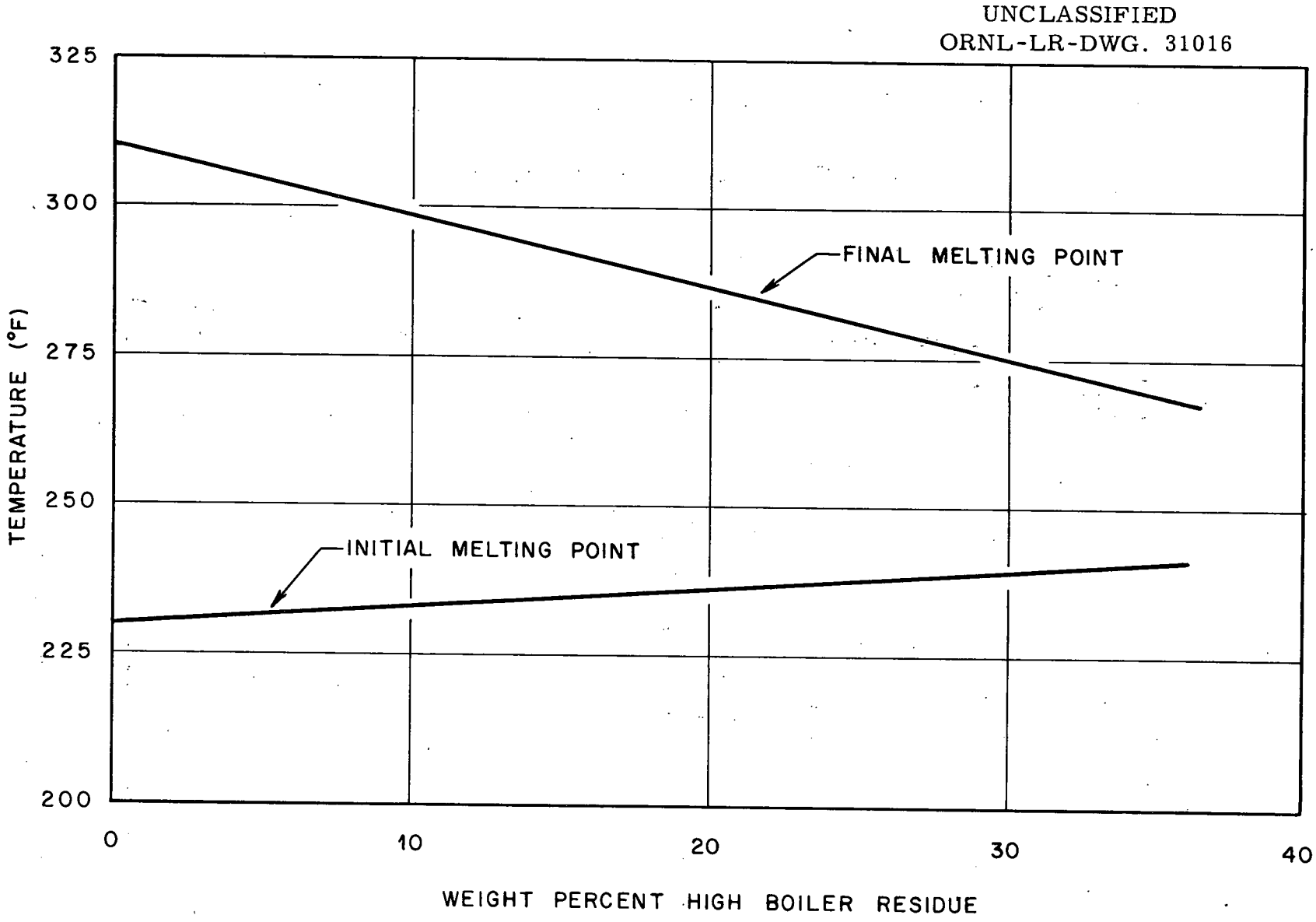

Fig. 41. Melting Point of Irradiated Santowax-R (NAA-2079)

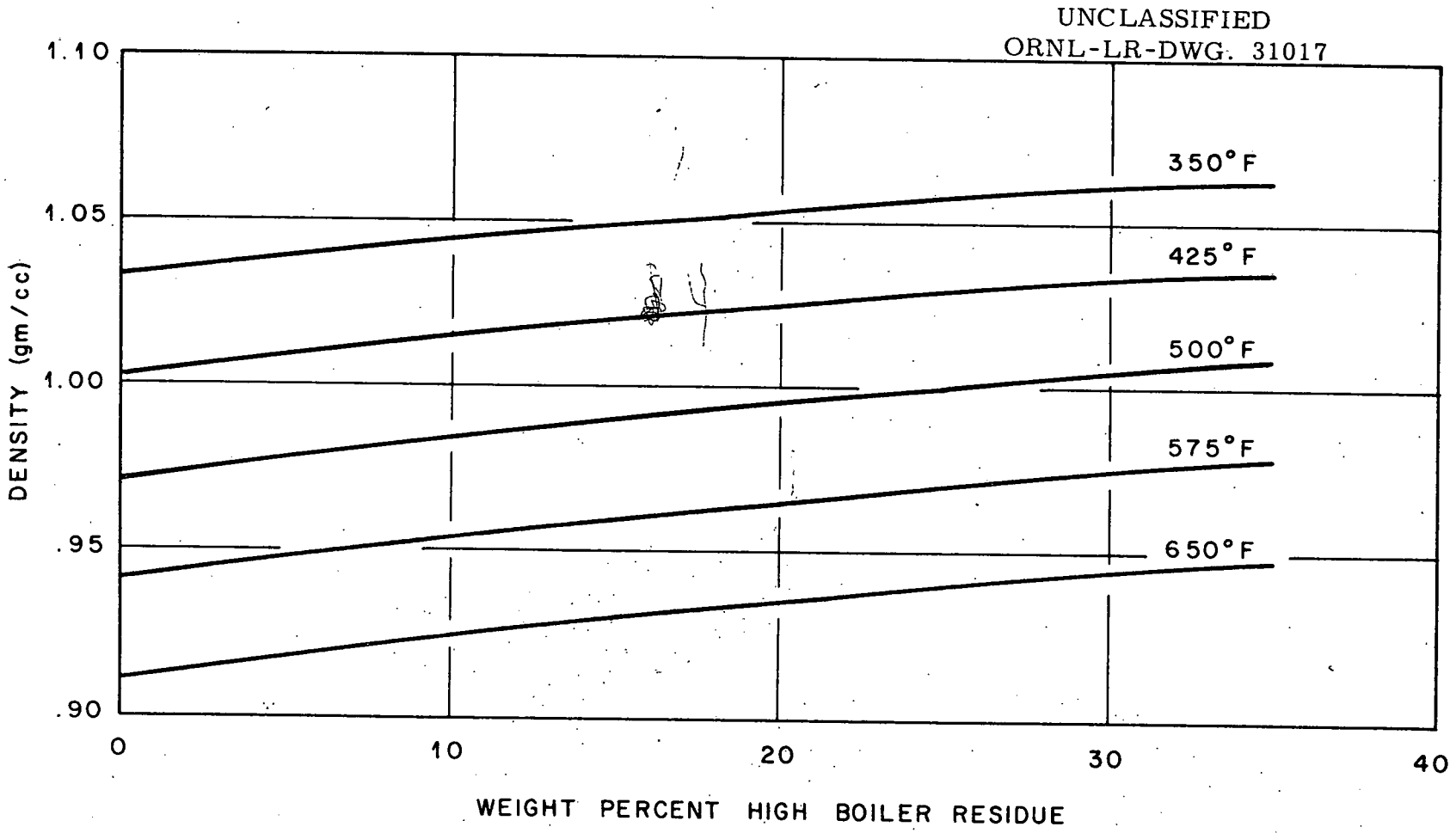

Fig. 42. Density of Irradiated Santowax-R (NAA-2079)

the surface of a 16 inch steel coolant pipe and at a position one and a half feet from the pipe are given in Table 16. The activities given in this table are for 1 ppm of the impurity in the coolant. The impurity content in Santowax-R is not as great as 1 ppm for some of these impurities. An estimate of the radiation due to impurities at the pipe surface based on a typical analysis of Santowax-R is 496 mr/hr. To this value one should add the radiation contributed by corrosion products in the coolant. The total radiation level at the pipe surface including these contributions is estimated to be 759 mr/hr. This amount seems quite high but it must be recalled that all this radiation is due to impurities and these impurities are continually being removed in the organic purification system.

TABLE 16

RADIATION LEVELS FROM 1 PPM CONCENTRATIONS OF VARIOUS IMPURITIES IN OMRE COOLANT

Element	Activity (dps/cu cm)	Radiation Level at Surface of 16 in. pipe (mr/hr)	Radiation level 1.5 ft from surface of pipe (mr/hr)
Na (1 ppm)	1.86×10^4	890	240
Mn (1 ppm)	2.01×10^5	3900	1200
Cl (1 ppm)	3.48×10^3	56	18
Hg (1 ppm)	2.13×10^4	27	9.1
Co (1 ppm)	3.52×10^4	990	340

TABLE 14

COMPARISON OF PROPERTIES OF DIPHENYL, "SANTOWAX-R", AND WATER

Property	Value of Property for Indicated Coolant		
	Water	Diphenyl	"Santowax-R"
Melting Point (°F)	32	158 (3-12)*	140 to 293 (3-16)
Boiling Point (°F)	212	491 (3-12)	700 (3-16)
Vapor Pressure at 700°F(psi)	3100	110 (3-17)	15 (3-16)
Density at 700°F(gm/cc)	.42	.72 (3-17)	.83 (3-18)
Viscosity at 700°F (centipoises)	.06	.18 (3-17)	.28 (3-14)
Specific Heat at 700°F $\frac{BTU}{lb-°F}$	5	.65 (3-12)	.56(at 550°F)**
Thermal Conductivity at 700°F (BTU/hr-ft-°F)	.185	.076 (3-12)	.076 (3-20)
Flash Point (°F)		235 (3-12)	375 (3-16)
Fire Point (°F)		253 (3-12)	460 (3-16)
Cost $/lb		.15	.1675 (3-15)

* Number in brackets is reference for value given

** Estimated from Specific Heat of tertiary eutectic of diphenyl, O-terphenyl and M-terphenyl.[3-12]

TABLE 15

EFFECTS OF HIGHER POLYMER CONCENTRATION ON THE ENGINEERING PROPERTIES OF SANTOWAX-R

Property	Value at the Indicated Higher Polymer Concentration	
	0%	30%
Thermal conductivity at 550°F (BTU/sq ft, hr, °F/ft	0.076	0.072
Specific Heat at 550°F (BTU/lb, °F)	0.56	0.56
Density at 600°F (lbs/cu ft)	55	57
Viscosity at 600°F (lbs/ft-hr)	0.94	1.41
Viscosity at 700°F (lbs/ft-hr)	0.675	1.01

ECONOMIC EVALUATION

Introduction

It is apparent that within the man-hour limitations of this project, we could hardly hope to construct a highly accurate and original forecast of either the capital or operating costs of our reference design. We have tried whenever possible to be guided by cost estimates appearing in the literature representing the best efforts of responsible study groups. When, either because of lack of design information or an adequate estimating basis, it was impossible to analyze the cost in detail, we have tried to place a cost figure on the equipment or system which we felt was high.

It was our sincere wish to present cost figures for the system which could be lowered by more careful study but not raised. To realize such an ambition would have required engineering the reactor complex using only those materials and fabrication techniques for which costs could be predicted with confidence. In addition it would have required that the reactor components with their specified materials and fabrication be known to be able to withstand the reactor operating environment for the required length of time. To even state these aims may serve to alert the reader to our immaturity in this field of engineering endeavor.

We have been able to construct our reactor system using materials, designs and fabrication techniques which fell within the range of conventional engineering practice. This means, in terms of economics, that we feel a high degree of confidence in the conservatism of our capital cost estimate.

Unfortunately, the chosen operating temperatures of our reactor system have required that our aluminum cladding on the fuel elements must operate in a temperature range above the temperatures consituting accepted engineering practice. Even though the best information and methods of analysis available indicate that our fuel element cladding is adequate, we must admit that there still remains some doubt that our elements will operate satisfactorily for the required length of time.

All in all, we feel that our operating cost estimate is based on a reasonable engineering extrapolation and that our reference design will be able to operate at a quite good economic point. However, we did wish to

point out that the desired degree of economic certainty was not achieved.

Capital Cost Estimates

The basis for our economic evaluation in this report is a preliminary memorandum entitled "Economic Evaluation" dated December 7, 1956 issued by the Technical Appraisal Task Force on Nuclear Power of the Edison Electric Institute. This memorandum represents an attempt by the group to more or less standardize or establish ground rules for power reactor system economic evaluations. The purpose was to permit easy comparison of different reactors. The pertinent portions of this memorandum are reproduced in the economics section of the appendix to this report.

Our capital cost estimate is presented in Table 17. The detailed descriptions of the structures, systems, or equipment whose capital costs are shown are to be found in other sections of the report.

TABLE 17

CAPITAL INVESTMENT IN THOUSANDS OF DOLLARS

Land and Rights			500
Structure and Improvements			8,810
Main Building			
Shell	4,250		
Other than shell	2,400		
Service Building	1,350		
Site Preparation	90		
Misc. Site Facilities	720		
Reactor Plant Equipment (Installed)			10,320
Reactor		2,058	
Vessell	1,408		
Special Shielding	650		
Fuel Handling Facilities		2,000	
Remote-Handling Equipment	1,000		
Conveying Equipment	500		
Storage	500		
Instrumentation and Control		2,000	

TABLE 17 (Con't)

Primary Coolant System (Installed)		1,968	
Main Heat Exchangers	1,100		
Purification System	30		
Pumps	278		
Organic Piping	260		
Instrumentation	60		
Auxiliaries			
Heat Up System	180		
Storage and Handling Facilities	60		
D_2O System (Installed)		2,194	
Purification System	1,500		
Pumps	118		
Piping	210		
Heat Exchangers	56		
Storage Tanks	44		
Auxiliaries			
Heat Up System	66		
Instrumentation	200		
Gas Handling and Storage		100	
Turbine Generator and Steam Cycle Costs (Installed)			7,867
Turbine Generator	4,970		
Special Foundations	90		
Condenser and Auxiliaries	118		
Circulating Water System	340		
Other Turbine Auxiliaries (lab system, etc.)	50		
Feed Water Heaters	85		
Storage Tanks	432		
Deep Wells			
Pumps	4		
Sinking and Casing	115		
Water Treating Equipment	138		
Blowdown Equipment	13		
Main Feed Pumps	26		
Misc. Pumps (Hotwell, Heater Drain, etc.)	21		

TABLE 17 (Con't)

Instrumentation	300	
Piping	1,165	
Accessories - Electrical		2,200
Miscellaneous Plant		800
Switch Gear, etc.		1,900
Total Direct Costs		32,397
Contingencies (10%)		3,239
Engineering - Special Tests and Management (10%)		3,239
GRAND TOTAL		38,875

We do not feel that a detailed defense of the capital cost estimate would add anything to the report. The estimates are for the most part taken from other studies, the rules established by the Edison Electric Institute Committee, or computed by more or less standard estimating procedures.

Operating Costs

As with all other costs in this report, the preliminary momorandum by the Edison Electric Institute group forms the basis for the estimate of operating costs. There are, however, many operating costs which are peculiar to this particular reactor. This section will be devoted to a discussion of the methods and assumptions used in arriving at these costs.

Fuel element fabrication, including installation in the reactor core was assumed to cost $20/kg. of uranium. Ignoring for the moment the cost of forming the UO_2, the cost of $20/kg. of U represents a charge of $51/lb. of fabricated aluminum. This appears to be a quite generous allowance for fuel fabrication, especially compared to quoted costs for Zircaloy-2 elements as low as $66/kg. of U appearing in the literature.[4-1].

Fissionable material rental is assumed to be 4% per annum based on a cost of $40/kg. of natural uranium. In computing burnup costs the uranium at $40/kg. is assumed to be completely used when taken from the reactor. Credit for the unburned U-235 and the plutonium is taken account of separately.

Shipping and processing costs for the aluminum clad UO_2 elements was assumed to be $20/kg. of U. The allowance for shipping was $6/kg. of U and for chemical processing $14/kg. of U. These figures were obtained by comparing

our fuel element to more or less standard types listed in an AEC press release on processing costs. Table 38 in the appendix shows the AEC estimates of processing costs with the fuel element most similar to ours underlined. Table 18 shows annual fuel consumption in tons/year, fuel burnup and associated costs in $/year as a function of irradiation in megawatt days/ton.

D_2O rental was assumed to be 4% per annum applied to a base cost of $28/lb. The allowance for D_2O depletion was taken as 4% per annum. There seems to be no standard figure for depletion allowance. Values in the range of 4 to 5% have been noted in the literature.

The cost of replacing the organic coolant which is destroyed by irradiation in the reactor has been estimated for our reactor at .2 mills per kwh of electricity produced. The details of the .2 mills/kwh estimate are presented in the appendix under organic make-up costs.

The credit for fissionable material produced is computed using the figures shown in Table 39 in the Appendix. The price schedule for plutonium as a function of higher isotope content was taken from the AEC price schedule published in the Federal Register, dated June 6, 1957. The credit for depleted uranium is computed from Table 39 in the appendix. The figures appearing in Table 39 were in turn computed using a formula developed by Manson Benedict[4-2]. Annual fissionable material credits as a function of irradiation time in mwd/ton are displayed in Table 19.

Carrying Charges

Carrying charges are computed by the rules outlined in the Edison Electric Institute paper. The only deviation is that we have carried the fuel fabrication cost of two complete cores rather than one as recommended. We have allowed for one-half of one core to be kept on hand ready for insertion in the core, one core in the reactor, and one-half of one core cooling prior to shipment to the chemical processing plant. Table 20 exhibits the carrying charges.

TABLE 18 ANNUAL FUEL CONSUMPTION AND COSTS AS A FUNCTION OF EXPOSURE

Irradiation in 10^3 med/t	Cycle Time in Months	Annual Fuel Consumption in tons/yr	Annual Fuel Burnup in $\$10^3$	Annual Fabrication Costs, $\$10^3$	Annual Shipping and Processing Costs $\$10^3$
1	5.53	234	8,500	4,250	4,250
2	11.06	117	4,260	2,130	2,130
3	16.59	78	2,840	1,420	1,420
4	22.12	58.5	2,125	1,065	1,065
5	27.65	46.8	1,702	852	852
6	33.18	39.0	1,420	710	710
7	38.71	33.4	1,214	607	607
8	44.24	29.3	1,067	533	533
9	99.77	26.0	946	473	473
10	55.3	23.4	852	426	426

Assumptions:

(1) Reactor Core Loading, 106 tons of U

(2) 25% Overall heat to electrical conversion efficiency

(3) 80% plant factor

(4) Plant capacity 200 net electrical MW

(5) Fuel Fabrication Cost $20/Kg of U

(6) Processing Cost $20/KG of U, ($14 Chemical Processing and waste disposal, $6/Kg of U Shipping Cost)

TABLE 19 - ANNUAL ISOTOPE CREDIT ASSUMING REACTOR GRADE Pu AT $28.50/GRAM

Irradiation 10^3 MWD/ton	Pu Conc. gms/ton	U-235 Conc. gms/ton	Annual Pu Credit, $\$10^3$	Annual Uranium Credit, $\$10^3$	Total Annual Credit, $\$10^3$
0	0	6450	0		11,250
1	980	5150	6,540	5,150	11,690
2	1600	4200	5,330	1,450	6,780
3	2050	3400	4,560	435	4,995
4	2400	2760	4,000	111	4,111
5	2550	2250	3,400	13.7	3,414
6	2640	1870	2,940	0	2,940

Assumptions:

(1) 106 Tons of U

(2) Pu at $28.50/gram

(3) Uranium Credit Calculated as shown in the Appendix

TABLE 20

CARRYING CHARGES FOR THE ODPR

Cost of Plant	
Land	$ 500,000
Reactor and Associated Equipment	24,038,000
Turbogenerator Plant	14,360,000
Total	38,898,000
Working Capital	5,390,000
Annual Carrying Costs	
Land at 11%	$ 55,000
Reactor and Associated Equipment at 15.25%	3,670,000
Turbogenerator Plant at 14%	2,010,000
Working Capital at 9%	485,000
Total	6,220,000
Total Carrying Charges, Mills/ kwh	4.45

Total Energy Costs

Total energy costs have already been presented in the Summary section of this report. As will become apparent later, we may wish to operate the reactor at something less than optimum conditions in order to ease the requirements on the fuel elements. Therefore, we have included Table 21 which shows the total energy costs for the reactor at 1,000 , 3,000 , and 6,000 mwd/ton.

Parametric Studies and General Observations

Operating Alternatives - We have already admitted elsewhere in the report that we are making an engineering extrapolation in using aluminum clad on our fuel elements in a condition where the surface temperature may rise to 750°F We feel that there are many ways in which we could reduce the severity of the operating conditions and still retain good economics.

For instance, it would be possible to reduce the maximum fuel element clad temperature to 700°F with a small loss in net power output. And hence, with a small effect on direct power costs.

Another alternative would be to vent the elements in the critical temperature zones of the reactor. Venting the elements would release some percentage of the fission product gases into the primary coolant system and allow for pressure equalization between the inside of the element and the outside. It is believed that this amount of fission product release into the coolant stream could be tolerated. Although the fuel element would still be called upon to operate above the temperature range where data on strength and creep are readily available, the load or stress would have been reduced to a very small value. This alteration to the fuel element design appears to have little or no effect on economics.

Still another possibility would be to run the fuel elements for only 1,000 mwd/ton. This would markedly reduce the stresses in the clad and also reduce the total creep occuring prior to removal. The economic penalty for operating the fuel elements to 1,000 mwd/ton instead of 3,000 mwd/ton would be serious, being of the order of 3 mills/kwh as shown in Table 21. While the penalty is large, it would not be disastrous, particularly if it were temporary.

We believe that our fuel elements as specified will operate satisfactorily, but since our operating conditions are fairly severe, we wished to point out ways of easing requirements without incurring any tremendous economic penalties.

The case for Enriched Uranium Fuel - The effect of overall reactor economics of using enriched uranium fuel was briefly investigated. The price of enriched uranium as UF_6 is shown in Table 40 in the appendix. The cost of converting UF_6 to UO_2 was assumed to be \$8/lb[4-3]. The results of the study are presented in Fig. 43 which shows net fuel costs in mills/kwh as a function of irradiation in mwd/ton for natural uranium, .978%, and 1.46% enrichment. The significant factor which makes the cost picture for enriched fuel worse than for natural uranium is the relatively high cost of the UF_6 to UO_2 conversion. This cost is of course avoided with natural uranium fuel since it is produced in the desired form by the refineries.

Zircaloy-2 Clad Fuel Elements - As an alternate to the cheap easy to fabricate, easy to process, aluminum clad elements we could have chosen to use Zircaloy-2 clad elements and process tubes. The effect of using Zircaloy-2 cladding and process tubes was investigated. Only the effect on fuel costs was checked. It was assumed that carrying charges were unaffected by the higher working capital requirements.

TABLE 21 TOTAL ENERGY COSTS

Irradiation (mwd/ton)	1,000	3,000	6,000
Annual Carrying Charges	$6,220,000	$6,220,000	$6,220,000
Annual Operating Costs			
Labor and Maintenance	1,300,000	1,300,000	1,300,000
Fuel Element Fabrication	4,250,000	1,400,000	700,000
Fissionable Material Rental	308,000	308,000	308,000
Fissionable Material Consumed	8,500,000	2,840,000	1,420,000
Shipping and Processing	4,250,000	1,420,000	710,000
Water and Miscellaneous Supplies	80,000	80,000	80,000
D_2O Rental (120 tons)	269,000	269,000	269,000
D_2O Depletion Allowance	269,000	269,000	269,000
Organic Makeup	280,000	280,000	280,000
Total Annual Cost	25,726,000	14,386,000	11,556,000
Less Fissionable Prod. Credit	11,690,000	4,995,000	2,940,000
Net Annual Cost	14,036,000	9,391,000	8,616,000
Energy Cost in Mills/KWH	10.02	6.70	6.15

The Effect of The New Plutonium Fair Price - The effect of the new plutonium guaranteed fair price schedule, $28.50/gram minimum, (Assuming $1.50 per gram for conversion of Pu salt to metal buttons) was studied. The total energy costs for the ODPR, assuming the old minimum plutonium credit of $12/gram are shown in Table 37 in the appendix. In general, the effect of the new plutonium price is significant only at irradiations of the order of 3,000 mwd/ton or less. It has a quite beneficial effect on energy costs for the ODPR since this reactor is designed to take advantage of all of the benefits attendant to short irradiations.

Fuel Loading - Effect of fuel loading was studied for a given reactor size and lattice spacing. The effect on plutonium production is shown in the physics section of the report. We do not believe we are at the optimum point with a specified loading of 106 tons of U ; however, our study indicates that overall energy cost of $3,000 mwd/ton would probably be altered by less than one-half of one mill/kwh. There is some economic gain to be achieved by adjusting the fuel loading upward by 20 to 40 tons. The increased fuel loading will also yield somewhat longer lifetimes. The small gain in lifetime, is of doubtful economic significance. Particularly, since the gain in plutonium production is more important at the lower irradiations. In any event, we do not feel that altering the fuel loading can change the economics of this reactor materially.

Conclusions - We certainly cannot lay claim to a unique economic position for the ODPR simply because the predicted overall energy costs lie in the range 6 to 7 mills/kwh. However, we do believe that with this reactor we have arrived at the usual energy costs predicted for nuclear power stations with fewer doubtful engineering extrapolations than most.

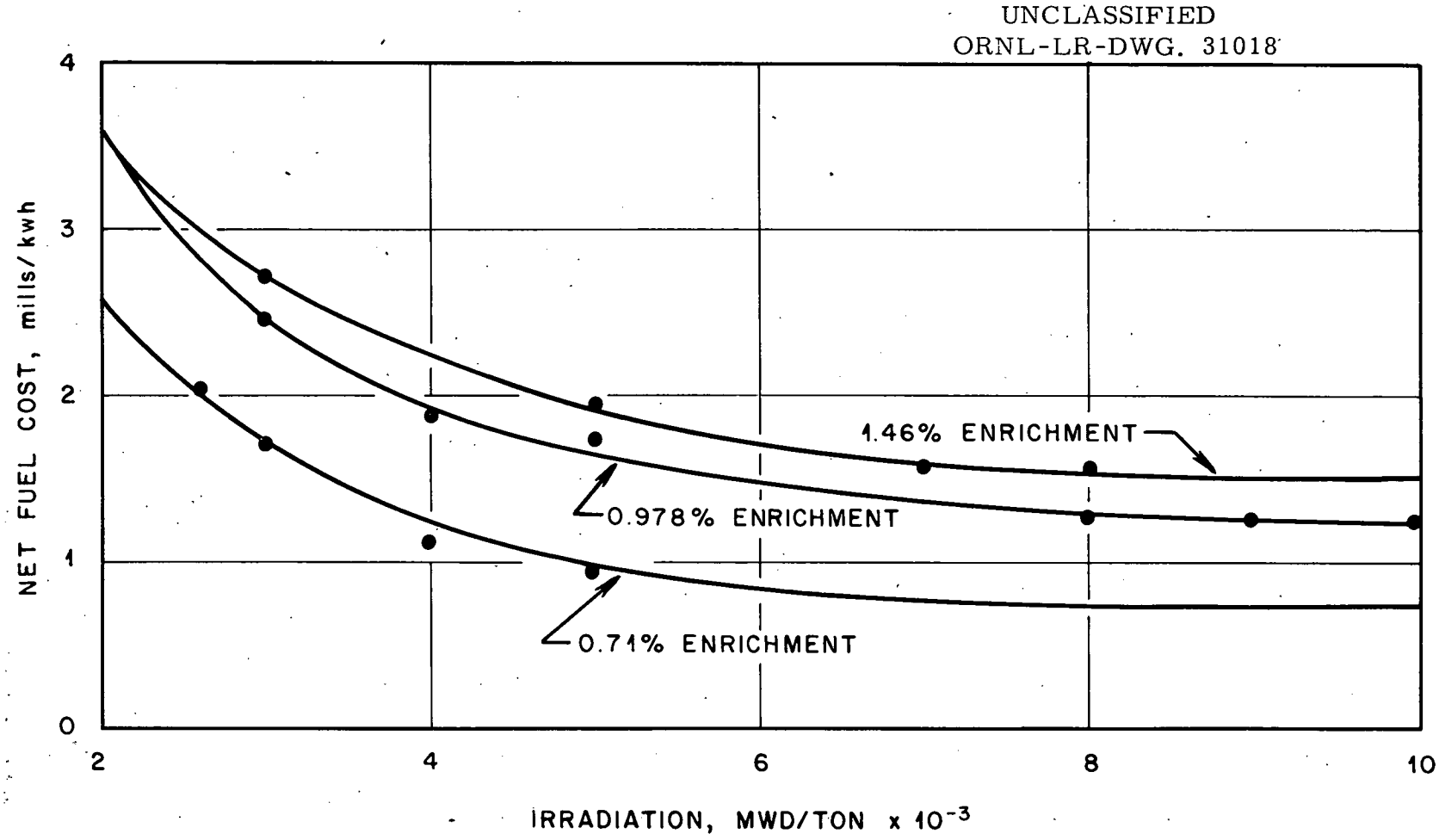

Fig. 43. Net Fuel Cost, Mills per KWH, Vs. Irradiation, Megawatt Days per Ton for Various Enrichments

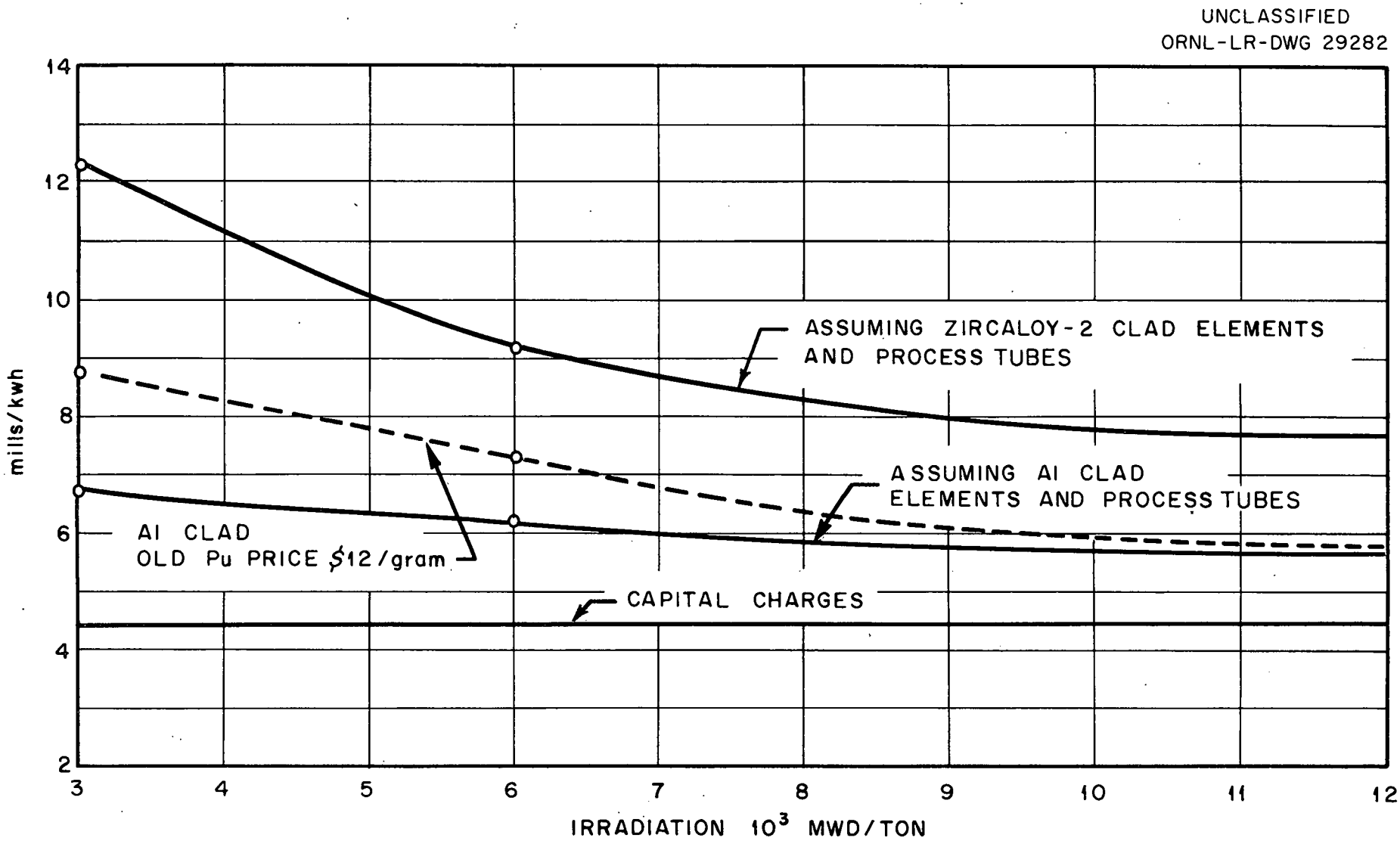

Fig. 44. Total Energy Costs vs. Irradiation

MAINTENANCE

Detailed operational procedures and personnel requirements is not discussed in this report. The general concept of how the operation of the reactor and plant would be influenced by equipment failures or other adverse operating conditions is discussed however in the section on Reactor Control and Instrumentation.

Maintenance of equipment outside of the reactor building will be conducted in a conventional manner since none of the equipment or materials to be handled will be radioactive. Special provisions, however, are necessary to allow maintenance of equipment inside the reactor building. The major pieces of equipment which will require special techniques are; the organic and the heavy water circulating-feed pumps, the reboiler-superheater units, the heavy water coolers, and the special indexing unit and crane system within the reactor vessel itself.

The eight organic recirculating-feed pumps are installed in pairs in four separately shielded compartments, thus requiring the outage of two pumps in order to repair or replace any one. This reduces plant capability to approximately 75% of full load rating during such outage. At least one spare pump is kept on hand for replacement purposes. If a pump requires maintenance it is shut down, along with the other pump in that cell, is valved off from the system outside the cell, and all organic in the pumps and piping within the cell is drained to the organic storage tank. The piping and pumps are remotely flushed with benzene and then water and allowed to radioactively cool for a short period of time before entrance into the cell may be accomplished. Radiation level within the cell is checked until it is down to permissible limit as prescribed by health physics, and then the pump may be replaced or maintained in place depending upon its activity. If pump itself is too "hot" to maintain in place it is replaced and moved to a storage area within the reactor building until its activity is down to a low enough level to permit direct maintenance. This replacement procedure minimized outage time.

The four D_2O recirculating-feed pumps are maintained in a similar manner as the organic pumps. The notable exceptions are that they require only a water flush and that each D_2O pump is individually shielded and the loss of one pump does not result in a load reduction since three pumps are designed

to supply normal demands.

The four reboiler-superheater units can each be maintained individually since they are in four separately shielded areas. An outage of one of these units results in a loss of capability of the plant of about 25%. These units, when shut down for maintenance, are sectionalized from the rest of the system and drained and flushed similar to the organic pumps. When activity in the cells of the unit out of service is down to permissible level, the unit head is removed and the maintenance performed. A number of leaky tubes in any one unit may be simply plugged off without any resultant load loss since there is some surplus surface area built into the system. If the number of tubes having leaks becomes too great, the tube bundle of that unit may be replaced by a spare bundle kept in readiness for such occasion, and the removed bundle can be retubed or otherwise repaired directly in a separate maintenance area.

Maintenance of the D_2O coolers is somewhat similar to that of the reboiler-superheater units, except that the outage of one of the D_2O coolers does not affect plant capability. One D_2O cooler is normally in service with instrumentation such that any leak detected in the cooler in service will automatically put the spare cooler in service and cut out the leaking unit and drain it. Flushing and subsequent maintenance is then performed manually.

The maintenance of the special indexing unit and associated equipment within the reactor must be done outside of the reactor vessel, therefore, provision is made in the top head of the reactor so that the entire indexing unit can be removed. The reactor must be out of service in order to accomplish this removal.

HAZARD EVALUATION

This reactor has many attractive features but there are certain dangerous characteristics and hazards which must be analyzed, evaluated, and the system designed to minimize the risks to operating personnel, the public and equipment.

Nuclear Reactors in general will not run away unless a number of serious mistakes in design and operation are committed. To minimize this possibility adequate control must be provided; the reliability and effect of mal-function of each piece of equipment and combination thereof must be analyzed and adequate supervision be planned.

Many other situations will arise which have to do with the protection of plant personnel and others at the site, the protection of investment, and the protection of the general public and property. These too must be analyzed and planned for.

Stability - The safety of this reactor depends upon its intrinsic built-in stability, reliability of conventional equipment, design such that equipment failure will not create hazardous conditions, and the operation and maintanance procedures planned. For example the reactor has a small but negative coefficient of reactivity, that is, the reactivity decreases with increasing coolant temperature, moderator temperature or both.

Problems and situations which arise during startup and shutdown, manipulation of the controls, loading and unloading of fuel and the control of all materials made radioactive by the reactor have been analyzed and are discussed in this report.

The possibility of release of fission products to the atmosphere is minimized in this reactor by the compatibility of UO_2 fuel and coolant, the integrity of the cladding, the fact that there will be no explosive chemical reaction between the fuel and coolant even though the cladding fail, the inherently low pressures encountered in the organic fluid, the leak tightness of the system and the gas tight spherical container vessel.

The possibility of this reactor becoming supercritical; melting down due to either loss of coolant during operation or to the delayed heat produced by radioactive fission products; or possible exothermic chemical reactions among its components have been analyzed.

A nuclear runaway does not represent a serious hazard to the general public since it would not be very violent -- nothing like an explosion even of ordinary chemical explosives. A blast shield is provided, however, around and above the reactor vessel to protect the container vessel from fragments resulting from explosion and thus confine the radioactive products of fission within this semi-spherical shell.

Chemical explosions can cause considerable violence and pressure in such containment vessels. In our reactor there is no possibility of a uranium water reaction or aluminum water reaction. The possibility of ignition of the organic requires oxygen. In order for this to occur the hot organic must be exposed to the atmosphere within the container vessel. The pressures which could occur from such a reaction are low. The maximum pressure in the container vessel should all the heavy water in the core somehow evaporate would also be low and containable. Thus the containment vessel is thought to be adequate for any reasonably conceivable incident.

The large excess reactivity of this reactor during initial operation and over its life must be eliminated by full insertion of most of the control rods throughout the core, with sufficient safeties above set for instantaneous drop and a sufficient number of shim rods inserted for flux flattening, shaping xenon oscillation, etc., and one for control.

A boric acid injection system and a moderator dump are incorporated as additional lines of defense to prevent run away. An increase in reactivity caused by the removal of a control rod will result in a power level and eventual temperature increase. The negative temperature coefficient will act to decrease the resultant reactivity insertion and eventually completely nulify it for some high power level and thus stabilize it. This coefficient should be both large and quick acting to stabilize the reactor without destruction occurring during transients resulting from the malfunction of equipment or operating errors. The principle change in temperature is due to the generation of fission heat in the fuel elements. This heating results in an increased absorption of neutrons as they slow down through the resonance region by a phenomena known as Doppler broadening of the U^{238} resonances. This is the primary negative component in our reactor and the first to act during reactivity insertions. The resultant heating of the coolant with its decrease in density however, results in a reduction in poisons and an increase in thermal

utilization. This effect is large and much greater than the Doppler effect. The subsequent increase in neutron temperature of the composite moderator which includes the moderating properties of the organic coolant result in a decrease in its moderating properties and result in an additional negative component.

The overall coefficient was found to be small but negative. The results of this computation will be found in the Engineering section on Controls. If some failure of the cooling system occurs, caused by the breakdown of the pumps, loss of pumping power, or mechanical failure of cooling piping, a serious situtation may evolve if the heat is not disposed of. To provide for these contingencies, a standby and emergency cooling system is incorporated in this design consisting of emergency pumps connected to a separate power supply and with special piping. Analysis of this system will be found under Reactor Emergency Cooling System in the Engineering Section.

The control system has been designed so that in the event of too high a power level, a serious reduction in coolant flow, or any major failure of fuel elements, the reactor will shut down in a short time interval to minimize damage. All potentially dangerous failures are monitored by instruments and control channels and signals are initialed with the control equipment set in motion to cause a scram, shutdown or cutback in power.

These monitors and channels are in duplicate, independent of each other and of different types. A power failure results in an automatic pickup of all control equipment by the battery backup.

The gas tight building will confine the fission products during an extended cooling period should an incident occur which results in the release of fission products from the reactor vessel.

The fission products may eventually be exhausted to the atmosphere via scrubbers and the high stack, provided during such time and weather conditions as to minimize the hazard to the public and/or property.

APPENDIX A

REACTOR ANALYSIS

Analysis of this reactor was done on the Oak Ridge automatic computer (ORACLE), using a code for large, heterogeneous thermal reactors which was developed by the Reactor Experimental Engineering Division, Oak Ridge National Laboratory (2-1). The code is based on a modified one-group Fermi age model, which is considered adequate for large heavy water moderated reactors. The code analyzes a unit cell of the heterogeneous core and uses the geometric buckling of the core to give results for the core as a whole.

The important outputs of the machine calculations (all as function of lifetime) are:

(1) effective reactivity (no xenon or samarium)
(2) concentration of U^{235}, U^{238}, Pu^{239}, Pu^{240}, Pu^{241} and fission products (except xenon and samarium)
(3) thermal neutron flux
(4) conversion ratio
(5) thermal neutron diffusion length in moderator and the core
(6) resonance escape probabilities for U^{235}, U^{238}, Pu^{239}, Pu^{240}, and Pu^{241}.
(7) fuel macroscopic fission and scattering cross-sections.

These outputs are computed as frequently as desired during fuel lifetime. However, computations should be made at least once every five chronological days of lifetime (at reference design power density) because the accuracy of the iterative process by which the solutions of equations are obtained has not been checked for longer intervals.

Nuclear Reactions Considered

The following nuclear reactions are considered in developing equations for the code:

$$U^{235} + n \longrightarrow \text{fission}$$

$$U^{238} + n \longrightarrow Pu^{239} + n \begin{cases} \nearrow \text{fission} \\ \searrow Pu^{240} + n \longrightarrow Pu^{241} \end{cases}$$

$$Pu^{241} + n \longrightarrow \text{fission}$$

The following nuclear reactions were also considered but the concentrations of U^{236} and Pu^{242} were neglected because of their low macroscopic absorption cross-sections.

$$U^{235} + n \longrightarrow U^{236}$$

$$Pu^{241} + n \longrightarrow Pu^{242}$$

It was assumed that the loss of U^{239} and Np^{239} (in the Pu^{239} production cycle) through neutron absorption was negligible. The following computations show the validity of this assumption.

P_A = probability of neutron absorption per unit time per nucleus

P_B = probability of beta decay per unit time per nucleus

$$P_A = \sigma_a \phi_T$$

$$P_B = \lambda = \frac{0.693}{T_{\frac{1}{2}}}$$

For a thermal neutron flux of 3×10^{13} N/cm^2 - sec

$$\left(\frac{P_A}{P_B}\right)_{U^{239}} = \frac{\sigma_a^{29} \phi_T}{\lambda_{29}} = \frac{3 \times 10^{13} \times 22 \times 10^{-24}}{4.9 \times 10^{-4}} = 1.35 \times 10^{-6}$$

$$\left(\frac{P_A}{P_B}\right)_{Np^{239}} = \frac{\sigma_a^{39} \phi_T}{\lambda_{29}} = \frac{3 \times 10^{13} \times 80 \times 10^{-24}}{3.5 \times 10^{-6}} = 6.85 \times 10^{-4}$$

Multiplication Constant (k)

The multiplication constant, k, is taken as the ratio of the neutron production rate to the neutron destruction rate. The value of k must be equal to or greater than one for the reactor to be operable.

The multiplication constant determined in this code does not account for xenon or samarium poisoning. The actual effective reactivity of the core is found by subtracting reactivity loss due to xenon and samarium from the computed multiplication constant. Xenon concentration is a function of the thermal neutron flux. Since the mode of operation of the reactor was taken to correspond to constant power, the thermal neutron flux, and consequently the

reactivity loss due to xenon, will vary with variation in fissionable isotope concentration. Since flux variation is small, the equilibrium xenon reactivity loss was taken as a constant. Mean value of flux was taken as 2.55×10^{13} n/cm^2 - sec (See figure 33b) and the equivalent equilibrium xenon and samarium reactivity loss as 3.4% (See Section II)

Neutron Production Rate (NPR)

General Formulation of NPR Equation - Neutron production rate is defined as the number of fission neutrons released per unit volume per unit time from fissions at all energies.

$$NPR = \epsilon^{28} \left\{ N^{25} \nu^{25} \left[\sigma_{ft}^{25} \phi_T + \int_{6 E_T}^{\infty} \sigma_f^{25} \phi \, dE \right] + N^{49} \nu^{49} \left[\sigma_{fT}^{49} \phi_T + \int_{6 E_T}^{\infty} \sigma_f^{49} \phi \, dE \right] + N^{41} \nu^{41} \left[\sigma_{fT}^{41} \phi_T + \int_{6 E_T}^{\infty} \sigma_f^{41} \phi \, dE \right] \right\} \quad (1)$$

In this equation the terms $N \nu \sigma_{fT} \phi_T$ and $N \nu \int \sigma_f \phi \, dE$ give the number of fission neutrons released per unit volume per unit time from fissions caused by thermal energy neutrons and by greater than thermal energy neutrons respectively. The latter term will be referrrd to as the resonance fission term, even though the limits of integration cover the whole range of neutron energy greater than thermal rather than just the resonance absorption range. ϵ^{28}, the fast fission factor, is the number of neutrons released by fission of U^{238} per neutron released by thermal and resonance fission of all fissionable isotopes. ϵ^{28} for this core was based on a formula for fast fission factor for a cluster of cylindrical natural uranium rods:

$$\epsilon = 1 + \tfrac{1}{2} (\epsilon_s - 1)(1 + \sqrt{n}) \quad (2)$$

ϵ_s is the fast fission factor for a single rod and is given by:

$$\epsilon_s = 1 + 0.0245 \, d$$

n = number of rods in cluster = 19

d = diameter of individual rod = 0.556 in.

For this reactor $\epsilon^{28} = 1.036$

Reduction of the general NPR equation - The asympotic equation for flux (A-1) may be substituted for ϕ in the resonance fission terms of the general NPR equation. This equation is

$$\phi = \frac{Q}{\xi \Sigma_s E}$$

Q, slowing down density, is the product of (1) the NPR, (2) the probability of reaching a given energy without being absorbed and (3) the probability of reaching a given energy without leaking from the system. Before the general NPR equation can be reduced to tractable form it is necessary to examine the formulation of the resonance escape probability and the non-fast leakage probability.

$p_i(E)$ = resonance escape probability, i.e., the probability that a neutron escapes capture in the i^{th} isotope in slowing down from fission energy to energy E. For a homogeneous system:

$$p_i(E) = 1 - \int_{E_o}^{E} \Sigma_a^i (E') \phi(E') dE'$$

Using the asymptotic flux approximation for a single neutron (A-1):

$$\phi(E') = \frac{p_i(E')}{\xi \Sigma_s E'}$$

$$p_i(E) = 1 - \int_{E_o}^{E} \frac{\Sigma_a^i (E') p_i(E') dE'}{\xi \Sigma_s E'} \qquad (3)$$

To modify for a heterogeneous system, Σ_a^i must be reduced by the ratio of the volume of fuel, V_F, to the volume of cell, V_c, and the flux must be decreased by the resonance flux disadvantage factor, ξ.

The resonance flux disadvantage factor for a cylindrical unit cell may be expressed (A-1)

$$\zeta = \frac{K_F' \quad R_{fuel}}{2} \qquad \frac{I_o \quad (K_F' \quad R_F)}{I_1 \quad (K_F' \quad R_F)}$$

where $$K_F' 2 = 3 \overline{\sum}_a^{fuel} \overline{\sum}_s^{fuel} \left(1 - 0.8 \frac{\overline{\sum}_a^{fuel}}{\overline{\sum}_t^{fuel}} \right)$$

Bars indicate the average values of the macroscopic cross-sections over the resonance energy region.

The heterogeneous resonance escape probability then becomes

$$p_i (E) = 1 - \int_E^{E_f} \Sigma_a (E') \quad \frac{V_F}{V_c} \quad \frac{p (E')}{\zeta \{ \Sigma_s (E')} \quad dE' \qquad (4)$$

Differentiating with respect to energy and rearranging terms

$$\frac{dp_i}{p_i} = - \sum_a^i \quad \frac{V_F}{V_c} \quad \frac{dE'}{\zeta \{ \Sigma_s E'} = - N^i \quad \sigma_a^i \quad \frac{V_F}{V_c} \frac{dE'}{\zeta \{ \Sigma_s E'}$$

Integrating

$$p_i (E) = \exp - \left[- \int_{E_o}^{E} \quad N_i \quad \frac{V_F}{V_C} \quad \frac{\sigma_a^i \quad dE'}{\zeta \{ \Sigma_s E'} \right]$$

N_i, V_F, V_C, and $\{$ are independent of energy and ζ and Σ_s may be assumed to be, so

$$p_i (E) \simeq \exp - \left[N_i \quad \frac{V_F}{V_C} \quad \frac{R_a^i (E)}{\zeta \{ \Sigma_s} \right] \qquad (5)$$

where $R_a^i (E) = \int_E^{E_o} \sigma_a^i (E') \quad \frac{dE'}{E'}$ (resonance absorption integral)

For U^{235}, Pu^{240}, and Pu^{241} the concentrations were assumed small enough to use infinite dilution values, and the resonance absorption integrals were calculated directly from equation 5. For U^{238}, the experimental value of R_a^i for UO_2 rods was used:

$$R_a^i = \int_{E_o}^{E} \sigma_a^i \quad \frac{dE}{E} = 11.5 + 22.1 \quad \frac{S}{M} \qquad (A\text{-}2)$$

Values for the resonance absorption integrals for this reactor are given in Table 22.

TABLE 22

VALUES OF RESONANCE ABSORPTION INTEGRALS

Isotope	R_a, barns
U^{235}	742
Pu^{239}	1880
Pu^{240}	8940
Pu^{241}	2060

The lower limit of the resonance (non-thermal) region was an energy equal to six times the mean thermal neutron energy. Neutron temperature was 250°F, mean thermal energy was 0.034 Mev (see Section F below).

Table 23 gives the resonance escape probability of the principal U and Pu isotopes and of the system as a whole for various fuel lifetimes. Figure 48a shows p of the system as a whole over lifetime.

TABLE 23

ISOTOPE RESONANCE ESCAPE PROBABILITIES

Lifetime (MWD/ton)	p^{28}	p^{25}	p^{49}	p^{40}	p^{41}	p^{system}
0	.906	.956	1.000	1.000	1.000	.866
525	.906	.960	.993	.999	1.000	.865
1181	.906	.965	.985	.995	1.000	.858
1837	.906	.969	.979	.989	1.000	.849
2494	.906	.973	.975	.983	.999	.843
3150	.907	.979	.970	.971	.998	.835

Fast Leakage - The probability of non-fast leakage for large reactors in the ordinary Fermi Age Model is

$$P_{NFL} = \frac{1}{1 + B^2 \tau}$$

The resonance flux for each isotope must be reduced by this quantity. It is therefore necessary to find the age from fission energy to resonance energy for each isotope which contributes to the resonance capture and to thermal energy.

(1) Mean Resonance Energy - A mean resonance energy for each isotope had to be selected. The values used in these calculations are shown in Table 24 (A-1)

TABLE 24

MEAN RESONANCE ENERGY OF U AND Pu ISOTOPES

ISOTOPE	ENERGY, ev
U^{238}	50
U^{235}	15
Pu^{239}	10
Pu^{240}	1
Pu^{241}	0.3

(2) Fermi Age - Calculation of Fermi age is based on the unit cell. Contents of the cell are considered homogenized, and Fermi age is given by:

$$\tau_{\text{mixture}} = \int \frac{\frac{dE}{E}}{3 (\xi \overline{\Sigma}_s)_{\text{mixture}} (\overline{\Sigma}_{tr})_{\text{mixture}}} \qquad (6)$$

where $(\xi \overline{\Sigma}_s)_{\text{mixture}} = \dfrac{\sum_{i=1}^{5} V_i (\xi \Sigma_s)_i}{V_i}$

$(\overline{\Sigma}_{tr})_{\text{mixture}} = \dfrac{\sum_{i=1}^{5} V_i (\xi \Sigma_{tr})_i}{V_i}$

The five components of the unit cell, and the area of each component per cell, are:

Heavy water	31.8 in^2
UO_2	4.6 in^2
Organic	2.65 in^2
Aluminum	4.41 in^2
Void	0.66 in^2

$$\tau_{mixture} = \int_{E_T}^{E_f} \frac{\frac{dE}{E} \sum_{\gamma=1}^{5} \sum_{i=1}^{5} V_{ij}}{3 \sum_{i=1}^{5} V_i (\xi \Sigma_s)_i \sum_{i=1}^{5} V_i (\Sigma_{tr})_i}$$

If it is assumed that Σ_s and Σ_{tr} are not highly dependent on energy and that the average energy of fission neutrons is 2 Mev, age may be written:

$$\tau(E) = \frac{1/3 \ln \frac{2 \times 10^6}{E}}{(\overline{\xi \Sigma_s})_{mix} (\overline{\Sigma}_{tr})_{mix}}$$

$\xi \Sigma_s$ and Σ_{tr} for aluminum and UO_2 are small and will therefore be neglected. Therefore,

$$(\xi \Sigma_s)_{mix} = \frac{V_{org}}{V_{total}} (\xi \Sigma_s)_{org} + \frac{V_{D_2O}}{V_{total}} (\xi \Sigma_s)_{D_2O}$$

$$(\Sigma_{tr})_{mix} = \frac{V_{org}}{V_{total}} (\Sigma_{tr})_{org} + \frac{V_{D_2O}}{V_{total}} (\Sigma_{tr})_{org}$$

For ORACLE studies it is convenient to modify the equations by defining

$$V_{total} = V_{org} + V_{D_2O}$$

This introduces a slight error in relative concentrations, but it is convenient because the Fermi age can be adjusted to account for varying amounts of fuel and aluminum in code parameter studies. Fuel and aluminum are considered to act as a void in neutron slowing down. Since $\tau \propto \frac{1}{\rho^2}$ (ρ = cell density)

$$\tau_1 \rho_1^2 = \tau_2 \rho_2^2$$

where τ_1 = Fermi age without voids
τ_2 = Fermi age with voids
ρ_1 = density without voids
ρ_2 = density with voids

$$\text{Then } \tau_2 = \tau_1 \left(\frac{\rho_1}{\rho_2}\right)^2 = \tau_1 \left(\frac{\text{area without voids}}{\text{area with voids}}\right)^2 \qquad (8)$$

The value of the slowing down power ($\xi\Sigma_s$) of each cell component is given by:

$$\xi \Sigma_s = \frac{1/3 \ln \frac{2 \times 10^6}{E_T}}{\tau(E_T)\ \Sigma_{tr}}$$

Date used in Fermi age calculations for this reactor are:

(τ D_2O) 200°F	128 cm^2	(A-2)
(τorganic) 600°F	91 cm^2	(A-4)
($\Sigma_{tr} D_2O$) 200°F	0.475 cm^{-1}	(A-2)
(Σ_{tr} organic) 600°F	0.268 cm^{-1}	(A-5)
($\xi \Sigma_s$ D_2O) 200°F	0.158 cm^{-1}	
($\xi_{D_2O} \Sigma_s$ organic) 600°F	0.126 cm^3	
V^{D_2O}	31.8 cm^3	
$V^{organic}$	2.65 cm^3	

The calculated age to thermal (0.034 ev) was 127 cm^2 without voids, 203 cm^2 with voids.

Table 25 gives the computed age to each isotope resonance (for mean resonance energies see Table 24).

TABLE 25

AGE TO ISOTOPE RESONANCES

ISOTOPE	τ_1 (NO VOIDS)	τ_2 (WITH VOIDS
U^{238}	82	131
U^{235}	91	146
Pu^{239}	94	150
Pu^{240}	111	178
Pu^{241}	121	194

(3) Variation of Fermi Age with Temperature - Fermi age is a function of material density and consequently of material temperature. An analytical expression of the latter relationship is derived here.

$$\tau = \int_{kT}^{E_f} \frac{dE}{E} \frac{}{3(\xi \Sigma_s)(\Sigma_{tr})} = \frac{\ln \frac{E_f}{kT}}{3(\xi \Sigma_s)(\Sigma_{tr})}$$

$$\Sigma_{tr} = \Sigma_s (1-\bar{\mu}) \quad \text{and} \quad \Sigma_s = \frac{N_o \rho}{\mu} \sigma_s$$

$$\bar{\mu} = \frac{2}{3A}$$

$$\tau = \frac{1}{(3\xi) \frac{N_o \sigma_s}{\mu} (1-\bar{\mu})} \frac{\ln \frac{E_f}{kT}}{\rho^2}$$

$$= \frac{C \ln \frac{E_f}{kT}}{\rho^2} \quad \text{if } \sigma_s \text{ is not a function of T}$$

$$\tau_B = \tau_A \left(\frac{\rho_A}{\rho_B}\right)^2 \frac{\ln \frac{E_f}{kT_B}}{\ln \frac{E_f}{kT_A}} \tag{9}$$

where

τ_A = Fermi age at temperature A (cm^2)
τ_B = Fermi age at temperature B (cm^2)
ρ_A = Density at temperature A
ρ_B = Density at temperature B
T_A = Temperature A (^oKelvin)
T_B = Temperature B (^oKelvin)

Application of p and Fast Leakage to General NPR Equation - The asymptotic equation for flux for the i^{th} isotope may now be represented by

$$\phi_i \cong \frac{NPR \prod_{i=1}^{i-1} p_j}{\xi \Sigma_s E(1 + B^2 \tau_i)}$$

The term $\prod_{i=1}^{i-1} p_j$ is the product of the resonance escape probabilities of the isotopes which have a resonance energy greater than that of the i^{th} isotope (see Table 24.) For example, the resonance flux seen by Pu^{239} would be

$$\phi_{49} = \frac{NPR \quad p^{28} \, p^{25}}{\xi \Sigma_s E(1+B^2 \tau_{49})}$$

The integral part of the term for Pu^{239} resonance fission in the general NPR equation could therefore be written:

$$\int_{6 E_T}^{\infty} \sigma_f^{41} \phi \, dE = \int_{6 E_T}^{\infty} \frac{\sigma_f^{41} \, NPR \quad p^{28} \, p^{25} \, dE}{\xi \Sigma_s E(1 + B^2 \tau^{49})}$$

Removing terms that are independent of the resonance energy

$$\int_{6 E_T}^{\infty} \sigma_f^{41} \phi \, dE = \frac{NPR \quad p^{28} \, p^{25}}{\xi \Sigma_s (1+ B^2 \tau^{49})} \int_{6 E_T}^{\infty} \sigma_f^{41} \frac{dE}{E}$$

and defining

$$R_a^i \equiv \int_{6 E_T}^{\infty} \sigma_f^i \frac{dE}{E} \qquad \text{(resonance fission integral)}$$

the general NPR equation may be written:

$$\frac{NPR}{\phi_T} = \frac{N^{25} \sigma_{ft}^{25} \nu_{25} + N^{49} \sigma_{ft}^{49} \nu^{49} + N^{41} \sigma_{ft}^{41} \nu^{41}}{\frac{1}{\epsilon_{28}} - \frac{1}{\xi \Sigma_s} \left[\frac{N^{25} \nu^{25} p^{28} R_F^{25}}{1 + B^2 \tau^{25}} + \frac{N^{49} \nu^{49} p^{28} p^{25} R_F^{49}}{1 + B^2 \tau^{49}} + \right.}$$

$$\left. + N^{41} \nu^{41} \frac{p^{28} \, p^{25} \, p^{49} \, p^{40} \, R_F^{41}}{1+B^2 \tau^{40}} \right] \qquad (10)$$

Figure 49 shows the variation of NPR with lifetime. Table 26 shows values of R_a calculated for this reactor.

TABLE 26

RESONANCE FISSION INTEGRALS FOR U AND PU ISOTOPES

ISOTOPE	R_a (barns)
U^{235}	502
Pu^{239}	1496
Pu^{241}	1576

Neutron Destruction Rate (NDR)

Neutron destruction rate is defined as the number of neutrons of all energies which are removed from the system by:

(1) thermal absorption by U^{235}, U^{238}, Pu^{239}, Pu^{240}, Pu^{241}, fission products, organic coolant and aluminum

(2) fast and thermal leakage

(3) fast absorption in U^{238}

(4) resonance absorption in U^{235}, U^{238}, Pu^{239}, Pu^{240}, and Pu^{241}

Resonance and fast neutron absorption by moderator, coolant and fission products are neglected.

The general equation for NDR is:

$$\begin{aligned} NDR = \phi_T \Big[& N^{28} \sigma_{aT}^{28} + N^{25} \sigma_{aT}^{25} + N^{49} \sigma_{aT}^{49} + N^{40} \sigma_{aT}^{40} + N^{41} \sigma_{aT}^{41} \\ & + N^{fP} \sigma_{aT}^{fP} + N^{D_2O} \sigma_{aT}^{D_2O} + N^{org} \sigma_{aT}^{org} + N^{al} \sigma_{aT}^{al} \Big] + \phi_T D_T B^2 \\ & + \frac{\epsilon^{28}-1}{\nu^{28}} (NPR) + N^{28} \int \sigma_a^{28} dE + N^{25} \int \sigma_a^{25} dE \\ & + N^{49} \int \sigma_a^{49} dE + N^{40} \int \sigma_a^{40} dE + N^{41} \int \sigma_a^{41} dE \\ & + NPR \; \frac{p^{28} p^{25} p^{49} p^{40} p^{41} B^2 \tau_T}{1 - B^2 \tau_T} \end{aligned} \qquad (11)$$

Using the asymptotic flux approximation in the resonance absorption terms and defining:

$$NPR' = \frac{NPR}{\phi_T}, \quad NDR' \equiv \frac{NDR}{\phi_T}, \quad R_a^i \equiv \int_{6E_T}^{\infty} \frac{\sigma_a^i \, dE}{E}$$

the general equation may be written

$$NDR' = \Sigma_{aT}\left(1 + L^2B^2\right) + \frac{\epsilon^{28} - 1}{\nu^{28}} \quad (NPR')$$

$$+ NPR' \quad \frac{p^{28}\, p^{25}\, p^{49}\, p^{40}\, p^{41}\, B^2}{1+B^2\,\tau_T}\,\tau_T +$$

$$+ \frac{NPR'}{\xi\,\Sigma_s}\left[\frac{N^{28}\,Ra^{28}}{1+B^2\,\tau_{28}} + \frac{N^{25}\,p^{28}\,Ra^{25}}{1+B^2\,\tau_{25}} + \frac{N^{49}\,p^{28}\,p^{25}\,Ra^{49}}{1+B^2\,\tau_{49}}\right.$$

$$\left. + \frac{N^{40}\,p^{28}\,p^{25}\,p^{49}\,Ra^{40}}{1+B^2\,\tau_{40}} + \frac{N^{41}\,p^{28}\,p^{25}\,p^{49}\,p^{40}\,Ra^{41}}{1+B^2\,\tau_{41}}\right] \quad (12)$$

where

$$\Sigma_{aT} \equiv N^{28}\,\sigma_{aT}^{28} + N^{25}\,\sigma_{aT}^{25} + N^{49}\,\sigma_{aT}^{49} + N^{40}\,\sigma_{aT}^{40} + N^{41}\,\sigma_{aT}^{41}$$

$$+ N^{fP}\,\sigma_{aT}^{fP} + N^{mod}\,\sigma_{aT}^{mod} + N^{org}\,\sigma_{aT}^{org} + N^{al}\,\sigma_{aT}^{al} \quad (13)$$

Figure 49 shows the variation of NDR with lifetime.

Isotope Concentration

The general equations for rate of change concentration of significant isotopes and fission products are

$$\frac{dN^{25}}{dt} = -N^{25}\,\sigma_{aT}^{25}\,\phi_T - N^{25}\int\sigma_a^{25}\,\phi\,dE$$

$$\frac{dN^{28}}{dt} = -N^{28}\,\sigma_{aT}^{28}\,\phi_T - N^{28}\int\sigma_a^{25}\,\phi\,dE$$

$$\frac{dN^{49}}{dt} = -N^{49}\,\sigma_{aT}^{49}\,\phi_T - N^{49}\int\sigma_a^{49}\,\phi\,dE + N^{28}\,\sigma_{aT}^{28} + N^{28}\int\sigma_a^{28}\,\phi\,dE$$

$$\frac{dN^{40}}{dt} = -N^{40}\,\sigma_{aT}^{40}\,\phi_T - N^{40}\int\sigma_a^{40}\,\phi\,dE + \frac{\sigma_{cT}^{49}}{\sigma_{aT}^{49}}\,N^{49}\,\sigma_{aT}^{49}\,\phi_T + N^{49}\int\frac{\sigma_{cT}^{49}}{\sigma_{aT}^{49}}\,\sigma_a^{49}\,\phi\,dE$$

$$\frac{dN^{41}}{dt} = N^{41}\,\sigma_{aT}^{41}\,\phi_T - N^{41}\int\sigma_a^{41}\,\phi\,dE + N^{40}\,\sigma_{aT}^{40}\,\phi_T + N^{40}\int\sigma_a^{40}\,\phi\,dE$$

$$\frac{dN^{fp}}{dt} = -N^{fp}\,\sigma_{aT}^{fp}\,\phi_T + \Sigma_f'\,\phi_T$$

Where Σ_f' is defined

$$\Sigma_f' \equiv N^{25}\,\sigma_{fT}^{25} + N^{49}\,\sigma_{fT}^{49} + N^{41}\,\sigma_{fT}^{41} + \frac{\epsilon^{28}-1}{\nu^{28}}\,\frac{NPR}{\phi_T}$$

$$+ \frac{1}{\phi_T}\left[N^{25}\int\sigma_f^{25}\,\phi\,dE + N^{49}\int\sigma_f^{49}\,\phi\,dE + N^{41}\int\sigma_f^{41}\,\phi\,dE\right] \quad (14)$$

The power density of the reactor has been assumed constant. Therefore, the fission products are formed at a constant rate. A thermal microscopic cross-section of 50 barns was assumed for each fission product formed. A higher value would have been more conservative and would perhaps have accounted better for resonance absorption of the fission products.

Using the asymptotic flux approximation for the resonance energy region and the following definitions:

$$\alpha_T^{49} \equiv \frac{\sigma_{cT}^{49}}{\sigma_{aT}^{49}}, \quad \alpha_R^{49} \equiv \frac{\sigma_c^{49}}{\sigma_a^{49}}, \quad R_a^i \equiv \int\sigma_a^i\,\frac{dE}{E}, \quad NPR' \equiv \frac{NPR}{\phi_T}$$

the general isotope concentration equations reduce to:

$$\frac{1}{\phi_T}\frac{dN^{25}}{dt} = -N^{25}\left[\sigma_{aT}^{25} + \frac{NPR'\,p^{28}\,R_a^{25}}{\xi\,\Sigma_s(1+B^2\,\tau^{25})}\right] \quad (15)$$

$$\frac{1}{\phi_T}\frac{dN^{28}}{dt} = -N^{28}\left[\sigma_{aT}^{28} + \frac{NPR'\,R_a^{28}}{\xi\,\Sigma_s\,(1+B^2\,\tau^{28})}\right] \quad (16)$$

$$\frac{1}{\phi_T}\frac{dN^{49}}{dt} = -N^{49}\left[\sigma_{aT}^{49} + \frac{NPR'\,p^{28}\,p^{25}\,R_a^{49}}{\xi\,\Sigma_s(1+B^2\,\tau^{49})}\right] + N^{28}\left[\sigma_{aT}^{28} + \frac{NPR'\,R_a^{28}}{\xi\,\Sigma_s(1\;B^2\;28}\right. \quad (17)$$

$$\frac{1}{\phi_T}\frac{dN^{40}}{dt} = -N^{40}\left[\sigma_{aT}^{40} + \frac{NPR'\,p^{28}\,p^{25}\,p^{49}\,R_a^{40}}{\xi\,\Sigma_s(1+B^2\,\tau^{40})}\right]$$

$$+ N^{49}\left[\alpha^{49}\,\sigma_{aT}^{49} + \frac{NPR'\,p^{28}\,p^{25}\,\alpha^{49}\,R_a^{49}}{\xi\,\Sigma_s(1+B^2\,\tau^{49})}\right] \quad (18)$$

$$\frac{1}{\phi_T}\frac{dN^{41}}{dt} = -N^{41}\left[\sigma_{aT}^{41} + \frac{NPR'\,p^{28}\,p^{25}\,p^{49}\,p^{40}\,p^{41}\,R_a^{41}}{\xi\,\Sigma_s\,(1+B^2\,\tau^{40})}\right] \quad (19)$$

$$+ N^{40}\left[\sigma_{aT}^{40} + \frac{NPR' \quad p^{28}\, p^{25}\, p^{49}\, R_a^{40}}{\xi \Sigma_s (1 + B^2 \quad \zeta^{40})}\right]$$

$$\frac{1}{\phi_T} \quad \frac{dN^{fp}}{dt} = - N^{fp} \quad \sigma_{aT}^{fp} + \Sigma_f'$$

Fuel Lifetime

The fuel lifetime is the product of the power density and time of reactor operation at the instant k becomes less than one.

Conversion Ratio

Conversion ratio is defined as the ratio of the macroscopic cross-section for the formation of fissionable material to the macroscopic cross-section for the destruction of fissionable material; based on thermal flux;

$$CR = \frac{\Sigma_{aT}^{28} + N^{28} \int_{6E_T}^{\infty} \sigma_a^{28} \frac{\phi}{\phi_T}\, dE + \Sigma_{aT}^{40} + N^{40} \int_{6E_T}^{\infty} \sigma_a^{40} \frac{\phi}{\phi_T}\, dE}{\Sigma_{aT}^{25} + N^{25} \int_{6E_T}^{\infty} \sigma_a^{25} \frac{\phi}{\phi_T}\, dE + \Sigma_{aT}^{49} + N^{49} \int_{6E_T}^{\infty} \sigma_a^{49} \frac{\phi}{\phi_T}\, dE + \Sigma_{aT}^{41} +}$$

$$+ N^{41} \int_{6E_T}^{\infty} \frac{\phi}{\phi_T} \sigma_a^{41}\, dE$$

Figure 48b shows the variation of conversion ratio with lifetime for the design reactor.

Thermal Cross-sections

The thermal absorption and fission cross-sections of U^{235} and Pu^{239} have been measured with mono-energetic neutrons to an accuracy of a few percent. When a distribution of neutron energy exists at thermal equilibrium, average thermal cross-sections must be used.

Assuming $\frac{1}{v}$ absorption and maxwellian distribution

$$\bar{\sigma} = \frac{\int \sigma(v)\, \phi(v)\, dv}{\int \phi(v)\, dv} = \frac{\int \frac{B}{v}\, n(v)\, v\, dv}{\int n(v)\, v\, dv} = \sqrt{\frac{\pi}{2}}\, \frac{B}{v_o}$$

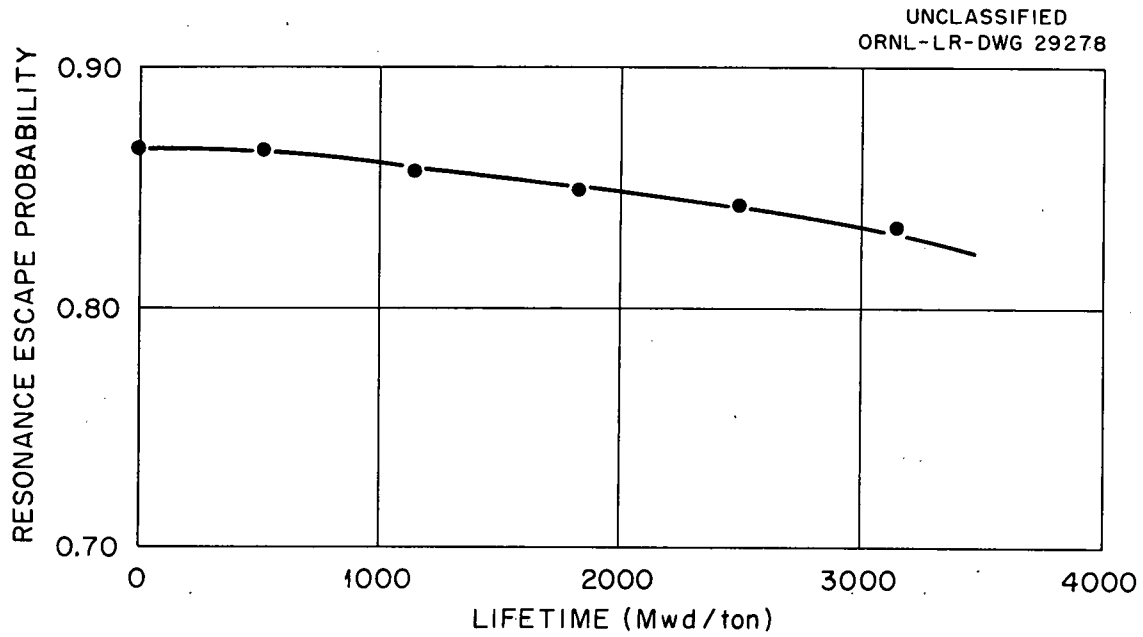

Fig. 48a: Resonance Escape Probability vs Lifetime

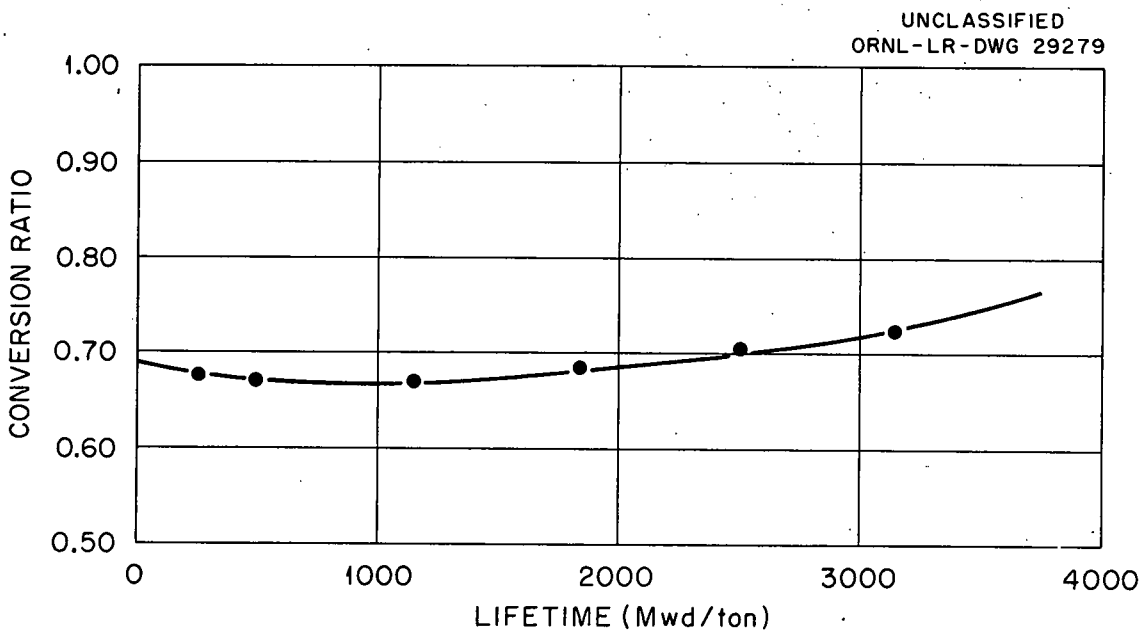

Fig. 48b: Conversion Ratio vs Lifetime

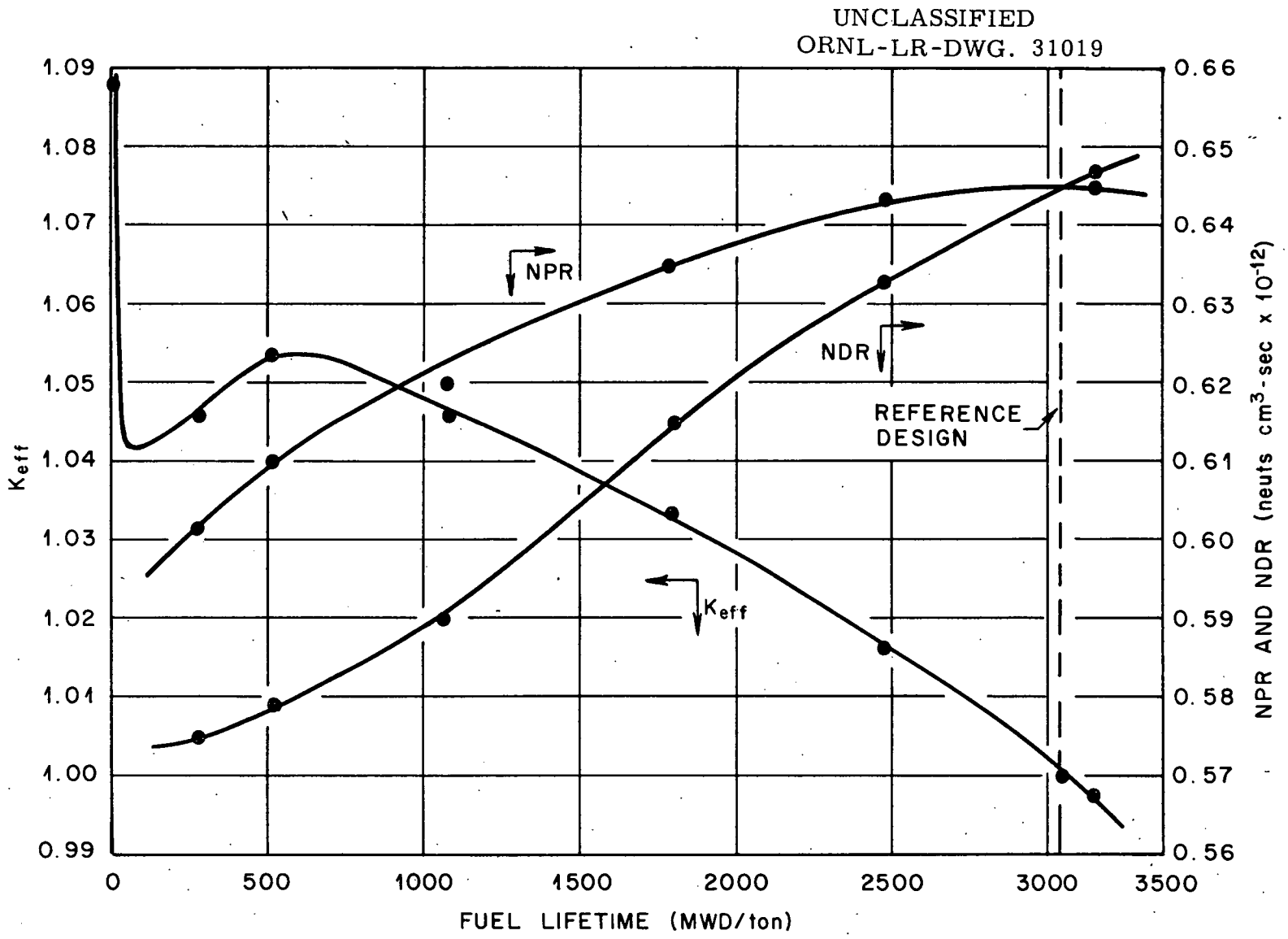

Fig. 49. K_{eff}, Neutron Production Rate and Neutron Destruction Rate

where v_o is the velocity of the neutrons in the distribution which have the most probable energy

Since $\frac{B}{v_o} = \sigma_o$ (cross section of neutron with velocity v_o)

$$\bar{\sigma} = \frac{\sqrt{\pi}}{2} \sigma_o$$

If, however, the cross-section is not 1/v, a correction that must be applied to $\bar{\sigma}$ (a-3). The effective cross section for a Maxwellian neutron distribution, the most probable neutron energy of which is E_o, is related to the cross-section for neutrons of the most probable energy in the distribution by the expression:

$$\bar{\sigma}(E_o) = f(E_o)\, \sigma(E_o)$$

For a 1/v absorber, $f(E_o) = 1$

For a non-1/v absorber, $f(E_o)$ is defined by:

$$f(E_o) = \frac{\int \sigma(E)\, \phi(v)\, dv}{\int \sigma(E_o)\, \frac{v_o}{v}\, \phi(v)\, dv}$$

Consequently for non-1/v absorbers, the average thermal cross-section is given by:

$$\bar{\sigma}(E_o) = f(E_o)\, \frac{\sqrt{\pi}}{2}\, \sigma(E_o)$$

A problem exists in selecting the most probable thermal neutron energy (E_o) upon which to base thermal cross-section determinations. To find this energy the temperatures of the components of the reactor were examined to find the temperature corresponding to that of the neutrons of most probable velocity in the system. The most probable neutron velocity is related to this temperature by $\frac{1}{2}\, m\, v_o^2 = k\, T_o$.

In a non-capturing medium, neutrons in thermal equilibrium with the medium have a Maxwellian distribution. In an absorbing medium, however, the absorption of neutrons of lower energy results in a"hardening" of the energy spectrum. Consequently the temperature corresponding to the most probable

velocity is somewhat higher. For a mixture of essentially non-absorbing moderator such as D_2O and poison such as terphenyl (which also serves as moderator), the temperature would be somewhat higher than the D_2O temperature.

In this case the D_2O temperature was 93°C (366°K). A neutron temperature of 400°K was assumed. The neutron energy corresponding to this temperature is 0.034 ev.

The table on page 176 gives cross-sections used in calculating reference design reactor.

Method of Calculation

The ORACLE uses the initial fuel concentrations and other input quantities in the NPR and NDR equations to compute the initial k. If k is greater than one, Σ_f' is then used to determine the thermal neutron flux which will give the proper power density. This flux and the time interval of calculation are then put into the isotope equation (equations 15-19 above), which are now in finite difference form, and new isotope concentrations are found. These concentrations are used to find a new value of k. If this k is greater than one, the operation is repeated until k falls below one. Figure 49 shows the variation of k_{eff}, with fuel lifetime for the reference design reactor. The k_{eff} shown is corrected for equilibrium xenon and samarium.

SYMBOLS

A = atomic mass number of nuclide

T^{49} = $\dfrac{cT^{49}}{aT^{49}}$

R^{49} = $\dfrac{c^{49}}{a^{49}}$

B^2 = geometric buckling

CR = conversion ratio

ξ = average logarithmic energy decrement per collision

D_T = thermal diffusion coefficient (cm)

E_1 = energy

E_T = thermal energy

ϵ or ε = fast fission factor

f = correction for non-1/v absorption by certain isotopes

I = Bessel function of first king (subscript is the order)

k = multiplication constant, when alone

λ = radioactive decay constant ($time^{-1}$)

L = thermal neutron diffusion length (cm)

μ = mean value of the cosine of the scattering angle in the laboratory coordinate system

n = number of fuel rods per cluster

NDR = neutron destruction rate ($neutrons/cm^3$-sec)

NPR = neutron production rate ($neutrons/cm^3$-sec)

ν = mean number of neutrons produced per fission (superscript indicates isotope - sec)

p = resonance escape probability (subscript designates isotope - see $\sim$)

P_{NFL} = probability of non-fast leakage

ϕ = neutron flux ($neutrons/cm^2$-sec)

ϕ_T = thermal neutron flux

Q = neutron slowing down density ($neutron/cm^3$-sec)

R_{Fuel} = radius of fuel rod of area equivalent to area of all rods in cluster

R_a = resonance absorption integral

R_f = resonance fission integral (barns)

ρ = density

σ = microscopic cross-section (barns)

Subscript indicates reaction and neutron energy

a = absorption

c = radiative capture

f = fission

t = total

T = thermal energy neutron

Superscript indicates isotope or material (also used in ν and p)

25 - U^{235} 41 - Pu^{241}

28 - U^{238} 49 - Pu^{239}

40 - Pu^{240} Al - aluminum

Σ = microscopic cross-section (cm^{-1})

Σ_f' = see equation 14

T = temperature (° Kelvin)

$T_{\frac{1}{2}}$ = half life of nuclide

τ = Fermi age (cm^2)

V = volume

v = velocity

$\mathcal{S}$ = resonance flux disadvantage factor

DATA USED IN ANALYSIS CALCULATIONS

	U^{235}	U^{238}	Pu^{239}	Pu^{240}	Pu^{241}	FP	D_2O	Al
σ_{aT}	514	1960	1000	250	936	77	8.6×10^{-2}	-
σ_a	65	-	168	795	140	-	-	
σ_s	10	8.3	9.6	9.6	9.6	-	14	-
ν	2.47	2.60	2.91	-	3.05	-	-	-
τ	146	131	150	178	194	-	-	-
R_a	742	-	1880	8940	2060	-	-	-
R_f	502	-	1496	1576	-	-	-	-

DENSITIES (gm/cm^3 AT INDICATED TEMPERATURES)

Al	$600^{\circ}F$	2.67
UO_2	$800^{\circ}F$	10.00
D_2O	$175^{\circ}F$	1.09
Terphenyl	$600^{\circ}F$	0.875

APPENDIX B

HEAT TRANSFER AND FLUID FLOW

Organic Heat Transfer Properties

The use of an organic fluid as the primary coolant for a reactor poses several engineering problems. Most important among these are the relatively poor heat transfer properties of the organics in general.

Comparison With Other Coolants -

1. Film Coefficient - Figure 50 shows the relative magnitude of the film coefficient, h, versus pumping power for an organic coolant as compared to water and CO_2, based on the Dittus-Boelter equation:

$$h = 0.023 \frac{k}{D} \left(\frac{VD}{\mu}\rho\right)^{0.8} \left(\frac{c_p}{k}\mu\right)^{0.4}$$

For a given pumpting power, the film coefficient for the organic fluid is approximately 20% of that for water, but somewhat better than CO_2.

Therefore, for a given film temperature drop, five times as much heat transfer area is required when using an organic as compared to water to transfer the same amount of heat. In practice this factor requires the use of a much higher film temperature drop, with resulting higher surface temperature, when using organic coolants. Even with the use of a high film temperature drop the heat transferred per unit area still tends to be less for an organic coolant, and this requires a larger degree of subdivision of the fuel than in water cooled systems.

2. Heat Capacity - As another means of comparing these fluids the product ρc_p, which is a measure of the bulk heat transfer properties of a fluid, is listed below.

Fluid	$c_p\rho$(BTU/F - Ft^3)
Water (550°F)	61.7
Diphenyl (650°)	32
CO_2(115 psig)	0.12

Thus for a given temperature rise across the reactor, twice as much organic as water is required to remove the same amount of heat.

ORNL-LR-Dwg.-31020
UNCLASSIFIED

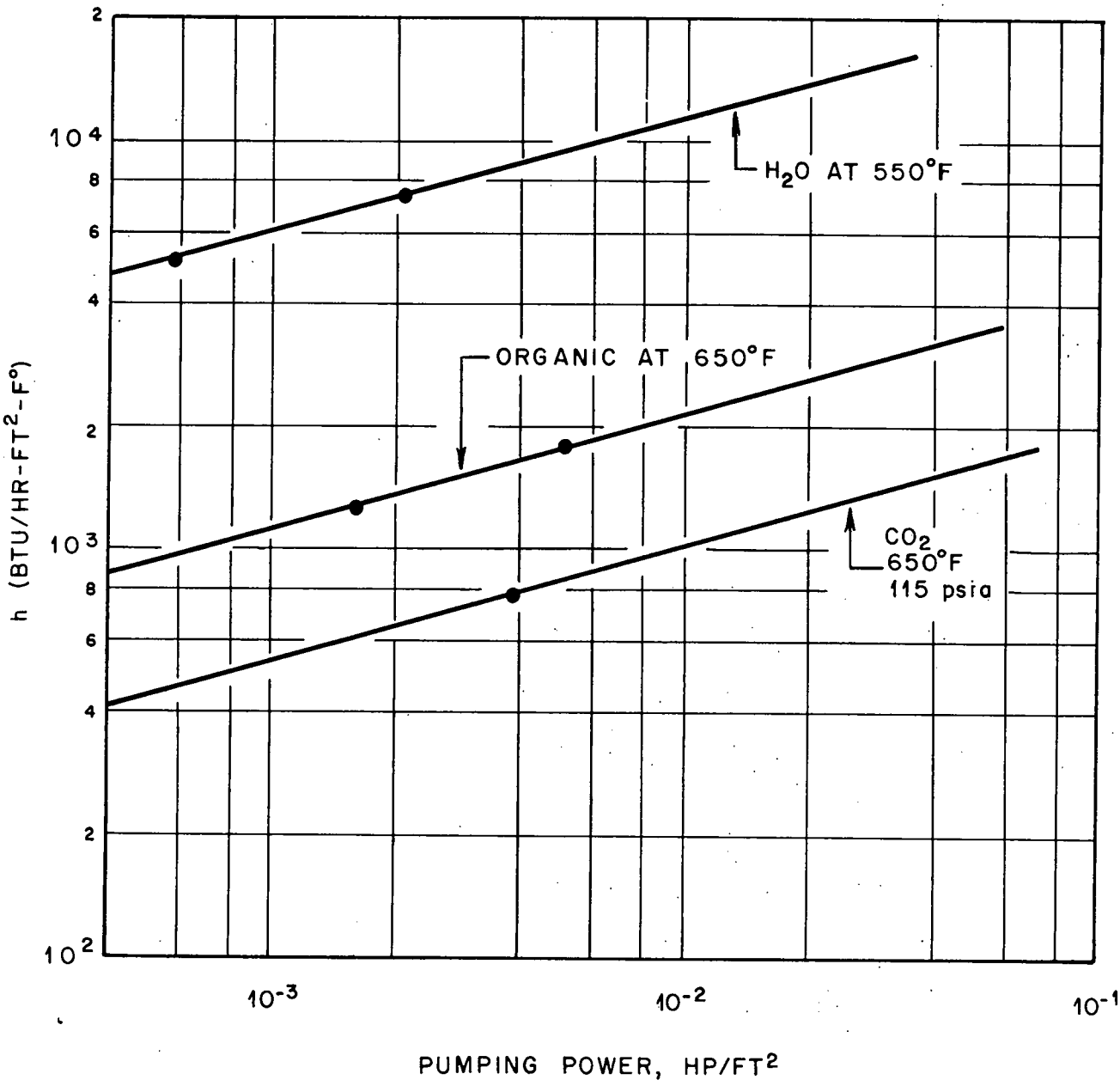

Fig. 50. h Vs. Pumping Power for 1-inch Diameter Tubing

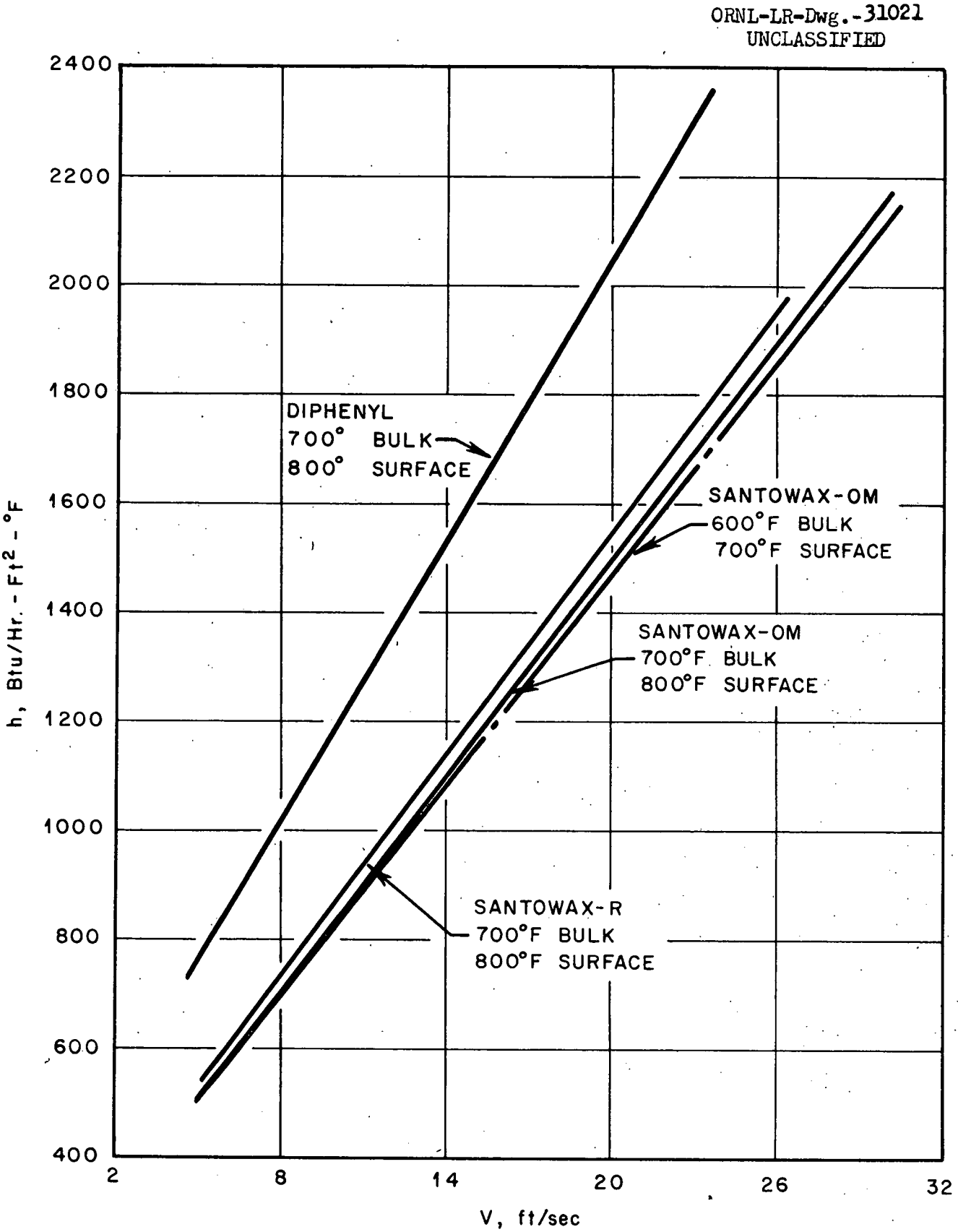

Fig. 51. Experimental Heat Transfer Coefficients for Unirradiated Diphenyl, Santowax-R, and Santowax-OM

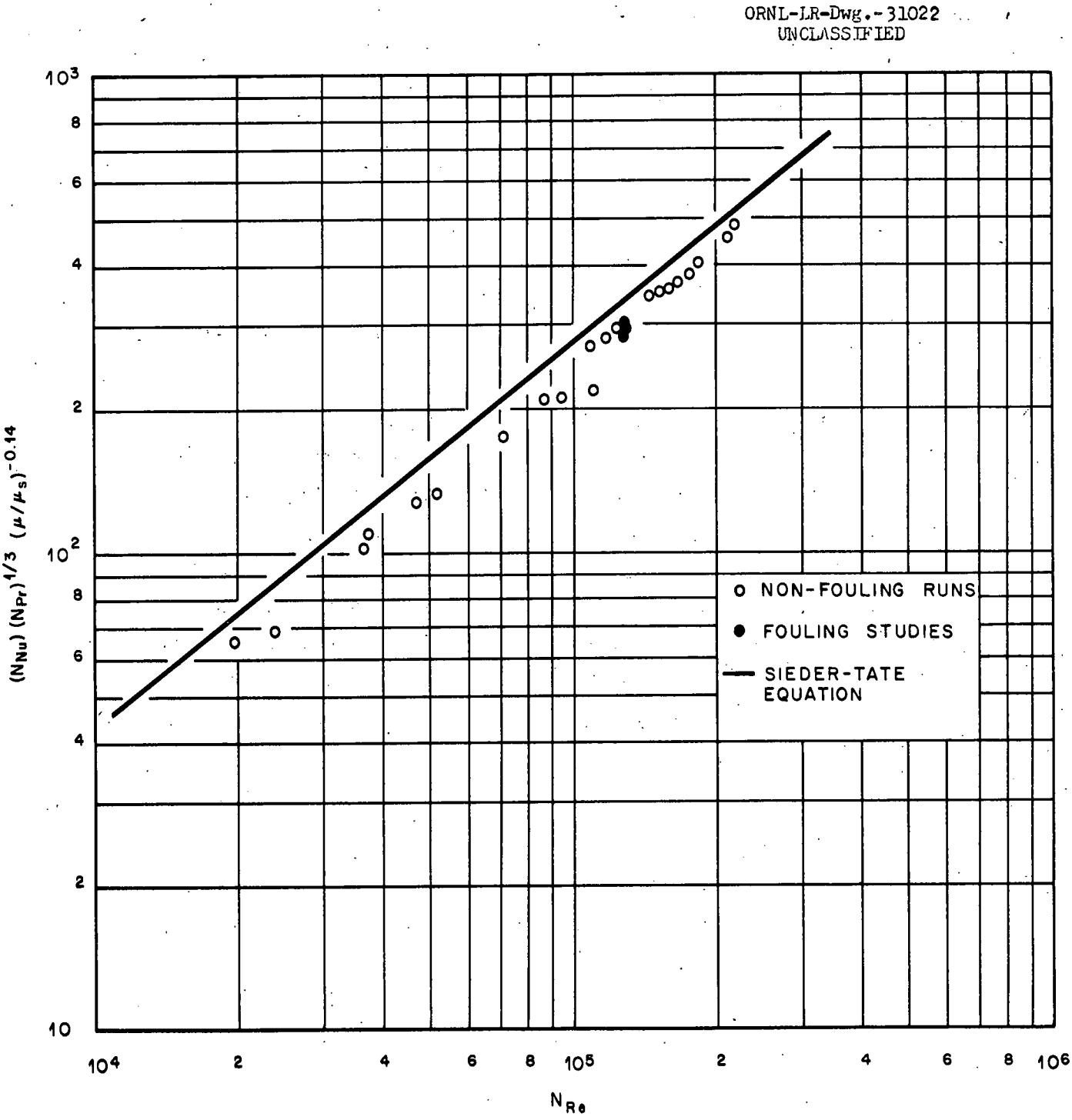

Fig. 52. Experimental Heat Transfer Coefficients for Santowax-R

Comparison of Organics - Among the organics themselves there is considerable variation in heat transfer properties. Figure 51 indicates the variation in film coefficient among the three possible coolants considered in this study. At a velocity of 25 ft/sec the film coefficient for Santo-wax R is 25% less than that for diphenyl, due primarily to the higher viscosity of the Santo-wax R.

Figure 52 shows the correlation of experimental data for Santo-wax R as compared to the Sieder-Tate equation:

$$h = \frac{0.027\ k}{D} \left(\frac{VD\rho}{\mu}\right)^{0.8} \left(\frac{C_p \mu}{k}\right)^{0.33} \left(\frac{\mu}{\mu_\omega}\right)^{0.14}$$

The graph indicates that the above equation may be used to predict the film coefficient within an accuracy of 10%.

Radiation Effects - The effect of irradiation upon the organics is to reduce their heat transfer properties, primarily by increasing the viscosity. Figure 53 shows the effect of higher boiling tars, which are formed upon irradiation, upon the film coefficient, h. Since it is desirable to operate at a high tar concentration in order to reduce the organic make-up, this effect is of considerable importance. At the tar concentration of 30% used in this study the film coefficient for Santo-wax R is estimated to be 83% of that for the unirradiated material.

Burn-Out Heat Flux - Reference B-1 has correlated experimental data for the maximum heat flux in diphenyl as a function of coolant velocity and the degree of subcooling of the fluid, T_{sub}. For a velocity of 15 ft/sec the maximum heat flux is given by the relation

$$Q/A_{critical} = 2310\ T_{sub} + 177{,}000$$

If this equation is applicable to Santo-wax R the maximum heat flux in the critical portion of the core will be approximately 465,000 B/Hr-Sq ft. Since the calculated maximum heat flux at full load is 242,000 B/Hr-Sq ft, the ratio of burnout flux to maximum operating flux will be 1.9.

Design Criteria

The aim of the heat transfer analysis was to satisfy the following conditions:

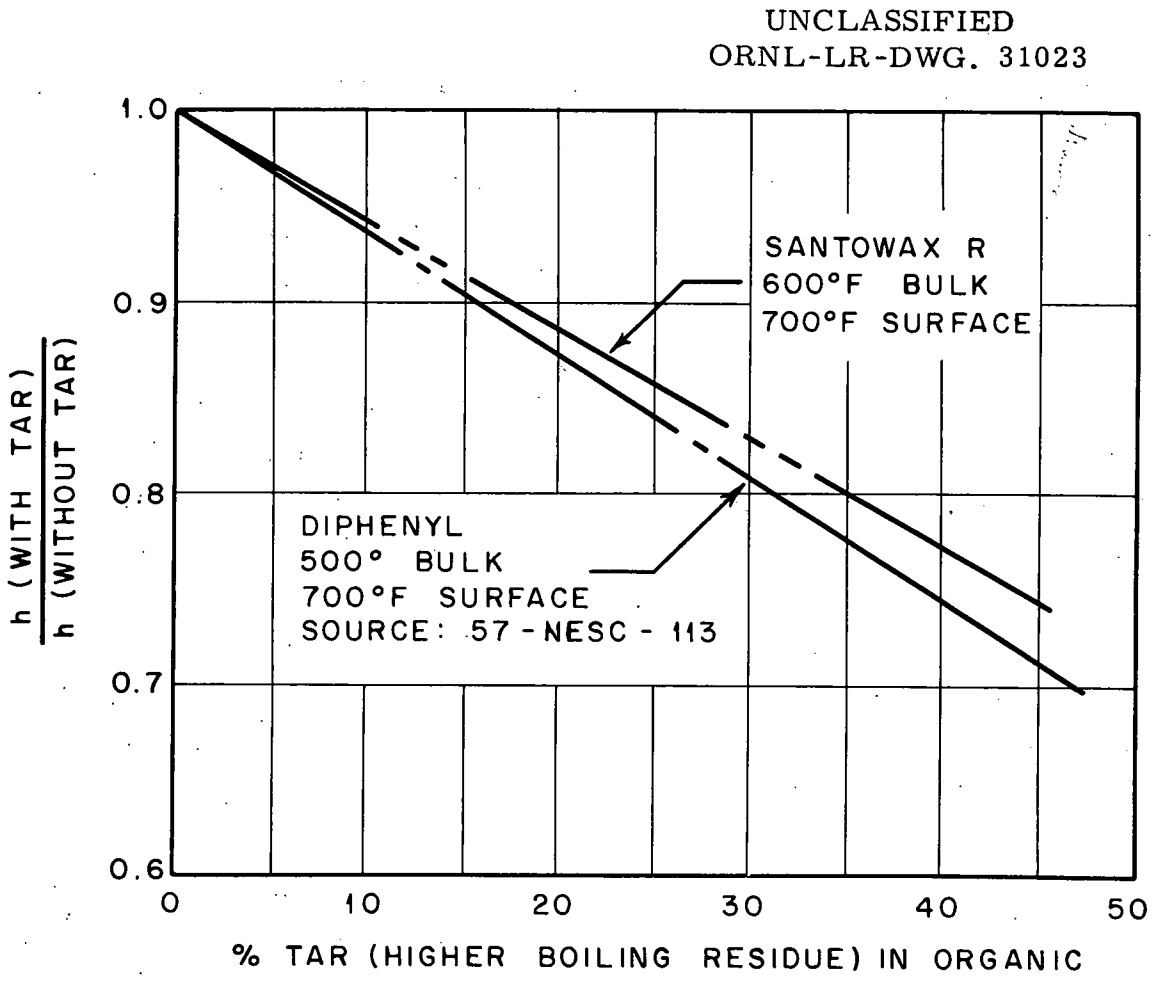

Fig. 53. Heat Transfer Coefficient Vs. Percent Tars

1. A maximum allowable surface temperature of 750°F
2. As high a reactor outlet temperature as possible, consistant with condition 1.
3. Use of a minimum number of fuel elements.
4. The amount of organic coolant in the core should be as small as possible, in order to reduce make-up and increase reactivity.
5. The energy required to pump the organic coolant should not be excessive.

As in any design, these requirements are in conflict, and the final design represents a compromise among them. No attempt was made to optimize the overall design because of the difficulty of assessing the relative worth of each of the requirements listed. However it is believed that the final design represents a reasonable compromise between these requirements.

Reactor Core Analysis

Method - Equations were derived for the maximum wall temperature in the reactor as outlined in references B-2, B-3 and B-4. These derivations are given at the end of this appendix. The various parameters involved were then varied to determine the effect of each one on the system. These included the number of fuel elements, coolant velocity, hydraulic diameter, coolant outlet temperature and temperature rise through the reactor. Figures 54 and 55 indicate the results of some of these studies. Figure 54 shows the variation in maximum wall temperature as a function of coolant temperature rise for constant reactor outlet temperature and constant power output. The graph indicates that an increase in coolant temperature rise tends to lower the maximum wall temperature somewhat. A high temperature rise is also desirable from the standpoint of reducing the amount of organic in the core. Figure 55 shows the effect of the fuel element spacing, which varies with the number of fuel elements for a constant reactor size, upon the maximum wall temperature. The pumping power is also plotted but it is of little significance in this range since the maximum surface temperature is the controlling factor.

Hot Channel Factors - Figure 56 shows the longitudional variation in bulk coolant and wall temperatures within the reactor for the final design, both with and without hot channel factors. Hot channel factors of 1.3 were used for both the bulk coolant temperature rise and the film temperature

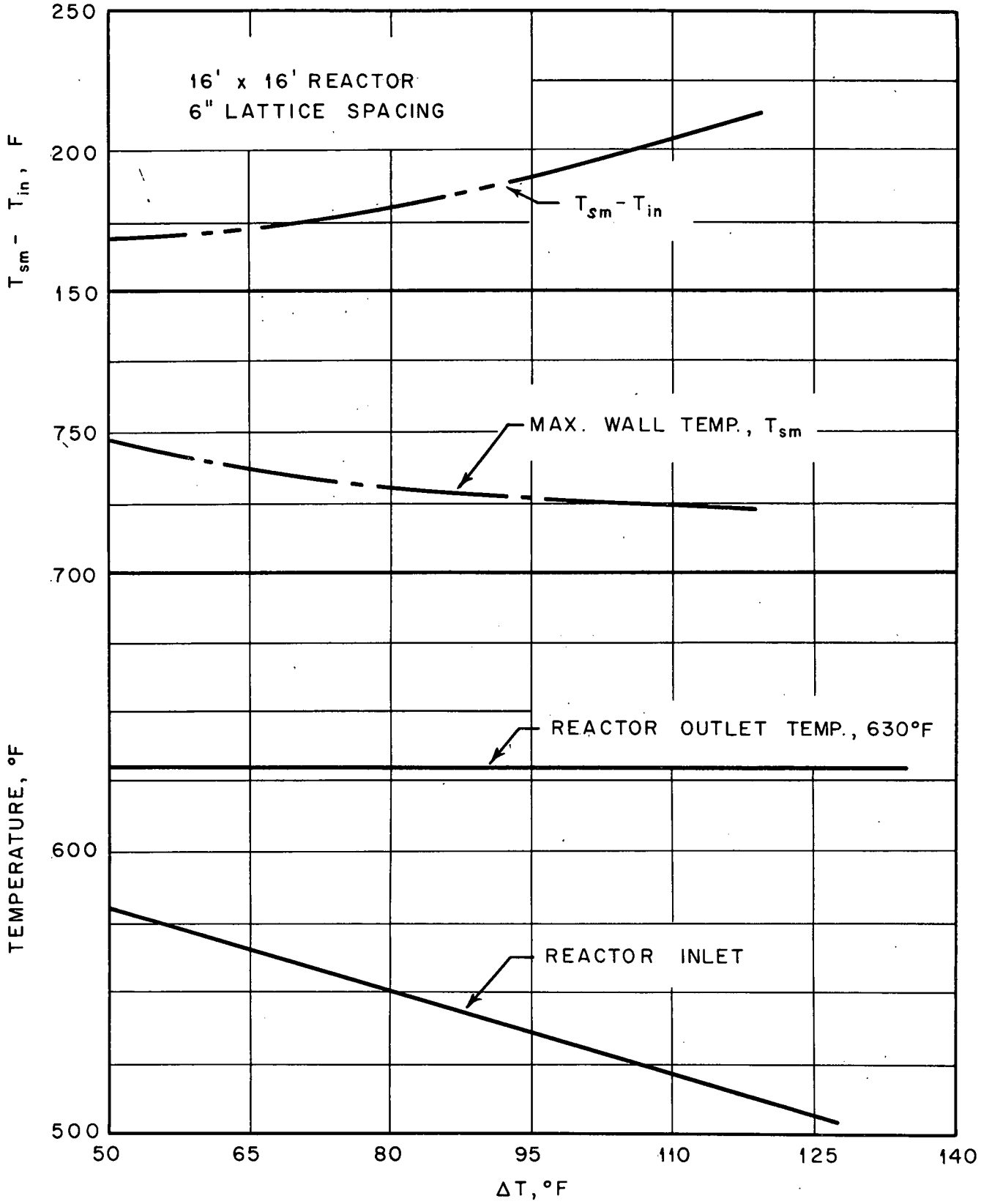

Fig. 54. Maximum Wall Temperature Vs. ΔT for Constant Power Output and Reactor Outlet Temperature

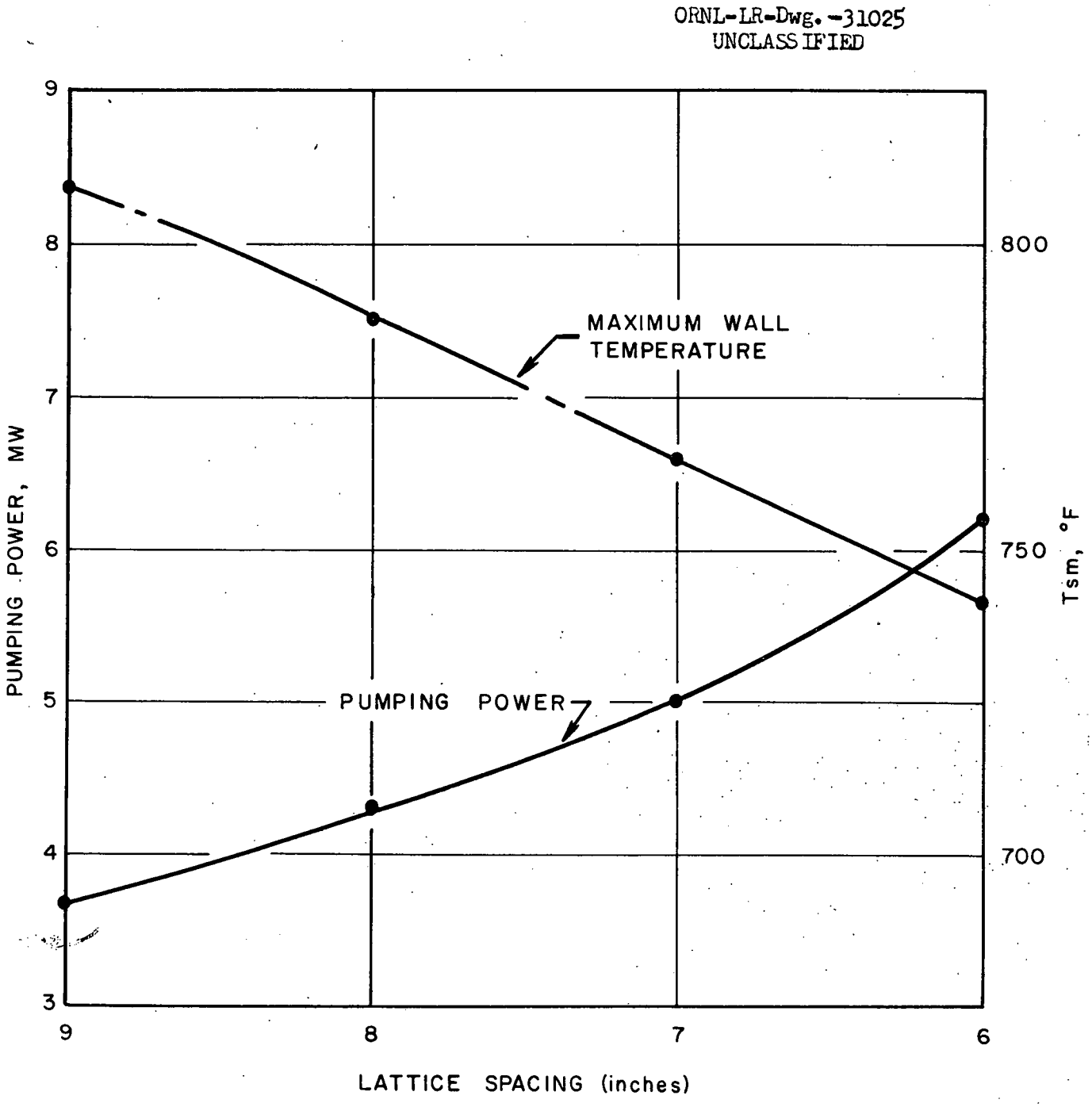

Fig. 55. Pumping Power and Maximum Wall Temperature Vs. Lattice Spacing for Constant Velocity and Power Output

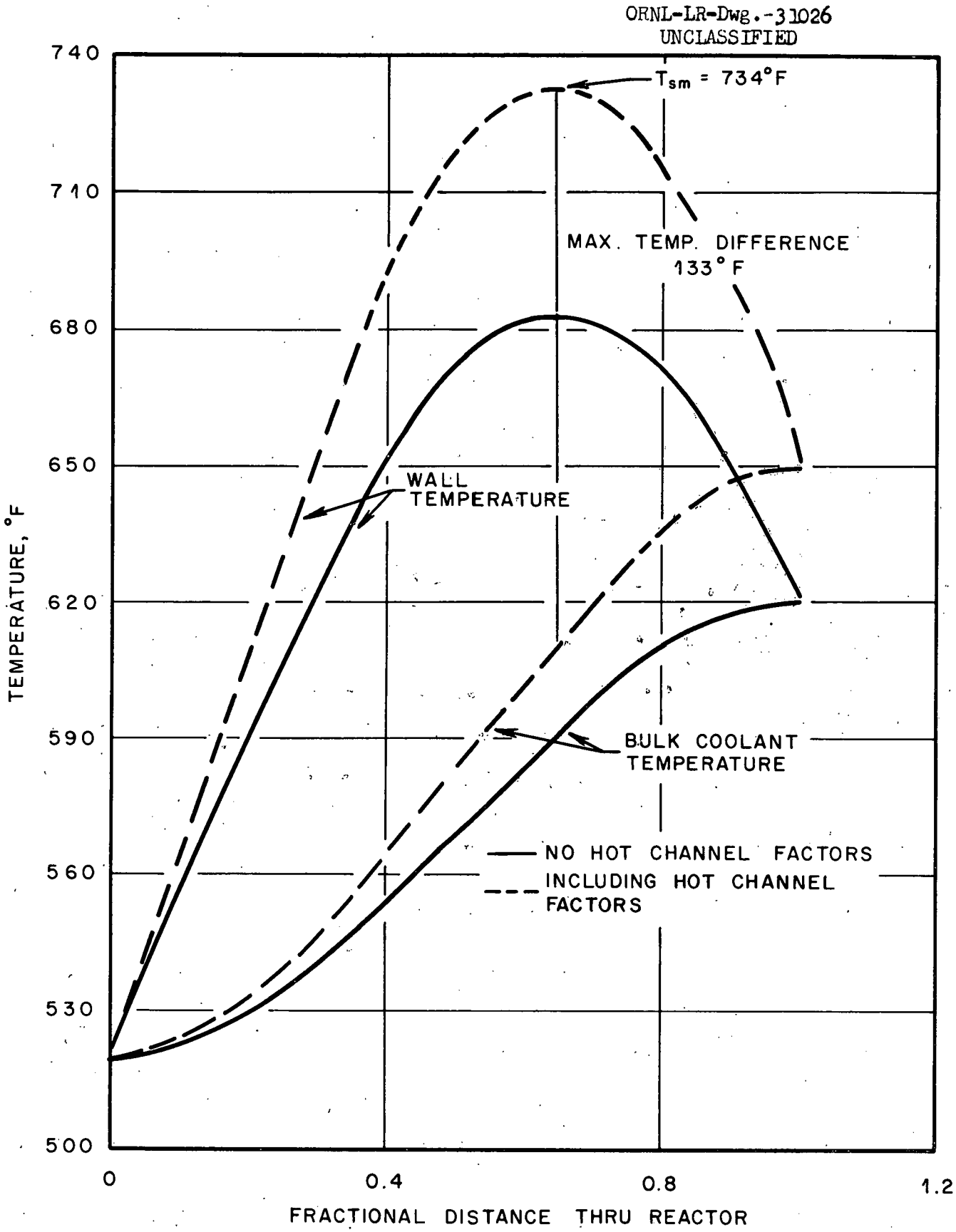

Fig. 56. Longitudinal Temperature Profile in Central Coolant Channel

UNCLASSIFIED
ORNL-LR-DWG. 23622

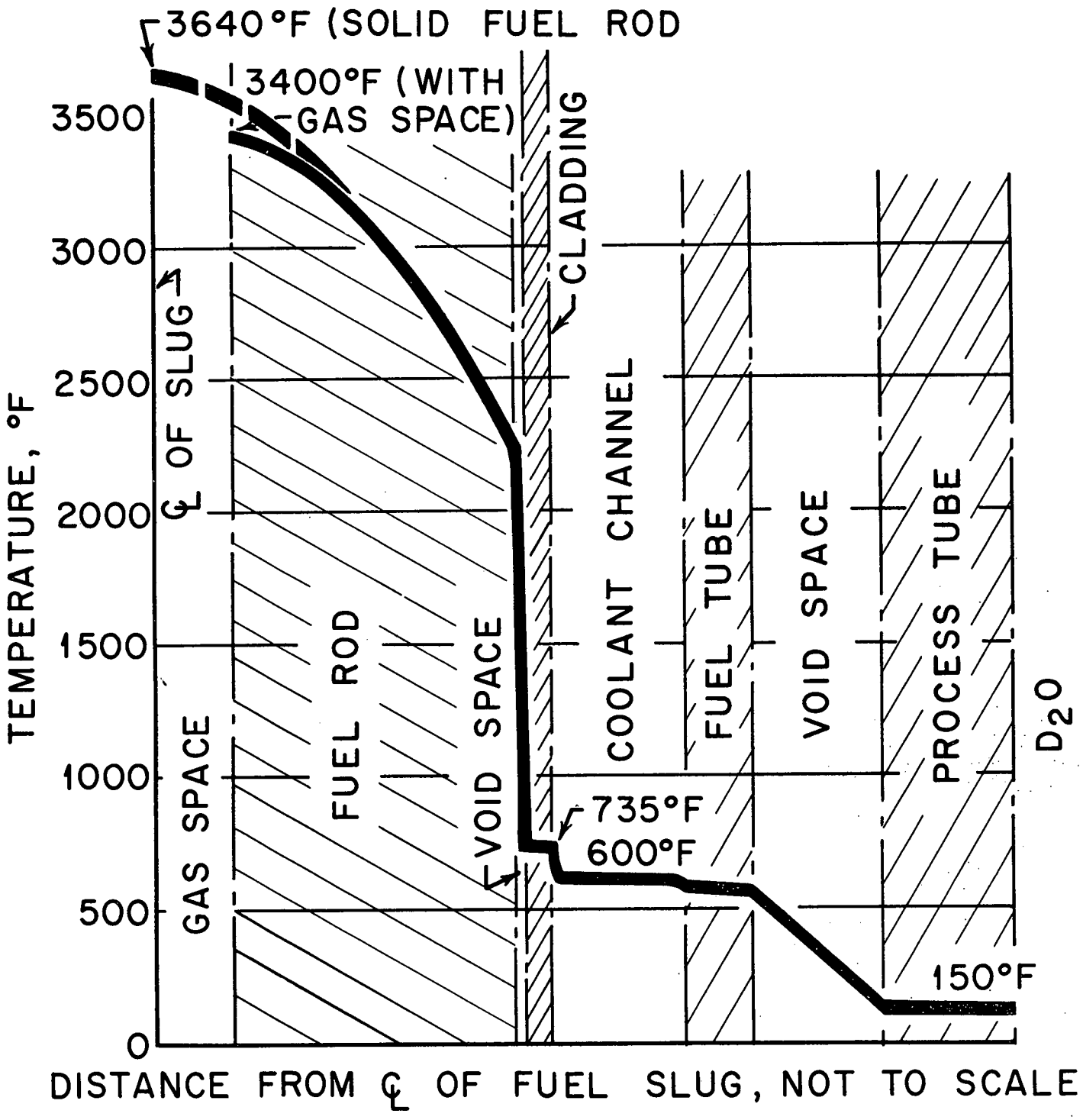

RADIAL TEMPERATURE DISTRIBUTION

difference in calculating the maximum wall temperature. No scale factor was used since experimental data (reference B-5) indicates that fouling does not occur. These factors are included to take account of local variations in tolerances, heat generation, coolant flow, etc., and it is assumed that all such adverse variations exist at the critical point in the reactor. While the values used for these factors are somewhat low compared to other reactor designs, it is believed that they are adequate for the following reasons:

1. Since the various coolant channels within a cluster are interconnected, local film boiling does not result in vapor binding of an entire channel, as in the case of a plate type element.
2. Loss of cladding integrity due to high temperature in a few elements is not considered a serious accident in this reactor.
3. Since the fuel is UO_2 there is little danger of meltdown.

Fuel Temperature - Figure 57 shows the radial temperature profile of a fuel element in the central region of the reactor, based on a radial clearance between the fuel and cladding of 0.002 in. at room temperature, and a gas pressure of one atmosphere. A more detailed calculation taking into account the variation of thermal conductivity of the fuel with temperature and heat transfer by radiation indicates that the maximum fuel temperature will be higher than shown in Figure 57, but still below its melting point of 5200°F. It should be noted that the maximum fuel temperature is very sensitive to the clearance between fuel and clad. For example, if a bond exists between the two the maximum fuel temperature will be under 2000°F.

Flux Distribution - Since detailed physics calculations were not available to predict the actual flux distribution within the core, an assumed distribution was used in the heat transfer analysis. In an unreflected cylindrical core the ratio of peak to average neutron flux is 2.31 in the radial direction and 1.57 in the axial direction. For the purposes of this study the core was assumed to have the same value of peak to average flux in the axial direction but a ratio of 2.0 in the radial direction, because of the D_2O reflector.

Since the reactor power output is directly proportional to the radial ratio of peak to average flux for a given maximum wall temperature, consideration

should be given to the possibility of flattening the flux in a more detailed study. Control rods tend to flatten the radial distribution at start-up but are of little value near the end of reactor life.

Pumping Power

The calculated value of the power required to move the organic coolant through the core, exclusive of entrance and exit plenum losses, is 8.5 MW. The ratio of pumping power to thermal reactor output is then 0.01. Reference B-6 suggests that the nominal design range for this ratio in a pressurized water cooled reactor should be 0.002 to 0.004. The higher pumping power in this reactor is due to the following:

1. High velocities must be used in the core in order to increase the heat transfer properties of the fluid.
2. The fluid is somewhat more viscous than water.
3. The fuel element chosen has a high friction factor.

The maximum organic velocity used in this study was 30 ft/sec, since no corrosion data was available at higher velocities.

In addition to the higher pumping power the accompanying high pressure drop through the core presents problems in the mechanical design of the core. Since the last of the factors listed above is the only one capable of significant variation once the decision to use an organic coolant has been made, consideration might be given to elements with a lower friction factor.

Steam Generators and Superheaters

The reference design conditions for the primary heat exchangers are shown in Figure 58. The logarithmic mean temperature differences and overall coefficients of heat transfer are given below:

Unit	Log Mean Temp. Diff., F	U B/Hr-Ft^2-F
Pre-heater	112	180
Steam Generator	111	240
Superheater	105	80

The poor heat transfer properties of the primary fluid are reflected in the high temperature driving forces required.

Some thought was given to the possibility of reducing the maximum wall temperature in the reactor by increasing the size of the primary heat exchangers. Figure 59 shows the effect of varying the reactor outlet

temperature upon the total heat transfer surface required in the primary heat exchangers. The large increase in evaporator size is due to the high temperature drop in the organic, which results in a "pinch-point" at the evaporator inlet. Doubling the size of the exchangers would reduce the reactor outlet temperature, and hence the maximum wall temperature, by fifty degrees.

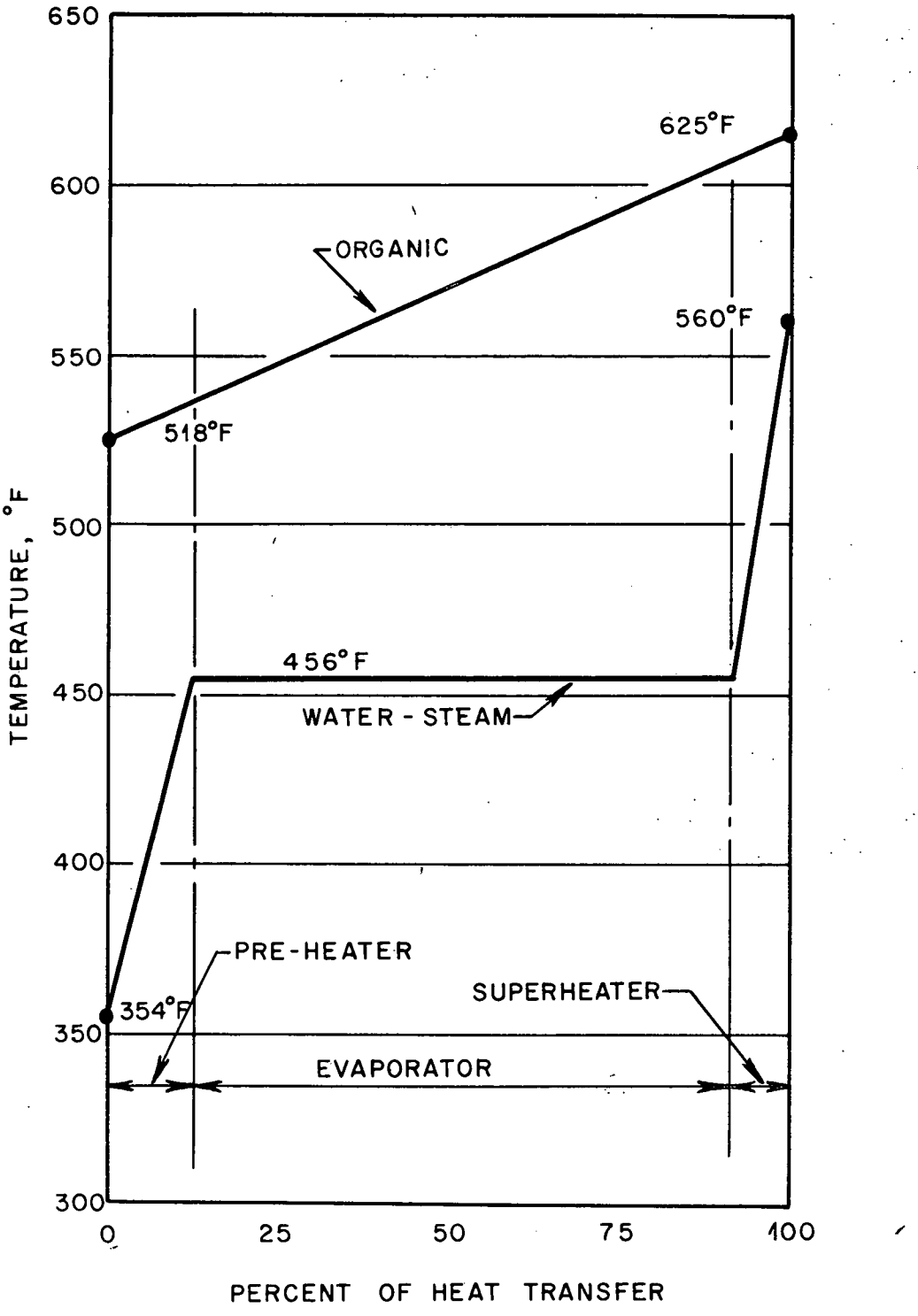

Fig. 58. Primary Coolant and Steam Cycle Temperature Diagram

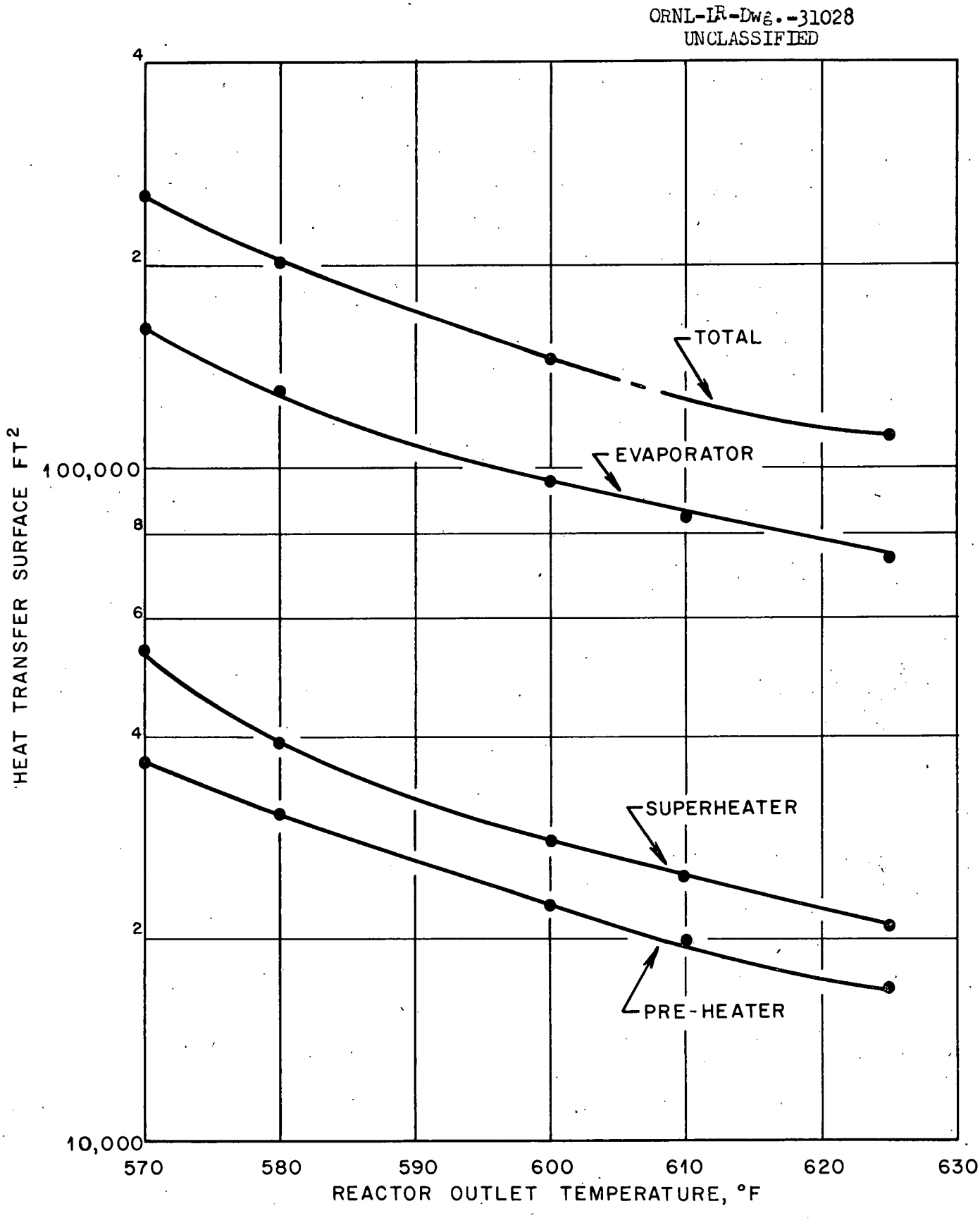

Fig. 59. Heat Exchanger Area Vs. Reactor Outlet Temperature for Constant Organic Temperature Rise = 107°F and Constant Steam Conditions

DERIVATION OF EQUATIONS USED IN HEAT TRANSFER ANALYSIS

Consider a fuel element located radially within the reactor at the point of average neutron flux and hence having the average radial heat generation rate. At any point x along the fuel rod the local heat generation rate is $q^{0111}(x)$. At steady state all heat generated in the fuel must be removed by the coolant. Therefore, in a differential length dx about x the balance equation is:

$$A_F \, dx \, q^{0111}(x) = \rho \, V \, A_c \, C_P \, d \, T_F$$

This equation may be rewritten:

$$d \, T_F = \left\{ \frac{A_f}{\rho V \, A_c \, C_P} \right\} q^{0111}(x) \, dx$$

Assuming that none of the terms in the bracket are a function of x, one may write:

$$T_F(x) - T_{in} = \left\{ \frac{A_F}{\rho V \, A_c \, C_P} \right\} \int_{x=0}^{x} q^{0111}(x) \, dx \qquad (1)$$

A second relation may be written in terms of the heat transfer to the coolant:

$$q^{0111}(x) \; A_F \, dx = h \, P \, dx \; \Theta \; (x)$$

But $A_F L = \upsilon$, the total volume of fuel per channel, and $PL = A_H$, the total heat transfer area per channel, so that

$$\Theta(x) = \frac{q^{0111}(x) \upsilon}{h \, A_H} \qquad (2)$$

In order to proceed the longitudional heat generation distribution must be known. If one assumes a cosine distribution with the origin of coordinates at the center of the reactor, then the local heat generation rate at any point along the channel may be written as

$$q^{0111}(x) = q_o \cos \left(\pi x/L \right)$$

where q_o is the heat generation rate at the center of the reactor. Integrating Equation 1,

$$T_F(x) - T_{in} = \left\{ \frac{A_F}{\rho A_c \, V \, C_P} \right\} q_o \int_{x=-L/2}^{x} \cos \left(\frac{\pi x}{L} \right) dx$$

$$= \left\{ \frac{A_F}{\rho A_c V C_P} \right\} \quad q_o \left(\frac{L}{\pi} \right) \left[\text{Sin} \left(\frac{\pi x}{L} \right) + 1 \right] \qquad (3)$$

Also, Equation (2) may be written as

$$\theta(x) = \frac{U q_o}{h A_H} \cos \left(\frac{\pi x}{L} \right) , \qquad (4)$$

if it is assumed that the film coefficient is not a function of x. The surface temperature, T_s, may be obtained by adding equations 3 and 4.

$$T_S(x) - T_{in} = \frac{U q_o}{h A_H} \cos \left(\frac{\pi x}{L} \right) + \frac{q_o A_F L}{\rho C_P A_c V \pi} \left[\text{Sin} \left(\frac{\pi x}{L} \right) + 1 \right] \qquad (5)$$

The overall heat balance for the coolant channel is

$$\rho V A_c C_P \Delta T = q_{Avg.} U$$

where

$$q_{Avg} = \frac{1}{L A_F} \int_{x=-L/2}^{L/2} q^{0111}(x) A_F \, dx = \frac{q_o}{L} \int_{-L/2}^{L/2} \cos \left(\frac{\pi x}{L} \right) dx = \frac{2}{\pi} q_o$$

Substituting for q_{Avg} and solving for ΔT:

$$\Delta T/2 = q_o \, U / \rho V A_c C_P \pi$$

So that equation 5 may be rewritten

$$T_S(x) - T_{in} = \frac{U q_o}{h A_H} \cos \left(\frac{\pi x}{L} \right) + \frac{\Delta T}{2} \left[1 + \text{Sin} \left(\frac{\pi x}{L} \right) \right] \qquad (6)$$

Also, since the maximum film temperature difference, θ_{ML}, can be seen from equation 4 to be: $\theta_{ML} = q_o \, U/h A_H$, it follows that

$$T_S(x) - T_{in} = \theta_{ML} \cos \left(\frac{\pi x}{L} \right) + \Delta T/2 \left[1 + \sin \left(\frac{\pi x}{L} \right) \right] \qquad (7)$$

To find the point of maximum surface temperature, T_{sm}, this relation may be differentiated and set equal to zero.

$$\frac{\Delta T \pi}{2L} \cos \left(\frac{\pi x}{L} \right) - \frac{\theta_{ML} \pi}{L} \text{Sin} \left(\frac{\pi x}{L} \right) = 0$$

The equation may be solved by making use of the trigonometric relation

$$a \text{ Sin } \gamma + b \cos \gamma = \sqrt{a^2 + b^2} \text{ Sin } (\gamma + \beta)$$

where

$$\text{Sin} \beta = \frac{9}{\sqrt{a^2 + b^2}}$$

Solving for x, and requiring the x be positive, since T_{sm} must lie above the center of the reactor,

$$x = \frac{L}{\pi}\beta = \frac{L}{\pi}\ \mathrm{Sin}^{-1}\left\{\frac{\Delta T\ \pi/2L}{\left[\left(\frac{\Delta T}{2}\right)^2\left(\frac{\pi}{L}\right)^2 + \theta_{ML}^2\left(\frac{\pi}{L}\right)^2\right]^{\frac{1}{2}}}\right\} =$$

$$\frac{L}{\pi}\ \mathrm{Sin}^{-1}\left\{\frac{\Delta T^2}{\Delta T^2 + 4\ \theta_{ML}^2}\right\}^{\frac{1}{2}}$$

To find T_{sm}, substitute this value of x into equation 6, to obtain

$$T_{sm} - T_{in} = \Delta T/2 + \tfrac{1}{2}\left[\Delta T^2 + 4\ \theta_{ML}^2\right]^{\frac{1}{2}} \qquad (8)$$

Since h is assumed to be constant along the channel, the film temperature difference at any point along the channel is proportional to $q^{0111}(x)$. Therefore

$$\theta_{ML}/\theta_{AL} = \pi/2$$

Rewriting equation 8

$$T_{sm} - T_{in} = \Delta T/2 + \tfrac{1}{2}\left[\Delta T^2 + \pi^2\ \theta_{AL}^2\right]^{\frac{1}{2}} \qquad (9)$$

Hot channel factors, $F_{\Delta T}$ and F_{θ}, may be included to take account of local variations which are assumed to occur simultaneously at the critical point in the channel. In addition, a factor F'_{θ} must be included to take account of the variation in film temperature with the radial location of the channel within the reactor. Since the individual channels will be orificed to maintain ΔT constant across each one, $F'_{\Delta T}$ will be unity.

To find F'_{θ}, let ψ be the ratio of peak to average heat generation within the reactor in the radial direction. Then, be definition,

$$\frac{h_m\ \theta_{Mal}}{h_A\ \theta_{AL}}\left[\frac{A_H}{A_H}\right] = \left[\frac{\rho A_c\ C_P\ \Delta T}{\rho A_c\ C_P\ \Delta T}\right]\frac{V_M}{V_A} = \psi$$

But, from the Sieder-Tate equation,

$$h \sim V^{0.8}$$

So that,

$$\frac{\theta_{MAL}}{\theta_{AL}} = \left(\frac{V_m}{V_A}\right)^{0.2} = \psi^{0.2} = F'_{\theta}$$

Equation 9 then becomes:

$$T_{sm} - T_{in} = \frac{F_{\Delta T}\ \Delta T}{2} + \tfrac{1}{2}\left[(F_{\Delta T}\Delta T)^2 + \pi^2\ (F'_{\theta}\ F_{\theta}\ \theta_{AL})^2\right]^{\frac{1}{2}} \qquad (10)$$

It is desirable to relate the average film temperature difference, Θ_{AL}, to other variables in the system. For the fuel element in question, the hydraulic diameter is given by

$$D_e = \frac{4 A_F L}{A_H + 2\pi R_T L}$$

Let K be the ratio of total surface area to the heat conducting surface. One may then write

$$D_e = \frac{4 A_c L}{A_H K}$$

The total heat transfer area in the reactor is $A_S = N A_H$, where N is the number of channels. Similarily, the total coolant flow area is $A_T = N A_c$. Using these relations, D_e may be written as

$$D_e = \frac{4 L A_T}{K A_s}$$

The total reactor thermal output, Q_r, is given by

$$Q_R = \frac{\Theta_{AL} h_A A_s}{3413} \qquad (11)$$

As indicated previously,

$$h_m/h_A = \psi^{0.8}$$

Writing equation 11 in terms of h_m and D_e,

$$Q_R = \frac{\Theta_{AL} h_m 4 L A_T}{3413 \psi^{0.8} K D_e} \qquad (12)$$

The film coefficient, h, may be written in terms of the Sieder-Tate equation:

$$h_m = K_1 K_2 0.027 \frac{K}{D_e} \left[\frac{V_m D_e \rho}{\mu}\right]^{0.8} \left[\frac{C_P \mu}{k}\right]^{0.33} \left[\frac{\mu}{\mu_W}\right]^{0.14}$$

The physical property values are for the unirradiated material and the factor K_1 is included to account for the change in h due to irradiation of the fluid. The factor K_2 is included to account for the increase in h due to increased turbulence within the fuel element caused by the spacer wires. The last term in the equation is close to unity and will be neglected. The reactor thermal output may also be expressed by

$$Q_R = \frac{V_A A_c C_P \Delta T \rho}{3413} = \frac{V_m A_c C_P \Delta T \rho}{\psi (3413)}$$

Making use of the factor α , which is the ratio of coolant cross-sectional area to reactor cross-sectional area,

$$\alpha = \frac{4 A_c}{\pi D^2}$$

and solving for V_m

$$V_m = \frac{Q_R \psi (3413) 4}{C_P \Delta T \rho \pi D^2 \alpha}$$

Substituting in equation 11, and solving for θ_{AL},

$$\theta_{AL} = \frac{45.2 \; Q_R^{0.2} \; D_e^{1.2} \; \Delta T^{0.8} \; D^{0.6} \; \alpha^{0.8} \; K \left[\frac{(C_P \mu)^{0.467}}{K^{0.67}} \right]}{(L/D) \; A_T \; K_1 \; K_2} \qquad (13)$$

Equation 13 can be used to solve for θ_{AL}, once the system has been physically described. Equation 10 may then be used to determine the maximum wall temperature in the reactor.

LIST OF SYMBOLS USED IN HEAT TRANSFER

A_c	Coolant cross-sectional area per channel	ft^2
A_f	Fuel cross-sectional area per channel	ft^2
A_s	Total heat transfer area in reactor	ft^2
A_h	Heat transfer area per channel	ft^2
A_t	Total coolant flow area in reactor	ft^2
c_p	Specific heat of coolant	B/#-F
D	Reactor Diameter	ft
D_e	Hydraulic diameter of coolant channel	ft
$F_{\Delta T}$	Hot channel factor for temperature rise through reactor	
F_θ	Hot channel factor for film temperature difference	
F'_θ	Ratio of average film temperature difference in central channel to average film temperature difference in reactor	
h	Film coefficient for heat transfer	$B/Hr-Ft^2-F$
k	Thermal conductivity of coolant	B/Hr-Ft-F
K	Ratio of total surface area to heat transfer area	
K_1	Ratio of film coefficient of coolant with tar concentration to that with no tars	
K_2	Ratio of film coefficient with spiral spacers to that with no spacers	
L	Reactor height	ft
N	Number of fuel elements in reactor	
P	Wetted perimeter of fuel element	Ft
$q^{o'''}$	Volumetric heat generation rate	$B/Hr-Ft^3$
Q_r	Reactor thermal output	KW
R_t	Radius of inner fuel element tube	Ft.
T_f	Coolant temperature	F
T_{in}	Reactor inlet coolant temperature	F
T_s	Fuel element wall temperature; T_{sm}, maximum fuel element wall temperature	F

V_a	Average coolant velocity in reactor; V_m, maximum coolant velocity	Ft/Hr
v	Volume of fuel per fuel element	ft^3
α	Ratio of coolant cross-sectional area to reactor cross-sectional area	
ΔT	Temperature rise of coolant through reactor	
θ_{AL}	Average film temperature difference in reactor	F
θ_{ML}	Maximum film temperature difference in average fuel element in reactor	F
θ_{MAL}	Average film temperature difference in central fuel element	F
μ	Viscosity of coolant	#/Hr-Ft
ρ	Density of coolant	$\#/Ft^3$
ψ	Ratio of peak to average radial heat generation rate	

APPENDIX C

CALCULATION OF STRESS IN FUEL ELEMENTS FROM BUILDUP OF STABLE FISSION PRODUCT GASES

The total thermal power of the reactor is 800 megawatts. The total volume of fuel is 1.08×10^7 cm^3. The average power density is then,

$$\frac{8 \times 10^8 \text{ watts}}{1.08 \times 10^7 \text{ cm}^3} = 74 \text{ watts/ cm}^3$$

There are 3.1×10^{10} fissions/sec/watt thus, the average number of fissions/ sec/cm^3 is 2.3×10^{12}.

The total yield of stable fission product gases (Xe and Kr) is about 25%. Thus, the average production of stable fission product atoms is

$$.25 \times 2.3 \times 10^{12} = 5.75 \times 10^{11} \text{ atoms/sec/cm}^3.$$

Since there are 6.023×10^{23} atoms per mole, the average gas production is

$$\frac{5.75 \times 10^{11}}{6.023 \times 10^{23}} = 9.55 \times 10^{-11} \text{ moles/sec/cm}^3$$

From the perfect gas law:

$$p = \frac{\eta RT}{V},$$

where p is pressure, T is temperature (absolute), V is volume, η is the number of moles, and R is the gas constant. The average temperature of the hottest fuel elements is about 2000°F or 1373°K. The volume of each element is 95.4 cm^3. The 1/8" hole in each UO_2 disk provides a free volume fraction of .05 or 4.77 cm^3. The density of the UO_2 is 92% of the theoretical density. It will be assumed that all the porosity (8%) is free volume, thus the free volume available for the fission product gases is 12 cm^3. Then,

$$p \frac{(\text{atm})}{(\text{sec})} = 9.55 \times 10^{-11} \text{ moles/sec/cm}^3 \times 95.4 \text{ cm}^3 \times 1.37 \times 10^3 \text{ °K} \times \frac{8.2 \times 10^{-2} \text{ liter atm/°K}}{1.2 \times 10^{-2} \text{ liters}}$$

$$p \frac{(\text{atm})}{(\text{sec})} = 85 \times 10^{-8} \quad \text{or} \quad p = 1.25 \times 10^{-5} \text{ psi/sec}$$

Assume that 1/2 atm of He occupies the free volume at room temperature. At 1373°K, this corresponds to a pressure of 35 psi, thus the total internal

pressure is

$$P = pt + 35 = \left[1.25 \times 10^{-5} (t) + 35\right] \quad \text{psi}$$

where t is the time in seconds, or

$$P = \left[4.5 \times 10^{-2} (t) + 35\right] \text{ psi}$$

where t is in hours.

The external pressure on the hottest fuel element is 125 psi, thus the net internal pressure is

$$P = 4.5 \times 10^{-2} (t) + 35 - 125$$

$$P = \left[4.5 \times 10^{-2} (t) - 90\right] \text{ psi}$$

The hoop stress caused by the internal pressure is given by

$\sigma = \frac{Pr}{T}$ where r is the radius of the element and T is the wall thickness. Since $r = .278$ in, and $T = .025$ in

$$\sigma = 11.1 P = 11.1 \left[4.5 \times 10^{-2} (t) - 90\right] \quad \text{psi}$$

This would be the stress if all of the stable fission gases were free to cause pressure which is not the case. If 20% of the gases are released the stress would be

$$\sigma = 11.1 \left[\frac{4.5}{5} \times 10^{-2} (t) - 90\right] = \left[.1 (t) - 1000\right] \quad \text{psi}$$

If 10% of the gases are released the stress would be

$$\sigma = \left[.05 (t) - 1000\right] \quad \text{psi}$$

If 1% of the gases are released the stress would be

$$\sigma = \left[.005 (t) - 1000\right] \quad \text{psi}$$

However, the fission rate in the hottest fuel elements is about 3 times that in an average element, thus the stress in the hottest fuel elements is as follows:

For 20% gas release : $\sigma = \left[.3 (t) - 1000\right]$ psi

For 10% gas release : $\sigma = \left[.15 (t) - 1000\right]$ psi

For 1% gas release : $\sigma = \left[.015 (t) - 1000\right]$ psi

Where σ is in psi and t is in hours.

The results of this calculation are plotted in Figure 10.

APPENDIX D

REACTOR CONTROL

Temperature Coefficient

Coolant Temperature Coefficient - A usual expression for effective multiplication factor is:

$$k_{eff} = \frac{\eta \epsilon p f}{1 + M^2 B_g^2} \qquad (a\text{-}1)$$

where

η = neutrons produced / neutrons absorbed in fuel

ϵ = fast fission factor

p = resonance escape probability

f = thermal utilization factor

$M^2 = L^2 + \tau$ = thermal diffusion area plus fermi age

B_g^2 = reactor buckling

An expression for the change in multiplication factor with coolant temperature or for coolant temperature coefficient is given by:(d-1,D-2)

$$\frac{\partial k_{eff}}{\partial T_c} = \frac{1}{\eta}\frac{\partial \eta}{\partial T_c} + \frac{1}{f}\frac{\partial f}{\partial T_c} + \frac{1}{\epsilon}\frac{\partial \epsilon}{\partial T_c} + \frac{1}{P}\frac{\partial P}{\partial T_c} - B_g^2 \frac{\partial M^2}{\partial T_c} \qquad (a\text{-}2)$$

where T_c = Coolant temperature

A change in coolant temperature affects the reactor in two basic ways:

1. the neutron temperature is changed which leads to altered nuclear cross sections,
2. The density of the coolant is changed thereby readjusting the thermal utilization of neutrons.

One uncertainty in the calculations of the temperature coefficient is the effect of the coolant temperature on the neutron temperature. The ratio of coolant to moderator columes is of the order of .1; however, the coolant contains much hydrogen and is located in the region where most of the absorptions take place. Also, it is calculated that approximately 25% of the energy deposited by neutrons slowing down is deposited in the coolant. It seems logical that a neutron temperature gradient would exist in each fuel cell with the temperature in the center of the cell determined mostly by the coolant temperature and the temperature at the interface between coolant

and moderator determined mostly by the moderator temperature. To get some approximation as to the relative weights of coolant and moderator temperatures on neutron temperature, the following relationship is assumed:

$$T_n = \frac{\Sigma_s^c}{\Sigma_s^c + \Sigma_s^m} T_c + \frac{\Sigma_s^m}{\Sigma_s^c + \Sigma_s^m} T_m \qquad \text{(a-3)}$$

Σ_s = macroscopic scattering cross section homogenized over unit cell, at approximately .1 ev or somewhat above thermal energy.

This expression reduces to:

$$T_n \approx .25\, T_c + .75\, T_m$$

where T_n = neutron temperature
T_m = moderator temperature
T_c = coolant temperature

Variation of η with temperature - The expression for η is:

$$\eta = \frac{\nu N^{25} \sigma_f^{25}}{N^{25} \sigma_a^{25} + N^{28} \sigma_a^{28}} \qquad \text{(a-4)}$$

$$= \frac{\nu}{\frac{\sigma_a^{25}}{\sigma_f^{25}} \quad \frac{N^{28}}{N^{25}} \frac{\sigma_a^{28}}{\sigma_f^{25}} f}$$

Using the values listed in BNL-325 this reduces to:

$$\eta = \frac{2.47}{1.18 + \frac{.664}{f}}$$

where ν = neutrons produced/fission
σ_a^{25} = thermal absorption cross section of U^{235}
σ_a^{28} = thermal absorption cross section of U^{238}
σ_f^{25} = thermal fission cross section of U^{235}
f = non 1/v factor for U^{235} cross sections.

It can be shown that

$$\frac{1}{\eta}\frac{\partial \eta}{\partial T_n} = \frac{2.47 \quad \left(\frac{.664}{f^2}\right)\frac{\partial f}{\partial T_n}}{\eta\,(1.18 + \frac{.664}{f})^2} \qquad \text{(a-5)}$$

This expression is valid for a neutron temperature of 410°K(which is the approximate value for this reactor). From BNL-325, $\frac{\partial f}{\partial T_n}$ is found to be approximately .00001 at 410°K. This leads to the result:

$$\frac{1}{\eta}\frac{\partial \eta}{\partial T_n} \quad (410^\circ K) = .37 \times 10^{-5}/^\circ C$$

If it is estimated that the change in neutron temperature per degree charge in coolant temperature is .25, then

$$\frac{1}{\eta}\frac{\partial \eta}{\partial T_c} \approx .1 \times 10^{-5}/^\circ C$$

Variation of ϵ with Temperature - It is generally assumed that the variation of ϵ with temperature is negligible. No attempt was made to determine such a variation, and it will be assumed to be zero.

Variation of f with Temperature - The variations in thermal utilization with temperature are due to two effects:

1. The density of the coolant changes resulting in a decrease of poison for an increase in temperature,
2. The disadvantage factor decreases with increasing temperature.

Both these effects tend to make the contribution of $\frac{1}{f}\frac{\partial f}{\partial T_c}$ positive. The following expression for f used was taken from the Reactor Handbook:[D-3]

$$\frac{1}{f} - 1 = F(K_o r_o)\left[\frac{N_1\ \sigma_{a1}\ V_1 + N_2\ V_2\ \sigma_{a2}}{N_o\ \sigma_{ao}\ V_o}\right] + X(K_2 r_1)\, K_2 r_2 \qquad \text{(a-6)}$$

All symbols are defined in the handbook.

The thermal utilization factor was calculated at two coolant temperatures 500°F and 600°F, or two neutron temperatures of 387°K and 401°K. It was assumed that the variation between these two temperatures was linear. The value of $\frac{1}{f}\frac{\partial f}{\partial T_c}$ was found to be approximately $3.6 \times 10^{-5}/^\circ C$.

Variation of p with Temperature - The variation of resonance escape with temperature is attributed to Doppler broadening of the resonance

absorption bands. This effect has been discussed repeatedly in the literature (D-2,D-4,D-5).

The expression for p according to the Reactor Handbook is:

$$P = e^{-1/G} \qquad \text{(a-7)}$$

where:

$$G = \left[\frac{N_2 V_2 (\overline{\xi \sigma_s})_2}{N_o V_o A (1 + 1.92\ S/M)} F(\bar{K}_o r_o) + X(\bar{K}_2 r_1 \bar{K}_2 r_2)\right.$$

All symbols are defined in the Reactor Handbook.

The x factor was found to be negligible and dropped. The quantity G may be written as $G = K/A$

where: $$K = \frac{N_2 V_2}{N_o V_o} \quad \frac{(\overline{\xi \sigma_s})_2}{(1 + 1.92\ S/M)} \quad F(\bar{K}_o r_o)$$

The quantity A varies with temperature and the following expression is obtained:

$$\frac{1}{P}\frac{\partial P}{\partial T_c} = -\frac{A}{K}\left(\frac{1}{A}\frac{\partial A}{\partial T_c} \cong -.208 \left(\frac{1}{A}\frac{\partial A}{\partial T_c}\right)\right. \qquad \text{(2-8)}$$

A value of $1/a\ \partial A/\partial T_c$ is taken from HW-37766 as 1.74×10^{-4}. This variation is a function of metal temperature instead of neutron temperature.

The value arrived at for $1/p\ \partial p/\partial T_c$ is then $-3.62 \times 10^{-5}/^{o}C$. This is a Doppler broadening effect alone. There is an additional effect due to the increased surface to mass ratio following an increase in temperature. This effect is also negative but small compared to the Doppler broadening[D-5] and was neglected.

Variation of M^2 with Temperature - An approximate expression for Fermi age is the following:

$$\tau = \frac{1}{3 \bar{\xi} \Sigma_t \Sigma_s} \ln \frac{E_o}{E_T} \qquad \text{(a-9)}$$

where

$\bar{\xi}$ = avg. log energy decrement/collision

T_n = neutron temperature

Σ_t = avg. macroscopic transport cross section

Σ_s = avg. macroscopic scattering cross section

E_o = fission avg. neutron energy

E_T = thermal avg. neutron energy

It was found that

$$\frac{\partial \tau}{\partial T_c} \approx .05 \text{ cm}^2/^\circ\text{C}$$

The expression used for L^2 was taken from the Reactor Handbook[D-3]. (all symbols are defined in the handbook)

$$L^2 = f_m L^2_m \qquad \text{(a-10)}$$

$$f_m = 1 - f \left[1 + \frac{N_1 \sigma_{a1} V_1}{N_o \sigma_{ao} V_o} F(K_o r_o) \right] \qquad \text{(a-11)}$$

L^2 was calculated at the same temperature at which f was calculated and the variations assumed linear between the temperature limits. $\frac{\partial L^2}{\partial T_c}$ was found to be approximately .1 $\text{cm}^2/^\circ\text{C}$.

Using a reactor, B_g^2 of 1.15×10^{-4}, the value for $B_g^2 \frac{\partial M^2}{\partial T_c}$ is seen to be approximately $1.65 \times 10^{-5}/^\circ\text{C}$.

Coolant Temperature Coefficient Summary

$\frac{1}{\epsilon} \frac{\partial \epsilon}{\partial T_c}$	0
$\frac{1}{n} \frac{\partial n}{\partial T_c}$	$.1 \times 10^{-5}$
$\frac{1}{P} \frac{\partial P}{\partial T_c}$	-3.62×10^{-5}
$\frac{1}{f} \frac{\partial f}{\partial T_c}$	3.6×10^{-5}
$-B_g^2 \frac{\partial M^2}{\partial T_c}$	-1.65×10^{-5}
$\frac{\partial k_{eff}}{\partial T_c}$	-1.55×10^{-5}

Moderator Temperature Coefficient - The expression used in calculating a coolant temperature coefficient may also be used in calculating a moderator temperature coefficient. However, two of the five terms may be neglected:

(1) $\frac{1}{\epsilon} \frac{\partial \epsilon}{\partial T_m}$ and (2) $\frac{1}{p} \frac{\partial p}{\partial T_m}$

Variations in ϵ are too small to be considered, and variations in p are brought about primarily by changing the temperature of the uranium metal which is insulated from the moderator.

1. $\frac{1}{f}\frac{\partial f}{\partial T_m}$

There is a variation in f with moderator-temperature that results from a flattening of the flux or decrease in the disadvantage factor with increasing neutron temperature. This is a positive contribution to the over all moderator coefficient. The magnitude is found in the same manner as before, i.e., by calculating a thermal utilization factor at two temperatures and assuming that the variation is linear with temperature. Values of f were calculated for moderator temperatures of 100°F and 200°F or neutron temperatures of 376°K and 418°K. The value of $\frac{1}{f}\frac{\partial f}{\partial T_m}$ was found to be $.4 \times 10^{-4}/^{o}C$.

2. $\frac{1}{\eta}\frac{\partial \eta}{\partial T_m}$

Values for the variation of η with neutron temperature were calculated in section A.1.a.(1) of this appendix. The variation of neutron temperature with moderator temperature $\left(\frac{\partial T_n}{\partial T_m}\right)$ was assumed to be approximately .75. This results in a value of approximately $.3 \times 10^{-5}/^{o}C$ for $\frac{1}{\eta}\frac{\partial \eta}{\partial T_m}$.

3. $B_g^2 \frac{\partial M^2}{\partial T_m}$

The change in L^2 was calculated in the same manner as when calculating the coolant temperature coefficient using the same equation It was determined that $\frac{\partial L^2}{\partial T_m}$ is of the order of .088.

The approximate expression for τ (equation a-9) was again used, and values were obtained at the two moderator temperatures (100°F and 200°F) and the variation assumed linear. The approximate value for $\frac{\partial \tau}{\partial T_m}$ was determined in this manner to be .12 $cm^2/^{o}F$.

The sum of these two effects gives a net effect for $B_g^2 \frac{\partial M^2}{\partial T_m}$ of $-2.37 \times 10^{-5}/^{o}C$.

Moderator Temperature Coefficient

$\frac{1}{\epsilon}\frac{\partial \epsilon}{\partial T_m}$	0
$\frac{1}{p}\frac{\partial p}{\partial T_m}$	0
$\frac{1}{\eta}\frac{\partial \eta}{\partial T_m}$	$.3 \times 10^{-5}/^{\circ}C$
$\frac{1}{f}\frac{\partial f}{\partial T_m}$	$.4 \times 10^{-5}/^{\circ}C$
$-B_g^2\frac{\partial M^2}{\partial T_m}$	$-2.37 \times 10^{-5}/^{\circ}C$
$\frac{\partial k_{eff}}{\partial T_m}$	$-1.67 \times 10^{-5}/^{\circ}C$

Control Rod Effectiveness

The analysis of the rods is based on the work done by Wheeler;

(1) The basic equation for the analysis is a transcendental equation of the form:[D-6, D-7]

$$Y_0(br_{eff}) - \frac{Y_1(bR)}{J_1(bR)} J_0(br_{eff}) = \frac{\tau}{L^2}\frac{2}{\pi}\left[K_0(Xr_{eff}) + \frac{K_1(Xr)}{I_1(Xr)} I_0(Xr_{eff})\right]$$

Where:

Y_0, Y_1, J_1, J_0, K_1, K_0, I_1, and I_0 are the Bessel functions

r_{eff} = effective radius of control rod

R = radius of zone affected by rod

τ = fermi age of reactor

L^2 = thermal diffusion area of reactor

$x = \sqrt{1/\tau + 1/L^2}$

b = parameter determined by trial and error solutions of equation.

This equation is solved by trial and error for the parameter b which is used for determining a parameter, δk_{local}, defined by Wheeler as:

(2) $\delta k_{local} = b^2 (L^2 + \tau)$

The δk_{local} is then multiplied by appropriate geometry factors to determine the worth of each rod. The effective radius of a circular rod is determined by the following equations:[D-1]

(3) $r_{eff} = r_o e^{-\frac{.71\lambda}{r_o}}$

r_o = radius of rod = 1.25"

λ = mean free path for neutrons in the moderator

The δk of each rod is determined according to Wheeler by the equation:

(4) $\delta k(rod) = \text{position factor} \times \frac{\pi R^2}{\pi \tilde{R}^2} \delta k_{local}$

R = radius of zone covered by rod

$\tilde{R}$ = radius of reactor

The position factor is defined by:

$$\text{Position factor} = \frac{\int_{\text{zone of rod}} n^2 \, d(vol)}{\int_{\text{reactor}} n^2 \, d(vol)}$$

(n = neutron density)

The position factor for a bare cylindrical reactor is $3.710 J_o^2 (2.408 r/R)$. Equation (1) was solved for b using the following parameters:

τ = 200 cm^2

L^2 = 50 cm^2

R = 19 cm

R_{eff} = 1.96 cm

The value for b was found to be .028. This value of b in turn gave a δk_{local} of .196.

To get the approximate worth of each rod, it was assumed that they were arranged in concentric circles according to the following table:

Group	No. of Rods	Radius	J_o^2 (2.405 r/R)
I	1	0	1.0
II	6	15"	.935
III	12	30"	.76
IV	18	45"	.531
V	24	60"	.296
VI	30	75"	.116
VII	40	90"	.0213

The δ k of each group was found by multiplying the δ k of a rod at that radius as determined by equation (4) by the number of rods in the group.

Group	δk_{local}	δ k/rod	No rods	δ k/Group
I	.196	.004	1	.004
II	.196	.00378	6	.0227
III	.196	.00304	12	.0365
IV	.196	.00222	18	.0400
V	.196	.00118	24	.0283
VI	.196	.00046	30	.0138
VII	.196	.000085	40	.0034
Total				.1487

APPENDIX E

SHIELDING

Calculation of Neutron Leakage

Neutron leakage is calculated by a consideration of the leakage probability for the equivalent bare reactor. This is a reactor having the same cell constants as the reference reactor. Corrections are then applied to the bare reactor to account for the effect of the reflector.

Reactor Data

B^2 radial = $.870 \times 10^{-4}$ cm^{-2}

L^2 = 67 cm^2

τ = 203 cm^2 (considering voids)

P_{re} = 0.91

Radius = 8.46 ft = 258 cm

Height = 16 ft = 490 cm

P_F = probability of fast leakage = $1 - e^{-B^2 g \tau} \cong B^2 g \tau$

P_T = probability of thermal leakage = $\frac{L^2 Bg^2}{1 + L^2 Bg^2} \cong L^2 Bg^2$

$B^2 g \tau = .870 \times 10^{-4} \times 2.03 \times 10^2 = .0177$

$L^2 Bg^2 = 67 \times .870 \times 10^{-4} = .00583$

P_F	.0177
P_T	.00583

Fast neutron production = 800×10^6 (watt) $\times 3.1 \times 10^{10} \left(\frac{\text{fission}}{\text{sec-watt}}\right) \times 2.5 \left(\frac{\text{neutron}}{\text{fission}}\right)$

$N_F = 6.2 \times 10^{19} \left(\frac{\text{Fast Neutrons}}{\text{sec.}}\right)$

$N_T = N_F \; P_{Re} \; P_{NFL} = 6.2 \times 10^{19} \times .91 \times .9823$

$N_T = 5.55 \times 10^{19} \left(\frac{\text{Thermal neutrons}}{\text{sec}}\right)$

Leakage(Into Reflector)

$$J_F = \frac{6.2 \times 10^{19} \times .0177}{2\pi \times 258 \times 490} = 1.38 \times 10^{12} \left(\frac{\text{fast neutrons}}{\text{cm}^2\text{-sec}}\right)$$

$$J_T = \frac{5.55 \times 10^{19} \times .00583}{2\pi \times 258 \times 490} = 4.07 \times 10^{11} \left(\frac{\text{thermal neutrons}}{\text{cm}^2\text{-sec}}\right)$$

The neutrons leaking into the reflector are attenuated as follows:

Energy	J To Reflector	Attenuation $e^{-T/\sqrt{\tau}}$ $e^{-T/L}$	J From Reflector
Fast	1.38×10^{12}	0.262	3.62×10^{11}
Thermal	4.07×10^{11}	0.92	3.72×10^{11}

and

$$\tau_{D_2O} = 130 \text{ cm}^2$$

$$L^2 D_2O = 25{,}734 \text{ cm}^2 \quad L = 162 \text{ cm}$$

Calculation of Fast Neutron Dose

The fast neutrons leaving the reflector are attenuated through the concrete biological shield. The leakage currect J_F is assumed to be isotropic and is transformed into an equivalent isotropic surface source.

$$D = 1/2 \; S_a \; e^{-\frac{Z}{\lambda}} \quad \text{when} \quad S_a = 2 \times 3.62 \times 10^{11}$$

$$\lambda = \frac{1}{\Sigma_R} = 10.6 \text{ cm} \quad \text{(For bayrites concrete Ref. E-1)}$$

assuming an allowable $D = 10 \; \frac{\text{fast neut}}{\text{cm}^2\text{-sec}}$

$$Z = 8.5 \text{ (ft.)}$$

Subsequent calculations indicated that the Gamma attenuation of Bayrites concrete was sufficient to allow a higher neutron dose rate if the attenuation of fast neutrons by inelastic scattering in the reactor vessel was considered.

ATTENUATION IN REACTOR VESSEL

$\lambda \cong$ 6 cm $\qquad Z$ = 1.5" (Thickness of Vessel Wall)

Sa = $3.62 \times 10^{11} \times 2$ $\qquad \frac{Z}{\lambda} = .635$

$D = \frac{1}{2}\,Sa\,E_1\left(\frac{Z}{\lambda}\right) \qquad E_1(.626) = 4 \times 10^{-1}$

$$D = \frac{1}{2} \times 3.62 \times 10^{11} \times 2 \times 4 \times 10^{-1} = 1.448 \times 10^{11} \left(\frac{\text{Fast Neutron}}{\text{cm}^2\ \text{sec}}\right)$$

8' Bayrites

ATTENUATION IN CONCRETE BIOLOGICAL SHIELD

$\lambda = \frac{1}{\Sigma_R}$ (For Bayrites concrete, Ref. E-1) = 10.6(cm)

$Sa = 2 \times 1.448 \times 10^{11} \left(\frac{\text{neuts}}{\text{cm}^2\text{-sec}}\right) \qquad Z = 8$ (ft)

$$D = \frac{Sa}{2}\, e^{-\frac{Z}{\lambda}} = \frac{1.448 \times 10^{11} \times 2}{2}\, e^{-\left(\frac{8 \times 12 \times 2.54}{10.6}\right)}$$

$$D = 1.448 \times 10^{11} \times 10^{-10} = 14.48 \left(\frac{\text{fast neutron}}{\text{cm}^2\text{-sec}}\right)$$

D = 3.2 Mr/Hr from Fig. Assuming 10 Mev neuts.

TABLE 27

CALCULATION OF γ SPECTRUM IN CORE

Material	Volume	Vol. Fraction (cm^3/cm^3 - cell)
Al	4.41	.1015
D_2O	31.8	.7310
$C_{18}H_{14}$	3.65	.0610
UO_2	4.60	.1060
	43.46	

$\phi \cong 2 \times 10^{13} \left(\frac{\text{neutrons}}{\text{cm}^2\text{ - sec}}\right)$ (over lifetime)

TABLE 28

NEUTRON CAPTURES BY MATERIALS IN CORE

Element	$\Sigma_c (cm^{-1})$	$\Sigma_c \phi \left(\frac{captures}{cm^3 - sec}\right)$
Al	1.36×10^{-3}	2.72×10^{10}
D_2	2.18×10^{-5}	4.36×10^{8}
O	$.47 \times 10^{-5}$	9.4×10^{7}
C_{18}	1.13×10^{-5}	2.26×10^{8}
H_{14}	6.45×10^{-5}	1.29×10^{9}
U^{238}	6×10^{-3}	1.2×10^{11}
U^{235}	1.71×10^{-3} (n, c)	3.42×10^{10}
O^2	9.45×10^{-7}	1.89×10^{7}

TABLE 29

CAPTURE GAMMA RELEASE

Element	Photons/100 Capt.			
	0-3	3-5	5-7	> 7
Al	13	77	21	35
D_2			100 (6)	
O_2	Negligible →			
C	30	100	--	--
H	100 (2.23)			
U^{238}	300 (3)	--	--	--
	200(1)	--	--	--
U^{235}	--	100(5)	--	--

We will assume that U^{238} gives one 3 Mev γ and 2 1-Mev γ's/capture. ($\sim$ 5 Mev binding energy). U^{235} will be assumed to emit 1-5 Mev/capture. Note that although the binding energy of oxygen is $\sim$4 Mev. its concentration is low enough to make it negligible.

TABLE 30

CAPTURE GAMMA SPECTRUM

Element	E_{av}	/100 Capt.	$\frac{\text{100 Capt.}}{\text{cm}^3 - \text{sec}}$	$\frac{\gamma\text{'s}}{\text{cm}^3 - \text{sec}}$
Al	1.5	13	2.72×10^8	3.52×10^9
	4.0	77	↓	2.09×10^{10}
	6	21		5.70×10^9
	> 7	35		9.50×10^9
H^2	6	100	4.36×10^6	4.36×10^8
C	1.5	30	2.26×10^6	6.78×10^7
	4.0	100	↓	2.26×10^8
H_1	2.23	100	1.29×10^7	1.29×10^9
U^{238}	1.0	200	1.2×10^9	2.4×10^{11}
	3.0	300	↓	3.6×10^{11}
U^{235}	5.0	100	3.42×10^8	3.42×10^{10}

TABLE 31

PROMPT GAMMA SPECTRUM

The Prompt Gamma Distribution Can Be Expressed As Follows:

$$N(E)\Big|_a^b = \int_a^b 7.5\, e^{-E}\, d \qquad \text{Ref. E-1}$$

a	b	e^{-b}	e^{-a}	$-7.5\,(e^{-b}-e^{-c})$ (Gammas/Fission)	$5 \times \Sigma_f \phi$ (Gammas/cm^3-sec)
0	3	1	1	7.3	1.46×10^{11}
3	5	.00667	.05	3.25×10^{-1}	6.50×10^{10}
5	7	.00091	.00667	4.33×10^{-2}	8.66×10^{9}
7		0	.00091	6.83×10^{-3}	1.37×10^{10}

$$N_f = \left(\frac{\text{No Fissions}}{cm^3 - \text{sec}}\right) = \Sigma_f \phi \cong 2 \times 10^{13} \times .943 \times 10^{-2}$$

$$N_\gamma \cong 2 \times 10^{11} \left(\frac{\text{fissions}}{cm^3 - \text{sec}}\right)$$

TABLE 32

TOTAL GAMMA SPECTRUM

E	Capture x 10^{-10}	Prompt x 10^{-10}	N(γ) x 10^{-10}	N (γ)E (γ) x 10^{-10}
1.0	.24		24	24
1.5	.358	14.6	14.96	22.4
2.23	.129		.129	.288
3.0	36		36	108
4.0	2.11	6.5	8.61	34.4
5.0	3.42		3.42	17.1
6.0	.612	.886	1.478	
> 7*	.950	1.37	2.43	
			90.92	233.67

* Use 8 for E > 7 $\quad \langle E(\gamma)\ 7\rangle = \frac{\Sigma N(\gamma)\, E(\gamma)}{N(\gamma)} = \frac{233.67}{90.92} = \underline{2.56 \text{ Mev}}$

The average Gamma Energy is therefore conservatively estimated to be approximately 3 Mev/γ .

Calculation of Gamma Attenuation in Core

The Mass Absorption Coefficient can be approximated as follows:

$$\left(\frac{\mu}{P}\right)_{\text{Core}} = \frac{\sum_i \left(\frac{\mu}{P}\right)_i P_i}{P_i}$$

(These values are obtained for E (γ) of 3 Mev)

TABLE 33

MASS ABSORPTION COEFFICIENTS

Material	$\left(\frac{\mu}{\rho}\right)_i$	ρ_i	$\left(\frac{\mu}{\rho}\right)_i \rho^i$
Al	.0330	.2760	.0091
D_2O	.0380	.7960	.0302
$C_{18}H_{14}$	.0416	.0535	.00223
U	.0435	.9300	.0405
O_2	.0359	.0125	.000448
Σ		2.0680	.0825

$$\left\langle \left(\frac{\mu}{\rho}\right) \right\rangle = \frac{.0825}{2.0680} \simeq .0400$$

$$\left(\frac{\mu}{\rho}\right) = .0400 = \frac{\mu}{2.06} \quad \therefore \mu = .04 \times 2.06 = .0825$$

$$\lambda = \frac{1}{\mu} = \frac{1}{.0825} = 12.1 \text{ cm}$$

The equivalent surface isotropic source for a slab source from Ref. is as follows:

$$S_a \text{ (isotropic)} = S_v \lambda \quad S_v = 90.92 \times 10^{10} \left(\frac{\gamma}{\text{cm}^3 - \text{sec}}\right)$$

when $\lambda = 12.1$ (for 3 Mev γ)

$$S_a \text{ (isotropic)} = 11.0 \times 10^{12} \left(\frac{\gamma}{\text{cm}^2 - \text{sec}}\right)$$

It is more convenient to use Gamma Energy Flux since the allowable dose rate for 3 Mev Gammas is $\frac{3340}{3} \simeq 1100 \left(\frac{\text{Mev.}}{\text{cm}^2 - \text{sec}}\right)$

$$\therefore S_a \text{ isotropic} = 11.0 \times 10^{12} \left(\frac{\gamma}{\text{cm}^2 - \text{sec}}\right) \times 3 \left(\frac{\text{Mev}}{\gamma}\right)$$

$$\delta_a^{\text{isotropic}} = 3.3 \times 10^{12} \frac{\text{Mev}}{\text{cm}^2 - \text{sec}}$$

The D_2O Reflector attenuates this gamma energy as follows:

$$\left(\frac{\mu}{\rho}\right)_{D_2O} \simeq \left(\frac{\mu}{\rho}\right)_{H_2O} \Bigg|_{3 \text{ Mev}} = .0396 \text{ and since} = 1.09 \text{ for } D_2O$$

$$\mu = .0396 \times 1.09 = .0431 \quad (\text{cm}^{-1})$$

$$\lambda = \frac{1}{\mu} = 23.2 \text{ cm (relaxation length)}$$

The D_2O reflector is only $6 \times 2.54 = 15.2$ cm. in thickness and therefore there is negligible gamma buildup. Using a B(R) of unity

$$D = \tfrac{1}{2} \quad S_a \quad E_1 \quad \left(\frac{Z}{\lambda}\right) \quad \text{Ref. E-2} \quad \left(\frac{Z}{\lambda}\right) = .655$$

From Ref. E-2 $\quad E_1(.665) = 512 \times 10^{-1}$

$$D = 8.45 \times 10^{12} \quad \frac{\text{Mev}}{\text{cm}^2 - \text{sec}}$$

A similar calculation is done for the reactor vessel wall using B (R) = 1

$$\left(\frac{\mu}{\rho}\right)_{Fe}^{3\text{Mev}} = .0359 \qquad Fe = 7.85 \ \frac{\text{Grams}}{\text{cm}^3} \qquad Z = 1.5 \times 2.54 = 2.81$$

$$\mu = .0359 \times 7.85 = .286 \ \text{cm}^{-1}$$

$$\lambda = \frac{1}{.286} = 3.5 \ \text{cm}$$

The γ energy leaving the reactor vessel after attenuation

$$D = \tfrac{1}{2} \delta_a \quad E_1 \left(\frac{Z}{\lambda}\right) \qquad \left(\frac{Z}{\lambda}\right) = 2.81$$

$$E_1 (2.81) = 1.7 \times 10^{-2} \quad \text{Ref. E-2}$$

$$S_a = 2 \times 8.45 \times 10^{12} \left(\frac{\text{Mev}}{\text{cm}^2 - \text{sec}}\right)$$

$$D = 1.435 \times 10^{9} \left(\frac{\text{Mev}}{\text{cm}^2 - \text{sec}}\right)$$

The gamma energy leaving the reactor vessel is attenuated through the concrete biological shield. Since the biological shield will be of reasonably large thickness we can expect Compton scattering to cause appreciable build-up. If we assume a linear $B(R) = \frac{Z}{\lambda}$

$$D = \frac{\delta_a}{2} \quad e^{-\frac{Z}{\lambda}}$$

when Z is the unknown.

$$\delta_a = 2 \times 1.435 \times 10^{9} \quad \frac{\text{Mev.}}{\text{cm}^2 - \text{sec}}$$

$$\mu \left(\text{For Bayrites concrete Ref. 2}\right) = .1093 \qquad D = \frac{3340}{3} = 1100 \left(\frac{\text{Mev}}{\text{cm}^2 - \text{sec}}\right)$$

$$\lambda = \frac{1}{.1093} = 9.15 \ (\text{cm}) \qquad \text{and } Z = 4.22 \ (\text{ft})$$

An important source of γ's is the radiative capture of a neutron. These capture gammas are usually quite hard and can penetrate long distances in the shield. For example, the capture gamma in the iron is about 7 Mev, while that in concrete is about 4 Mev.

For this calculation we will assume that the attenuation of thermal neutrons through the reactor vessel results in a capture gamma volume source in the Iron and that the interface of reactor vessel and the biological shield acts as a surface source for these capture gammas. Since the reactor vessel is only $1\frac{1}{2}$ " thick this is a fairly close conservative estimate.

The reactor vessel is assumed to be an infinite slab to obviate any multi-region problems. In this case:

$$\phi(x) = \frac{3 J_T e^{-K}}{K \lambda_{tr}}$$

For Iron

$$N = 8.47 \times 10^{22} \left(\frac{\text{Atoms}}{\text{cm}^3}\right)$$

$$\Sigma_s = 8.47 \times 10^{22} \left(\frac{\text{Atoms}}{\text{cm}^3}\right) \times 11 \left(\frac{\text{cm}^2}{\text{Atom}}\right) = .93 \ (\text{cm}^{-1})$$

$$\Sigma_a = 0.21 \ (\text{cm}^{-1})$$

$$\mu = \frac{2}{3A} = \frac{2}{3 \times 56} = .0119$$

$$\lambda_{tr} = \frac{1}{.93(1-.0199)} = 1.09 \ (\text{cm})$$

$$L^2 = \frac{\lambda_{tr}}{3 \Sigma_a} = \frac{1.09}{3 \times .21} = 1.73 \ (\text{cm}^3) \therefore L = 1.31 \text{ cm}$$

$$K = \frac{1}{L} = .764 \ (\text{cm}^{-1}) \qquad J_T = 3.72 \times 10^{11} \left(\frac{\text{Thermal Neut.}}{\text{cm}^2\text{-sec}}\right)$$

$$\phi(x) = \frac{(3)(3.72 \times 10^{11}) e^{-.764x}}{.764 \times 1.09} = 1.34 \times 10^{12} \ e^{-.764x}$$

To calculate the capture gammas in the iron an average thermal flux in the Iron was calculated, as follows

$$\overline{\phi(x)} = \frac{\int_0^{1.5 \times 2.54} e^{-.764 x} \, dx}{1.5 \times 2.54}$$

$$\bar{\phi}(x) = 4.36 \times 10^{11} \left(\frac{\text{Neuts}}{\text{cm}^2\text{-sec}}\right)$$

$$\text{(Neutron capture rate)} = \Sigma_a \bar{\phi}(x) = 4.36 \times 10^{11} \left(\frac{\text{neuts}}{\text{cm}^2\text{-sec}}\right) \times 0.21 \left(\frac{\text{cm}^2}{\text{cm}^3}\right)$$

$$\text{(Neutron capture rate)} = 9.15 \times 10^{10} \left(\frac{\text{Capt.}}{\text{cm}^2 - \text{sec}}\right)$$

Ref. E-1 indicates that the average number of γ's released per neutron capture is 1.7 $\frac{\gamma}{\text{Capture}}$. Since the binding energy of the neutron is 7.73 Mev the average energy of the capture gamma is $\frac{7.73}{1.7} \tilde{=} 6$ Mev.

$$\delta_r = \text{Capture gamma production} = 9.15 \times 10^{10} \left(\frac{\text{capture}}{\text{cm}^3 - \text{sec}}\right) \times 1.7 \left(\frac{\gamma}{\text{capture}}\right)$$

$$\delta_v = 1.56 \times 10^{11} \left(\frac{\gamma}{\text{cm}^3 - \text{sec}}\right)$$

Transformation of this volume source to an equivalent isotropic surface source.

$\rho_a = \delta_v \lambda$ $\qquad$ $\delta_v = 1.56 \times 10^{11} \left(\frac{\gamma}{\text{cm}^2\text{-sec}}\right)$ OR

$\delta_a = 6.25 \times 10^{11} \left(\frac{6 \text{ Mev } \gamma\text{'s}}{\text{cm}^2 - \text{sec}}\right)$ $\qquad$ $\lambda = \frac{1}{\mu} = \frac{1}{.237} = 4.22$ (cm)

Using a linear B(R)

$$D = \frac{\delta_a}{2} e^{-Z/\lambda} \qquad D_{\text{allowable}} \tilde{=} \frac{3340}{6} \tilde{=} 557 \left(\frac{\text{Mev}}{\text{cm}^2\text{-sec}}\right)$$

and $Z = 6$ ft. $\qquad$ $\lambda = 9.15$ For Bayrites Concrete 6 Mev

The dose rate from 8' thick bayrites concrete

$$D = 6.25 \times 10^{11} \; e^{\frac{-8 \times 12 \times 2.54}{9.15}}$$

$$D = \frac{6.25 \times 10^{11}}{2 \times 3.549 \times 10^{11}} = .880 \left(\frac{\gamma}{\text{cm}^2 - \text{sec}}\right)$$

$$D = 8 \times 10^{-6} \times 10^{3} \times .880 \tilde{=} 8 \times 10^{-3} \text{ Mr/Hr}$$

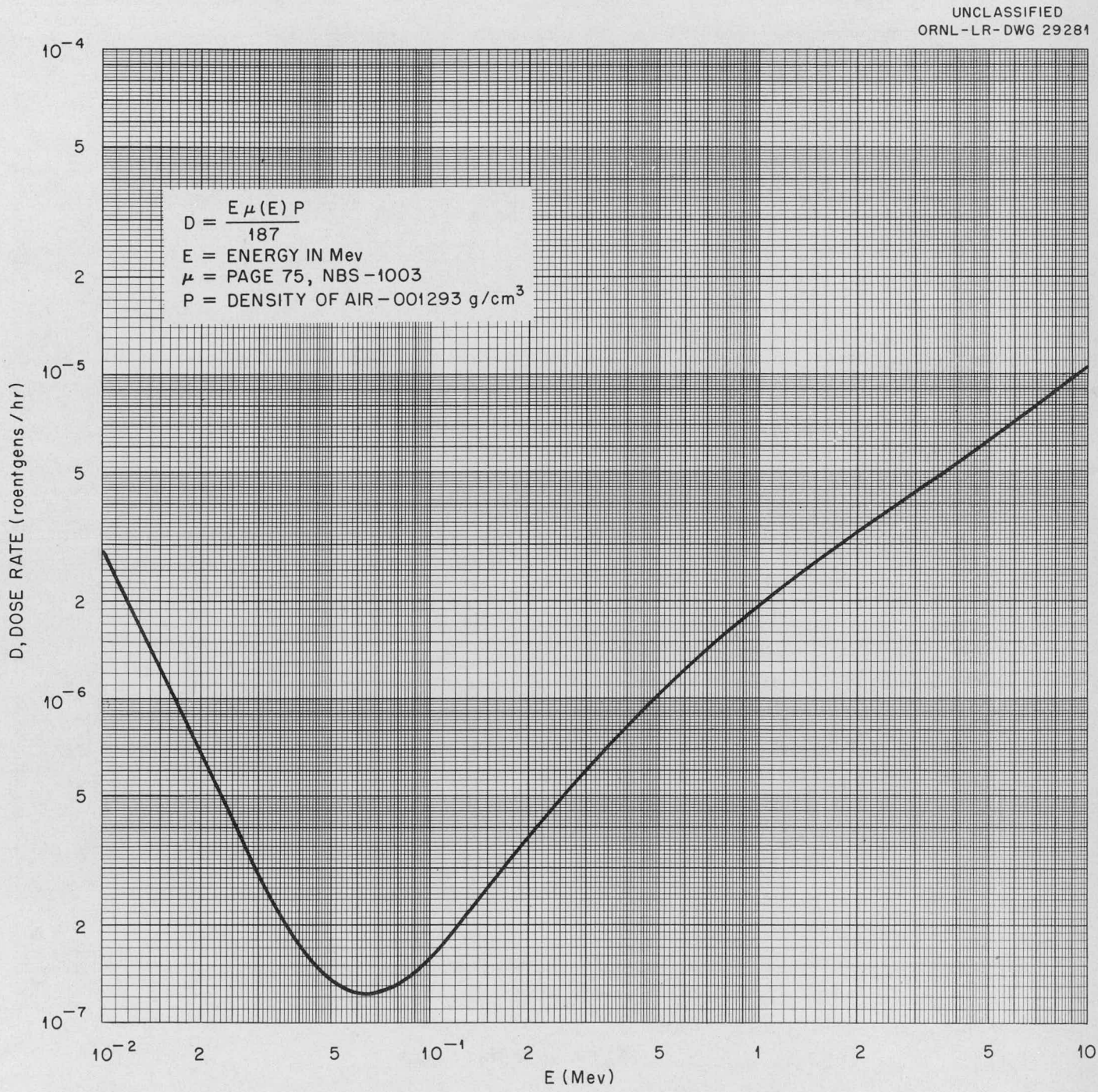

Fig. 60. Gamma Dose Rate Due to 1 photon / cm^2 · sec.

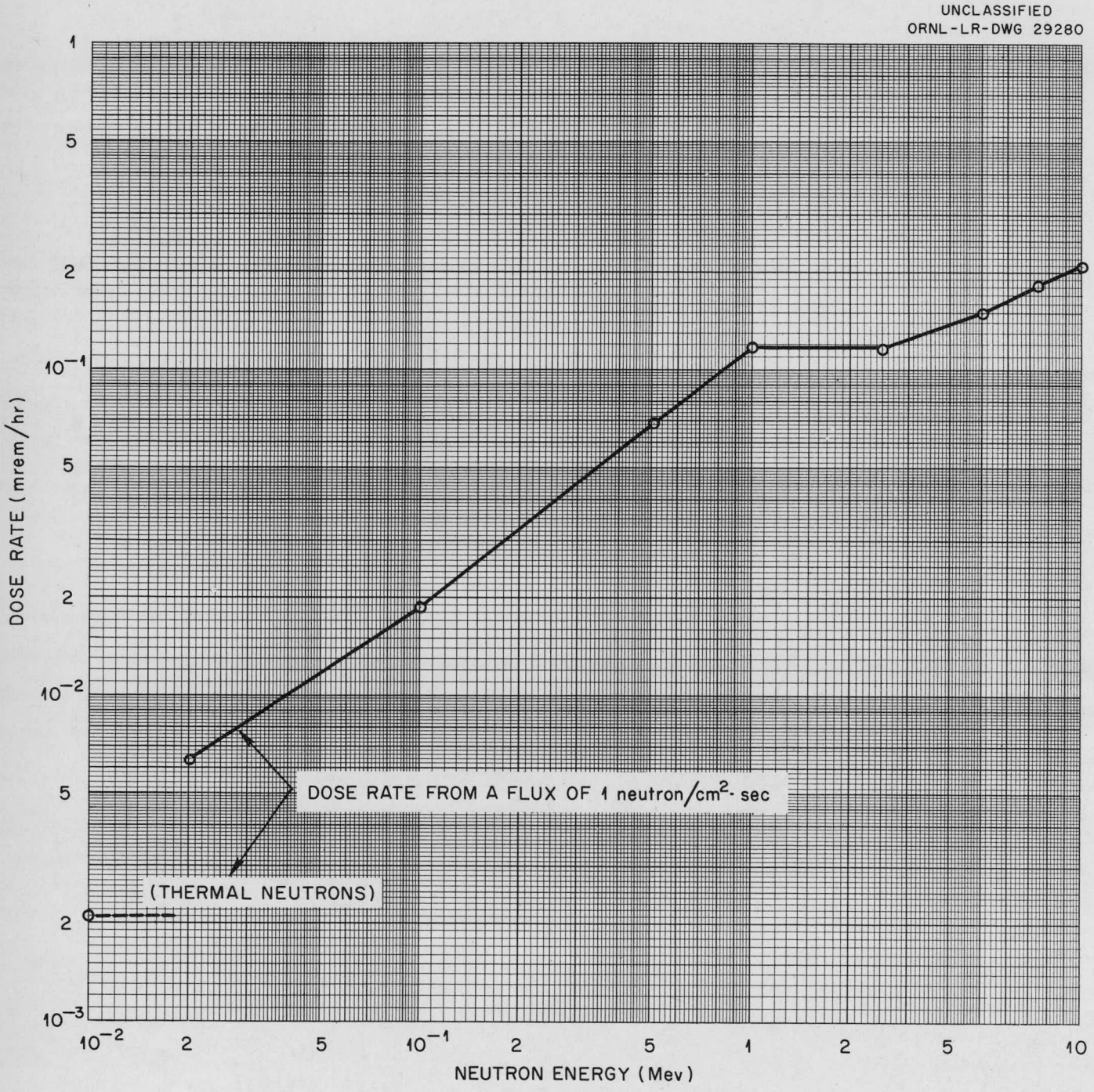

Fig. 61. Curve to Convert Neutron Flux to Dose Rate.

Capture gammas are also released by absorption of neutrons in the concrete. These neutrons enter the concrete as fast neutrons and then are slowed down by the concrete. Using the rough approximation of age replacement length of τ/λ enables the capture gammas to be transformed to an equivalent isotropic surface source at a depth of τ/λ in the shield.

From previous

$$S_a = 1.448 \times 2 \times 10^{11} \quad \left(\frac{\text{fast neuts.}}{\text{cm}^2 - \text{sec}} \right)$$

$$\frac{\tau}{\lambda} \tilde{=} 30 \text{ cm} \qquad \text{Ref. E-2}$$

Using a linear B (R) to account for scattering buildup

$$D = \frac{S_a}{\gamma} \; e^{-\frac{z}{\lambda}}$$

$z = 244 \text{ cm} - 30 \text{ cm} = 214 \text{ cm}$

$\lambda = 9.15$ Bayrites concrete for 4 Mev γ's

$$D = \frac{1.448 \times 2 \times 10^{11}}{2} \; e^{\frac{-214}{9.15}}$$

$$D = 8.2 \left(\frac{\gamma}{\text{cm}^2 - \text{sec}} \right)$$

D = .41 Mr/Hr Fig. 60

APPENDIX F

MATERIALS

From the straight line plots in Figure 36 in the Materials Selection Section the functional relationship between stress, strain, and time for the aluminum alloy X-2219 was determined as follows:

The slope of the log creep rate vs. log stress curve (for 600°F)was determined by:

$$\text{slope} = \frac{\log 1 - \log .1}{\log 6400 - \log 2100} = 2.06$$

The equation of the straight line is given by:

$$\text{slope} = \frac{\log c - \log .1}{\log \sigma - \log 2100} -$$

where C is the creep rate in % deformation in 1000 hours and σ is stees in psi.

The equation can be rewritten:

$$C = .1 \left(\frac{\sigma}{2100}\right)^{2.06}$$

Since $C = \epsilon/t$ where ϵ is the strain in % deformation and t is time in thousands of hours, the equation becomes:

$$\epsilon = .1\, t \left(\frac{\sigma}{2100}\right)^{2.06}$$

In a similar way the equation for the line at 750°F ("$\frac{1}{2}$" extrapolation was found to be:

$$\epsilon = .1\, t \left(\frac{\sigma}{1000}\right)^{2.15},$$

and that for the "$\frac{1}{4}$" extrapolation was:

$$\epsilon = .1t \left(\frac{\sigma}{560}\right)^{2.18}$$

APPENDIX G

POWER PLANT CALCULATIONS

The power plant calculations for this system are essentially the same as those for any conventional steam power plant cycle, with the heat for generating the steam in this case being supplied by the hot organic fluid. A summary of the miscellaneous heater data is shown in Table 4, and the steam cycle flow and heat balance is shown in Fig. 19 and 20. A calculation of the overall plant heat balance is shown on a subsequent page.

A calculation of heat transformed into work in the turbine at full load is as follows:

	10^6 Btu/hr
Throttle to first extraction stage:	
$(2.563 \times 10^6)(1277-1203)$	189.662
First to second extraction stage:	
$(2.372 \times 10^6)(1203-1145)$	137.576
Second to third extraction stage:	
$(2.170 \times 10^6)(1145-1068)$	167.090
Third to fourth extraction stage:	
$(2.109 \times 10^6)(1068-1031)$	78.033
Fourth extraction to condenser inlet:	
$(1.920 \times 10^6)(1031-928)$	197.760
Total	770.121×10^6 Btu/hr
Equivalent mw	225.6 mw

Assuming a generator efficiency of 98.5%, the generator output would be:

$(225.6)(.985)$	222.2 mw
Auxiliary power is:	18.94 mw
Net electrical output is:	203.26 mw
Overall plant efficiency is:	
$\frac{203.26}{800} \times 100$	25.4%

OVERALL PLANT HEAT BALANCE

	10^6 Btu/hr	%
Heat Input at Reactor	2,730.400	100.0
Heat loss to moderator and shield	273.040	10.0
	2,457.360	90.0
Heat Loss Due To Radiation, etc.	9.300	0.3
	2,448.060	89.7
Heat Loss to Circulating Water	1,666.560	61.1
	781.500	28.6
Heat Loss to Turbine Auxiliaries	11.379	0.4
	770.121	28.2
Generator Equivalent Heat Loss	11.753	0.4
	758.368	27.8
Auxiliary Power Equivalent Heat Loss	64.642	2.4
	693.726	25.4

APPENDIX H

ORGANIC MAKE UP ANALYSIS

Energy Absorption of Organic

Slowing Down of Fast Neutrons - The energy absorbed per unit volume of the organic due to fast neutron scattering is equal to the product of the fast neutron scattering reaction rate, the average fractional energy loss per collision and the average energy of the fast neutrons.

$$\Delta E_n \left(\frac{\text{Mev absorbed}}{\text{cm}^3, \text{ sec}} \right) = \phi_F \ \bar{E}_n \left[(\Sigma_s)_H \ (q)_H + (\Sigma_s)_c \ (q)_c \right]$$

The fast flux (ϕ_F) was assumed to be twice the thermal flux, or 2 x 2 x 10^{13} neutrons/cm^2, sec. To be conservative, it was further assumed that the fast flux remains uniform in the fuel region. The average energy ($\bar{E}_n$) of the fast neutrons was assumed to be 2.0 Mev.

$(\Sigma_s)_H = 0.119 \text{ cm}^{-1}$*, $(q)_H = 0.632$ fractional energy loss per collision

$(\Sigma_s)_c = 0.087 \text{ cm}^{-1}$, $(q)_c = 0.147$

therefore,

$$\Delta E_n = 7.05 \times 10^{12} \text{ Mev/cm}^3, \text{ sec}$$

Since the density of the organic = 924 gm/cc,

$$\Delta E_n = 1.22 \text{ watts/gram}$$

Gamma Photon Energy Deposition - The major sources of gamma photons in the core are from direct fission, fission product decay, and neutron captures in the organic coolant and aluminum structural material.

(1) Prompt Fission and Fission Product Gammas - Each fission produces 7.5 gamma photons directly and 5.9 as a result of fission product decay[H-2], all of which are assumed to have an average energy of 1 Mev. Hence the gamma production rate due to fission and fission products is equal to the product of the fission tate per unit volume of fuel, the fuel volume, and the number of gamma photons per fission

---

* The values for $(\Sigma_s)_H$, $(q)_H$, $(\Sigma_s)_c$, and $(q)_c$ are from Ref. H-1

$$S\left(\frac{\text{photons}}{\text{sec, fuel tube}}\right) = 2.3 \times 10^{12} \left(\frac{\text{fissions}}{\text{cm}^3 \text{ of fuel, sec}}\right) \times 14500 \left(\frac{\text{cm}^3}{\text{fuel tube}}\right)$$

$$\times 13.4 \left(\frac{\text{photons}}{\text{fission}}\right) = 4.47 \times 10^{17}$$

The power density used is an average value based on a total reactor power output of 800 MW of heat.

In order to obtain a simple expression for energy absorption in the organic, the photon production rate in each tube was replaced by a line source of equivalent strength in the center of the tube. The organic was placed around the source so that the cylinder thus formed would equal the volume of organic in a fuel tube. This transformation gives a conservative estimate (higher than the actual) of the energy picked up by the organic because no allowance is made for γ attenuation by the fuel or structural material and the assumed path length of γ's through the organic is much longer than the true average path length.

Hence the energy absorbed is:

$$\Delta E_\gamma \left(\frac{\text{Mev absorbed}}{\text{sec, tube}}\right) = \int_{du} \mu_E^{\text{Total}} (\text{cm}^{-1}) \bar{E}_\gamma \left(\frac{\text{Mev}}{\text{photon}}\right)$$

$$\times \Gamma \left(\frac{\text{photons}}{\text{cm}^2\text{, sec}}\right) \, dV \, (\text{cm}^3)$$

where:

μ_E^{Total} = energy absorption coefficient for the organic = 0.0265 cm^{-1} for 1 Mev photons (Ref. H-3)

$\bar{E}_\gamma$ = average energy of a gamma photon = 1 Mev

$\Gamma = \dfrac{S\, e^{-\mu_a^{\text{total}}}}{2\pi r}$

μ_a^{Total} = linear absorption coefficient for the organic = 0.0628 cm^{-1} for 1 Mev photons (Ref H-3)

r = effective radius of the organic cylinder = 2.34 cm

dV = $2\pi r \, dr \, dl$

l = height of cylinder = 488 cm

Therefore,

$$\Delta E_\gamma = l \, \mu_E^{\text{total}} \, \bar{E}_\gamma \, S \int_{r=0}^{r=2.34} e^{-\mu_a^{\text{total}}} \, r \, dr$$

$$= 2.58 \times 10^{16} \text{ Mev absorbed/sec, tube} = 0.535 \text{ watts/gram}$$

This accounts for the energy deposited by fission and fission product γ's released in the same tube through which the organic is flowing.

In order to take into account the energy deposition of gamma photons originating in adjacent fuel tubes, a gamma flux reaching a neighboring tube was estimated. This was done by first homogenizing the fuel and organic in a tube, and thus obtaining a new effective radius (3.86 cm) for the cylinder and a new μ_a^{total} (0.583 cm^{-1}). Then the flux leaving a fuel tube is:

$$\Gamma = S \left(\frac{\text{original line source}}{2\pi r}\right) e^{-\mu_a^{total} r} = 4 \times 10^{12} \frac{\text{photons}}{cm^2, sec}$$

A build up factor of 2 was assumed since the path length through the cylinder was about equal to two attenuation lengths. Finally, the flux was reduced by geometric attenuation and absorption in the D_2O moderator. (μ_a^{total} = 0.07 cm^{-1}, path length = 9 cm.) Thus the flux which enters an adjoining fuel tube is:

$$\Gamma = 1.42 \times 10^{12} \text{ photons}/cm^2, sec$$

The organic in the adjoining tube was assumed to occupy a rectangular parallelopiped 10 cm wide, 1.7 cm thick, and 488 cm. long (same volume as the cylinder), in the direct line of above flux. The energy absorbed under these apparently conservative assumption is:

$$\Delta E_j^* = 0.0104 \text{ watts/gram, adjoining tube}$$

For each fuel tube there are 6 adjoining tubes, thus the total from all adjoining tubes is .062 watts/cm. Since this amount is small the contribution from tubes at a greater distance than the adjoining tubes was neglected. Thus the total energy absorbed from direct fission and delayed fission product γ's is $\Delta e_\gamma + \Delta E^*_\gamma = 0.597$ watts/cm.

(2) Neutron Capture Gammas - The same procedure was followed to calculate energy absorption in the organic due to neutron capture gammas. In order to determine a source strength of these gammas, the product of the neutron capture reaction rate and the volume of aluminum and organic was used.

$$S\left(\frac{\text{captures}}{sec, tube}\right) = \phi_T \Sigma_a V \left(\frac{\text{volume}}{\text{tube}}\right)$$

The final results for the gamma energy deposition in the organic are tabulated below:

	Photons Per Cap.	Photon Energy Mev.	Line Source Strength, Photons per cm, per sec, per tube	Energy Absorbed by Organic, watts/gram
Prompt and Fission Product Gammas	13.4	1.0	9.16×10^{14}	0.597
Organic Capture Gammas	1(3)	2.23(3)	3.01×10^{12}	0.004
Aluminum Capture Gammas	2(3)	4.0(3)	8.13×10^{12}	0.018
			Total	0.619

The total energy absorbed in the organic is 1.22 + 0.62 or 1.84 watts/gm. In order to take into account the energy absorbed by the organic above and below the core and to further insure that this estimate is conservative, a 1.5 factor was used. The final answer then becomes 2.76 watts/gram.

Decomposition Rate of Organic

It was assumed that Santo-wax-R has the same decomposition characteistics as meta-terphenyl. From a plot[H-4] of % polymer concentration versus energy absorbed for meta-terphenyl at 400°C, (See Figure 62) a decomposition rate for Santo-wax-R was estimated by obtaining the slope at 30% polymer concentration. The value obtained was

0.47% decomposition/μ amp hour per gram of mixture

Since the graph was plotted for 1 Mev electrons, the decomposition value can also be expressed as

0.47% decomposition/watt hour per gram of mixture

A factor of 1.05 was used to account for gas formation in the total decomposition rate.

Therefore, the decomposition rate of the Santo-wax-R in the reactor is:

$$\text{tar formation} = 0.0047 \left(\frac{\text{grams of tar formation}}{\text{watt hour per gram}}\right) 2.76 \left(\frac{\text{watts}}{\text{gram}}\right)$$

$$\times 5.75 \times 10^{6} \text{ (grams)} = 7.55 \times 10^{4} \text{ grams/hr} = 167 \text{ lbs/hr}$$

Total decomposition rate = (167)(1.05) = 175 lbs/hr

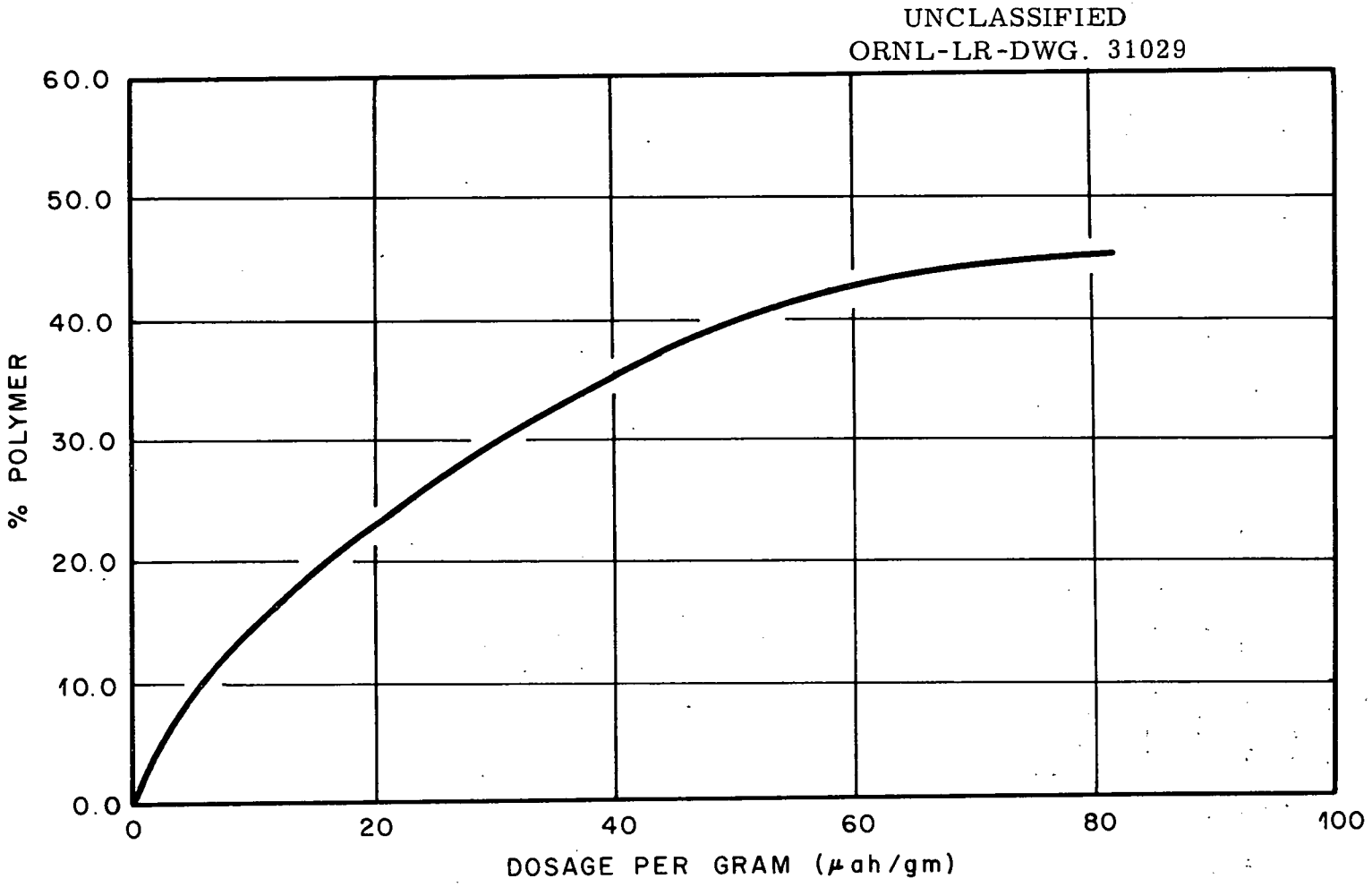

Fig. 62. Statitron Irradiated m-Terphenyl at 400°C (1-Mev Electron)

Organic Make Up Costs

Santo-wax-R, as used in the reactor, is a byproduct (the still bottoms) of biphenyl manufacture consisting of 80% terphenyls and 20% higher boilers. Since the purification system will remove these higher boilers, 1.25 lbs of Santo-wax-R must be added per lb. of coolant decomposition in the core. At $0.1675 per pound, the cost of coolant make up becomes:

$$\text{Cost} = \left(\frac{175 \text{ lbs. of decomp}}{\text{hr}}\right)\left(\frac{125 \text{ lbs of Santo-wax-R}}{\text{lb of decomp}}\right)\left(\frac{\$0.1675}{\text{lb of Santo-wax-R}}\right)$$

$$= \$36.6/\text{hr} = 0.183 \text{ mills/KWH}$$

Rounded figure: 0.2 mills/KWH

APPENDIX I

ECONOMICS AND COST DATA

TABLE 34

ANNUAL ISOTOPE CREDIT ASSUMING REACTOR GRADE Pu AT $ 12/ GRAM

Irradiation 10^3 MWD ton	Pu Conc. gms/ton	U-235 Conc. gms/ton	Annual Pu Credit, 10^3	Annual Uranium Credit, 10^3	Total Annual Credit, 10^3
1	980	5150	2750	5150	7900
2	1600	4200	2240	1450	3690
3	2050	3400	1920	435	2355
4	2400	2760	1685	111	1796
5	2550	2250	1430	13.7	1440
6	2640	1870	1235		1235

Assumptions:

(1) .8 Plant Factor

(2) .25 Over-all Plant Efficiency

(3) Pu at 12/gram

(4) U credit as shown in Appendix

TABLE 35

ENERGY COST ESTIMATE ASSUMING THE OLD REACTOR GRADE PU CREDIT

	3000 MWD/ton		6000 MWD/ton	
	Annual Charge $\$10^3$	Charge Mills/KWH	Annual Charge $\$10^3$	Charge Mills/KWH
Operating Cost	8,186		5,346	
Credit Fissionable Material Prod.	2,355		1,235	
Net Operating Cost	5,831	4.16	4,111	2.94
Total Carrying Charge	6,220	4.45	6,220	4.45
Total Cost	12,021	8.61	10,331	7.39

Assumptions:

(1) .8 Plant Factor

(2) .25 Overall Plant Efficiency

(3) Pu at $12/gram

(4) U Credit as Shown in Appendix

TABLE 36

ANNUAL FUEL COST AS A FUNCTION OF EXPOSURE ASSUMING ZIRCALOY-2CLAD

Irradiation 10^3 MWD/ton	Annual Fuel Consumption tons/yr	Annual Fuel Burnup $\$10^3$	Annual Fuel Element Fabrication $\$10^3$	Annual Shipping Proc. Costs 10^3
1	234	8,500	17,000	6,370
2	117	4,260	8,520	3,190
3	78	2,840	5,670	2,130
4	58.5	2,125	4,250	1,600
5	46.8	1,702	3,410	1,280
6	39.0	1,420	2,840	1,065
7	33.4	1,214	2,430	910
8	29.3	1,067	2,130	800
9	26.0	946	1,890	710
10	23.4	852	1,705	640

Assumptions:

(1) .8 Plant Factor

(2) .25 Overall Plant Efficiency

(3) 200 MW Plant Capacity

(4) Fuel Fabrication Costs of $80/kg

(5) Processing and Shipping Cost $30

TABLE 37

TOTAL ENERGY COST FOR ODPR ASSUMING ZIRCALOY-2 CLADDING AND $12/GRAM FOR REACTOR GRADE Pu

Operating Costs

Operation	3,000 MWD/ton Annual Cost 10^3	Mills/KWH	6,000 MWD/ton Annual Cost 10^3	Mills/KWH	12,000 MWD/ton Annual Cost 10^3	Mills/KWH
Labor and Maintenance	1,300		1,300		1,300	
Fuel Element Fabrication	5,670		2,840		1,420	
Fissionable Material Rental	308		308		308	
Cost of Fissionable Mat. Consumed	2,840		1,420		710	
Shipping and Processing	2,130		1,055		532	
Water and Miscellaneous Supplies	80		80		80	
D_2O Rental	269		269		269	
D_2O Depletion Allowance	269		269		269	
Organic Make Up	280		280		280	
Total operating cost	13,146		7,831		5,168	
Credit Fissionable Material Prod.	2,385		1,235		608	
Net Operating Costs	10,761	7.69	6,596	4.7	4,560	3.26
Annual Carrying Charges	6,220	4.45	6,220	4.45	6,220	4.45
Total Annual Cost	16,981	12.14	12,816	9.15	10,780	7.71

TABLE 38

FUEL PROCESSING COSTS

Nucleonics, May 1957 New Item

AEC Estimated Processing Costs

	Batch Size (Kg U)	Proc. Rate Kg U/day	Plant Time days	Annual Charge in $1,000	Unit Charge $/Kg U
Fuel Type A	35	28	4.3	65.8	1880
Fuel Type A	190	28	13.6	208	1095
Fuel Type B	20 +	44	3.5	26.8	2680
Fuel Type B	60	44	4.4	67.3	1120
Fuel Type C	120,000	1000	128	1459	12
Fuel Type D	20,000	1000	28	428	21

Fuel type A - Plate assemblies of approximately 90% enrichment U as an Al alloy, Al clad; processing composition is 7.5% U, 92.5% Al; assumed burn-up is 20% of U-235

Fuel type B - Plate assemblies of approximately 90% enrichment U as a Zr alloy, Zircaloy-2 clad; processing composition is 1.5% U, 98.5% Zircaloy-2; assumed burn-up is 25% of the U-235

Fuel type C - Slugs and plate assemblies of normal U, Al clad; processing composition 95% U, 5% Al; assumed irradiation is 800 MWD/ton

Fuel type D - Rod shaped elements of normal or depleted U, Zr and SS clad; processing compositions varies but is mostly U or UO_2

AEC Radiochemical Processing Charges

Reactor	Batch size (Kg U)	Proc. Rate Kg U/day	Plant Time days	Annual Charge in $1,000	Unit Charge $/Kg U
Common Wealth Edison	14,500	1000	22.5	344	24
Consumer PPD Nebraska	24,400	1000	32.4	396	20
Consolidated Edison	8,140 Th 1,980	1000 Th 24-U	16.1	246	30 Th 1240 U
PRDC					
Core	5,475	150	44.5	681	124
Blanket	32,300	1000	40.3	617	19
Elk River					
Core	12	44	3.3	50.5	4200
Blanket	6,850+	1000	13.8	42.8 ‡	31
Wolverine	20 +	88	3.3	10.1 ‡	2500
Yankee Atomic Electric	22,000	1000	30.0	459	21

* Annual unless otherwise stated,

Every fifth year,

Average for each year

The above charges are for processing delivered fuel elements to decontaminated nitrates and are based on AEC estimates of various reactors. In practice batch sizes will be determined as outlined in AEC statement of March 12. There are orders of magnitude estimates of irradiated fuel processing charges to illustrate pricing policy. They do not constitute a commitment on the part of the government.

Fuel characteristics assumed

Comm. Ed. - UO_2 pellets in Zircaloy-2 tubluar assemblies; U of 1.5% enrichment, processing composition is 76% UO_2 24% Zircaloy-2; assumed burn-up is about 60% of the U-235.

CPPD - Slug assemblies of Uranium of 2.3% enrichment; S.S. clad; processing composition is 91% U, 9% SS; NaK bond; Assumed burn-up is about 16% of the U-235

Con. Ed. - Alternate U and Th plates in assembly; the U is of about 90% enrichment as a Zr alloy and is clad with Zircaloy-2 as is the Th; processing composition is 53% Zr, 3% U, 44% Th; assumed burn-up is 57% of the U-235 and 49% of the U-233.

PRDC - Core - Pin assemblies of U of 27% enrichment as a Mo alloy, Zr clad; processing composition is 72% U, 8% Mo, 3% Zr, 17% S.S.; assumed burnup is about 4% of the U-235

Blanket - Rod assemblies of depleted U, S.S. clad; processing composition is 80% U, 20% S.S., Na bond; assumed irradiation is about 4000 g/t Pu

RCPA - Core - Plate assemblies of U of about 90% enrichment as a Zr alloy, Zr clad; processing composition is 3% U 97% Zr; assumed burn-up is 40% of the U-235

Blanket - Plate assemblies of normal U as a Zr-Nb alloy, Zr clad; processing composition is 65% U, 34% Zr, 1% Nb; assumed irradiation is to about 4000 g/t Pu

Wolverine UO_2SO_4 Solution ; U of about 90% enrichment; assumed burnup to 48% U-235

Yankee UO_2 pellets in S.S. tubular assemblies; U of 25% enrichment; processing composition is 85% UO_2, 15% S.S. ; assumed irradiation is 6400 MWD/ton.

TABLE 39

U-235 AND Pu PRICES FOR VARIOUS EXPOSURES

Depleted Uranium Credit computed from the formula

$$*C(U)\ (\$/Kg \text{ of contained U}) = 37.48\ (2X-1)\ \ln\frac{449X}{1-X} + 449\ (X-.00222)$$

where X = the weight fraction of U-235 in Uranium. Enrichment as a function of Exposure as computed by our physics group for the ODPR.

Exposure	% Enrichment	$/Kg of U	$/gm of Contained U-235
0	.71	40	5.63
1000	.587	25.1	4.27
2000	.462	13.3	2.88
3000	.374	6.15	1.64
4000	.304	2.10	.69
5000	.248	.32	.13
6000	.206	0	0

Plutonium Credit as a function of Exposure, assuming an initial conversion ratio of .8 - Computed from price schedule published in the June 6, 1957 issue of the Federal Register

Exposure	$/gm of Contained Pu
400	38.1
800	33.6
1200	29.3
1600	28.50
2000	28.50
4000	28.50

* This formula appeared in the March 1957 issue of Chemical Engineering Progress in an article by Manson Benedict.

UNITED STATES ATOMIC ENERGY COMMISSION
WASHINGTON 25, D. C.
November 17, 1956

TABLE 40

Base Charges for Enriched Uranium, as UF_6, f.o.b. Oak Ridge, varying with U-235 enrichment.

Weight Fraction (U-235 in Total U)	Charge ($/Kg. Contained U)	Weight Fraction (U-235 in Total U)	Charge ($/Kg Contained U)
.0072	40.50	.040	535.50
.0074	42.75	.045	616.50
.0076	45.25	.050	698.25
.0078	47.50	.060	862.50
.0080	50.00	.070	1,028.00
.0082	52.50	.080	1,195.00
.0084	55.00	.090	1,362.00
.0086	57.50	.10	1,529.00
.0088	60.00	.15	2,374.00
.0090	62.75	.20	3,223.00
.0092	65.25	.25	4,078.00
.0094	67.75	.30	4,931.00
.0096	70.50	.35	5,793.00
.0098	73.00	.40	6,654.00
.010	75.75	.45	7,515.00
.011	89.00	.50	8,379.00
.012	103.00	.55	9,245.00
.013	117.00	.60	10,111.00
.014	131.25	.65	10,979.00
.015	145.50	.70	11,850.00
.020	220.00	.75	12,721.00
.025	297.00	.80	13,596.00
.030	375.50	.85	14,475.00
.035	455.00	.90	15,361.00

* *

Guaranteed Fair Prices to be Paid for Plutonium and Uarnium-233 Produced by Licensees, and Delivered to the AEC During the Period July 1, 1962 to June 30, 1963.

A. Plutonium, as metal buttons, f.o.b. AEC Plant
Base Price : $12/gr Plutonium

B. Uranium-233, as Uranyl (233) nitrate, f.o.b., Oak Ridge, Tenn.
Base Price: $15/gr U-233

December 7, 1956

D R A F T

EDISON ELECTRIC INSTITUTE

TECHNICAL APPRAISAL
TASK FORCE ON NUCLEAR POWER

ECONOMIC EVALUATION

In order to provide a common basis for economic evaluation of various nuclear power plant concepts, the methods and rates outlined herein should be used.

Because of varying financial arrangements, differences in local tax rates, cost of bond interest, etc, no one set of fixed charge rates will apply to all locations or at all times in the future. However, by using a uniform set of rates for the various types of nuclear plants and an explanation of the rates used, adjustments to over-all estimated costs can be made by any prospective nuclear power plant builder to fit the conditions in his area.

CAPITAL COSTS

Capital costs of a nuclear power plant should include all costs normally covered by a production plant in service account. They should include the cost of land and land rights, structures and equipment of a permanent or semi-permenent nature and an item for interest during construction.

Land and Land Rights

Except for a specific location, the cost of land cannot be estimated. However, for purposes of comparing cost of alternative nuclear power plants, a uniform cost for land of $500,000 should be used for each estimated project cost.

Structure and Equipment

Estimated costs of structures and equipment should include the cost of all permanent and semi-permenent buildings, the nuclear steam generator, turbo-generator units (including any required for emergency or auxiliary supply), and all accessory structures and equipment. Not to be included in the capital cost of the plant are the cost of fertile and fissionable material, any special moderator material (such as heavy water) or the cost of core fabrication.

All estimates should include an allowance for engineering but not the cost of preliminary major research and development expenses.

Interest During Construction

The allowance for interest during construction should be computed at 6% of the cost of the plant, including the cost of land.

Working Capital

Because of the present basis of accounting for fissionable material after usage and also deferred payment of taxes, processing costs, etc, the amount of working capital required will be limited largely to materials and supplies, including spare parts and equipment, cost of special moderator material such as heavy water (unless leased), and the cost of fabricating the first core, including the cost of purchased fertile material but not including leased fissionable material.

The allowance for working capital should be computed or determined as follows:

4% of plant cost (excluding land), plus

The cost of fabricating the first core, plus

The cost of purchased fertile material in the first core, plus

The cost of special moderator material (unless leased).

PRELIMINARY RESEARCH AND DEVELOPMENT COSTS

Rather than convert the cost of major non-recurring preliminary research and development expenses to an annual basis, the total amount of such expenses should be separately stated. These expenses would normally include preliminary research and test costs which might be necessary to determine the physical and operating characteristics of certain materials and plant components before a reactor design can be finalized.

FIXED CHARGE RATES

The attached tabulation entitled "Fixed Charge Rates for Nuclear Power Plant Economic Evaluation" summarizes the fixed charge rates to be used for the various plant components.

Bond Interest and Return on Equity Capital

The annual cost of these items is based on an over-all rate of return of 6% and assumes that 50% of the plant cost will be financed with bonds having an interest rate of 3-$\frac{1}{2}$% and 50% by capital from other sources - common stock, preferred stock, surplus.

While a bond interest rate of 3-½% is substantially below present interest rates, its use herein is based upon an approximate average of the lowest and highest interest rates on Class A or better electric light and power investor owned public utility bonds issued during the past two decades.

Local Taxes

The local tax rate of 2% is based upon the average amount paid in State and local taxes by investor owned electric utilities in percent of plant investment as reported by the Edison Electric Institute.

Income Taxes

The income tax computation is based upon a 52% tax rate and assumes that amortization accruals will apply equally to bond and equity capital during the assumed lives, reducing in later years the interest deductions for Federal income tax purposes.

Amortization

For amortization, a sinking fund rate is used based upon a 6% return on reinvested amortization accruals. An average life of 20 years has been assumed for the complete plant. While this is lower than that ordinarily used for a conventional power plant, it is probable, at least in the early stages of development, that the turbine equipment will be at a somewhat lower pressure and temperature than modern conventional practice, and progress in reactor development is likely to be rapid. Consequently the lower life upon which the computations are based is intended to cover a more rapid rate of depreciation because of technological obsolescence rather than a shorter physical life.

Insurance

Insurance normally carried on a conventional plant and third party liability insurance should be computed at 0.5% of plant cost (excluding land).

INTERIM REPLACEMENTS

The amortization period used assumed equal life for the reactor and turbine plant. In some types of plant, this assumption may be realistic. However in other types, the life of many of the component parts of the reactor may be less than 20 years and require periodic replacement within the 20 year life of the plant as a whole. For example, assume for a particular plant the nuclear steam generator represents 50% of the original cost and that 50% of this part of the plant will need to be replaced once during the 20 year period. The annual charge to cover these interim replacements would be 1.25%. No ground rule can be made as to a specific allowance for this item and it is left to the judgment of the individual evaluating a particular type of reactor.

OPERATING COSTS

From year to year, operating costs in a nuclear power plant are likely to undergo large variations as fuel expenses, processing costs, credit for recovered materials, fabricating costs, etc, are not likely to be at a uniform rate. For purposes outlined herein, evaluations should be limited to average steady state operating conditions rather than a year by year analysis of operating expenses and output.

Labor and Maintenance

In general, operating labor costs will consist of the annual costs of the fixed operating force stationed at a nuclear power plant, including the cost of fringe benefits, company overheads, etc. In large plants, the operation will probably consist of a high degree of completeness. On the other hand, small plants are likely to be self contained units, requiring substantially less full time operating personnel.

It is also likely that in the larger plants, a substantial part of the maintenance will be conducted by full time personnel assigned to the plant while in the smaller plants, most of the maintenance will be conducted by periodic overhaul or as required as a result of failure of some component part. Maintenance will also vary with the size, complexity and type of plant.

Rather than have each reporting group prepare a manning schedule and make separate estimates of labor and maintenance costs, more uniform results for comparative purposes can be obtained by the use of the simple thumb rule given below. Investigation of estimated operating labor and maintenance costs of a few proposed large projects indicate that the results obtained by this thumb rule computation agree closely with the estimates. The results so obtained will of course by subject to further refinement by any prospective nuclear power plant builder.

Estimated Annual Operating
Labor & Maintenance Costs

Over 100,000 Kw electric capacity - $500,000 plus
$4.00 per Kw of electric capacity

50,000 to 100,000 Kw electric capacity - $200,000 plus
$7.00 per Kw of electric capacity

Less than 50,000 Kw electric capacity - $100,000 plus
$9.00 per Kw of electric capacity

Fuel Element Fabrication

The estimated cost of fuel fabrication should include the cost of control rods, cladding material and converting UF-6, plutonium metal Uranyl (233) Nitrate, and fertile material to the forms required. It should also include the cost of shipping the fissionable materials from Oak Ridge to the fabricator and the cost of shipping fabricated fuel elements to the site.

Fertile Material

The cost of natural or depleted uranium should be based on the price currently quoted by the Atomic Energy Commission. A price of $43.00 per kilogram for thorium metal should be used.

Rental of Fissionable Material

The rental charge for fissionable material should be computed at a rate of 4% per annum and should be based upon the charges set forth in the attached United States Atomic Energy Commission tabulation dated November 17, 1956. Allowance should be made for rental charges from the date upon which fissionable material is shipped from the Atomic Energy Commission facility to the date upon which accounting for such fissionable material is completed.

Cost of Fissionable Material Consumed and Credit for Fissionable Material Produced

The cost of fissionable material consumed and lost should be based upon the charges for fissionable materials as given in the attached United States Atomic Energy Commission tabulation dated November 17, 1956. Credits for fissionable materials produced should be in accordance with the current price to be paid for such materials by the Atomic Energy Commission.

Shipping

This item should include the cost of shipping spent fuel elements or fission products to the processing and disposal sites.

Processing and Waste Disposal

This item should include the cost of reprocessing spent fuel and the cost of disposing of fission products.

TOTAL ANNUAL COST

The over-all annual cost of each project should be reduced to a unit cost per kilowatt hour at 40%, 60%, and 80% annual capacity factors. The attached tabulation entitled "XYZ Nuclear Power Plant and Estimate of Power Cost" illustrates the application of the rates given herein to a hypothetical heterogeneous nuclear power plant and the computation of over-all costs per kilowatt hour at the various capacity factors.

December 7, 1956

FIXED CHARGE RATES FOR NUCLEAR POWER PLANT ECONOMIC EVALUATION

	Land and Land Rights	Structures and Equipment	Working Capital
Annual Rates - % of Cost			
Bond Interest	1.75	1.75	1.75
Return on Equity Capital	4.25	4.25	4.25
Local Taxes	2.00	2.00	--
Income Taxes	2.85	2.85	2.85
Amortization	-	2.70	-
Insurance	-	0.50	-
Total Excluding Interim Replacements	10.85	14.05	8.85
Rounded to	11.0	14.0	9.0

Interim Replacements - In addition to an allowance for amortization, some allowance in the estimate of annual fixed costs should be made for interim replacement of various units of property during the 20 year life assumed above. For some types of reactors, such as pressurized water, these replacements will be small. For other types such as a homogeneous reactor, replacements during the 20 year period may be substantial because of corrosions, erosion, etc.

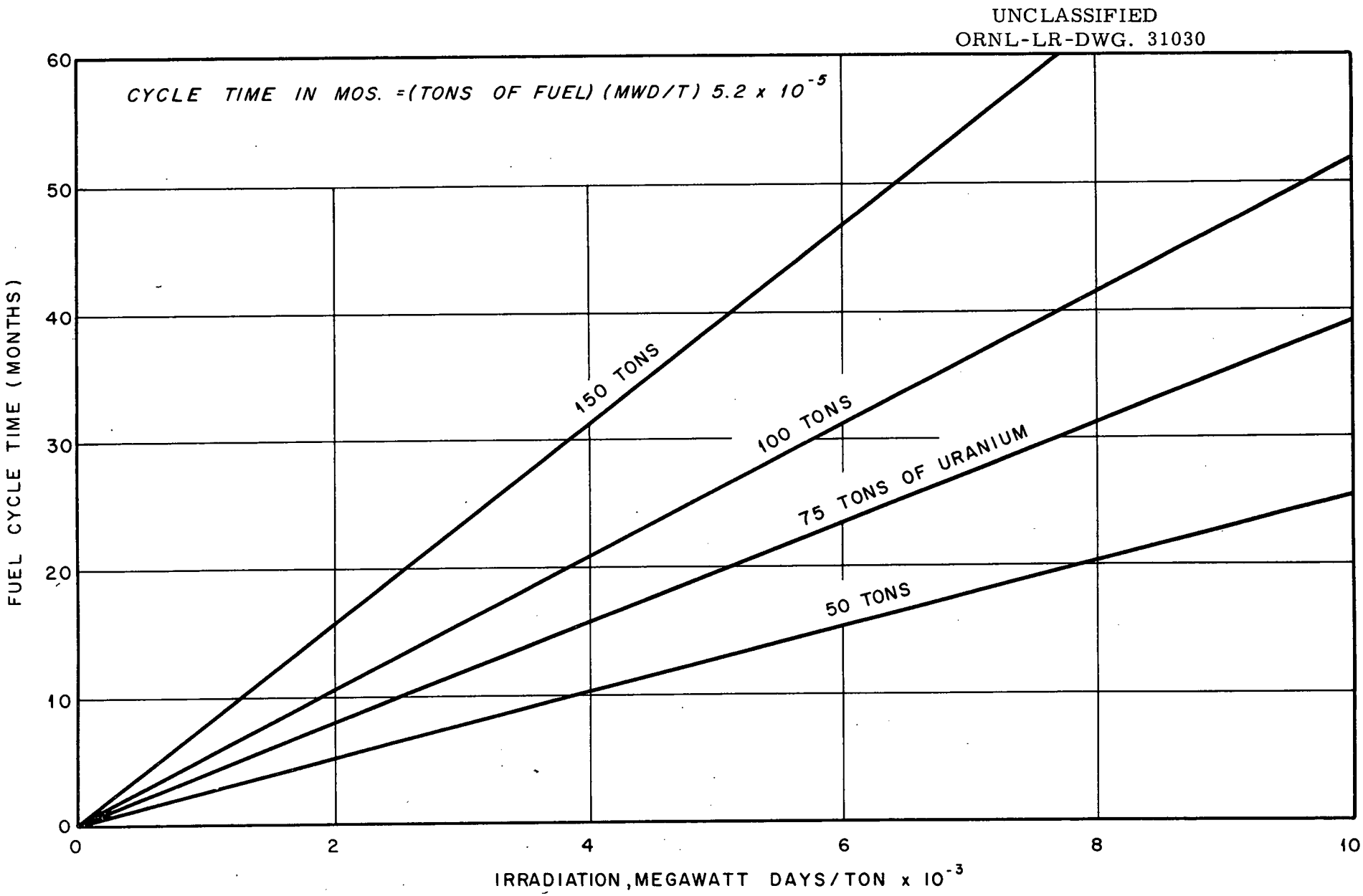

Fig. 45. Fuel Cycle Time in Months Versus Irradiation in MWD/Ton Assuming a 0.8 Load and an Electrical Conversion Efficiency of 25% and an Electrical Capacity of 200 MW

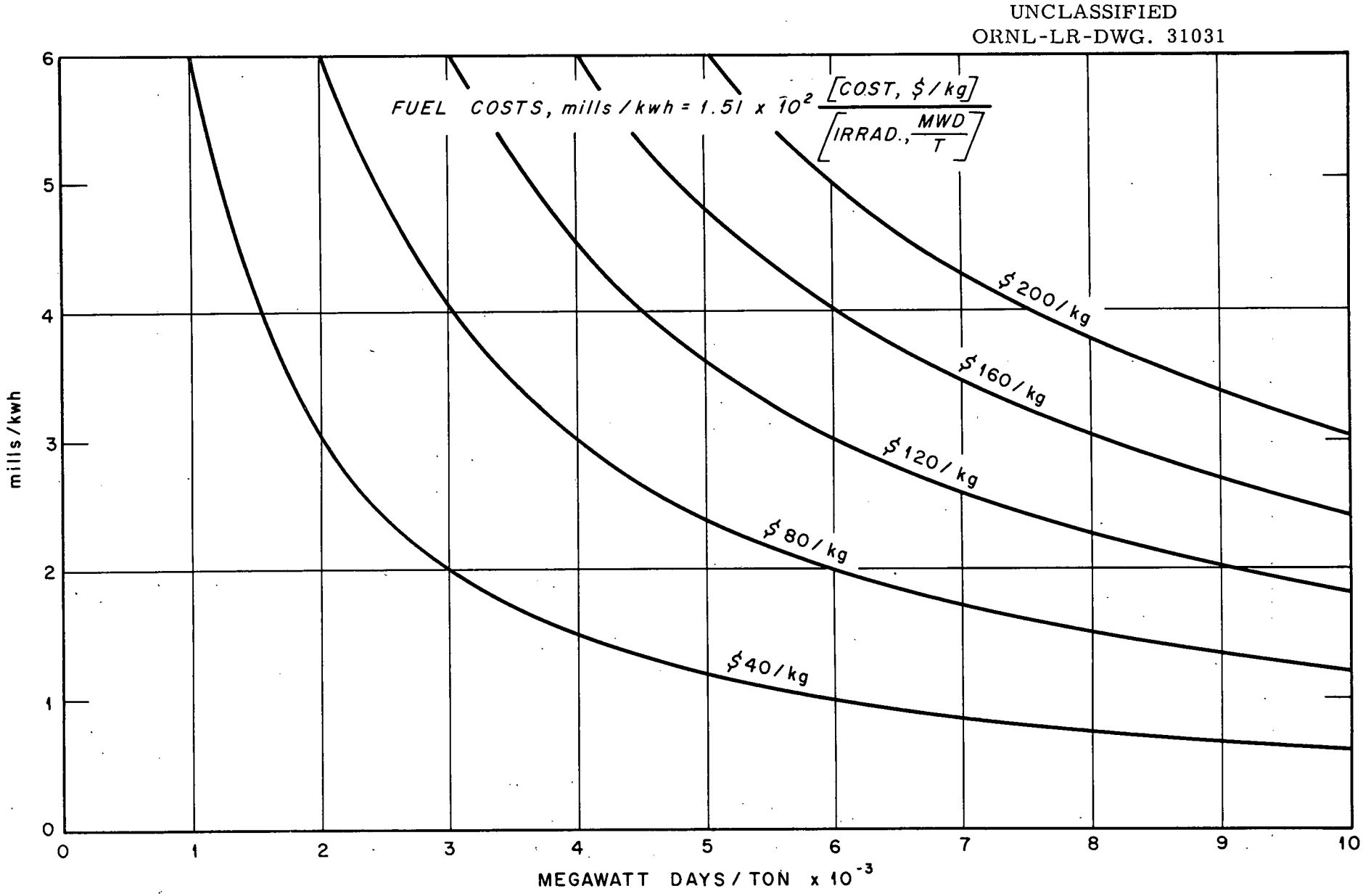

Fig. 46. Fuel Burn up Costs, mills/kwh, Vs. Irradiation Time, Megawatt Days/Ton for Various Core Costs in Dollars per Kilogram - Assuming a 25% Electrical Conversion Efficiency

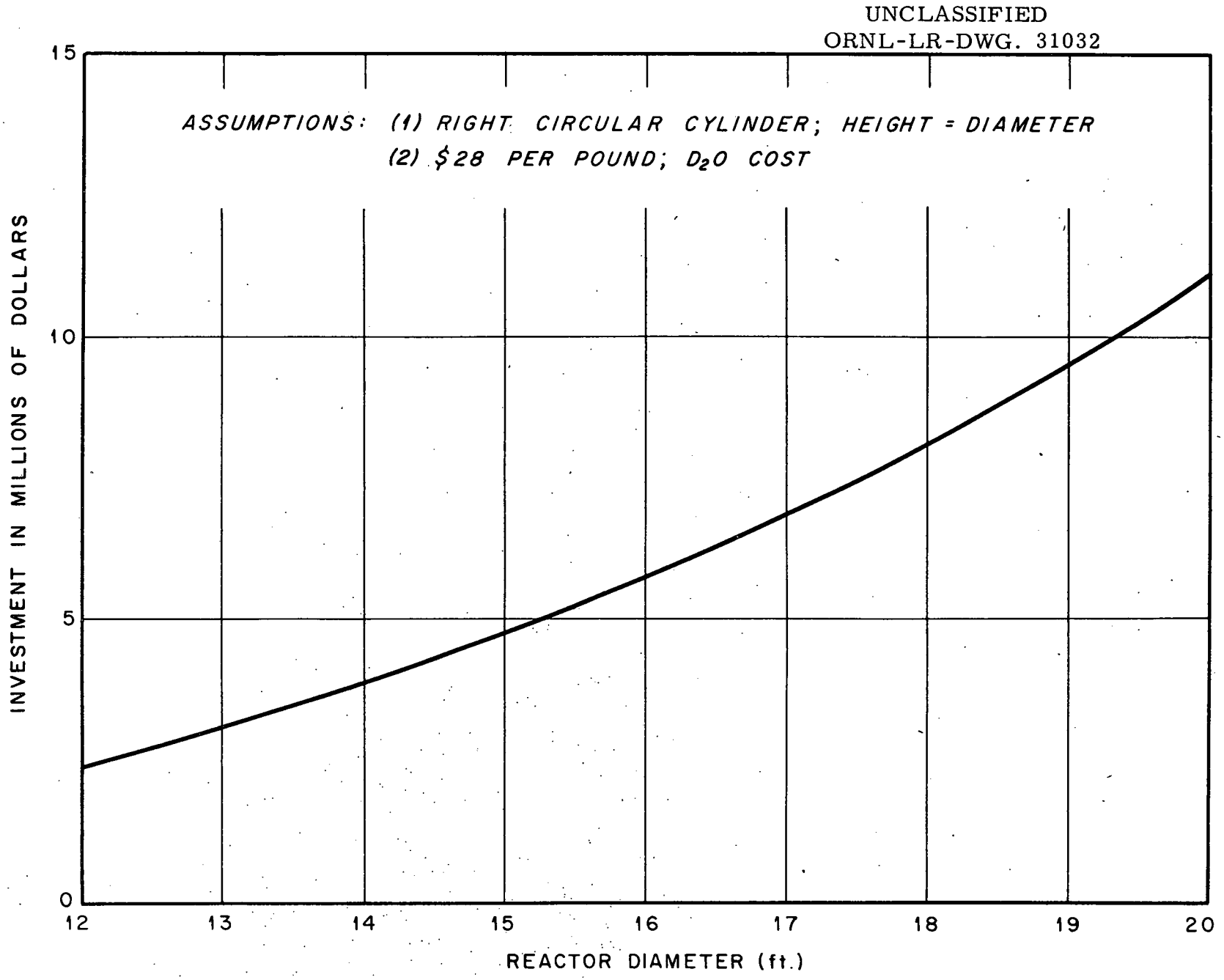

Fig. 47. D_2O Capital Investment Versus Reactor Radius (Diam.)

REFERENCES

1-1 National Bureau of Standards Handbooks: "Maximum Permissible Amount of Radioactivity in the Human Body and Maximum Permissible Concentrate in Air and Water", No. 52.
"Permissible Dose for External Sources from Ionizing Radiation, No. 59
"Regulating of Radiation Exposures by Legislative Means," No. 61

1-2 "Preliminary Design and Cost Estimate of A Heavy Water Moderated and Cooled Fifty Megawatt Nuclear Power Plant", NPG-16, April 1, 1954 (Declassified)

1-3 Shimazaki, T.T. and Freede, W.J., "Determining Coolant Flow In SRE Fuel Elements", Nucleonics, Vol. 15, No. 2, February, 1957.

1-4 Shimazaki, T.T., and Freede, W.J., "Heat Transfer and Hydraulic Characteristics of the SRE Fuel Element:, Reactor Heat Transfer Conference, New York, 1956

1-5 Shimazaki, T.T., "Friction Factor and Orifice Coefficient for SRE Fuel Element Assembly", NAA-SR-1100.

1-6 Bettis Technical Review, "Reactor and Plant Engineering", Vol. 1, No. 1, May, 1957.

1-7 Technical Progress Reports, Pressurized Water Reactor Project, WAPD-MRP-52 through WAPD-MRP-67.

1-8 Lewis, W.B., "Natural Uranium-Heavy Water Reactors for Low Cost Power", DL-29

1-9 Lustman, B., "Release of Fission Gases from UO_2", WAPD-173

1-10 Schultz, M.A. "Control of Nuclear Reactors and Power Plants", McGraw-Hill, 1955

2-1 Jaye, S., "Oracle Code for Large, Heterogeneous Thermal Reactors", Oak Ridge National Laboratory, To be Published.

2-2 Hausner, H.H. and Mills, R.G., "Uranium Dioxide for Fuel Elements," Nucleonics, Vol 15, No. 7, July 1957

2-3 Murray, R.L., "Nuclear Reactor Physics" Prentice-Hall, 1957

2-4 Glasstone, S., "Principles of Nuclear Reactor Engineering, Ed. 1, D. Van Nostrand Co., Inc. 1955

2-5 The Reactor Handbook, Volume I, Physics , AECD-3645

3-1 Technical Progress Reports, Pressurized Water Reactor Project, WAPD-MRP-52 through WAPD-MRP-67

3-2 Hausner, H.H., and Mills, R.G., "Uranium Dioxide for Fuel Elements", Nucleonics, Vol. 15, No. 7, July 1957

3-3 "Organic Moderated Reactor Experiment; First Progress Report; October 1955 to July 1956, NAA-SR-1700, p. 30

3-4 "High Velocity Corrosion Study in Organic Media", Mine Safety Appliances Company, Technical Report No. 54

3-5 "Corrosion Studies in Organic Heat-Exchange Media", Battelle Memorial Institute, BMI-1160

3-6 Lingafelter, J.W., "Feasibility Study on Magnesium Alloy Process Tubing for Organic Coolants", HW-47921

3-7 Marin, J., "Engineering Materials, Their Mechanical Properties and Applications, Prentice-Hall, Inc., New York, 1954, p. 271

3-8 Ibid, p. 264

3-9 "Compilation of Organic Moderator and Coolant Technology", TID-7007, Part I

3-10 Bolt, R.O., and Carrol, S.G., "Summary Evaluation of Organics as Reactor Moderator-Coolants", AECD-3711

3-11 McGoff, M.J., and Mausteller, J.W., "In-Pile Testing of Monoisopropyl Biphenyl", MSA-IR-55

3-12 McEwen, M., "Preliminary Engineering Studies, Organic Reactor Coolant Moderators", R and E-Cr-964

3-13 Private Communication from C.A. Trilling, Atomics International, Division of North American Aviation, Inc.

3-14 "OMR Electric Power Plant", Atomics International, Division of North Americal Aviation, Inc., AI-1673

3-15 Private Communication from M. McEwen, Monsanto Chemical Company

3-16 Monsanto Technical Bulletin, O-125, January 1956

3-17 Nuclear Science and Engineering, Vol. 2, 1956

3-18 "Organic Moderated Reactor Experiment; First Progress Report; October 1955 to July 1956, NAA-SR-1700, p. 148

3-19 Ibid, p. 149

3-20 "Summary of Santowax-R Heat Transfer and Fouling Runs in the Laboratory Heat Transfer Loop", Inter-Office Letter from D. Huber and M. Silverberg to D. W. Bareis, Atomics International Division of North American Aviation, Inc.

3-21 Colichman, E.L., and Fish, R., "Pyrolytic and Radiolytic Recomposition Rate Studies on Ortho, Meta, and Para-Terphenyls", NAA-SR-1287

3-22 "Organic Moderated Reactor Experiment; First Progress Report; Oct. 1955 to July 1956", NAA-SR-1700, p. 118

4-1 Iskenderian, et al, "Heavy Water Reactors for Industrial Power Including Boiling Reactors", UN-P/495-USA

4-2 Benedict, M., "Fuel Cycles in Single Region Thermal Reactors", (Part II), Chemical Progress, March 1957

4-3 "Enriched Versus Natural Uranium", Nucleonics, June 1957

A-1 Glasstone, S., Edlund, M.C., "The Elements of Nuclear Reactor Theory", D. Van Nostrand, 1952

A-2 The Reactor Handbook, Volume I, Physics - AECD-3645

A-3 Hughes, D.J., Schwartz, R.B."Neutron Cross Sections," BNL-325

A-4 Brown, W.W., "Neutron Age and Diffusion Length Measurements in Diphenyl", NAA-SR-Memo-1706

A-5 Conerty, M.C., et al, "Calculation of Fast and Thermal Group Constants with application of Diphenyl", KAPL-1643

B-1 Sato, K., "Determination of Burnout Limits of Polyphenyl Coolants", AGC-AE-32, 1957

B-2 Palladino, N.J., "The Thermal Design of Nuclear Power Reactors" ASME Paper No. 54-SA-58

B-3 Glasstone, S., "Principles of Nuclear Reactor Engineering", Ed. 1, D. Van Nostrand Co., Inc., 1955

B-4 Gilliland, E.R., Bareis, D. and Feick, G., "Heat Removal From Nuclear Reactors", NP-155

B-5 Report for D. Huber and M. Silverberg to D. W. Bareis, "Summary of Santowax-R Heat Transfer and Fouling Runs in the Laboratory Heat Transfer Loop", Inter-office Letter.

B-6 Freund, G.A. and London, A.L., "A General Method for Comparing Thermal Performance of Fuel Element Geometries and Coolants for Non-Boiling Reactors", ANL-5589

D-1 Kaplan and Chernick, The Brookhaven Nuclear Reactor Theory and Nuclear Design, BNL-152, 1952

D-2 Kaplan and Chernick, "Uranium Graphite Lattices- The Brookhaven Reactor", Proceedings of the International Conference on the Peaceful Uses of Atomic Energy; p. 606, 1955

D-3 The Reactor Handbook, Volume I, Physics, AECD-3645, 1955

D-4 Goertzel, "An Estimation of Doppler Effect in Intermediate and Fast Reactors", Proceedings of the International Conference on the Peaceful Uses of Atomic Energy, P/613, 1955

D-5 Davis, M.W., "Resonance Capture of Neutrons by Uranium Cylinders:, HW-37766, 1955

D-6 Wheeler, J.A., "Principles of Nuclear Power, Chapter 22, Control", N-2292, 1944

D-7 Wigner, Weinberg, Williamson, "Efficiency of Control Rods Which Absorb Only Thermal Neutrons", CP-1461, 1944

E-1 Blizard, E.P., "Nuclear Radiation Shielding", Oak Ridge National Laboratory, Oak Ridge, Tennessee

E-2 Rockwell, T., Reactor Shielding Design Manual, D. Van Nostrand Co., Inc. New York 1956

H-1 Makazato, S. and Gercke, R.J., "Organic In-Pile Loop Naa-18" NAA-SR-1592

H-2 Maienschien, F.C., "Chart Showing Current Values for the Distribution of Energy Released by The Fission of U-235 Induced by Thermal Neutrons", ORNL-CF-56-10-9, Oak Ridge National Laboratory, Oak Ridge, Tennessee, 1956

H-3 Rockwell, T., Reactor Shielding Design Manual, D. Van Nostrand Co., Inc., New York, 1956

H-4 Cochman and Fish, Pyralytic and Radiolytic Decomposition Rate Studies of Ortho-, Meta-, and Para-Terphenyls, NAA-SR-1287

GENERAL BIBLIOGRAPHY

1. Beeley, R.J., "Reactor Evaluation Quarterly Progress Report for August - October 1953", NAA-SR-845
2. Edison Electric Institute, "Economic Evaluation", prepared by the Technical Appraisal Task Force on Nuclear Power.
3. Freund, G.A., "The Case for Organic Coolant Moderators for Power Reactors", Nucleonics, Volume 14, No. 8, August 1956, p. 58
4. Gaedkoop, J.A. and Jensen, G., (editors), "Proceedings of the Kjeller Conference on Heavy Water Reactors".
5. Lane, J.A., "Reactor Economic Data", Progress in Nuclear Energy VIII, p. 349
6. LeTourneau, B.W. and Grimble, R.E., "Engineering Hot Channel Factors for Nuclear Reactor Design", Nuclear Science and Engineering Volume I, October, 1956
7. Lewis, W.B., "The Heavy-Water Reactor for Power", DL-25
8. Lewis, W.B., "Canadian Experiments Aim at Economic Nuclear Power", Nucleonics, Volume 14, No. 10, October 1956, p. 28
9. Shimazaki, T.T., "Heat Transfer Considerations in the Use of Organic Cluids", No. 57, NESC-113
10. "Proceedings of the SRE-OMRE-Forum", TID-7525, NAA-SR-1804